



PhD's thesis XXX Cycle

ON THE RENORMALIZATION OF THE SINGLET EXTENSION OF THE STANDARD MODEL

A Theoretical Study of High Energy Physics

Gabriele Ria

Supervisor: Davide Meloni
Program Coordinator: Giuseppe Degrassi
Department of Mathematics and Physics
Università degli Studi Roma Tre
Rome, Italy 2017

Contents

Introduction	3
1 Model Setup	5
1.1 The Scalar Lagrangian	5
1.2 The Yukawa Lagrangian	10
1.3 Gauge-Fixing and Ghost Lagrangian	12
1.4 Theoretical and Experimental Constraints	14
1.4.1 Theoretical Constraints	14
1.4.2 Experimental Constraints	15
1.4.3 Global Constraints	17
1.5 Parameter Values	18
2 Singlet Decay Widths at Tree-Level	21
2.1 LO Decay Width to Gauge Bosons	22
2.2 LO Decay Width to Fermions	23
2.3 LO Decay Width to Higgs Bosons	23
2.4 LO Decay Width to massless Gauge Bosons	23
2.5 LO Total Decay Width and Branching Fractions	25
3 Renormalization of the SSM	29
3.1 Renormalization Schemes	33
3.2 Renormalization Conditions and Counterterms	36
3.2.1 Explicit Form of the OS Counterterms	38
3.2.2 Explicit Form of the iOS Counterterms	40
3.2.3 Explicit Form of the MF Counterterms	41
3.2.4 Equivalence of the MF and iOS Schemes	42
4 Singlet Decay Widths at the Next-to-Leading Order	44
4.1 NLO Decay Width to Gauge Bosons	45
4.2 NLO Decay Width to Fermions	50
4.3 NLO Decay Width to Higgs Bosons	55
4.4 NLO Total Decay Width	56

4.5	NLO Application of the MF renormalization scheme	58
5	Numerical Results	60
5.1	Dependence on s_α and w	60
5.2	Dependence on m_S	63
5.3	A Comment on the Gauge Dependence	71
	Conclusions	73
	Appendix	75
A -	SSM Tadpole Amplitudes	75
	Tadpole for the H Field	75
	Tadpole for the S Field	76
B -	SSM Self-energy Amplitudes	76
	Self-Energy for the W Boson	76
	Self-Energy for the Z Boson	77
	Self-Energy for the $Z\gamma$ Mixing	78
	Self-Energy for the γ Boson	78
	Self-Energy for the H Boson	79
	Self-Energy for the S Boson	80
	Self-Energy for the HS Mixing	81
	Self-Energy for the Top Quark	83
C -	SSM Three Point Functions	83
	One-Loop Corrections to SZZ Vertex	83
	One-Loop Corrections to SWW Vertex	88
	One-Loop Corrections to SHH Vertex	92
	One-Loop Corrections to Stt Vertex	94
D -	Loop Integral Expressions: $\mathcal{A}_0, \mathcal{B}_0, \mathcal{B}_{00}, \mathcal{B}_1$	97

Introduction

In June of 2012, the LHC experiment [1, 2] has finally completed the spectrum of the Standard Model with the discovery of the Higgs boson, predicted in the 60's by Higgs [3, 4], Englert, Brout [5], Guralnik, Hagen and Kibble [6]. However, the structure and the physics behind the Higgs sector are not completely clear and this represents a possible gateway to the manifold conceivable extensions of the Standard Model (SM). One of the simplest renormalizable enlargement of the Higgs sector is constructed by adding to the SM Lagrangian one additional spinless real electroweak singlet, which develops its own vacuum expectation value [7, 8, 9, 10, 11, 12, 13, 14].

Beside being easy to implement, the physics of a scalar singlet has received a lot of attention in the recent years for several reasons; among them, it can help in solving the issues related to the metastability of the electroweak vacuum [15, 16] if the Higgs potential receives a correction due to new physics which modify it at large field values [17] and it could provide a door to hidden sectors [18] to which it is coupled. The singlet model has the advantage of depending on relatively few parameters and this implies a feasible experimental study at the LHC for the analysis of the new physic effects in the Higgs boson couplings, searches for heavy SM-like Higgs bosons [19, 20] and direct searches for resonant di-Higgs production [21, 22, 23]; in the absence of linear and triple self-interactions, this model possesses a \mathbb{Z}_2 -symmetry and the singlet can be a viable candidate for dark matter, although for masses somehow larger than 500 GeV [24, 25] the couplings of the dark matter to the known particles occur only through the mixing of the singlet field with the SM Higgs boson. Without a \mathbb{Z}_2 -symmetry a strong first order electroweak phase transition is allowed and additional sources of \mathcal{CP} violation occur in the scalar potential. In this thesis we limit ourselves to a situation where the new singlet s^0 communicates with the $SU(2)_L$ doublet ϕ only via a quartic interaction of the form,

$$\kappa (\phi^\dagger \phi) (s^0)^2 .$$

This implies that the would-be Higgs boson of the SM mixes with the new singlet leading to the existence of two mass eigenstates, the lighter of which (H) is the experimentally observed Higgs boson whereas the heaviest one (S) is a new state not seen so far in any collider experiments. We call this model the *Singlet Extension of the SM* (**SSM**). Since only ϕ is coupled to ordinary matter, the main production mechanisms and decay channels of H and S are essentially the same as those of the usual SM Higgs particle, with couplings rescaled by quantities which depend on the scalar mixing angle, called α , whose bounds have been

discussed in details in [10, 11, 26, 27]. For masses larger than $\gtrsim 200$ GeV, the most important decay channels of the heavy state S are those to a pair of vector bosons $S \rightarrow VV$ and, when kinematically allowed ($m_S > 2m_H$), to a pair of lighter scalars and top quarks, $S \rightarrow HH, \bar{t}t$. With the run II at LHC, the exploration of the scalar sector is expected to reveal more details. So, the comparison between theory and data requires precise predictions obtained through higher-order calculations. To this aim, we evaluated the radiative corrections to the main decay rates $\Gamma(S \rightarrow ZZ, W^+W^-, \bar{t}t, HH)$ and studied in details their dependence on the singlet mass m_S as well as on the mixing angle α and the singlet vev w . Interestingly enough, the SSM scalar sector implies no natural way of defining the renormalized scalar mixed mass (or alternatively, the scalar mixing angle) and the non-diagonal fields through a physically motivated renormalization scheme. As a consequence, it is possible to construct different prescriptions to renormalize the non-diagonal scalar sector; nevertheless, we have to pay attention to their definitions since some of them manifest a gauge dependence in the physical observables. To compute the next-to-leading order (NLO) EW decay rates, we use the "*improved on-shell*" renormalization scheme which is totally gauge-invariant [29]. To give a comment on the gauge dependence effect on the renormalized decay widths we also consider a second scheme, called "*minimal field*", which exhibits a gauge dependence [29]. The minimal field scheme is defined by renormalization conditions which need the introduction of a renormalization scale μ_R . We prove that it is possible to obtain a gauge independent result by fixing this scale at $\mu_R^2 = (m_H^2 + m_S^2)/2$ since, for this specific value, the improved on-shell and the minimal field schemes are equivalent.

The main result of this thesis is that for the singlet scalar mass range $200 \leq m_S \leq 1000$ GeV the gauge independent EW corrections to the decay widths reach a maximum of $\mathcal{O}(6\%)$ in the W^+W^- channel, $\mathcal{O}(5\%)$ in the ZZ channel and $\mathcal{O}(4\%)$ in the $HH, \bar{t}t$ channels for masses lower than 450 GeV and almost independently on the mixing angle α (the HH channel is the only one to show a more pronounced mixing dependence in the mass region for which its NLO correction is maximal), whereas for larger masses ($m_S \gtrsim 700$ GeV) these corrections take negative values. Besides, we discuss the impact of the QCD corrections on the $S \rightarrow \bar{t}t$ channel which can be directly deduced by the SM QCD one-loop contributions to the Higgs decay into a top quark pair. For the total decay width $\Gamma(S \rightarrow all)$, we obtain a maximum correction of $\mathcal{O}(6\%)$ for $m_S \sim 200$ GeV. Finally, we have analyzed the impact of the gauge dependence on the decay rates with respect to μ_R for two fixed values of $m_S = 400, 1000$ GeV and found that it causes a variation on the NLO decay widths which is less than $\lesssim |3|\%$ in all decay channels.

The structure of the thesis is as follows: in Chap.1 we recall the relevant features of the SSM and its theoretical and experimental constraints; in Chap.2, we describe and analyze the full set of the leading-order (LO) expressions of the scalar singlet decay widths; in Chap.3 we illustrate the details of our renormalization procedure that we apply in Chap.4 to discuss the structure of the $\Gamma(S \rightarrow ZZ, W^+W^-, \bar{t}t, HH, all)$ renormalized decay widths. The radiative corrections to these decay rates are numerically computed in Chap.5; the last chapter is devoted to our conclusions.

Chapter 1

Model Setup

In this chapter we describe the singlet extension of the Standard Model (we will use the short notation, SM and SSM, to indicate the Standard Model and its singlet extension, respectively). In comparison with the SM, the SSM is characterized by adding one real spinless scalar field which transforms as a singlet under $SU(3)_C \times SU(2)_L \times U(1)_Y$ and affects the same Lagrangians where the SM Higgs field appears. The full SSM Lagrangian is defined as,

$$\mathcal{L}_{\text{SSM}} = \mathcal{L}_{\text{gauge}} + \mathcal{L}_{\text{fermions}} + \mathcal{L}_{\text{QCD}} + \mathcal{L}_{\text{scalars}} + \mathcal{L}_{\text{Yukawa}} + \mathcal{L}_{\text{GF}} + \mathcal{L}_{\text{ghosts}}. \quad (1.1)$$

The first three terms, which include the gauge and fermionic kinetic parts, the couplings between fermions and gauge bosons and the full quantum chromodynamics (QCD), are given by the respective SM expressions [28]. On the other hand, the remaining terms (the Lagrangians of the scalars, the Yukawa interactions, the gauge-fixing and ghosts terms) contain the new scalar singlet field and need a more detailed discussion which will be the subject of the next sections.

1.1 The Scalar Lagrangian

The scalar sector is defined by

$$\mathcal{L}_{\text{scalars}} = (\mathcal{D}^\mu \phi)^\dagger (\mathcal{D}_\mu \phi) + (\partial^\mu s^0)(\partial_\mu s^0) - \mathcal{V}_{\text{SSM}}(\phi, s^0), \quad (1.2)$$

where \mathcal{D}^μ is the SM covariant derivative and $\mathcal{V}_{\text{SSM}}(\phi, s^0)$ is the scalar potential which is made up of the usual SM Higgs potential, with ϕ representing the SM scalar field, augmented with the new contributions due to quadratic and quartic terms of the new scalar field, represented by s^0 , and a portal interaction among s^0 and ϕ as specified below:

$$\mathcal{V}_{\text{SSM}}(\phi, s^0) = \mu^2(\phi^\dagger \phi) + \lambda(\phi^\dagger \phi)^2 + \mu_s^2 (s^0)^2 + \rho (s^0)^4 + \kappa (\phi^\dagger \phi)(s^0)^2,$$

where s^0 is a true isospin singlet (with hypercharge $Y = 0$), $\phi = [\eta^+, \phi^0 + i\eta_3/\sqrt{2}]^T$, $\phi^0 = (v + h)/\sqrt{2}$ (the value of v is obtained as a function of the Fermi constant G_F , $v \equiv (\sqrt{2}G_F)^{-1/2} =$

246.22 GeV) and $\eta^\pm = (\eta_1 \pm i\eta_2)/\sqrt{2}$ and η_3 are the Goldstone bosons. Notice that the potential $\mathcal{V}_{\text{SSM}}(\phi, s^0)$ exhibits a \mathbb{Z}_2 -symmetry under which $s^0 \rightarrow -s^0$, so that linear and trilinear terms in s^0 are not allowed.

Beside the vev of the ϕ field, we also consider the possibility that s^0 acquires a non-zero vacuum expectation value (vev) w , and thus the expansion of the field around its classical minimum is set as $s^0 = (w+s)/\sqrt{2}$. The full expansion around the vevs of $\mathcal{V}_{\text{SSM}}(\phi, s^0)$ involves the linear terms for the scalar fields, h and s , from which we can define the tadpole relations:

$$T_\phi = \mu v^2 + v^3 \lambda + \frac{v w^2 \kappa}{2}, \quad T_{s^0} = \mu_s w^2 + w^3 \rho + \frac{v^2 w \kappa}{2}. \quad (1.3)$$

The minimization conditions of the scalar potential are given by: $T_\phi, T_{s^0} = 0$ ¹. The most immediate consequence of the potential $\mathcal{V}_{\text{SSM}}(\phi, s^0)$ is that a non-diagonal mass matrix is generated for the two neutral states h and s that, in the gauge basis, has the following form:

$$\mathcal{M}_{\text{gauge}}^2 = \begin{pmatrix} 2\lambda v^2 & \kappa v w \\ \kappa v w & 2\rho w^2 \end{pmatrix}. \quad (1.4)$$

Considering all couplings as real parameters, the positivity of the mass matrix is ensured requiring that [17]

$$\lambda > \frac{\kappa^2}{4\rho}, \quad \lambda, \rho > 0. \quad (1.5)$$

To have physical propagating particles in the SSM, it is necessary to consider eigenstates with specific masses. The physical scalar masses can be achieved through the following orthogonal rotation:

$$U(\alpha) \cdot \mathcal{M}_{\text{gauge}}^2 \cdot U(\alpha)^{-1} = \text{diag}(m_H^2, m_S^2), \quad (1.6)$$

where $m_{H,S}$ are the physical masses and $U(\alpha)$ is the rotation matrix whose action on the scalar fields as follows:

$$\begin{pmatrix} H \\ S \end{pmatrix} = U(\alpha) \begin{pmatrix} h \\ s \end{pmatrix} = \begin{pmatrix} \cos \alpha & -\sin \alpha \\ \sin \alpha & \cos \alpha \end{pmatrix} \begin{pmatrix} h \\ s \end{pmatrix}, \quad (1.7)$$

with $\alpha \in [-\pi/2, \pi/2]$. After the orthogonal transformation, the tree-level masses of the particles in the mass basis are given by [17, 29]:

$$m_{H,S}^2 = \lambda v^2 + \rho w^2 \mp \frac{\rho w^2 - \lambda v^2}{\cos 2\alpha}, \quad (1.8)$$

¹Notice that the potential is stationary at:

$$v^2 = \frac{4\rho\mu^2 - 2\kappa\mu_s^2}{\kappa^2 - 4\lambda\rho}, \quad w^2 = \frac{4\lambda\mu_s^2 - 2\kappa\mu^2}{\kappa^2 - 4\lambda\rho}$$

and, in turn, a mapping between the Lagrangian states and the physical fields H and S is realized:

$$\phi^0 = \frac{1}{\sqrt{2}}(v + H \cos \alpha + S \sin \alpha) \quad , \quad s^0 = \frac{1}{\sqrt{2}}(w - H \sin \alpha + S \cos \alpha). \quad (1.9)$$

In the rest of this thesis we will consider the H field as the lightest mass eigenstate and we identify it with the Higgs boson whose mass of 125 GeV has been already measured at LHC [31], so we always consider $\text{sign}(\rho w^2 - \lambda v^2) \times \text{sign}(\cos 2\alpha) > 0$. While the mass of the light scalar field is kept fixed, we will limit ourselves to the mass range $200 \leq m_S \leq 1000$ GeV (which corresponds to the bound $0.018 \leq |\sin \alpha| \leq 0.36$ [29]). The mixing angle α can be expressed in terms of the model parameters and vevs so that,

$$\tan 2\alpha = \frac{\kappa v w}{\rho w^2 - \lambda v^2}. \quad (1.10)$$

Notice that in the limit $(v/w) \ll 1$, the expressions for the masses and mixing are well approximated by:

$$m_H^2 \simeq 2v^2 \left(\lambda - \frac{\kappa^2}{4\rho} \right) = 2v^2 \lambda_{\text{sm}} \quad , \quad m_S^2 \simeq 2\rho w^2 + \frac{\kappa^2 v^2}{2\rho} \quad , \quad \sin \alpha \simeq \frac{\kappa v}{2\rho w}, \quad (1.11)$$

which clearly show that the SM quartic coupling λ_{sm} receives a correction proportional to the ratio among the portal coupling κ and the quartic of the s^0 field [16].

Now, the couplings of the H and S fields with gauge bosons arising from the covariant derivative in eq.(1.2) are similar to the SM Higgs ones rescaled by an appropriate mixing factor:

$$\mathcal{D}_\mu \phi \rightarrow \left[\partial_\mu + ig \frac{\sigma_i}{2} W_\mu^i(x) + ig' \frac{Y}{2} B_\mu(x) \right] \left(\frac{1}{\sqrt{2}}(v + H \cos \alpha + S \sin \alpha + i\eta_3) \right), \quad (1.12)$$

where g and g' are the electroweak constants, W_μ^i ($i = 1, 2, 3$) and B_μ are the gauge boson fields in the gauge basis of $SU(2)_L$ and $U(1)_Y$ respectively, while the Pauli matrices σ_i and the hypercharge Y are the generators of the respective groups. In addition, the scalar singlet field insertion gives no contributions to the gauge boson squared masses which get the same SM form:

$$\begin{aligned} (\mathcal{D}^\mu \phi)^\dagger (\mathcal{D}_\mu \phi) &\rightarrow \frac{1}{2} \begin{pmatrix} 0 & v \end{pmatrix} \left(g \frac{\sigma_i}{2} W^{\mu i} + g' \frac{Y}{2} B^\mu \right)^\dagger \left(g \frac{\sigma_j}{2} W_\mu^j + g' \frac{Y}{2} B_\mu \right) \begin{pmatrix} 0 \\ v \end{pmatrix} = \\ &= \frac{1}{2} \frac{v^2}{4} \left[g^2 (W_\mu^1)^2 + g^2 (W_\mu^2)^2 + (-g W_\mu^3 + g' B_\mu)^2 \right]. \end{aligned} \quad (1.13)$$

As usual the fields $W_\mu^{1,2,3}$, B_μ can be shifted in the mass basis through the orthogonal transformation defined in terms of the Weinberg mixing angle θ_W :

$$\gamma_\mu = (\sin \theta_W W_\mu^3 + \cos \theta_W B_\mu) \quad \text{with } m_\gamma^2 = 0, \quad (1.14)$$

$$Z_\mu = (\cos \theta_W W_\mu^3 - \sin \theta_W B_\mu) \quad \text{with } m_Z^2 = \frac{(g^2 + g'^2)v^2}{4}, \quad (1.15)$$

$$W_\mu^\pm = \frac{(W_\mu^1 \mp iW_\mu^2)}{\sqrt{2}} \quad \text{with } m_W^2 = \frac{g^2 v^2}{4}. \quad (1.16)$$

The pure scalar interactions are obtained by expanding $\mathcal{V}_{\text{SSM}}(\phi, s^0)$ in terms of the physical scalar fields so that the trilinear and quartic couplings can be schematically written as ²:

$$\mathcal{V}_{\text{SSM}}(\phi, s^0) \supset C_{\mathcal{S}_1 \mathcal{S}_2 \mathcal{S}_3} \mathcal{S}_1 \mathcal{S}_2 \mathcal{S}_3 + C_{\mathcal{S}_1 \mathcal{S}_2 \mathcal{S}_3 \mathcal{S}_4} \mathcal{S}_1 \mathcal{S}_2 \mathcal{S}_3 \mathcal{S}_4, \quad (1.17)$$

where \mathcal{S} can be one among H, S, η_3 and η^\pm . Below we report a list of the coefficients $C_{\mathcal{S}_1 \mathcal{S}_2 \mathcal{S}_3}$ and $C_{\mathcal{S}_1 \mathcal{S}_2 \mathcal{S}_3 \mathcal{S}_4}$:

$$C_{SSS} = -3ic_\alpha s_\alpha (c_\alpha v + s_\alpha w) \kappa - 6i(s_\alpha^3 v \lambda + c_\alpha^3 w \rho), \quad (1.18)$$

$$C_{HHH} = -3ic_\alpha s_\alpha (s_\alpha v - c_\alpha w) \kappa - 6i(c_\alpha^3 v \lambda - s_\alpha^3 w \rho), \quad (1.19)$$

$$C_{HSS} = -i[c_\alpha v (c_\alpha^2 - 2s_\alpha^2) + s_\alpha w (2c_\alpha^2 - s_\alpha^2)] \kappa - 6i(c_\alpha s_\alpha^2 v \lambda - c_\alpha^2 s_\alpha w \rho), \quad (1.20)$$

$$C_{HHS} = -i[s_\alpha v (s_\alpha^2 - 2c_\alpha^2) + c_\alpha w (c_\alpha^2 - 2s_\alpha^2)] \kappa - 6i(c_\alpha^2 s_\alpha v \lambda - c_\alpha s_\alpha^2 w \rho), \quad (1.21)$$

$$C_{H\eta_3\eta_3} = -i(2c_\alpha v \lambda - s_\alpha w \kappa), \quad (1.22)$$

$$C_{H\eta^+\eta^-} = -i(2c_\alpha v \lambda - s_\alpha w \kappa), \quad (1.23)$$

$$C_{S\eta_3\eta_3} = -i(c_\alpha w \kappa + 2s_\alpha v \lambda), \quad (1.24)$$

$$C_{S\eta^+\eta^-} = -i(c_\alpha w \kappa + 2s_\alpha v \lambda), \quad (1.25)$$

$$C_{HHHH} = -6i(c_\alpha^4 \lambda + c_\alpha^2 s_\alpha^2 \kappa + s_\alpha^4 \rho), \quad (1.26)$$

$$C_{SSSS} = -6i(c_\alpha^4 \rho + c_\alpha^2 s_\alpha^2 \kappa + s_\alpha^4 \lambda), \quad (1.27)$$

$$C_{HHSS} = -i(c_\alpha^4 - 4c_\alpha^2 s_\alpha^2 + s_\alpha^4) \kappa - 6ic_\alpha^2 s_\alpha^2 (\lambda + \rho), \quad (1.28)$$

$$C_{HHHS} = -6i(c_\alpha^3 s_\alpha \lambda - c_\alpha s_\alpha^3 \rho) + 3ic_\alpha s_\alpha c_{2\alpha} \kappa, \quad (1.29)$$

$$C_{HSSS} = -3ic_\alpha s_\alpha c_{2\alpha} \kappa - 6i(c_\alpha s_\alpha^3 \lambda - c_\alpha^3 s_\alpha \rho), \quad (1.30)$$

$$C_{HH\eta_3\eta_3} = -i(s_\alpha^2 \kappa + 2c_\alpha^2 \lambda), \quad (1.31)$$

$$C_{SS\eta_3\eta_3} = -i(c_\alpha^2 \kappa + 2s_\alpha^2 \lambda), \quad (1.32)$$

$$C_{HS\eta_3\eta_3} = -is_\alpha c_\alpha (2\lambda - \kappa), \quad (1.33)$$

$$C_{HH\eta^+\eta^-} = -i(s_\alpha^2 \kappa + 2c_\alpha^2 \lambda), \quad (1.34)$$

$$C_{SS\eta^+\eta^-} = -i(c_\alpha^2 \kappa + 2s_\alpha^2 \lambda), \quad (1.35)$$

$$C_{HS\eta^+\eta^-} = -is_\alpha c_\alpha (2\lambda - \kappa), \quad (1.36)$$

²We generated all Feynman rules for the SSM model using FEYNRULES [30].

with $s_\alpha = \sin \alpha$ and $c_\alpha = \cos \alpha$. It is important to observe that, starting from the mass matrix in the gauge basis (see eq.(1.4)), we can define the quartic couplings at tree-level (LO) in terms of the physical scalar masses and the mixing angle and, in the case of higher order calculations, these also become functions of the tadpoles in the mass basis ³ $T_{H,S}$ and the (symmetric) off-diagonal element of the physical mass matrix, called δm_{HS}^2 :

$$\begin{aligned} \mathcal{M}_{\text{gauge}}^2 + \begin{pmatrix} T_\phi/v & 0 \\ 0 & T_{s^0}/w \end{pmatrix} &= U(\alpha)^{-1} \cdot \begin{pmatrix} m_H^2 & \delta m_{HS}^2 \\ \delta m_{HS}^2 & m_S^2 \end{pmatrix} \cdot U(\alpha) = \\ &= \begin{pmatrix} m_H^2 c_\alpha^2 + m_S^2 s_\alpha^2 + \delta m_{HS}^2 s_{2\alpha} & \delta m_{HS}^2 c_{2\alpha} + s_\alpha c_\alpha (m_S^2 - m_H^2) \\ \delta m_{HS}^2 c_{2\alpha} + s_\alpha c_\alpha (m_S^2 - m_H^2) & m_H^2 s_\alpha^2 + m_S^2 c_\alpha^2 - \delta m_{HS}^2 s_{2\alpha} \end{pmatrix}. \end{aligned} \quad (1.38)$$

Using the definition of $\mathcal{M}_{\text{gauge}}^2$ shown in eq.(1.4), the quartic couplings are given by:

$$\lambda = \frac{m_H^2}{2v^2} c_\alpha^2 + \frac{m_S^2}{2v^2} s_\alpha^2 - \frac{c_\alpha T_H + s_\alpha T_S}{2v^3} + \frac{\delta m_{HS}^2}{2v^2} s_{2\alpha}, \quad (1.39)$$

$$\rho = \frac{m_H^2}{2w^2} s_\alpha^2 + \frac{m_H^2}{2w^2} c_\alpha^2 - \frac{c_\alpha T_S - s_\alpha T_H}{2w^3} - \frac{\delta m_{HS}^2}{2w^2} s_{2\alpha}, \quad (1.40)$$

$$\kappa = \frac{m_S^2 - m_H^2}{2vw} s_{2\alpha} + \frac{\delta m_{HS}^2}{vw} c_{2\alpha}, \quad (1.41)$$

with $T_H, T_S, \delta m_{HS}^2 = 0$ at tree-level. A fundamental feature of the SSM potential is that, at large m_S values, the portal interaction between the scalar singlet and the $SU(2)_L$ doublet leads to a positive tree-level threshold correction for the Higgs quartic coupling, which allows to avoid the potential instability of the Standard Model electroweak vacuum. The renormalization group equations (RGEs) for the portal (κ) and quartic (λ and ρ) couplings above the scale m_S are given by [16, 17],

$$\begin{aligned} (4\pi)^2 \frac{\partial \lambda}{d \ln \mu} &= \frac{3}{4} \left[g^4 + \frac{(g^2 + g'^2)^2}{2} \right] - 6y_t^4 + 12 \left[y_t^2 - \frac{g'^2 + 3g}{4} \right] \lambda + 24\lambda^2 + \kappa^2, \\ (4\pi)^2 \frac{\partial \kappa}{d \ln \mu} &= 3 \left[y_t^2 - \frac{g'^2 + 3g}{4} \right] \kappa + 2\kappa(3\lambda + 2\rho) + 2\kappa^2, \\ (4\pi)^2 \frac{\partial \rho}{d \ln \mu} &= 2\kappa^2 + 20\rho^2, \end{aligned} \quad (1.42)$$

where μ is the RGE running scale and y_t is the yukawa coupling associated with the top quark (the contributions due to the other fermions is negligible [32]). We observe that λ receives

³The tadpoles T_{ϕ, s^0} are rotated in the mass basis as

$$\begin{pmatrix} T_H \\ T_S \end{pmatrix} = \begin{pmatrix} \cos \alpha & -\sin \alpha \\ \sin \alpha & \cos \alpha \end{pmatrix} \begin{pmatrix} T_\phi \\ T_{s^0} \end{pmatrix}. \quad (1.37)$$

a linear and positive contributions in terms of κ^2 , which prevent it from becoming negative under the following conditions:

- $m_S < \Lambda_{\text{inst}} \sim 10^{10}$ GeV where Λ_{inst} is the SM instability scale [32].
- $(\kappa/8\pi)^2 \ln(\Lambda_{\text{inst}}/m_S)$ has to be quite large.

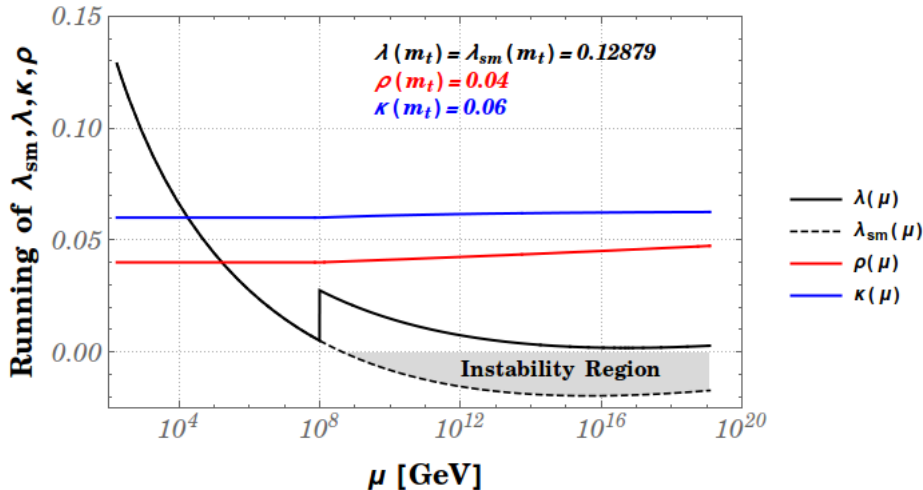


Figure 1.1: *Running of the quartic couplings for representative parameter choice: $m_S = 10^8$ GeV, $\lambda(m_t) = \lambda_{\text{sm}}(m_t) = 0.12879$, $\rho(m_t) = 0.04$ and $\kappa(m_t) = 0.06$.*

We show in Fig.(1.1) an example of running quartic couplings which is obtained for fixed values of λ , λ_{sm} , κ , ρ at a scale $m_t = 173.21$ GeV, namely $\lambda(m_t) = \lambda_{\text{sm}}(m_t) = 0.12879$, $\rho(m_t) = 0.04$ and $\kappa(m_t) = 0.06$, and $m_S = 10^8$ GeV. We can see that, thanks to the positive threshold at the singlet mass (for large values of m_S we have $\lambda \sim \lambda_{\text{sm}} + \kappa^2/4\rho$), the quartic coupling λ never enters into the instability region ⁴.

1.2 The Yukawa Lagrangian

The Yukawa Lagrangian includes the complete set of fermionic mass terms and interactions of the fermions and scalar bosons in the SSM. As discussed above, the kinetic terms of the fermions ($\mathcal{L}_{\text{fermions}}$) are the same of the SM:

$$\mathcal{L}_{\text{fermions}} = \sum_{\text{fermions}} i\bar{\psi}(D^\mu\gamma_\mu)\psi, \quad (1.43)$$

⁴Notice that we chose as initial condition $\kappa > 0$. However, the stabilization mechanism becomes more complicated when the running quartic couplings are analyzed with respect to negative κ values. In this case the stability condition is given by $-\kappa(\mu) < [\lambda(\mu)\rho(\mu)]^{1/2}$ and with the positive shift of λ it is essentially canceled out. This implies that the stability condition is much more constraining than in the case $\kappa > 0$ (see [16] for more details).

where $\bar{\psi} = \psi^\dagger \gamma^0$, ψ is the fermionic spinor field and the sum runs over all fermions, which are divided in three generations. In Tab.(1.1), the spinor fields are classified in terms of five representations of $SU(3)_C \times SU(2)_L \times U(1)_Y$.

Spinor Field	ψ^I [color, weak iso-spin, hypercharge]
LH leptons	$L_L^i [1, 2, -1]$
RH leptons	$l_R^i [1, 1, 2]$
LH quarks	$Q_L^i [3, 2, +1/3]$
RH up-type quarks	$u_R^i [3, 1, +4/3]$
RH down-type quarks	$d_R^i [3, 1, -2/3]$

Table 1.1: *Spinor field as representations of $SU(3)_C \times SU(2)_L \times U(1)_Y$. Here, $i = 1, 2, 3$ is the flavor index and LH, RH stand for the left- and right-handed fermions, respectively.*

We consider for simplicity the neutrinos to be massless and this implies that these exist in a LH state only. It is well known in the SM that a term like $-m_f \bar{\psi} \psi = -m_f (\bar{\psi}_L \psi_R + \bar{\psi}_R \psi_L)$ is not invariant under an $SU(2)_L \times U(1)_Y$ transformation and the absence of such a term implies massless fermions. Considering the complex Higgs doublet ϕ , which in the notation of Tab.(1.1) is a $[1, 2, 1]$ state, one can construct an invariant $SU(2)_L \times U(1)_Y$ interaction term as: $-y_f \bar{\psi}_L \phi \psi_R$, where y_f is the Yukawa coupling. When the Higgs field acquires the vev after the spontaneous symmetry breaking, we obtain the fermion masses proportional to the respective Yukawa coupling. However, this mechanism only gives mass to the "down" fermions. It is possible to write a new term in the Lagrangian which is gauge invariant and gives mass to the "up" fermions as follows: $-y_f \bar{\psi}_L \tilde{\phi}^c \psi_R$, where $\tilde{\phi}^c = i\sigma_2 \phi^\dagger$. So, in the most general case, the expression for the Yukawa Lagrangian is written as,

$$-\mathcal{L}_{\text{Yukawa}} = Y_{ij}^d \bar{Q}_L^i \phi d_R^j + Y_{ij}^u \bar{Q}_L^i \tilde{\phi}^c u_R^j + Y_{ij}^l \bar{L}_L^i \phi l_R^j + h.c., \quad (1.44)$$

where now Y_{ij}^d , Y_{ij}^u and Y_{ij}^l are arbitrary 3×3 complex matrices which include all Yukawa couplings arising from the three fermionic generations of leptons and quarks.

In addition, we can observe that it is not possible to construct a mass terms for the fermions by substituting the Higgs doublet ϕ with the new scalar singlet s^0 since the Yukawa interactions, written in terms of the singlet field, are not gauge invariant under $SU(2)_L \times U(1)_Y$ transformations. This implies that the new insertion of the scalar singlet gives no contributions to the fermion masses but appears only in the interaction terms between the Higgs doublet and the fermionic fields, with proportionality to s_α :

$$Y_{ij} \bar{\psi}_L^i \left(\frac{1}{\sqrt{2}} (v + H c_\alpha + S s_\alpha + i\eta_3) \right) \psi_R^j. \quad (1.45)$$

1.3 Gauge-Fixing and Ghost Lagrangian

In this section we describe the structure of the remaining Lagrangians, \mathcal{L}_{GF} and $\mathcal{L}_{\text{ghosts}}$, and their dependence on the scalar singlet field. Generally, \mathcal{L}_{GF} and $\mathcal{L}_{\text{ghosts}}$ are needed to quantize the Yang-Mills theories which contains the gauge bosons expressed as vector fields [28]. Since the degrees of freedom corresponding to the vector fields exceed those of the physical gauge fields, the quantization of the full SSM Lagrangian requires the choice of a specific gauge in order to remove the additional unphysical degrees of freedom. It is well-known that in this type of model the gauge-invariance plays a fundamental role in the renormalization procedure. This implies that the gauge-fixing becomes useful to check the gauge independence of higher order calculations, as it was discussed for the SSM in [29]. In order to define \mathcal{L}_{GF} , we introduce the F functions defined as:

$$F_{\pm} = \left(\partial_{\mu} \mp ie\tilde{\delta}_1 A_{\mu} \mp ig \cos \theta_W \tilde{\delta}_2 Z_{\mu} \right) W^{\pm} \pm i\xi'_{\text{W}} \frac{g}{2} \left(v + \tilde{\delta}_3 H + \tilde{\delta}_4 S \pm i\tilde{\delta}_5 \eta_3 \right) \eta^{\pm}, \quad (1.46)$$

$$F_Z = \partial_{\mu} Z^{\mu} + \xi'_Z \frac{g}{2 \cos \theta_W} \left(v + \tilde{\delta}_6 H + \tilde{\delta}_7 S \right) \eta_3, \quad (1.47)$$

$$F_{\gamma} = \partial_{\mu} A^{\mu}, \quad (1.48)$$

where e is the electromagnetic coupling constant, $\tilde{\delta}_i$ is the non-linear gauge parameters while ξ_i and ξ'_i ($i = \gamma, Z, W$) are the linear gauge parameter related to the gauge and Goldstone bosons, respectively. Notice that the non-linear case is described by the F functions non-linearly dependent on the scalar and gauge fields⁵. The gauge-fixing Lagrangian is defined in the following form:

$$\mathcal{L}_{\text{GF}} = -\frac{1}{2\xi_{\gamma}} |F_{\gamma}|^2 - \frac{1}{2\xi_Z} |F_Z|^2 - \frac{1}{\xi_{\text{W}}} F_+ F_-. \quad (1.49)$$

We recover the linear gauge fixing (usually indicated with R_{ξ}) by setting up $\tilde{\delta}_i = 0$ (with $\xi_i = 1$ we define the 't Hooft- Feynman gauge). In addition, we can fix $\xi'_{\text{W},Z} = \xi_{\text{W},Z}$ in order to cancel the mixing terms $\eta^{\pm} W^{\pm}$ and $\eta_3 Z$ arising from \mathcal{L}_{GF} , thus avoiding the presence of new unnecessary and intricate interaction terms at tree-level. On the other hand, the insertion in \mathcal{L}_{GF} of the additional non-linear gauge parameters $\tilde{\delta}_i$ ($i = 1, \dots, 7$) modifies the Feynman rules which become more complicated. We could also tune the $\tilde{\delta}_i$ values to reduce the number of diagrams and simplify some of the vertices (for instance, with $\tilde{\delta}_1 = 1$, the vertex $W^{\pm} \eta^{\mp} \gamma$ is canceled out and $W^{\pm} W^{\mp} \gamma$ assumes a more simple form). In order to fix the gauge in the non-Abelian Yang-Mills theories we have to introduce a new set of anticommuting fields, called *ghost* (proposed by L. Faddeev and V. Popov [36]). The main feature of the these fields

⁵The definitions of the F functions and the treatment of the non-linear gauge fixing in the SM can be found in [34, 35].

is that their quantum excitations have the wrong relation between spin and statistic to be a physical particles. Besides, the ghosts can appear as virtual states described by the following Lagrangian [28]:

$$\mathcal{L}_{\text{ghosts}} = \bar{u}_i^a (-\partial^\mu \mathcal{D}_\mu^{ab}) u_i^c = \bar{u}_i^a (-\partial^2 \delta^{ac} - g \partial^\mu f^{abc} A_\mu^b) u_i^c, \quad (1.50)$$

where \mathcal{D}_μ^{ab} is the covariant derivate, g is the gauge constant, f^{abc} are the structure constants of the gauge group (which can be $SU(2)$ or $SU(3)$ for the vector boson and gluon fields, respectively), A_μ are the gauge fields of the respective gauge groups and u_i (\bar{u}_i) (with $i = \pm, Z, \gamma$) are the Faddeev-Popov ghosts (anti-ghosts). Thus, we can write for a general non-Abelian gauge theory a complete Lagrangian (\mathcal{L}_{FP}) which includes all of the gauge-fixing effect as [28]:

$$\mathcal{L}_{\text{FP}} = -\frac{1}{4} F^{\mu\nu a} F_{\mu\nu}^a + \frac{1}{2\xi} |\partial^\mu A_\mu^a|^2 + \bar{\psi} (i \mathcal{D}^\mu \gamma_\mu - m) \psi + \bar{u}_i^a (-\partial^\mu \mathcal{D}_\mu^{ab}) u_i^c, \quad (1.51)$$

where $|\partial^\mu A_\mu^a|^2/2\xi$ can get additional terms which are non-linearly dependent on the scalar and gauge fields, as mentioned above. With the insertion of the ghost Lagrangian, \mathcal{L}_{FP} shows a new symmetry, called BRST symmetry [37], which is defined in terms of an infinitesimal anticommuting parameter ε :

$$\begin{aligned} \delta_{\text{BRST}} A_\mu^a &= \varepsilon \mathcal{D}_\mu^{ab} u_b, & \delta_{\text{BRST}} \psi &= ig \varepsilon u_a t^a \psi, & \delta_{\text{BRST}} u^a &= -\frac{1}{2} g \varepsilon f^{abc} u_b u_c, \\ \delta_{\text{BRST}} \bar{u}^a &= \varepsilon B^a, & \delta_{\text{BRST}} B^a &= 0, \end{aligned}$$

where t^a are the generators of the gauge group considered and B is an auxiliary field which has to be introduced to get the BRST-invariance of \mathcal{L}_{FP} ⁶. Considering the non-linear gauge fixing, the BRST transformations can be also defined for the scalar fields [29]:

$$\delta_{\text{BRST}} \eta_3 = \frac{g}{2} \left[(\eta^- u^+ + \eta^+ u^-) - \frac{u_Z}{\cos \theta_W} (v + c_\alpha H + s_\alpha S) \right], \quad (1.52)$$

$$\delta_{\text{BRST}} \eta^\pm = \mp \frac{ig}{2} \left[u^\pm (v + c_\alpha H + s_\alpha S \mp i \eta_3) + \frac{\sin 2\theta_W u_\gamma + \cos 2\theta_W}{\cos 2\theta_W} \eta^\pm \right], \quad (1.53)$$

$$\delta_{\text{BRST}} H = \frac{g c_\alpha}{2} \left[i(\eta^- u^+ - \eta^+ u^-) + \frac{u_Z}{\cos \theta_W} \eta_3 \right], \quad (1.54)$$

$$\delta_{\text{BRST}} S = \frac{g s_\alpha}{2} \left[i(\eta^- u^+ - \eta^+ u^-) + \frac{u_Z}{\cos \theta_W} \eta_3 \right]. \quad (1.55)$$

Notice that these BRST transformations depend on the S field only with proportionality to s_α . The results of this thesis have been obtained in the linear R_ξ gauge imposing $\tilde{\delta}_i = 0$, $\xi_i = 1$

⁶As discussed in [28], the introduction of the new auxiliary field B^a is given by the following substitution: $|\partial^\mu A_\mu^a|^2/2\xi \rightarrow \xi |B^a|^2/2 + B^a \partial^\mu A_\mu^a$.

and considering the gauge-dependence analysis in the SSM renormalization procedure (which we will treat in detail in the next sections) performed in [29]. There, the authors work with $\tilde{\delta}_i \neq 0$ in order to define a gauge independent renormalization scheme for the mixing scalar sector which must provide equivalent results with both $\tilde{\delta}_i = 0$ and $\tilde{\delta}_i \neq 0$.

1.4 Theoretical and Experimental Constraints

The SSM is subject to many constraints which are of a theoretical or experimental nature. These constraints have been explicitly discussed in the literature and we briefly have summarized them here.

1.4.1 Theoretical Constraints

- **Perturbative Unitarity:**

The tree-level perturbative unitarity, which emerges purely from theoretical aspects of electroweak symmetry breaking, has to be preserved. To this aim, it is sufficient that the scalar sector fulfills the following sum rules for the couplings between fermion, vector and scalar particles, which we call g_{nff} and g_{nVV} for scalar-fermion and scalar-vector interactions, respectively [38]:

$$\sum_n g_{nVV}^2 = g_{H_{\text{sm}}VV}^2 \quad , \quad \sum_n g_{nVV} g_{nff} = g_{H_{\text{sm}}VV} g_{H_{\text{sm}}ff} \quad , \quad (1.56)$$

where $n = H, S$ and H_{sm} is the SM Higgs field. Notice that the SSM exhibits the sum rules given above since $g_{HVV, Hff} = c_\alpha g_{H_{\text{sm}}ff, H_{\text{sm}}ff}$ and $g_{SVV, Hff} = s_\alpha g_{S_{\text{sm}}ff, H_{\text{sm}}ff}$, thus preserving the unitarity constraints. Besides, we can set a constraint on the SSM scalar masses via a relation on the partial wave amplitudes $a_J(s)$, associated with $2 \rightarrow 2$ processes given by [8]:

$$|\text{Re } a_J(s)| \leq \frac{1}{2}. \quad (1.57)$$

This allows us to find a $(m_S - m_H - \alpha)$ subspace where the perturbative unitarity is valid up to any energy scale. We therefore need to calculate the tree-level amplitudes for the $x_a x_b \rightarrow y_a y_b$ process, where $x_a x_b$ and $y_a y_b$ can be $\{ZZ, W^+W^-, HH, SS, HS\}$. Calculating the normalized five dimensional scattering matrix and imposing eq.(1.57) to each eigenvalues, one obtains, for small mixing angle ($s_\alpha \sim 0$), the element of the scattering matrix associated with $SS \rightarrow SS$ is decoupled from the other SM matrix elements and an lower limit on w is posed:

$$w^2 \gtrsim \frac{3m_S^2}{16\pi} \quad , \quad \text{for } a_0(SS \rightarrow SS) \leq \frac{1}{2}. \quad (1.58)$$

However, in the case of large s_α values, all partial wave contributions needs to be considered to determine a valid prediction of the lower limit on the allowed heavy scalar mass.

- **Potential Stability and Perturbativity of the scalar couplings:**

Typically, the stability of the scalar potential is described by the conditions in eq.(1.5) while the perturbativity of a general coupling x requires that:

$$|x(\mu)| \leq 4\pi, \quad (1.59)$$

which, for the SSM, are $x = (\lambda, \kappa, \rho)$. At the electroweak scale, $\mu = v$, we have no additional constraints in the (s_α, w) - parameter space when we test the perturbative unitarity condition. So, it is instructive to understand what are the energy scales for which the perturbativity of the scalar couplings and the potential stability remain valid. To achieve this goal, we have to consider eq.(1.5) and eq.(1.59) valid at an arbitrary scale μ and the renormalization group equations (reported in eq.(1.42)) are needed to evaluate the coupling $\lambda(\mu)$, $\kappa(\mu)$ and $\rho(\mu)$. By fixing a reference value for μ_{SSM} larger than μ_{SM} we can study the conditions arising from the perturbativity of the coupling and the stability of the scalar potential up to this benchmark scale so that we can define the (s_α, w) -parameter space for which these are verified [8, 10]. By the perturbativity of κ , we can determine a restriction in the large w and s_α regions while, if we analyze the perturbativity of λ and ρ , we obtain an upper limit on s_α and w , respectively. For instance, we report the conditions on s_α and w (discussed in [10]) obtained for fixed values of m_S and μ_{SSM} , namely $m_S = 600$ GeV and $\mu_{\text{SSM}} = 2.7 \times 10^{10}$ GeV: $|s_\alpha| \lesssim 0.3$ and $w \gtrsim 2v$.

1.4.2 Experimental Constraints

- **The W boson mass:**

The experimental value of the W boson mass is given by [39, 40, 41]:

$$m_W^{\text{exp}} = 80.385 \pm 0.015 \text{ GeV}. \quad (1.60)$$

The computation of the electroweak precision parameter Δr ⁷ imposes limits on the SSM parameter space when it is confronted with the experimental W boson mass measurement. The introduction of Δr implies that the theoretical expression of the W

⁷Following the standard conventions in the literature, the Δr definition is obtained matching the muon lifetime expression in the four fermions Fermi interaction to the equivalent calculation performed within the SM:

$$m_W^2 \left(1 - \frac{m_W^2}{m_Z^2}\right) \simeq \frac{\pi \alpha_{\text{em}}}{\sqrt{2} G_F} (1 + \Delta r), \quad (1.61)$$

where α_{em} is the fine structure constant at zero momentum ($\alpha_{\text{em}}(0) = e^2/4\pi$).

boson mass is shifted as $m_W \rightarrow m_W(1 + \Delta m_W/m_W)$ with,

$$\frac{\Delta m_W}{m_W} \sim \frac{s_W^2}{s_W^2 - c_W^2} \frac{\Delta r}{2}, \quad (1.62)$$

with $s_W = \sin \theta_W$ and $c_W = \cos \theta_W$. For $\Delta r = 0$ one gets the theoretical tree-level value $m_W^{\text{thLO}} = 80.94$ GeV. In the SM case, the best-fit value of Δr is given by $\Delta r_{\text{SM}} \simeq 0.038$, which shifts the value of the W boson mass to $(m_W^{\text{th}})_{\text{SM}} = 80.36$ GeV, a roughly 20 MeV away from the experimental result in eq.(1.60). The calculation of Δr include new physics effects could be relevant to impose parameter space constraints but also to explain the SM difference $|(m_W^{\text{th}})_{\text{SM}} - m_W^{\text{exp}}| \simeq 20$ MeV. For the SSM, this analysis has been performed in [26] and its conclusions are the following:

- i) Defining $\Delta r_{\text{SSM}} = \Delta r_{\text{SM}} + \delta r_{\text{SSM}}$, the SSM deviation from SM value (δr_{SSM}) is not large and generates a variation amounting to a maximum of $\mathcal{O}(10\%)$. The tension with the experimental result is reduced by the fact that $\Delta r_{\text{SSM}} > \Delta r_{\text{SM}}$ which implies that $(m_W^{\text{th}})_{\text{SSM}} < (m_W^{\text{th}})_{\text{SM}}$ (with $|(m_W^{\text{th}})_{\text{SM}} - (m_W^{\text{th}})_{\text{SSM}}| \sim 1 - 70$ MeV).
- ii) The SSM contributions to Δr and m_W are dependent on the scalar mixing angle and it is possible to derive upper bounds on $|s_\alpha|$ (especially for $m_S \gtrsim 300$ GeV) by comparing the $(m_W^{\text{th}})_{\text{SSM}}$ with m_W^{exp} . For example, the upper bound on $|s_\alpha|$ associated with $m_S = 1000$ GeV is $|s_\alpha|_{\text{max}} = 0.19$ (more upper bounds associated with different values of the singlet scalar mass are listed in Table.II of [26]).

- **Electroweak Parameters S,T and U:**

Similarly to the case discussed above, we can obtain other constraints on m_S and s_α from the electroweak precision observables (EWPO) which are the oblique parameters S , T and U defined as:

$$\begin{aligned} \frac{\alpha_{\text{em}}}{4s_W^2 c_W^2} S &= \frac{\bar{\Sigma}^{ZZ}(m_Z^2) - \bar{\Sigma}^{ZZ}(0)}{m_Z^2}; & \alpha_{\text{em}} T &= \frac{\bar{\Sigma}^{WW}(0)}{m_W^2} - \frac{\bar{\Sigma}^{ZZ}(m_Z^2)}{m_Z^2}; \\ \frac{\alpha_{\text{em}}}{4s_W^2} U &= \frac{\bar{\Sigma}^{WW}(m_W^2) - \bar{\Sigma}^{WW}(0)}{m_W^2} - c_W^2 \frac{\bar{\Sigma}^{ZZ}(m_Z^2) - \bar{\Sigma}^{ZZ}(0)}{m_Z^2}, \end{aligned} \quad (1.63)$$

where the $\bar{\Sigma}^{VV}(k^2)$ denotes the purely singlet model contributions to the gauge boson self-energy. However, the next-to-leading order (NLO) EWPO corrections generate weaker constraints on the mixing angle than the bounds obtained from the Δr analysis and do not contribute to new limits on w values being independent from it [10, 26].

- **Signal Strength of the Higgs Boson:**

The Higgs signal strength $|\mu|$ is defined in the general "beyond-SM" case (bSM) as:

$$\mu \equiv \frac{\sigma_{\text{bSM}}}{\sigma_{\text{SM}}} = \frac{c_\alpha^4 \Gamma_{\text{SM}}(m_H)}{c_\alpha^2 \Gamma_{\text{SM}}(m_H) + s_\alpha^2 \Gamma_{\text{hidden}}(m_H)}, \quad (1.64)$$

where $\Gamma_{\text{SM, hidden}}$ are the decay widths of the Higgs boson in the SM and in a possible hidden sector. In the SSM we have $\mu_{\text{SSM}} = c_\alpha^2$. Concerning the Higgs signal strength, we can use the following values [42, 43]:

$$\mu_{\text{LHC}} = 1.30 \pm 0.18 \quad , \quad \mu_{\text{CMS}} = 0.80 \pm 0.14 \quad \Rightarrow \quad \bar{\mu}_{\text{exp}} = 1.05 \pm 0.11. \quad (1.65)$$

As a consequence of the comparison between μ_{SSM} and $\bar{\mu}_{\text{exp}}$ up to 2σ -level deviations, the upper (lower) limits are obtained: $|s_\alpha| \lesssim 0.42$ ($|s_\alpha| \gtrsim 0.91$).

1.4.3 Global Constraints

It is interesting to analyze the unification of the full sets of constraints discussed above. In Fig.(1.2) and in Tab.(1.2), which are deduced from Figure I and Table I of [29] (in the Figure I, the scalar singlet mass is indicated with m_H instead of m_S), we report the allowed values of s_α and w associated with the mass range of our interest, $200 \leq m_S \leq 1000$ GeV, which will be used in our numerical analysis. From Tab.(1.2), we note that the mixing angle values can be included in the global range $0.018 \leq |\sin \alpha| \leq 0.36$ while the lower bound on the singlet vev is $w_{\min} = 0.85 v$. On the other hand, it is interesting to identify the values of w and $|s_\alpha|$ which are valid for every choice of m_S . The minimum value of w increases as m_S increases. This automatically implies that $w_{\min} = 4.34 v$ is a good choice for the m_S values of our interest. In a similar way, the range of $|s_\alpha|$ is restricted to the following interval: $|s_\alpha| \in [|s_\alpha|_{\min}^{\text{ms}=200 \text{ GeV}}, |s_\alpha|_{\max}^{\text{ms}=1000 \text{ GeV}}] = [0.09, 0.17]$. As a result, the study of the physical observables as a function of m_S requires:

$$|s_\alpha| \in [0.09, 0.17] \quad \text{and} \quad w \geq 4.34 v. \quad (1.66)$$

m_S [GeV]	$ s_\alpha $	w_{\min} [GeV]
200	[0.09,0.36]	0.85 v
300	[0.067,0.31]	1.25 v
400	[0.055,0.27]	1.69 v
500	[0.046,0.24]	2.13 v
600	[0.038,0.23]	2.56 v
700	[0.031,0.21]	3.03 v
800	[0.027,0.21]	3.45 v
900	[0.022,0.19]	3.85 v
1000	[0.018,0.17]	4.34 v

Table 1.2: Values of m_S considered in our numerical analysis, the ranges of $|s_\alpha|$ and the corresponding w_{\min} . Table extracted from Table I of [29].

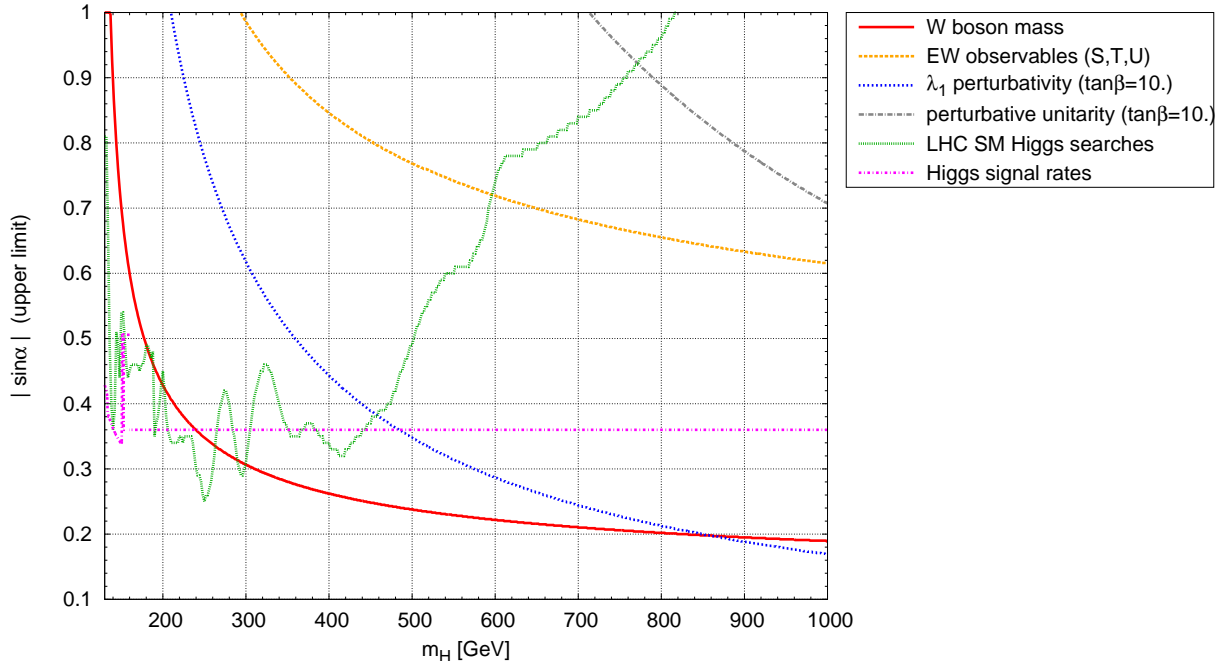


Figure 1.2: *Summary of the constraints as a function of $|\sin \alpha|$ and m_S . This figure is extracted from [29] and we directly report the original caption in terms of our notation and bibliography: "Maximal allowed values for $|\sin \alpha|$ in the high mass region, for a heavy boson mass in the range $m_S \in [130, 1000]$ GeV, from the following constraints: i) W boson mass measurement (red, solid) [26]; ii) electroweak precision observables tested via the oblique parameters S , T and U (orange, dashed); iii) perturbativity, of the RG-evolved coupling λ (blue, dotted), evaluated for an exemplary choice $w = 10v$, iv) perturbative unitarity (grey, dash-dotted), v) direct LHC searches (green, dashed), and vi) Higgs signal strength measurement (magenta, dash-dotted). For masses $m_S \in [300, 800]$ the W boson mass measurement yields the strongest constraint [26]. The present plot corresponds to an update of figure 8 from [10], where the latest constraints from the combined signal strength [44] have been taken into account."*

1.5 Parameter Values

Here, we give a summary of the input parameter values which will be needed in our analysis. The SM central values are taken from [50]:

- **Fine structure constant**

The fine structure constant α_{em} is given at $Q^2 = 0$ (Thompson limit):

$$\alpha_{\text{em}} = \alpha_{\text{em}}(0) = 1/137.035999139.$$

At $Q^2 = m_W^2$, it becomes $\alpha_{\text{em}}(m_Z^2) \approx 1/128$.

- **Fermi constant**

The experimental value of the Fermi constant is:

$$G_F = 1.1663787 \times 10^{-5} \text{ GeV}^{-2} .$$

- **Weinberg mixing**

The experimental value of s_W is:

$$s_W = \sqrt{0.23155} . \quad (1.67)$$

- **Strong coupling constant**

We define the strong coupling constant as α_s and its experimental value at $Q^2 = m_Z^2$ is:

$$\alpha_s(m_Z^2) = 0.1182 .$$

- **Higgs and Gauge boson masses**

The scalar and gauge boson masses are fixed to:

$$m_H = 125.09 \text{ GeV} \quad , \quad m_W = 80.385 \text{ GeV} \quad , \quad m_Z = 91.1876 \text{ GeV} .$$

- **Fermion masses**

We have only considered t , b , c and τ since the other fermions have comparably negligible masses:

$$m_t = 173.21 \text{ GeV} \quad , \quad m_b = 4.18 \text{ GeV} \quad , \quad m_c = 1.27 \text{ GeV} \quad , \quad m_\tau = 1776.86 \text{ MeV} .$$

- **CKM matrix element**

In the computation of the singlet decay rates no Cabibbo-Kobayashi-Maskawa matrix elements (V_{CKM}) are involved at LO. At the NLO we have verified that it is a good approximation to fix the mixing to the quark sector to be vanishingly small. For completeness, report here the best fit values of the quark mixing:

$$V_{\text{CKM}} = \begin{pmatrix} V_{ud} & V_{us} & V_{ub} \\ V_{cd} & V_{cs} & V_{cb} \\ V_{td} & V_{ts} & V_{tb} \end{pmatrix} = \begin{pmatrix} 0.97417 & 0.2248 & 4.09 \times 10^{-3} \\ 0.22 & 0.995 & 40.5 \times 10^{-3} \\ 8.2 \times 10^{-3} & 0.04 & 1.009 \end{pmatrix} \quad (1.68)$$

- **Scalar mixing angle, singlet mass and vev**

The full set of constraints on the SSM parameters gives us the range of the mixing angle, $|s_\alpha| \in [0.09, 0.17]$, and the minimum value of w , $w_{\min} = 4.34 v$, which are allowed for every choice of the singlet mass values included in the following range: $200 \leq m_S \leq 1000 \text{ GeV}$.

We have to fix a set of independent variables in the scalar sector needed for the numerical analysis. We choose w , m_S and α and express at tree-level λ , ρ and κ according to eqs.(1.39 - 1.41):

$$\lambda = \frac{m_H^2 c_\alpha^2 + m_S^2 s_\alpha^2}{2v^2} \quad , \quad \rho = \frac{m_S^2 c_\alpha^2 + m_H^2 s_\alpha^2}{2w^2} \quad , \quad \kappa = \frac{(m_S^2 - m_H^2)s_{2\alpha}}{2vw} . \quad (1.69)$$

In Tab.(1.3) we give an numerical values of λ , ρ and κ computed for representative parameter choices: $s_\alpha = (0.1, 0.35)$, $w = (5v, 10v)$ and $m_S = (300, 500, 700, 1000)$ GeV.

w = 5 v		s_α = 0.1			s_α = 0.35		
<i>m_S</i>	λ	κ	ρ	λ	κ	ρ	
300	0.135	0.024	0.029	0.204	0.08	0.0267	
500	0.148	0.077	0.082	0.366	0.253	0.073	
700	0.168	0.156	0.16	0.608	0.513	0.142	
1000	0.21	0.323	0.327	1.124	1.065	0.29	
w = 10 v		s_α = 0.1			s_α = 0.35		
<i>m_S</i>	λ	κ	ρ	λ	κ	ρ	
300	0.135	0.012	0.007	0.204	0.04	0.007	
500	0.148	0.038	0.02	0.366	0.127	0.018	
700	0.168	0.078	0.04	0.608	0.257	0.036	
1000	0.21	0.162	0.082	1.124	0.532	0.073	

Table 1.3: *Example of λ , κ and ρ values for representative parameter choices.*

Chapter 2

Singlet Decay Widths at Tree-Level

It is interesting to determine whether and how the new scalar boson can be produced at the LHC experiments and what the process topologies will be. To make predictions of physical observables, we should connect the results of calculations, evaluated through a field theory (e.g decay amplitudes) with experimental data at a collider (e.g decay widths). The main scope of this thesis is the computation of the dominant singlet decay rates at the NLO. First of all, we clearly need the LO formulas for all partial decay widths of the new scalar boson which we consider to be heavier than any other SM particle. In the SSM, since the singlet mixes with the Higgs field, we can parametrize the total decay rate in the following form:

$$\Gamma^{\text{LO}}(S \rightarrow \text{All}) = \Gamma^{\text{LO}}(S \rightarrow HH) + s_\alpha^2 \Gamma^{\text{LO}}(H_{\text{sm}} \rightarrow gg, \gamma\gamma, Z\gamma, ZZ, WW, \bar{f}f), \quad (2.1)$$

where $\Gamma^{\text{LO}}(H_{\text{sm}} \rightarrow \dots)$ have to be evaluated in terms of m_S instead of m_H . In the next paragraphs we will list a summary of all partial LO decay widths of the processes $S \rightarrow ij$ which can be evaluated using the general expression for the two body decay rate given by the integration of the squared amplitude over the two-body Lorentz-invariant phase space and defined as [28]:

$$\Gamma(S \rightarrow ij) = \frac{\sqrt{m_S^4 + m_i^4 + m_j^4 - 2m_S^2 m_i^2 - 2m_S^2 m_j^2 - 2m_i^2 m_j^2}}{16\pi m_S^3 n_i! n_j!} \sum_{\text{d.o.f}} |\mathcal{M}|^2, \quad (2.2)$$

where \mathcal{M} is decay amplitude, the summation is performed over all degrees of freedom (d.o.f) corresponding to the physical particles in the process, $n_{i,j}$ is the number of identical particles in the final state and $m_{i,j}$ are the masses of the decay products.

2.1 LO Decay Width to Gauge Bosons

The decay rate of the scalar S into two real gauge bosons gets contributions from longitudinally (L) and transversally ($\pm\pm$) polarized gauge bosons. The LO amplitude is given by,

$$\mathcal{M}^{\text{LO}}[S(k) \rightarrow V(p, a)V(q, b)] = e \frac{m_V^2}{s_W m_W} s_\alpha \times [g^{\mu\nu} \epsilon_\mu^a(p) \epsilon_\nu^b(q)], \quad (2.3)$$

where $V = W^\pm, Z$ and (p, q) , (a, b) are the four-momenta of the vector bosons and their polarizations, respectively. A straightforward computation of the decay width gives [45]:

$$\Gamma^{\text{LO}}(S \rightarrow VV) = \frac{G_F}{16\sqrt{2}\pi} m_S^3 s_\alpha^2 (1 + \delta_V) \sqrt{1 - 4x_V} (1 - 4x_V + 12x_V^2), \quad (2.4)$$

where $x_V = m_V^2/m_S^2$ and $\delta_V = 0, 1$ for $V = Z, W^\pm$, respectively. The longitudinally and transversally polarized decay rates to gauge boson pair are given by:

$$\{\Gamma^{\text{LO}}(S \rightarrow VV)\}^{\pm L} = (\Gamma^{\text{LO}}(S \rightarrow VV))^{\pm\pm} = 0, \quad (2.5)$$

$$\{\Gamma^{\text{LO}}(S \rightarrow VV)\}^{\pm\pm} = \frac{G_F}{16\sqrt{2}\pi} m_S^3 s_\alpha^2 (1 + \delta_V) \sqrt{1 - 4x_V} \times (4x_V^2), \quad (2.6)$$

$$\{\Gamma^{\text{LO}}(S \rightarrow VV)\}^L = \frac{G_F}{16\sqrt{2}\pi} m_S^3 s_\alpha^2 (1 + \delta_V) \sqrt{1 - 4x_V} \times (1 - 4x_V + 4x_V^2). \quad (2.7)$$

We can note the dominance of the longitudinal vector bosons in the decay of a heavy scalar singlet ($x_V \rightarrow 0$),

$$\frac{\Gamma^{\text{LO}}(S \rightarrow V_\pm V_\mp)}{\Gamma^{\text{LO}}(S \rightarrow V_L V_L)} = \frac{x_V^2/2}{[1 - x_V^2/2]^2}, \quad (2.8)$$

where this implies that, for high m_S values (TeV scale), the total contribution due to the sum of vector boson decay rates can be expressed as,

$$\Gamma^{\text{LO}}(S \rightarrow VV) \simeq \frac{G_F}{16\sqrt{2}\pi} (1 + \delta_V) m_S^3. \quad (2.9)$$

For completeness, we also report the case with a virtual gauge boson in the final state ($m_V < m_S < 2m_V$); summing over all decay channels available of the virtual W^* or Z^* , the widths are given by [46]:

$$\Gamma^{\text{LO}}(S \rightarrow W^*W) = \frac{3g^4 m_S}{512\pi^3} s_\alpha^2 \mathcal{F}(m_W/m_S), \quad (2.10)$$

$$\Gamma^{\text{LO}}(S \rightarrow Z^*Z) = \frac{g^4 m_S}{2048\pi^3} \frac{7 - \frac{40s_W^2}{3} + \frac{160s_W^4}{9}}{c_W^4} s_\alpha^2 \mathcal{F}(m_Z/m_S), \quad (2.11)$$

where,

$$\mathcal{F}(x) = \frac{3 - 24x^2 + 60x^4}{\sqrt{4x^2 - 1}} \arccos\left(\frac{3x^2 - 1}{2x^3}\right) + (3 - 18x^2 + 12x^4)|\ln x| - |1 - x^2| \left(\frac{47x^2 - 13}{2} + \frac{1}{x^2}\right). \quad (2.12)$$

2.2 LO Decay Width to Fermions

Since the coupling of S to fermions is proportional to the fermion mass (m_f) and the mixing angle (s_α), the fermionic decay width will be proportional to $s_\alpha^2 m_f^2$ and the matrix element takes the following form:

$$\mathcal{M}^{\text{LO}}[S(k) \rightarrow \bar{f}(p)f(q)] = i\bar{U}(p) \frac{e m_f^2}{2s_W m_W} s_\alpha V(q), \quad (2.13)$$

where U, V are the spinors of the fermions with momenta p and q . Using eq.(2.2) we get [47],

$$\Gamma^{\text{LO}}(S \rightarrow \bar{f}f) = s_\alpha^2 N_c \frac{m_S m_f^2}{16\pi v^2} (1 - 4x_f)^{3/2}, \quad (2.14)$$

where m_f is the mass of the fermion, $x_f = m_f^2/m_S^2$ and $N_c = 1, 3$ for leptons and quarks, respectively.

2.3 LO Decay Width to Higgs Bosons

When kinematically accessible, the heavy scalar decay to Higgs boson pair is guaranteed by the tree-level interaction C_{HHS} of eq.(1.21):

$$\Gamma^{\text{LO}}(S \rightarrow HH) = \frac{(C_{HHS})^2}{32\pi m_H} \sqrt{1 - \frac{4m_H^2}{m_S^2}}. \quad (2.15)$$

2.4 LO Decay Width to massless Gauge Bosons

Since neither $S\gamma\gamma$ nor Sgg interactions are present at the LO, the decay rates $S \rightarrow \gamma\gamma, Z\gamma, gg$ are defined through loops of gauge bosons and/or fermions. Thus, these decays are suppressed by the loop factor $\alpha_{(\text{em,s})}^2/16\pi^2$ and this implies that the branching ratios are relatively small, of the order of 10^{-4} . Starting from $S \rightarrow \gamma\gamma$, we have (for the SM Higgs boson, the decay width into two photons was calculated in [48]):

$$\Gamma^{\text{LO}}(S \rightarrow \gamma\gamma) = s_\alpha^2 \frac{\alpha_{\text{em}}^2 g^2}{1024\pi^3} \frac{m_S^3}{m_W^2} \left| \sum_i N_{ci} Q_i^2 A_i^{\gamma\gamma}(\tau_i) \right|^2, \quad (2.16)$$

where $i = \eta^\pm, f, W^\pm$, $\tau_i = 4m_i^2/m_S^2$ and $A_i^{\gamma\gamma}(\tau_i)$ is defined as:

$$A_\eta^{\gamma\gamma}(\tau_\eta) = \tau_\eta^2 [\tau_\eta^{-1} - f(\tau_\eta)], \quad (2.17)$$

$$A_f^{\gamma\gamma}(\tau_f) = -2\tau_f [1 + (1 - \tau_f)f(\tau_f)], \quad (2.18)$$

$$A_W^{\gamma\gamma}(\tau_W) = 2 + 3\tau_W [1 + (2 - \tau_W)f(\tau_W)], \quad (2.19)$$

with

$$f(\tau) = \begin{cases} \arcsin[\sqrt{1/\tau}]^2 & \text{if } \tau \geq 1, \\ -\frac{1}{4} \left(\ln \frac{1+\sqrt{1-\tau}}{1-\sqrt{1-\tau}} - i\pi \right)^2 & \text{if } \tau < 1. \end{cases} \quad (2.20)$$

In the case of $S \rightarrow Z\gamma$, the calculation is similar to the two-photons case and the decay width given by [49]:

$$\Gamma^{\text{LO}}(S \rightarrow Z\gamma) = s_\alpha^2 \frac{\alpha_{\text{em}}^2 g^2 m_S^3}{512\pi^3 m_W^2} \left(1 - \frac{m_Z^2}{m_S^2}\right)^3 |A^{Z\gamma}(\tau_V, \tau_f, \lambda_V, \lambda_f)|^2, \quad (2.21)$$

where $\lambda_i = 4m_i^2/m_Z^2$ and,

$$A^{Z\gamma}(\tau_V, \tau_f, \lambda_V, \lambda_f) = \sum_f \frac{2N_{cf}Q_f(2Q_f s_W - T_f^3)}{s_W c_W} [I_1(\tau_f, \lambda_f) - I_2(\tau_f, \lambda_f)] - \frac{c_W}{s_W} \left\{ 4(3 - t_W^2)I_2(\tau_W, \lambda_W) + \left[\frac{(2 + \tau_W)t_W^2 - 2}{\tau_W} - 5 \right] I_1(\tau_W, \lambda_W) \right\}, \quad (2.22)$$

with the parametric integrals given by the following expressions:

$$I_1(\tau, \lambda) = \frac{\tau\lambda}{2(\tau - \lambda)} + \frac{\tau^2\lambda}{(\tau - \lambda)^2} \left[g(\tau) - g(\lambda) + \frac{\lambda(f(\tau) - f(\lambda))}{2} \right], \quad (2.23)$$

$$I_2(\tau, \lambda) = \frac{\tau\lambda}{2(\tau - \lambda)} [f(\tau) - f(\lambda)], \quad (2.24)$$

$$g(\tau) = \begin{cases} \sqrt{\tau - 1} \arcsin(\sqrt{1/\tau}) & \text{if } \tau \geq 1, \\ \frac{1}{2}\sqrt{1 - \tau} \left(\ln \frac{1+\sqrt{1-\tau}}{1-\sqrt{1-\tau}} - i\pi \right) & \text{if } \tau < 1. \end{cases} \quad (2.25)$$

Notice that, for $S \rightarrow \gamma\gamma$ and $Z\gamma$, the W -loop contributions is ~ 5 times t -loop contributions. Finally, the $S \rightarrow gg$ can be obtained from eqs.(2.16-2.20) by neglecting the (W^\pm, η^\pm) -loops and using the substitution, $\alpha_{\text{em}}^2 N_{cf}^2 Q^4 \rightarrow 2\alpha_s^2$, so that:

$$\Gamma^{\text{LO}}(S \rightarrow gg) = s_\alpha^2 \frac{\alpha_s^2 g^2 m_S^3}{512\pi^3 m_W^2} \left| \sum_i A_f^{gg}(\tau_f) \right|^2, \quad (2.26)$$

with $A_f^{gg}(\tau_f) = A_f^{\gamma\gamma}(\tau_f)$.

2.5 LO Total Decay Width and Branching Fractions

Disregarding for the moment what we have discussed in the previous section about m_S , s_α and w we analyze here the behavior of the LO decay rates with respect to s_α , w and m_S . Calling for simplicity $\Gamma^{\text{LO}}(S \rightarrow \text{All}) = \Gamma_{\text{TOT}}$, we report it in the left panel of Fig.(2.1) as a function of m_S for different values of $(s_\alpha, w) = (0.1, 5v)$ and $(0.2, 10v)$, while in the right panel Γ_{TOT} is displayed in the $s_\alpha - w$ plane for two fixed values of m_S : $m_S = 400, 1000$ GeV.

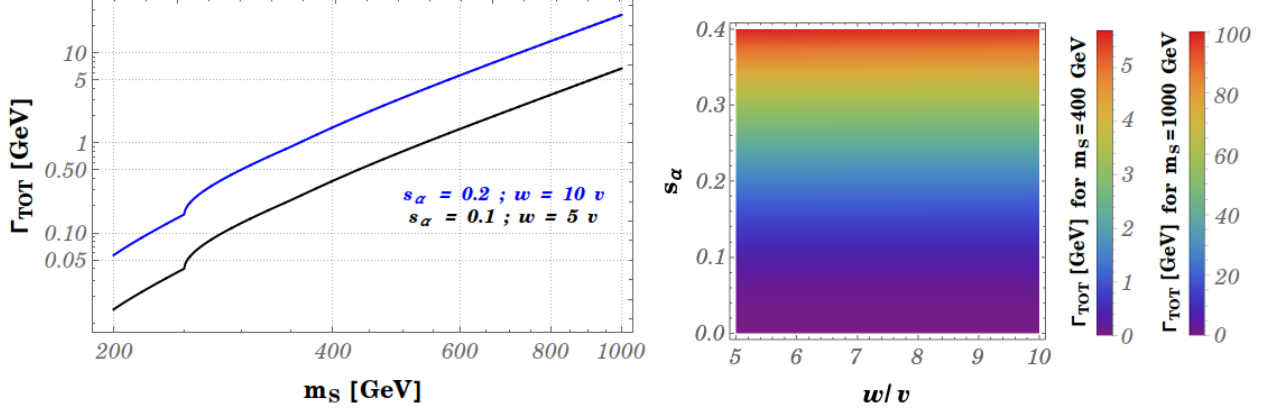


Figure 2.1: *Left plot:* $\Gamma^{\text{LO}}(S \rightarrow \text{All})$ as a function of the m_S for the two fixed sets of parameters: $s_\alpha = 0.1$, $w = 5v$ (black line) and $s_\alpha = 0.2$, $w = 10v$ (blue line). *Right plot:* $\Gamma^{\text{LO}}(S \rightarrow \text{All})$ in the $s_\alpha - w$ plane for two fixed values of m_S , namely $m_S = 400, 1000$ GeV.

We observe that Γ_{TOT} increases as s_α and w increase. In particular, the s_α -dependence is much stronger than the w -dependence since the full set of partial decay widths within Γ_{TOT} are proportional to s_α^2 (only C_{HHS} is a non-trivial function of s_α) while w only appears in the partial decay width $\Gamma^{\text{LO}}(S \rightarrow HH)$ suppressed by the typical small values characterizing κ and ρ (see Tab.(1.3)). In order to quantify this small dependence on w , we illustrate in Fig.(2.2) an example where the ratios $\Gamma_{\text{TOT}}^{s_\alpha=0.2}/\Gamma_{\text{TOT}}^{s_\alpha=0.1}$ and $\Gamma_{\text{TOT}}^{s_\alpha=0.35}/\Gamma_{\text{TOT}}^{s_\alpha=0.1}$ are computed for two different values of w , namely $w = 5v, 10v$. Neglecting the Higgs boson decay channel, the red lines confirm that Γ_{TOT} is fully proportional to s_α^2 (see eq.(4.45)): $\Gamma_{\text{TOT}}^{s_\alpha=s_1}/\Gamma_{\text{TOT}}^{s_\alpha=0.1} = (s_1/0.1)^2$. In this respect, the difference between the red (solid) and black (solid and dashed) curves is entirely due to the w and s_α dependences in eq.(1.21) which produce a variation for the defined ratios with $s_\alpha = 0.2$ and $s_\alpha = 0.35$ reaching a maximum of $\mathcal{O}(1\%)$ and $\mathcal{O}(6\%)$, respectively. Now, we can analyze the branching fractions of all partial decay channels. Defining $\text{BR}_{Sij}^{\text{LO}} = \Gamma^{\text{LO}}(S \rightarrow ij)/\Gamma_{\text{TOT}}$, we illustrate in Fig.(2.3) the dominant (right plot) and the rare decays (left plot) computed for the representative values $s_\alpha = 0.2$ and $w = 5v$. In addition, we have studied in Tab.(2.1), for fixed $m_S = 400$ GeV, and in Tab.(2.2), for fixed $m_S = 1000$ GeV, the s_α - and the w - dependences of all decay channels choosing three values of s_α and w : $s_\alpha = 0.1, 0.2, 0.35$ and $w = 5v, 10v, 15v$. We also calculate $\text{BR}_{HH}^{\text{LO}}$ for negative s_α values ($s_\alpha = -0.1, -0.2, -0.35$) since $\Gamma(S \rightarrow HH)$ is the only decay width not symmetric under a

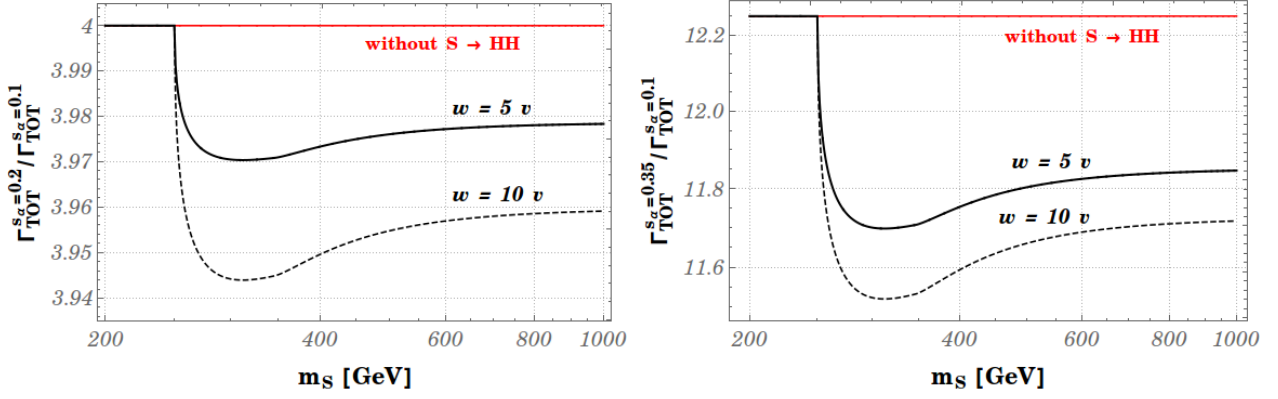


Figure 2.2: $\Gamma_{\text{TOT}}^{s_\alpha=0.2} / \Gamma_{\text{TOT}}^{s_\alpha=0.1}$ (left plot) and $\Gamma_{\text{TOT}}^{s_\alpha=0.35} / \Gamma_{\text{TOT}}^{s_\alpha=0.1}$ (right plot) as a function of the m_S for two fixed values $w = 5v$ (solid) and $w = 10v$ (dashed). The red line shows the considered ratios without the partial decay width $\Gamma^{\text{LO}}(S \rightarrow HH)$.

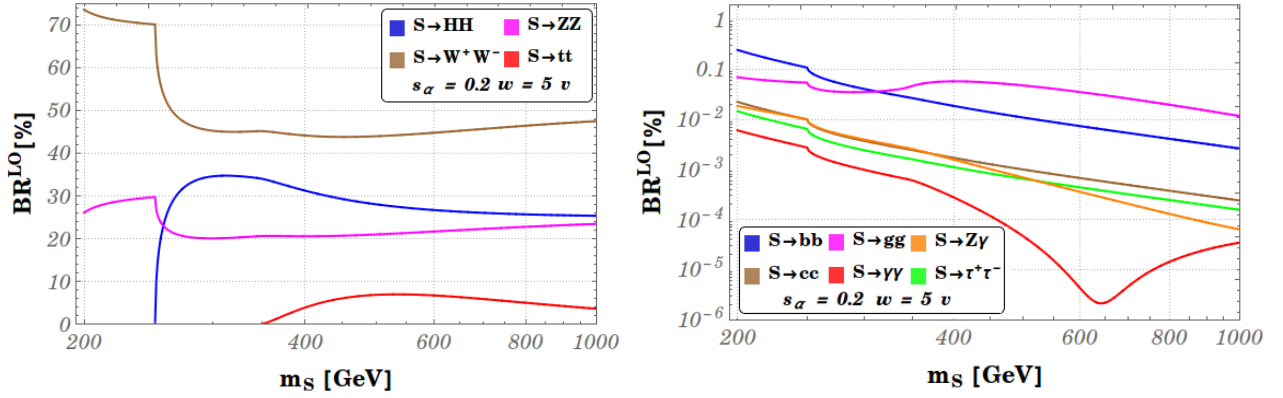


Figure 2.3: Dominant (left plot) and rare (right plot) decay channels computed for $s_\alpha = 0.2$ and $w = 5v$. Notice the different scale on the vertical axes.

sign flip of kind $s_\alpha \rightarrow -s_\alpha$. In the left plot of Fig.(2.3), we can observe at $m_S = 2m_H \sim 250$ GeV the decrease of $\text{BR}_{SZZ, SWW}^{\text{LO}}$ since Γ_{TOT} receives the new contribution related to the decay mode $S \rightarrow HH$ which becomes kinematically accessible at these mass values. Neglecting the behavior of $\text{BR}_{S\gamma\gamma}^{\text{LO}}$ for $m_S \gtrsim 600$ GeV, the $\text{BR}_{Sij}^{\text{LO}}$ depicted in the right plot of Fig.(2.3) show a global decrease for larger m_S values. In Tab.(2.1) and Tab.(2.2), we see that $\text{BR}_{SWW}^{\text{LO}}$, $\text{BR}_{SZZ}^{\text{LO}}$ and $\text{BR}_{Stt}^{\text{LO}}$ grow almost entirely with s_α while $\text{BR}_{SHH}^{\text{LO}}$ decreases as $|s_\alpha|$ increases, especially for negative s_α . In addition, $\text{BR}_{SHH}^{\text{LO}}$ grows with w for positive s_α values but it decreases as w increases in the negative mixing case.

$ s_\alpha $	w/v	$s_\alpha > 0$ $\text{BR}_{\text{SHH}}^{\text{LO}}$	$s_\alpha < 0$ $\text{BR}_{\text{SHH}}^{\text{LO}}$	$s_\alpha > 0$ $\text{BR}_{\text{SWW}}^{\text{LO}}$	$s_\alpha > 0$ $\text{BR}_{\text{SZZ}}^{\text{LO}}$	$s_\alpha > 0$ $\text{BR}_{\text{S}\bar{t}t}^{\text{LO}}$
0.1	5	31.7	30.0	43.8	20.5	3.9
0.2	5	31.3	27.9	44.1	20.6	3.9
0.35	5	28.8	23.1	45.7	21.3	4.0
0.1	10	31.3	30.4	44.1	20.6	3.9
0.2	10	30.4	28.7	44.7	20.9	4.0
0.35	10	27.4	24.5	46.6	21.8	4.1
0.1	15	31.2	30.6	44.2	20.6	3.9
0.2	15	30.1	29.0	44.8	20.9	4.0
0.35	15	26.9	25.0	46.9	21.9	4.2

Table 2.1: *Branching fractions of all decay channels computed for fixed values: $|s_\alpha| = 0.1, 0.2, 0.35, w = 5v, 10v, 15v$ and $m_S = 400 \text{ GeV}$. The $\text{BR}_{\text{HH}}^{\text{LO}}$ is computed for positive and negative s_α values while the other branching fractions are only computed for $s_\alpha > 0$.*

$ s_\alpha $	w/v	$s_\alpha > 0$ $\text{BR}_{\text{SHH}}^{\text{LO}}$	$s_\alpha < 0$ $\text{BR}_{\text{SHH}}^{\text{LO}}$	$s_\alpha > 0$ $\text{BR}_{\text{SWW}}^{\text{LO}}$	$s_\alpha > 0$ $\text{BR}_{\text{SZZ}}^{\text{LO}}$	$s_\alpha > 0$ $\text{BR}_{\text{S}\bar{t}t}^{\text{LO}}$
0.1	5	25.8	24.3	47.2	23.3	3.7
0.2	5	25.4	22.4	47.5	23.5	3.7
0.35	5	23.2	18.3	48.8	24.1	3.8
0.1	10	25.4	24.6	47.4	23.5	3.7
0.2	10	24.6	23.1	47.9	23.7	3.7
0.35	10	22.0	19.5	49.6	24.5	3.8
0.1	15	25.3	24.8	47.5	23.5	3.7
0.2	15	24.4	23.4	48.1	23.8	3.7
0.35	15	21.6	19.9	49.9	24.7	3.9

Table 2.2: *Branching fractions of all decay channels computed for fixed values: $|s_\alpha| = 0.1, 0.2, 0.35, w = 5v, 10v, 15v$ and $m_S = 1000 \text{ GeV}$. The $\text{BR}_{\text{HH}}^{\text{LO}}$ is computed for positive and negative s_α values while the other branching fractions are only computed for $s_\alpha > 0$.*

Finally, the branching fractions corresponding to the rare decay channels are totally independent from s_α and w (considering the s_α and w values reported in Tab.(2.1) and Tab.(2.2)) and give:

- **For $m_S = 400$ GeV:**

$$\text{BR}_{S\bar{b}b}^{\text{LO}} = 0.02\%, \text{BR}_{S\bar{c}c}^{\text{LO}} = 0.002\%, \text{BR}_{Sgg}^{\text{LO}} = 0.06\%, \text{BR}_{S\tau^+\tau^-}^{\text{LO}} = 0.001\%, \text{BR}_{SZ\gamma}^{\text{LO}} = 0.002\% \text{ and } \text{BR}_{S\gamma\gamma}^{\text{LO}} = 0.0003\%;$$

- **For $m_S = 1000$ GeV:**

$$\text{BR}_{S\bar{b}b}^{\text{LO}} = 0.003\%, \text{BR}_{S\bar{c}c}^{\text{LO}} = 0.0002\%, \text{BR}_{Sgg}^{\text{LO}} = 0.01\%, \text{BR}_{S\tau^+\tau^-}^{\text{LO}} = 0.0002\%, \text{BR}_{SZ\gamma}^{\text{LO}} = 0.00006\% \text{ and } \text{BR}_{S\gamma\gamma}^{\text{LO}} = 0.00003\%.$$

Chapter 3

Renormalization of the SSM

It is typical of quantum field theories to contain divergent amplitudes (in terms of Ultraviolet "UV" and/or Infrared "IR" divergences) when higher order corrections are taken into account. At the tree-level, the parameters in the Lagrangian (called "bare") are directly connected to the experimental quantities. As a consequence of the higher order corrections, the bare quantities differ from the corresponding physical ones for the UV- and/or IR-divergent factors which arise from the loop integral calculations. However, the so-called *regularization procedure* ensures that these integrals become convergent and allows us to isolate their divergent terms. We consider an example of UV-divergent loop integral to introduce the regularization concept:

$$\mathcal{I}(k, m) = \int \frac{d^4k}{(2\pi)^4} \frac{1}{(k^2 - m^2 + i\varepsilon)^2}, \quad (3.1)$$

where k is the momentum associated with the internal propagator, m is the mass of the particle which circles in the loop and $+i\varepsilon$ indicates the loop Feynman prescription [28]. Two of the most used regularization processes are: i) the Pauli-Villars regularization [51]; ii) the Dimensional regularization [52]. The first one subtracts the same loop integral with a much larger mass, called Λ (regulator), as follows:

$$\int \frac{d^4k}{(2\pi)^4} \frac{1}{(k^2 - m^2 + i\varepsilon)^2} \xrightarrow{\text{regularized}} \int \frac{d^4k}{(2\pi)^2} \left[\frac{1}{(k^2 - m^2 + i\varepsilon)^2} - \frac{1}{(k^2 - \Lambda^2 + i\varepsilon)^2} \right], \quad (3.2)$$

where the subtracted piece needed to regulate UV divergence is regarded as a contribution of another massive field (Pauli-Villar field) with the same quantum numbers and opposite statistics as the original field. This method has the benefit of maintaining the Lorentz invariance in the momentum space. As a result, the propagator for large momenta decreases faster, which ensures the convergence of the integrals. After the Wick rotation, the divergences manifest themselves as logs and powers of Λ^2 and $\mathcal{I}(k, m)$ gives:

$$\mathcal{I}(k, m) \xrightarrow{\text{regularized}} -\frac{i}{16\pi^2} \ln \left(\frac{m^2}{\Lambda^2} \right). \quad (3.3)$$

Even though Pauli-Villars approach works for the photon at one-loop order, it fails in more complicated scenarios like non-Abelian gauge theories (violation of the gauge invariance) or multi-loop calculations (many Pauli-Villars fields have to be introduced).

On the contrary, the dimensional regularization (which will be used throughout the rest of this thesis) avoids these problem. The main feature is the integration over the loop momenta in D dimension, defined as $D = 4 - 2\epsilon$, where ϵ is a small parameter which works as regulator. In this approach, the usual divergent form is given in terms of ϵ as follows [28]:

$$\int \frac{d^D k}{(2\pi)^D} \frac{1}{(k^2 - m^2 + i\epsilon)^2} = \frac{i}{16\pi^2} \left[\frac{1}{\epsilon} - \ln\left(\frac{m^2}{4\pi}\right) + \gamma_{\text{EM}} \right], \quad (3.4)$$

where γ_{EM} is the Euler-Mascheroni constant $\gamma_{\text{EM}} \sim 0,5772$ [53].

A regularized quantum field theory is obtained thanks to the *renormalization* which is the fundamental technique to consistently identify and remove the "infinities". As soon as all divergences are regulated, they have to be canceled against each other in a consistent way in order to obtain a finite result for each physical quantity. In this thesis, we have used for the renormalization procedure the so-called *counterterm approach* by which the bare Lagrangian parameters X_0 are expressed as the sum of finite renormalized quantities X and the divergent renormalization constants δX , called counterterms:

$$X_0 \rightarrow X + \delta X. \quad (3.5)$$

These are fixed by the *renormalization conditions* which connect the physical and renormalized parameters and can be arbitrarily defined, as we will illustrate in the next section. Notice that the radiative corrections modify the normalization factor of the fields by adding an infinite part. This causes that the Green functions could be divergent, even if we obtain finite S-matrix elements, and implies that the fields also have to be renormalized in order to get finite propagators and vertices. Consistently to the Lagrangian parameters, a bare field ϕ_0 can be renormalized by a similar procedure:

$$\phi_0 = \sqrt{Z_\phi} \phi \sim \left(1 + \frac{\delta Z_\phi}{2}\right) \phi, \quad (3.6)$$

where Z_ϕ is called *field renormalization constant*.

Let us introduce the renormalized quantities and counterterms of our interest:

- **Gauge Sector:**

The gauge boson masses m_V (with $V = Z, W$), the Weinberg angle θ_W and the electric charge e counterterms are defined in the following way:

$$(m_V^2)_0 = m_V^2 + \delta m_V^2, \quad (3.7)$$

$$(\theta_W)_0 = \theta_W + \delta\theta_W, \quad (3.8)$$

$$e_0 = (1 + \delta Z_e)e. \quad (3.9)$$

Obviously, the insertion of $\delta\theta_W$ implies that the relations between the mass and gauge basis in eq.(1.14) and eq.(1.15) are not valid to all orders. We also need the field renormalization constants for W^\pm , Z^0 and γ defined as:

$$W_0^\pm = \left(1 + \frac{1}{2}\delta Z_W\right) W^\pm, \quad (3.10)$$

$$\begin{pmatrix} Z_0 \\ \gamma_0 \end{pmatrix} = \begin{pmatrix} 1 + \frac{\delta Z_Z}{2} & \frac{\delta Z_{Z\gamma} - \delta\theta_W}{2} \\ \frac{\delta Z_{\gamma Z}}{2} + \delta\theta_W & 1 + \frac{\delta Z_\gamma}{2} \end{pmatrix} \begin{pmatrix} Z \\ \gamma \end{pmatrix}, \quad (3.11)$$

where in the last line we explicitly show the counterterms entering in the mixing matrix of the neutral gauge bosons. Notice that we can rewrite $\delta\theta_W$ as $\delta s_W^2/(2s_W c_W)$ using: $\delta\theta_W = \delta s_W/c_W$ and $\delta s_W = \delta s_W^2/(2s_W)$.

Typically, the gauge-fixing and the ghost Lagrangian, \mathcal{L}_{GF} and $\mathcal{L}_{\text{ghosts}}$, are considered in terms of already renormalized quantities [29, 35]. In this way, no additional counterterms have to be introduced for the linear $(\xi_i)_0$, $(\xi'_i)_0$ gauge parameters: $(\xi_i)_0$, $(\xi'_i)_0 \equiv \xi_i$, ξ'_i .

- **Fermion Sector:**

The fermion mass counterterms and the left and right -handed fermionic fields are defined through:

$$(m_f)_0 = m_f + \delta m_f, \quad (3.12)$$

$$f_{0i}^{\text{L,R}} = \left(\delta_{ij} + \frac{1}{2}\delta Z_{fij}^{\text{L,R}}\right) f_j^{\text{L,R}}, \quad (3.13)$$

where $f^{\text{L,R}} = P^{\text{L,R}} f$ with $P^{\text{L,R}} = (1 \mp \gamma_5)/2$.

- **Higgs Sector:**

Considering $\mathcal{L}_{\text{scalar}}$ of eq.(1.2) expressed in the gauge basis, we have that the bare parameters, the scalar masses and the vevs counterterms are shifted as:

$$\lambda_0 = \lambda + \delta\lambda, \quad (3.14)$$

$$\rho_0 = \rho + \delta\rho, \quad (3.15)$$

$$\kappa_0 = \kappa + \delta\kappa, \quad (3.16)$$

$$\mu_0^2 = \mu^2 + \delta\mu^2, \quad (3.17)$$

$$(\mu_s)_0^2 = \mu_s^2 + \delta\mu_s^2, \quad (3.18)$$

$$v_0 = v + \delta v, \quad (3.19)$$

$$w_0 = w + \delta w, \quad (3.20)$$

while the gauge field renormalization constants and the tadpole counterterms are given by:

$$\phi_0 = \left(1 + \frac{\delta Z_\phi}{2}\right) \phi, \quad (s^0)_0 = \left(1 + \frac{\delta Z_{s^0}}{2}\right) s^0, \quad (3.21)$$

$$(T_\phi)_0 = T_\phi + \delta t_\phi, \quad (T_{s^0})_0 = T_{s^0} + \delta t_{s^0}. \quad (3.22)$$

We can also define the counterterms in the mass basis where the mixing angle and the scalar masses arise (after the diagonalization α , m_S and m_H become functions of the scalar Lagrangian parameters):

$$\alpha_0 = \alpha + \delta\alpha, \quad (3.23)$$

$$(m_H^2)_0 = m_H^2 + \delta m_H^2, \quad (3.24)$$

$$(m_S^2)_0 = m_S^2 + \delta m_S^2. \quad (3.25)$$

Notice that, differently from the approach of [29], we have introduced the mixing angle counterterm $\delta\alpha$ instead of the mixed mass counterterm δm_{HS}^2 . The insertion of $\delta\alpha$ corresponds to shift the rotation matrix as

$$U(\alpha) \rightarrow U'(\alpha + \delta\alpha) = U(\alpha) + U(\delta\alpha),$$

where the application of $U'(\alpha + \delta\alpha)$ now diagonalizes the loop corrected mass matrix. However, the two approaches are related as follows ¹:

$$\delta m_{HS}^2 = (m_S^2 - m_H^2)\delta\alpha \quad (3.27)$$

As a consequence of such a relation, the full set of counterterms associated with the mixing scalar sector are defined according to the choice of δm_{HS}^2 or $\delta\alpha$.

Promoting eq.(1.7) to be valid to all orders ($\alpha_0 \equiv \alpha$), we obtain the following field renormalization constants associated with the scalar physical fields,

$$\begin{pmatrix} H_0 \\ S_0 \end{pmatrix} = \begin{pmatrix} 1 + \frac{\delta Z_H}{2} & \frac{\delta Z_{HS}}{2} \\ \frac{\delta Z_{SH}}{2} & 1 + \frac{\delta Z_S}{2} \end{pmatrix} \begin{pmatrix} H \\ S \end{pmatrix}, \quad (3.28)$$

and the mixed mass counterterm δm_{HS}^2 has to be used.

On the other hand, we can also avoid to promote the mixing angle to be fixed to all orders, as it was previously stated for $\delta\theta_W$, and this implies that the two physical scalar fields are shifted to the renormalized fields and the wave function renormalization constants as

$$\begin{pmatrix} H_0 \\ S_0 \end{pmatrix} = \begin{pmatrix} 1 + \frac{\delta Z_H}{2} & \frac{\delta Z_{HS}}{2} - \delta\alpha \\ \frac{\delta Z_{SH}}{2} + \delta\alpha & 1 + \frac{\delta Z_S}{2} \end{pmatrix} \begin{pmatrix} H \\ S \end{pmatrix}. \quad (3.29)$$

¹To determine the relation which links the two approaches, we have required the off-diagonal terms of the following matrix are zero:

$$U'(\alpha + \delta\alpha) \cdot \left[U(\alpha)^{-1} \cdot \begin{pmatrix} m_H^2 & \delta m_{HS}^2 \\ \delta m_{HS}^2 & m_S^2 \end{pmatrix} \cdot U(\alpha) \right] U'(\alpha + \delta\alpha)^{-1} = \text{diag}(m_H^2, m_S^2). \quad (3.26)$$

In this case δm_{HS}^2 has to be replaced by $\delta\alpha$ as described in eq.(3.27).

The tadpoles in the mass basis (T_H and T_S) are related to those in the gauge basis (T_ϕ and T_{s^0}) by the mixing,

$$\begin{pmatrix} T_H \\ T_S \end{pmatrix}_0 = \begin{pmatrix} c_\alpha & -s_\alpha \\ s_\alpha & c_\alpha \end{pmatrix} \begin{pmatrix} T_\phi \\ T_{s^0} \end{pmatrix}_0, \quad (3.30)$$

where T_ϕ and T_{s^0} follow the relations in eq.(3.22).

- **Three-point Vertex:**

We define the vertex counterterms as,

$$V_0 = V(1 + \delta V), \quad (3.31)$$

where V_0 is a short-hand notation for a generic coupling.

3.1 Renormalization Schemes

The choice of the renormalization scheme involves the counterterm definitions which are necessary to absorb the UV-divergent contributions from higher order amplitudes. We will fix the renormalization constants for the masses and fields through the so-called *on-shell scheme* (**OS**)² which allows us to choose the counterterms such that the physical and the finite renormalized parameters are the same to all orders of perturbation theory. For the counterterms associated with the scalar mixed mass (or alternatively, the scalar mixing angle) and non-diagonal fields, we can construct a set of schemes which are not necessarily bound to the OS conditions since there is no natural way of defining these counterterms through a physically motivated renormalization scheme. In this regard, we have to pay attention to the definitions of these schemes since some of them manifest a gauge dependence in the physical observables. We will introduce the renormalization of the mixing scalar sector through two different schemes, called *minimal field* (**MF**) and *improved on-shell* (**iOS**), where the first one contains gauge-dependent counterterms while the second one is completely gauge-invariant [29].

Now, we clarify the formulation of the OS renormalization conditions discussing an example where only one spinless self-interacting scalar particle is considered (for example, it can get trilinear or quartic self-couplings as shown in lower panel of Fig.(3.1)), described by the bare field Υ_0 and bare mass m_0 , and working on the propagator and two-point correlation function definitions. The bare definitions corresponding to this scalar field are shifted as: $\Upsilon_0 \rightarrow (1 + \delta Z_\Upsilon/2)\Upsilon$ and $m_0^2 \rightarrow m^2 + \delta m^2$. The treatment concerning the MF and iOS renormalization conditions can be described subsequently.

²This renormalization scheme was proposed for the first time in [54].

The bare propagator of the Υ_0 field, which we call $\mathcal{G}_0(p^2)$, can be defined as [28]:

$$\begin{aligned}\mathcal{G}_0(p^2) &= \int d^4x \langle \Omega | T \Upsilon_0(x) \Upsilon_0^*(0) | \Omega \rangle e^{ip \cdot x} = \\ &= \sqrt{Z_\Upsilon^*} \left[\int d^4x \langle \Omega | T \Upsilon(x) \Upsilon^*(0) | \Omega \rangle e^{ip \cdot x} \right] \sqrt{Z_\Upsilon} = \\ &= \sqrt{Z_\Upsilon^*} \hat{\mathcal{G}}(p^2) \sqrt{Z_\Upsilon},\end{aligned}\tag{3.32}$$

where the integral is computed over all space-time configurations x , $|\Omega\rangle$ is the vacuum state of this scalar toy theory, T is the time-ordering operator and $\hat{\mathcal{G}}(p^2)$ is the renormalized propagator (the quantities Q to be renormalized will be denoted through the "hat" symbol, \hat{Q}).

The bare propagator $\mathcal{G}_0(p^2)$ can also be defined as the sum of all *one-particle irreducible*³ (1PI) contributions to the self energy of the scalar field Υ_0 , indicated with $i\Sigma_{1\text{PI}}(p^2)$ (see Fig.(3.1)) [28]:

$$\begin{aligned}\mathcal{G}_0(p^2) &= \frac{i}{p^2 - m_0^2} + \frac{i}{p^2 - m_0^2} (i\Sigma_{1\text{PI}}(p^2)) \frac{i}{p^2 - m_0^2} + \dots + \frac{i}{p^2 - m_0^2} \left(\frac{-\Sigma_{1\text{PI}}(p^2)}{p^2 - m_0^2} \right)^n = \\ &= \frac{i}{p^2 - m_0^2} \left[1 + \left(\frac{-\Sigma_{1\text{PI}}(p^2)}{p^2 - m_0^2} \right) + \dots + \left(\frac{-\Sigma_{1\text{PI}}(p^2)}{p^2 - m_0^2} \right)^n \right] = \\ &= \frac{i}{p^2 - m_0^2} \left[\frac{1}{1 + \frac{\Sigma_{1\text{PI}}(p^2)}{p^2 - m_0^2}} \right] = \frac{i}{p^2 - m_0^2 + \Sigma_{1\text{PI}}(p^2)},\end{aligned}\tag{3.33}$$

where n represents the infinite 1PI loop-levels. By comparing eq.(3.32) and eq.(3.33), we

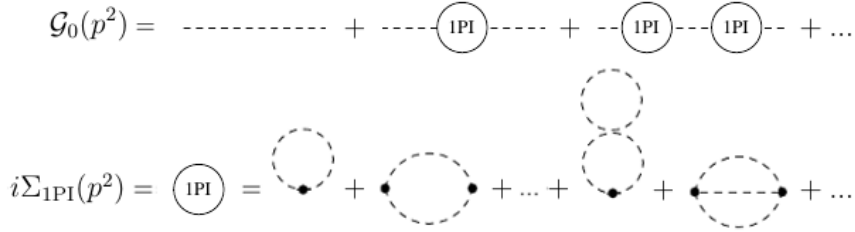


Figure 3.1: *Upper plot: 1PI-loop structure of the propagator $\mathcal{G}_0(p^2)$; lower plot: examples of loops contained in the 1PI contribution to the self-energy; the "black dots" depict the positions where the external propagators have to be connected.*

³These contributions are described by the complete set of self energy loop-contributions which cannot be separated into two distinct diagrams by a cut of one internal line. As shown in Fig.(3.1), the tadpoles (which can be separated into two distinct diagrams by a single cut) are excluded for simplicity since it is possible to assume an appropriate renormalization condition which removes them [28].

obtain the following renormalized propagator in terms of the physical quantities:

$$\begin{aligned}\hat{\mathcal{G}}(p^2) &= \frac{i}{\sqrt{Z_\Upsilon^*} \left[p^2 - m^2 - \delta m^2 + \Sigma_{\text{1PI}}(p^2) \right] \sqrt{Z_\Upsilon}} \approx \\ &\approx \frac{i}{p^2 - m^2 + \hat{\Sigma}_{\text{1PI}}(p^2)},\end{aligned}\quad (3.34)$$

and this automatically implies that $\hat{\Sigma}_{\text{1PI}}(p^2)$ is given by,

$$\hat{\Sigma}_{\text{1PI}}(p^2) = \Sigma_{\text{1PI}}(p^2) + (p^2 - m^2) \left(\frac{\delta Z_\Upsilon^* + \delta Z_\Upsilon}{2} \right) - \delta m^2, \quad (3.35)$$

with $\sqrt{Z_\Upsilon^*}$, $\sqrt{Z_\Upsilon}$ expanded as eq.(3.6). Using these compact results, the two-point correlation function (the inverse of the propagator) can be directly defined as:

$$\begin{aligned}\hat{\Gamma}(p^2) &= i[p^2 - m^2 + \hat{\Sigma}_{\text{1PI}}(p^2)] \approx \\ &\approx i(p^2 - m^2) \left(1 + \frac{\partial \hat{\Sigma}_{\text{1PI}}(p^2)}{\partial p^2} \Big|_{p^2=m^2} \right) = i(p^2 - m^2) (-i) \frac{\partial \hat{\Gamma}(p^2)}{\partial p^2} \Big|_{p^2=m^2},\end{aligned}\quad (3.36)$$

where the last row is obtained after an expansion around the pole of the propagator at $p^2 = m^2$.

At this point, the formulation of the OS renormalization conditions, which requires that physical and finite renormalized parameters are equivalent to all orders of perturbation theory, becomes more intuitive by considering two main assumptions:

i) The renormalized mass parameter of the physical particle is fixed by imposing that it is equal to the physical mass and by the fact that the real parts of the pole of the corresponding propagator is equivalent to the zero of the 1PI self energy contributions:

$$Re\{(-i)\hat{\Gamma}(m^2)\} = 0 \quad \rightarrow \quad Re\{\hat{\Sigma}_{\text{1PI}}(m^2)\} = 0; \quad (3.37)$$

ii) The physical field Υ is properly normalized through fixing the residue of the propagator at its pole to i :

$$Re \left\{ \frac{\partial \hat{\Gamma}(p^2)}{\partial p^2} \Big|_{p^2=m^2} \right\} = i \quad \rightarrow \quad Re \left\{ \frac{\partial \hat{\Sigma}_{\text{1PI}}(p^2)}{\partial p^2} \Big|_{p^2=m^2} \right\} = 0; \quad (3.38)$$

In our toy model these conditions are equivalent to:

$$\delta m^2 = Re \Sigma_{\text{1PI}}(m^2) \quad \text{and} \quad \delta Z_\Upsilon = -Re \Sigma'_{\text{1PI}}(m^2), \quad (3.39)$$

where Σ' is a short-hand notation for $\Sigma'(p^2) = \partial \Sigma(p^2)/\partial p^2$. It is important to point out that, in the case where the scalar field develops a non-zero vacuum expectation value, the renormalization condition for the tadpole T_Υ has to be considered.

3.2 Renormalization Conditions and Counterterms

We will apply the same treatment discussed above to the SSM Lagrangian fields in order to determine the renormalization conditions through their respective propagators or two-point correlation functions⁴. For the two-point correlation functions we have:

$$\begin{aligned} \hat{\Gamma}_{\mu\nu}^{\mathcal{V}\mathcal{V}'}(p^2) &= -ig^{\mu\nu}(p^2 - m_{\mathcal{V}}^2)\delta^{\mathcal{V}\mathcal{V}'} - \\ &\quad - i\left(g^{\mu\nu} - \frac{p^\mu p^\nu}{p^2}\right)\hat{\Sigma}_T^{\mathcal{V}\mathcal{V}'}(p^2) - i\frac{p^\mu p^\nu}{p^2}\hat{\Sigma}_L^{\mathcal{V}\mathcal{V}'}(p^2), \end{aligned} \quad (3.40)$$

$$\begin{aligned} \hat{\Gamma}_{ij}^f(p) &= i(\not{p} - m)\delta_{ij} + \\ &\quad + i[\not{p}(P^L\hat{\Sigma}_{ij}^{f,L} + P^R\hat{\Sigma}_{ij}^{f,R}) + (m_{f,i}P^L + m_{f,j}P^R)\hat{\Sigma}_{ij}^{f,S}], \end{aligned} \quad (3.41)$$

$$\hat{\Gamma}^{\mathcal{S}\mathcal{S}'}(p^2) = i(p^2 - m_{\mathcal{S}}^2)\delta^{\mathcal{S}\mathcal{S}'} + i\hat{\Sigma}^{\mathcal{S}\mathcal{S}'}(p^2). \quad (3.42)$$

Here, the functions corresponding to the gauge bosons are defined in the 't Hooft-Feynman gauge which will be used throughout the rest of this work; furthermore, $\Sigma_{1\text{PI}}$ is now indicated as Σ , $m_{\mathcal{S}/\mathcal{V}}$ is the mass of the incoming particle and $(\mathcal{V}\mathcal{V}', \mathcal{S}\mathcal{S}')$ can be one of the combinations $\{WW, ZZ, \gamma\gamma, \gamma Z, Z\gamma\}$ and $\{HH, SS, HS, SH\}$, respectively. $\hat{\Sigma}_T^{\mathcal{V}\mathcal{V}'}$ and $\hat{\Sigma}_L^{\mathcal{V}\mathcal{V}'}$ are the transverse and longitudinal contributions to the self-energies while the superscripts $\hat{\Sigma}_{ij}^{f,L}$, $\hat{\Sigma}_{ij}^{f,R}$ and $\hat{\Sigma}_{ij}^{f,S}$ stand for the left-handed, right-handed and scalar parts of the renormalized self-energies. The definitions of $\hat{\Sigma}(p^2)$ are given by [29, 33]:

$$\widetilde{Re}\hat{\Sigma}_T^{WW}(p^2) = \widetilde{Re}\Sigma_T^{WW}(p^2) + \delta Z_W(p^2 - m_W^2) - \delta m_W^2, \quad (3.43)$$

$$Re\hat{\Sigma}_T^{ZZ}(p^2) = Re\Sigma_T^{ZZ}(p^2) + \delta Z_Z(p^2 - m_Z^2) - \delta m_Z^2, \quad (3.44)$$

$$Re\hat{\Sigma}_T^{\gamma\gamma}(p^2) = Re\Sigma_T^{\gamma\gamma}(p^2) + p^2\delta Z_{\gamma\gamma}, \quad (3.45)$$

$$Re\hat{\Sigma}_T^{\gamma Z}(p^2) = Re\Sigma_T^{\gamma Z}(p^2) + \frac{1}{2}\delta Z_{\gamma Z}(2p^2 - m_Z^2) + m_Z^2\delta\theta_W, \quad (3.46)$$

$$Re\hat{\Sigma}^f(p^2) = Re\hat{\Sigma}_V^f(p^2) + Re\hat{\Sigma}_A^f(p^2), \quad (3.47)$$

$$Re\hat{\Sigma}^{HH}(p^2) = Re\Sigma^{HH}(p^2) + \delta Z_H(p^2 - m_H^2) - \delta m_H^2, \quad (3.48)$$

$$Re\hat{\Sigma}^{SS}(p^2) = Re\Sigma^{SS}(p^2) + \delta Z_S(p^2 - m_S^2) - \delta m_S^2, \quad (3.49)$$

$$\begin{aligned} Re\hat{\Sigma}^{HS}(p^2) &= Re\hat{\Sigma}^{SH}(p^2) = Re\Sigma^{HS}(p^2) + (m_H^2 - m_S^2)\delta\alpha + \\ &\quad + \left[\frac{\delta Z_{HS}}{2}(p^2 - m_H^2) + \frac{\delta Z_{SH}}{2}(p^2 - m_S^2) \right], \end{aligned} \quad (3.50)$$

where \widetilde{Re} takes the real part of the loop integrals only and it does not remove the imaginary parts arising from the various couplings of the theory (e.g. from complex CKM matrix elements; if these coupling are chosen to be real, the replacement $\widetilde{Re} \rightarrow Re$ is valid at the

⁴The only three-point function needed is associated with $e^+e^-\gamma$ vertex. This fixes δZ_e .

one-loop order) while $\hat{\Sigma}_{V,A}^f(p^2)$ in eq.(3.47) are defined as:

$$\hat{\Sigma}_V^f(p^2) = \not{p}\Sigma_V^f(p^2) + (\not{p} - m_f)\delta Z_{fV} + m_f\Sigma_S^f(p^2) - \delta m_f, \quad (3.51)$$

$$\hat{\Sigma}_A^f(p^2) = -\not{p}\gamma_5(\Sigma_A^f(p^2) + \delta Z_{fA}), \quad (3.52)$$

with $\delta Z_{fV,A} = (\delta Z_f^L \pm \delta Z_f^R)/2$ and $\Sigma_{V,A}^f = (\Sigma^{fL} \pm \Sigma^{fR})/2$.

We can impose the following conditions on the renormalized self-energy functions in the OS scheme [33, 55]:

$$\begin{aligned} \text{Re}\hat{\Sigma}^{HH}(m_H^2) &= 0, & \text{Re}\hat{\Sigma}'^{HH}(p^2)|_{p^2=m_H^2} &= 0, \\ \text{Re}\hat{\Sigma}^{SS}(m_S^2) &= 0, & \text{Re}\hat{\Sigma}'^{SS}(p^2)|_{p^2=m_S^2} &= 0, \\ \widetilde{\text{Re}}\hat{\Sigma}_T^{WW}(m_W^2) &= 0, & \widetilde{\text{Re}}\hat{\Sigma}'_T{}^{WW}(p^2)|_{p^2=m_W^2} &= 0, \\ \text{Re}\hat{\Sigma}_T^{ZZ}(m_Z^2) &= 0, & \text{Re}\hat{\Sigma}'_T{}^{ZZ}(p^2)|_{p^2=m_Z^2} &= 0, \\ \text{Re}\hat{\Sigma}_T^{\gamma\gamma}(0) &= 0, & \text{Re}\hat{\Sigma}'_T{}^{\gamma\gamma}(p^2)|_{p^2=0} &= 0, \\ \text{Re}\hat{\Sigma}_T^{Z\gamma}(m_Z^2) &= 0, & \text{Re}\hat{\Sigma}'_T{}^{Z\gamma}(0) &= 0, \\ \widetilde{\text{Re}}\hat{\Sigma}_V^f(m_f^2) &= 0, & \widetilde{\text{Re}}\hat{\Sigma}'_{V,A}{}^f(p^2)|_{p^2=m_f^2} &= 0. \end{aligned} \quad (3.53)$$

Notice that no renormalization condition for the mixing scalar sector is fixed. These conditions are set up in the MF and iOS schemes as:

- **Improved on-shell (iOS)**

This scheme requires that loop-induced $S - H$ or $H - S$ transitions vanish for on-shell external scalar states:

$$\text{Re}\hat{\Sigma}^{HS}(p^2)|_{p^2=m_H^2} = 0 \quad , \quad \text{Re}\hat{\Sigma}^{HS}(p^2)|_{p^2=m_S^2} = 0. \quad (3.54)$$

- **Minimal field (MF):**

Here, the off-diagonal renormalized self-energies are canceled out at an arbitrary renormalization scale, called μ_R :

$$\text{Re}\hat{\Sigma}^{HS}(p^2)|_{p^2=\mu_R^2} = 0. \quad (3.55)$$

As a consequence of eq.(3.55), we can note that for $\mu_R^2 \neq m_H^2, m_S^2$ the physical H and S states can oscillate when we compute vertices with scalar legs on their mass shell ($p^2 = m_H^2, m_S^2$) since the off-diagonal terms in the propagator matrix, which we call $\Delta_{\text{scalar}}^{-1}$, are different from zero:

$$\Delta_{\text{scalar}}^{-1}|_{\text{MF}} = \begin{pmatrix} p^2 - m_H^2 + \hat{\Sigma}^{HH}(p^2) & \hat{\Sigma}^{HS}(p^2)|_{p^2=\mu_R^2} \\ \hat{\Sigma}^{SH}(p^2)|_{p^2=\mu_R^2} & p^2 - m_S^2 + \hat{\Sigma}^{SS}(p^2) \end{pmatrix}. \quad (3.56)$$

Thus, these vertices need the following additional finite terms (for any scalar leg) which compensate the residual $S - H$ or $H - S$ loop contributions [29, 56]:

$$\hat{Z}_{HS} = -\frac{Re\hat{\Sigma}^{HS}(m_H^2)}{m_H^2 - m_S^2} \quad , \quad \hat{Z}_{SH} = -\frac{Re\hat{\Sigma}^{HS}(m_S^2)}{m_S^2 - m_H^2}. \quad (3.57)$$

Obviously, the diagonal fields depend on the OS conditions and this implies that $\hat{Z}_H = \hat{Z}_S = 1$.

3.2.1 Explicit Form of the OS Counterterms

From the full set of OS renormalization conditions in eq.(3.53) and eqs.(3.43-3.49) we can extract the following counterterms:

- **Mass Counterterms:**

$$\delta m_f = m_f \widetilde{Re}[\Sigma_V^f(m_f^2) + \Sigma_S^f(m_f^2)], \quad (3.58)$$

$$\delta m_H^2 = Re\Sigma^{HH}(m_H^2), \quad (3.59)$$

$$\delta m_S^2 = Re\Sigma^{SS}(m_S^2), \quad (3.60)$$

$$\delta m_W^2 = \widetilde{Re}\Sigma_T^{WW}(m_W^2), \quad (3.61)$$

$$\delta m_Z^2 = Re\Sigma_T^{ZZ}(m_Z^2). \quad (3.62)$$

- **Field Renormalization Constants:**

$$\delta Z_{fV} = -\widetilde{Re}\Sigma_V^f(m_f^2) - 2m_f^2 \widetilde{Re}(\Sigma_V^f(p^2) + \Sigma_S^f(p^2))\big|_{p^2=m_f^2}, \quad (3.63)$$

$$\delta Z_{fA} = -\widetilde{Re}\Sigma_A^f(m_f^2) - 2m_f^2 \widetilde{Re}\Sigma_A^f(p^2)\big|_{p^2=m_f^2}, \quad (3.64)$$

$$\delta Z_H = -Re\Sigma'^{HH}(p^2)\big|_{p^2=m_H^2}, \quad (3.65)$$

$$\delta Z_S = -Re\Sigma'^{SS}(p^2)\big|_{p^2=m_S^2}, \quad (3.66)$$

$$\delta Z_W = -\widetilde{Re}\Sigma_T'^{WW}(p^2)\big|_{p^2=m_W^2}, \quad (3.67)$$

$$\delta Z_Z = -Re\Sigma_T'^{ZZ}(p^2)\big|_{p^2=m_Z^2}, \quad (3.68)$$

$$\delta Z_{\gamma\gamma} = -Re\Sigma_T'^{\gamma\gamma}(p^2)\big|_{p^2=0}, \quad (3.69)$$

$$\delta Z_{\gamma Z} = 2Re\frac{\Sigma_T^{\gamma Z}(0)}{m_Z^2} + \frac{\delta s_W^2}{s_W c_W}. \quad (3.70)$$

- **Tadpoles:**

$$\delta T_H = -T_H \quad , \quad \delta T_S = -T_S. \quad (3.71)$$

• **Derived Quantities:**

$$\delta Z_W = \delta Z_{\gamma\gamma} + \frac{c_W}{s_W} \delta Z_{\gamma Z}, \quad (3.72)$$

$$\delta s_W^2 = -\delta c_W^2 = c_W^2 \left(\frac{\delta m_Z^2}{m_Z^2} - \frac{\delta m_W^2}{m_W^2} \right), \quad (3.73)$$

$$\delta Z_e = -\frac{1}{2} \delta Z_{\gamma\gamma} + \frac{s_W}{c_W} \frac{\text{Re} \Sigma_T^{\gamma Z}(0)}{m_Z^2}, \quad (3.74)$$

where the constant δZ_e is obtained by requiring the electric charge to be equal to the full $\bar{f}f\gamma$ -vertex in the Thompson limit and imposing that all corrections to the $\bar{f}f\gamma$ coupling vanish on-shell and for zero momentum transfer (we use f to be more general since this result is independent on the fermion species) [33]⁵. Concerning the correction to the electric charge (δZ_e) we need to clarify the appearance of ambiguities associated with the definition of the mass singularities due to light fermions (quarks and leptons) in $\ln(m_Z^2/m_f^2)$. The first approach is related to the fine structure constant $\alpha_{\text{em}}(q^2)$, at $Q^2 = m_Z^2$, which has to be imposed as input parameter. This choice modifies the definition of δZ_e as [33]:

$$\delta Z_e|_{Q^2=m_Z^2} = \delta Z_e|_{Q^2=0} - \frac{1}{2} \Delta \alpha_{\text{em}}(m_Z^2), \quad (3.75)$$

where $\Delta \alpha_{\text{em}}(m_Z^2)$ depends on the light-fermion contributions only (denoted with the index "light"):

$$\Delta \alpha_{\text{em}}(m_Z^2) = -\delta Z_{\gamma\gamma}^{\text{light}} + \left(\frac{\text{Re} \Sigma_T^{\gamma\gamma}(m_Z^2)}{m_Z^2} \right)^{\text{light}}. \quad (3.76)$$

Notice that these light-terms are canceled out when eq.(3.74) and eq.(3.76) are inserted in eq.(3.75).

The second approach is based on the so-called *modified on-shell mass scheme* (MOMS) [57], in which the electric charge is replaced by the Fermi constant G_F via

$$\frac{G_F}{\sqrt{2}} = \frac{e^2}{8s_W^2 m_W^2} \frac{1}{1 - \Delta r}. \quad (3.77)$$

The quantity Δr represents finite corrections to G_F ; these are well known and up to $\mathcal{O}(\alpha_{em}^2)$ are given by [57, 58]:

$$\Delta r = \frac{\widetilde{\text{Re}} \hat{\Sigma}_T^{WW}(0)}{m_W^2} + \frac{\alpha_{\text{em}}}{4\pi s_W^2} \left[\left(\frac{7}{2s_W^2} - 2 \right) \ln c_W^2 + 6 \right] + \mathcal{O}(\delta r_{\text{SSM}}), \quad (3.78)$$

⁵Our expression of δZ_e differs from the one quoted in [33] because of a different sign convention in the definition of the covariant derivative, see eq.(1.12).

where $\widetilde{Re}\hat{\Sigma}_T^{WW}(p^2)$ is the renormalized transverse self-energy of the W boson at momentum transfer p defined in eq.(3.43); the second term is due to the vertex-box loop corrections in the muon decay process and $\mathcal{O}(\delta r_{\text{SSM}})$ includes the negligible contributions arising from the insertion of the scalar singlet field ⁶.

The use of G_F instead of the electric charge amounts to shift $\delta Z_e \rightarrow \delta Z'_e = \delta Z_e - \Delta r/2$; if in Δr we use the "derived form" of δZ_W of eq.(3.72) then the cancellation of the $\delta Z_{\gamma\gamma}$ in the final counterterm expression is guaranteed and no problem arises from the light fermion loop contributions. This is verified as follows:

$$\begin{aligned} \delta Z'_e &= \delta Z_e - \frac{\Delta r}{2} = \left(-\frac{1}{2}\delta Z_{\gamma\gamma} + \frac{s_W}{c_W} \frac{Re\Sigma_T^{\gamma Z}(0)}{m_Z^2} \right) + \left(-\frac{\widetilde{Re}\hat{\Sigma}_T^{WW}(0)}{2m_W^2} - \frac{\mathcal{C}_{\text{muon}}}{2} \right) = \\ &= \left(-\frac{1}{2}\delta Z_{\gamma\gamma} + \frac{s_W}{c_W} \frac{Re\Sigma_T^{\gamma Z}(0)}{m_Z^2} \right) + \left(-\frac{\widetilde{Re}\Sigma_T^{WW}(0)}{2m_W^2} + \frac{\delta Z_W}{2} + \frac{\delta m_W^2}{2m_W^2} - \frac{\mathcal{C}_{\text{muon}}}{2} \right) = \\ &= \left(\frac{s_W}{c_W} \frac{Re\Sigma_T^{\gamma Z}(0)}{m_Z^2} \right) + \left(-\frac{\widetilde{Re}\Sigma_T^{WW}(0)}{2m_W^2} + \frac{c_W}{2s_W}\delta Z_{\gamma Z} + \frac{\delta m_W^2}{2m_W^2} - \frac{\mathcal{C}_{\text{muon}}}{2} \right), \end{aligned} \quad (3.79)$$

where $\delta Z_{\gamma Z}$ is defined in eq.(3.70) and $\mathcal{C}_{\text{muon}}$ represents the vertex-box loop corrections described by second term in eq.(3.78) (by substituting the numerical values of its parameters we obtain: $\mathcal{C}_{\text{muon}} \sim 0.0066$). Thus, the full expanded form of $\delta Z'_e$ is given by:

$$\delta Z'_e = \frac{\delta m_W^2}{2m_W^2} + \frac{\delta s_W^2}{2s_W^2} + \frac{Re\Sigma_T^{\gamma Z}(0)}{s_W c_W m_Z^2} - \frac{\widetilde{Re}\Sigma_T^{WW}(0)}{2m_W^2} - \frac{\mathcal{C}_{\text{muon}}}{2}. \quad (3.80)$$

It is important to observe that, differently from the α_{em} -approach where we have m_W and m_Z as input values, in the MOMS scheme m_W is not an input parameter. It is replaced by G_F in the following way:

$$m_W^2 = \frac{m_Z^2}{2} \left(1 + \sqrt{1 - \frac{4\pi\alpha_{\text{em}}}{\sqrt{2}G_F m_Z^2} \left[\frac{1}{1 - \Delta r} \right]} \right), \quad (3.81)$$

with $\Delta r \simeq 0.04$.

3.2.2 Explicit Form of the iOS Counterterms

The iOS definitions of $\delta Z_{HS,SH}^{\text{ios}}$ (we indicate with the superscript "ios" the counterterm of the mixing scalar sector arising from the iOS renormalization conditions) are determined using eq.(3.50) and eq.(3.54). These equations lead to [29],

$$\frac{\delta Z_{HS}^{\text{ios}}}{2} = \frac{Re\Sigma^{HS}(m_S^2)}{m_H^2 - m_S^2} + \delta\alpha^{\text{ios}}, \quad \frac{\delta Z_{SH}^{\text{ios}}}{2} = \frac{Re\Sigma^{HS}(m_H^2)}{m_S^2 - m_H^2} - \delta\alpha^{\text{ios}}. \quad (3.82)$$

⁶In the SSM, the new contributions to Δr generates a maximum variation of $\mathcal{O}(0.1)\%$ for $|s_\alpha| \sim 0.2$ [26].

On the other hand, the mixed mass (mixing angle) counterterm is defined in the following way [29]:

$$\delta m_{HS}^{2\text{ios}} = (m_S^2 - m_H^2) \delta\alpha^{\text{ios}} = \text{Re}\Sigma^{HS}(p^{*2}) \Big|_{p^{*2} = \frac{m_H^2 + m_S^2}{2}}, \quad (3.83)$$

where p^{*2} is fixed to the average mass. The reason for such a choice of p^{*2} lies on the fact that the mixed scalar self-energy at p^{*2} is independent on the gauge-fixing scheme. The gauge independence of the iOS scheme is also discussed in [59] where it is shown how the mixed scalar self energy at $p^{*2} = (m_H^2 + m_S^2)/2$ coincides with the gauge invariant part of the same quantity obtained through the so-called *pinch technique*, which generally allows the construction of off-shell Green's functions in non-Abelian gauge [60] or extended scalar [61] theories that are independent of the gauge-fixing parameter. For example, in [61] the authors calculate the NLO corrections to the Higgs boson couplings based on the OS renormalization scheme by using the pinch technique to remove the gauge dependence. The cancellation of the gauge dependence is also directly proven in the Higgs boson two-point functions computed in the linear R_ξ gauge by adding "pinch-terms" which are extracted from vertex corrections and box diagrams of a fermionic scattering process of the type $\bar{f}f \rightarrow \bar{f}f$.

3.2.3 Explicit Form of the MF Counterterms

To fix the non-diagonal scalar field renormalization $\delta Z_{HS}^{\text{mf}}$ (the superscript "mf" indicates the counterterm of the mixing scalar sector arising from the MF renormalization conditions) are determined using eq.(3.50) and eq.(3.54), we consider the renormalization factor for the bare scalar doublet $(\phi)_0$ and singlet fields $(s^0)_0$ in the gauge basis (reported in eq.(3.21)). This prescription is very similar to the renormalization procedure of the Higgs sector used in SM extensions like the 2HDM [62] and the MSSM [56]. Using the same orthogonal transformation introduced for the mass eigenstates, the physical wave functions for the scalar fields can be expressed in terms of the gauge basis ones $\delta Z_{\phi,s^0}$ as [29]:

$$\delta Z_H^{\text{mf}} = c_\alpha^2 \delta Z_\phi + s_\alpha^2 \delta Z_{s^0}, \quad (3.84)$$

$$\delta Z_S^{\text{mf}} = c_\alpha^2 \delta Z_{s^0} + s_\alpha^2 \delta Z_\phi, \quad (3.85)$$

$$\delta Z_{HS,SH}^{\text{mf}} = s_\alpha c_\alpha (\delta Z_\phi - \delta Z_{s^0}) = \frac{1}{2} t_{2\alpha} (\delta Z_H^{\text{mf}} - \delta Z_S^{\text{mf}}), \quad (3.86)$$

with $t_{2\alpha} = \tan 2\alpha$. These relations simplify in the so-called " $\overline{\text{MS}}$ scheme" where $\delta Z_{s^0}^{\overline{\text{MS}}} = 0$ ⁷ [29]:

$$\delta Z_H^{\text{mf}} = c_\alpha^2 \delta Z_\phi, \quad \delta Z_S^{\text{mf}} = s_\alpha^2 \delta Z_\phi, \quad \delta Z_{HS,SH}^{\text{mf}} = s_\alpha c_\alpha (\delta Z_H^{\text{mf}} - \delta Z_S^{\text{mf}}). \quad (3.87)$$

⁷The use of the $\overline{\text{MS}}$ scheme also allows us to neglect the counterterm δw in the physical definition of w , which is promoted to be an independent input parameter. Thus, no singlet vev counterterm appears in the one-loop calculations: $\delta w^{\overline{\text{MS}}} = 0$. Since δZ_{s^0} does not appear in the iOS scheme prescription, the renormalization condition on δw can be automatically imposed: $\delta w_{\text{ios}}^{\overline{\text{MS}}} = 0$.

Notice that $\delta Z_{HS}^{\text{mf}}$ is not an independent counterterm; in addition the mixed mass (mixing angle) counterterm is obtained by imposing the renormalization condition in eq.(3.55). In doing so, we have:

$$\delta m_{HS}^{2\text{mf}} = (m_S^2 - m_H^2)\delta\alpha^{\text{mf}} = \text{Re}\Sigma^{HS}(\mu_R^2) + \delta Z_{HS}^{\text{mf}} \left(\mu_R^2 - \frac{m_H^2 + m_S^2}{2} \right). \quad (3.88)$$

3.2.4 Equivalence of the MF and iOS Schemes

Assuming $p^{*2} = \mu_R^2 = (m_H^2 + m_S^2)/2$, we can prove the equivalence of the MF and the iOS schemes at this scale⁸. To this aim, it is enough to take into account a three-point interaction where there is at least one of the SSM scalar fields.

Let us consider a generic $S \rightarrow ij$ interaction described by the LO coupling g_{Sij} , where i and j can be any possible fields which interact with the S field. For simplicity, we neglect only the $S \rightarrow HH$ channel which implies a more complicated NLO coupling structure (the equivalence which we will discuss below can be easily proven for the $S \rightarrow HH$ case). The counterterms associated with MF and iOS schemes only appear in the renormalized coupling at the NLO (g_{Sij}^{NLO}) which is described by the generic Feynman diagrams reported in Fig.(3.2) and assumes the following form (for simplicity we use the δm_{HS}^2 prescription where no mixing angle counterterm arises):

$$g_{Sij}^{\text{NLO}} = g_{Sij} \left[1 + \frac{\delta Z_S + \delta Z_i + \delta Z_j}{2} + \frac{g_{Hij}}{g_{Sij}} \left(\frac{\delta Z_{HS}}{2} + \hat{Z}_{SH} \right) + \frac{\delta g_{Sij}}{g_{Sij}} + \delta V_{Sij} \right], \quad (3.89)$$

where $\delta Z_{S,i,j}$ are the renormalization constants associated with the three external fields, g_{Hij} represents the general Hij coupling which multiplies the counterterms due to the mixing of $S \rightarrow H$, δg_{Sij} can be expressed in terms of the counterterms which depend on the parameters contained in the g_{Sij} expanded form and δV_{Sij} is associated with the vertex correction. The only terms, which have different definitions in the two renormalization schemes, are those in eq.(3.89) inside the parenthesis (...):

$$\left(\frac{\delta Z_{HS}}{2} + \hat{Z}_{SH} \right) = \frac{\delta Z_{HS}}{2} + \frac{\text{Re}\hat{\Sigma}^{HS}(m_S^2)}{m_H^2 - m_S^2}, \quad (3.90)$$

with $\hat{Z}_{SH} = 0$ for the iOS renormalization condition (see eq.(3.54)). Therefore, we can verify the equivalence of these schemes discussing the following relation:

$$\frac{\delta Z_{HS}^{\text{ios}}}{2} \stackrel{?}{=} \frac{\delta Z_{HS}^{\text{mf}}}{2} + \frac{\text{Re}\hat{\Sigma}^{HS}(m_S^2)}{m_H^2 - m_S^2}, \quad (3.91)$$

⁸Obviously, the equivalence of these schemes implies that the gauge dependence of the MF scheme disappears only if $\mu_R^2 = (m_H^2 + m_S^2)/2$.

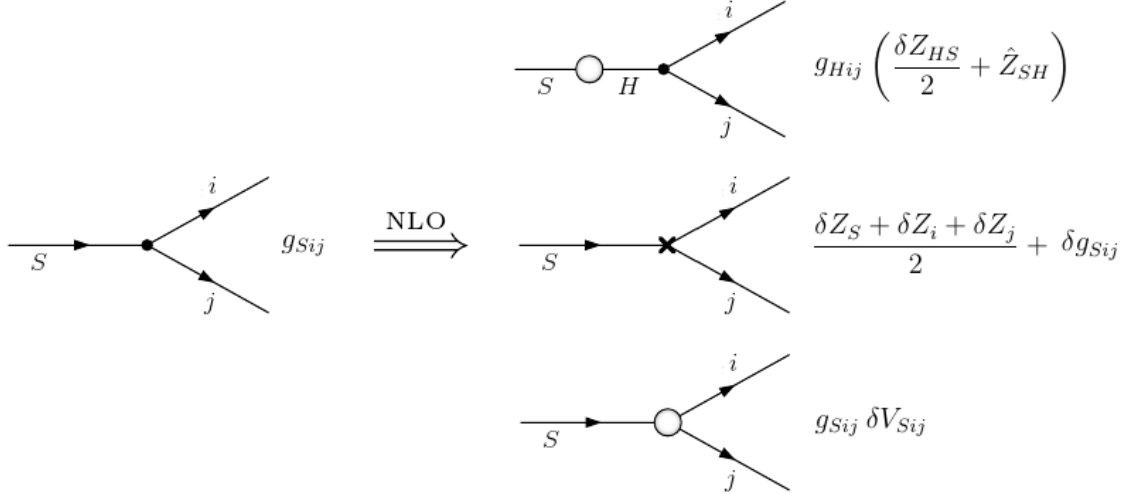


Figure 3.2: *Feynman diagrams associated with the NLO corrections to the LO coupling g_{Sij} with $ij \neq HH$.*

where the renormalized mixed scalar self energy, $Re\hat{\Sigma}^{HS}(p^2)$, is defined in eq.(3.50) and has to be expanded only in terms of the MF counterterms. Now, we must consider the following aspects of MF renormalization scheme: i) the definition of $\delta m_{HS}^{2\text{mf}}$, shown in eq.(3.88); ii) the relation between the mixed field renormalization constants: $\delta Z_{HS}^{\text{mf}} = \delta Z_{SH}^{\text{mf}}$. Using such definitions, eq.(3.50) becomes:

$$Re\hat{\Sigma}^{HS}(p^2) = Re\Sigma^{HS}(p^2) - Re\Sigma^{HS}(\mu_R^2) + \delta Z_{HS}^{\text{mf}}(p^2 - \mu_R^2). \quad (3.92)$$

Introducing eq.(3.82), eq.(3.83) and eq.(3.92) into eq.(3.91), we get:

$$\begin{aligned} \frac{Re\Sigma^{HS}(m_S^2) - Re\Sigma^{HS}(p^{*2})}{m_H^2 - m_S^2} &\stackrel{?}{=} \frac{Re\Sigma^{HS}(m_S^2) - Re\Sigma^{HS}(\mu_R^2)}{m_H^2 - m_S^2} + \\ &+ \frac{\delta Z_{HS}^{\text{mf}}}{m_H^2 - m_S^2} \left(\frac{m_H^2 + m_S^2}{2} - \mu_R^2 \right). \end{aligned} \quad (3.93)$$

This equivalence is confirmed by substituting $p^{*2} = \mu_R^2 = (m_H^2 + m_S^2)/2$; in fact the last term is cancelled out and the remaining terms become identical.

Hereafter,

we will treat the NLO decay rates of our interest in terms of the iOS counterterms preserving the gauge invariance in the physical observables. On the other hand, we separately give a comment on the gauge-dependent results using the MF prescription for fixed values of $\mu_R^2 \neq p^{*2}$ in order to roughly analyze the impact of the gauge dependence on the decay rates.

Chapter 4

Singlet Decay Widths at the Next-to-Leading Order

In order to calculate the NLO decay widths, we have to absorb the higher order contributions in the absolute square of the process amplitudes ($|\mathcal{M}_{Sij}^{\text{NLO}}|^2$):

$$|\mathcal{M}_{Sij}^{\text{NLO}}|^2 = |\mathcal{M}_{Sij}^{\text{LO}} + \mathcal{M}_{Sij}^{\text{1L}}|^2 \approx |\mathcal{M}_{Sij}^{\text{LO}}|^2 + 2\text{Re}[\mathcal{M}_{Sij}^{\text{LO}}\mathcal{M}_{Sij}^{\text{1L}*}] + \mathcal{O}_{2\text{L}}, \quad (4.1)$$

with i, j generic fields entering the process under study (the superindices "1L" and "2L" stand for "one-loop" and "two-loops", respectively). Notice that we are neglecting the "2L" - orders (NNLO). We can define the amplitudes $\mathcal{M}_{Sij}^{\text{LO,1L}}$ in the following way:

$$\mathcal{M}_{Sij}^{\text{LO}} = g_{Sij} A^{\text{LO}} \quad , \quad \mathcal{M}_{Sij}^{\text{1L}} = g_{Sij} A^{\text{LO}} \delta A^{\text{1L}}, \quad (4.2)$$

where g_{Sij} is the interaction coupling, A^{LO} includes the polarization or spinorial structures (in the scalar case $A^{\text{LO}} = 1$) and δA^{1L} represents all possible NLO correction terms. Following eq.(2.2), Γ^{LO} becomes proportional to $g_{Sij}^2 \sum_{\text{d.o.f}} |A^{\text{LO}}|^2$ and the decay rate at NLO assumes the following form:

$$\Gamma^{\text{NLO}} \approx \Gamma^{\text{LO}} [1 + 2\delta A^{\text{1L}}]. \quad (4.3)$$

The one-loop corrected decay width may also receive a supplementary contribution due to real corrections which occur when some of the external particles are charged. These additional contributions are typically called "brems-strahlung" and "gluons-strahlung" processes (we will discuss in details these contributions for $S \rightarrow W^+W^-$, $f\bar{f}$ decay rates) in the case of photon and gluon emissions, respectively. As a consequence of the external charged states, δA^{1L} is affected by infrared (IR) divergences since photon or gluon propagators may appear in the loops. In this case, the role of the brems- and gluons- strahlung processes is to regularize these divergences and we generally have:

$$\Gamma^{\text{NLO}} \approx \Gamma^{\text{LO}} [1 + 2\delta A^{\text{1L}}] + \Gamma^{\text{brems}} + \Gamma^{\text{gluon}}, \quad (4.4)$$

where the last term represents the photon and the gluon emission contributions to the process. We will determine in the next sections the NLO decay widths for the dominant S decay channels.

4.1 NLO Decay Width to Gauge Bosons

In this section we apply the renormalization procedure described in Sect.3.2 to the vertex of the scalar field S with two gauge bosons. The tree-level amplitude for the $S \rightarrow VV$ decays (with $V = W^\pm, Z$) is given by:

$$\mathcal{M}^{\text{LO}}[S(k) \rightarrow V(p, a)V(q, b)] = \mathcal{M}_{SVV}^{\text{LO}} = -i \rho_V \times [g^{\mu\nu} \epsilon_\mu^a(p) \epsilon_\nu^b(q)], \quad (4.5)$$

where p and q are the four momenta of the vector bosons and a, b their polarizations.

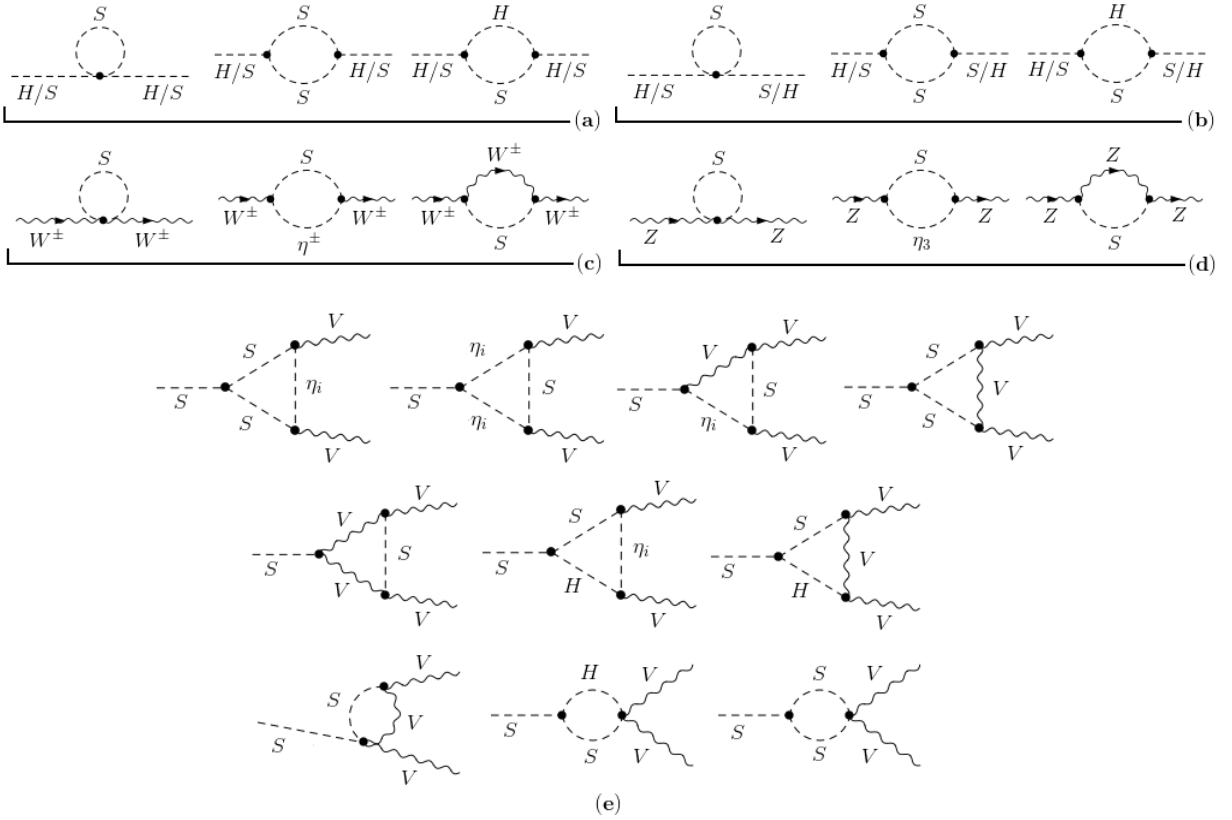


Figure 4.1: Fig.(a): S field contributions to the scalar self-energies; Fig.(b): S field contributions to the mixed scalar self-energies; Fig.(c): S field contributions to the W boson self energies; Fig.(d): S field contributions to the Z boson self energies; Fig.(e): S field contribution to the SVV vertex.

Here ρ_V is the SSM bare coupling ¹ defined as

$$\rho_V = e \frac{m_V^2}{s_W m_W} s_\alpha. \quad (4.7)$$

The related Feynman diagrams associated with the NLO corrections are reported in Fig.(4.1); we only show the contributions due to the insertion of the S field in the loops since diagrams with external S fields are similar to those of the SM quoted in [57] with the external Higgs replaced by S .

The bare coupling and the one-loop corrections to the SVV vertex can be put in the following form [57]:

$$\mathcal{V}^{\mu\nu} = \mathcal{V}_0^{\mu\nu} + \rho_V T_V^{\mu\nu}, \quad (4.8)$$

where ρ_V has been defined in eq.(4.7) and $\mathcal{V}_0^{\mu\nu} = \rho_V g^{\mu\nu}$. The generic expansion of $T_V^{\mu\nu}$ in terms of 2-index tensors is given by [57]:

$$T_V^{\mu\nu} = \mathcal{A}_V k^\mu k^\nu + \mathcal{B}_V q^\mu q^\nu + \mathcal{C}_V k^\mu q^\nu + \mathcal{D}_V q^\mu k^\nu + \mathcal{E}_V g^{\mu\nu} + i\mathcal{F}_V \epsilon^{\mu\nu\rho\sigma} k_\rho q_\sigma, \quad (4.9)$$

where k and q are the four-vectors of the external gauge bosons. The coefficient $\mathcal{A}_V, \dots, \mathcal{F}_V$ have to be ultra-violet (UV) finite whereas the term proportional to the antisymmetric tensor $\epsilon^{\mu\nu\rho\sigma}$ vanishes due to the charge conjugation invariance for external Z bosons and also if the gauge bosons are on the mass-shell. We decide to set the external squared momenta $[p^2, k^2, q^2]$ in the $S(k)V(k, a)V(q, b)$ vertex as $[m_S^2, m_V^2, m_V^2]$. We take real gauge bosons, so that only the coefficients \mathcal{D}_V and \mathcal{E}_V become relevant. Since the counterterms arising from the quantities in eq.(4.7) are included in the coefficient \mathcal{E}_V , we put it in the form $\mathcal{E}_V = \delta\rho_V + \delta V_V^\mathcal{E}$, where the symbol δV indicates the three point function at the one loop level and $\delta\rho_V$'s are:

$$\delta\rho_W = \frac{\delta m_W^2}{2m_W^2} - \frac{\delta s_W^2}{2s_W^2} + \delta Z_W + \delta Z_e + \frac{\delta Z_S}{2} + \frac{c_\alpha}{s_\alpha} \left(\frac{\delta Z_{HS}^{\text{ios}}}{2} - \delta\alpha^{\text{ios}} \right) + \frac{\delta s_\alpha^{\text{ios}}}{s_\alpha}, \quad (4.10)$$

$$\delta\rho_Z = \frac{\delta m_Z^2}{m_Z^2} - \frac{\delta m_W^2}{2m_W^2} - \frac{\delta s_W^2}{2s_W^2} + \delta Z_Z + \delta Z_e + \frac{\delta Z_S}{2} + \frac{c_\alpha}{s_\alpha} \left(\frac{\delta Z_{HS}^{\text{ios}}}{2} - \delta\alpha^{\text{ios}} \right) + \frac{\delta s_\alpha^{\text{ios}}}{s_\alpha}. \quad (4.11)$$

Notice that we obtain $\delta\rho_V$ independent from the mixing angle counterterm using the following substitution: $\delta s_\alpha^{\text{ios}} = c_\alpha \delta\alpha^{\text{ios}}$. The other counterterms entering the previous expressions have been listed in Subsect.(3.2.1-3.2.2). To avoid the explicit presence of the light fermions contributions to the NLO results, we use the MOMS scheme which means that $\delta Z_e \rightarrow \delta Z'_e$

¹Notice that for the lightest mass eigenstate H the following replacement applies in eq.(4.41):

$$S(k) \rightarrow H(k) \quad \Longrightarrow \quad \rho_V \rightarrow \rho_V c_\alpha / s_\alpha. \quad (4.6)$$

(discussed below eq.(3.78)). Performing the MOMS shift, we determine a compact form of $\delta\rho_V$ which now we call $\delta\rho_V'$:

$$\delta\rho_V' = \delta Z_V + \frac{\delta Z_S}{2} + \frac{c_\alpha}{s_\alpha} \frac{\delta Z_{HS}^{\text{ios}}}{2} + \frac{\delta m_V^2}{m_V^2} - \frac{\widetilde{Re}\Sigma_T^{WW}(0)}{2m_W^2} + \frac{Re\Sigma_T^{AZ}(0)}{s_W c_W m_Z^2} - \mathcal{C}_{\text{muon}}. \quad (4.12)$$

The coefficient \mathcal{E}_V is UV-finite both for Z and W external boson pairs, as it can be explicitly verified from the expressions of the bosonic and fermionic divergent parts quoted in Tab.(4.1) for all counterterms (which are divided by a common factor $g^2/(16\pi^2 \epsilon)$). Regarding the finite

	\mathcal{E}_W	\mathcal{E}_Z	UV _{bosonic}	UV _{fermionic}
δZ_W	✓	✗	19/6	-4
δZ_Z	✗	✓	$\frac{-1+2c_W^2+18c_W^4}{6c_W^2}$	$\frac{-20+40c_W^2-32c_W^4}{3c_W^2}$
$\delta Z_S/2$	✓	✓	$\frac{s_\alpha^2(2c_W^2+1)}{4c_W^2}$	$-\frac{s_\alpha^2 \sum_f N_c m_f^2}{4m_W^2}$
$c_\alpha \delta Z_{HS}^{\text{ios}}/2s_\alpha$	✓	✓	$\frac{c_\alpha^2(2c_W^2+1)}{4c_W^2}$	$-\frac{c_\alpha^2 \sum_f N_c m_f^2}{4m_W^2}$
$\delta m_W^2/m_W^2$	✓	✗	$\frac{6-31c_W^2}{6c_W^2}$	$4 - \frac{\sum_f N_c m_f^2}{2m_W^2}$
$\delta m_Z^2/m_Z^2$	✗	✓	$\frac{7+10c_W^2-42c_W^4}{6c_W^2}$	$\frac{20-40c_W^2+32c_W^4}{3c_W^2} - \frac{\sum_f N_c m_f^2}{2m_W^2}$
$-\widetilde{Re}\Sigma_T^{WW}(0)/2m_W^2$	✓	✓	$\frac{2c_W^2-1}{2c_W^2}$	$\frac{\sum_f N_c m_f^2}{4m_W^2}$
$Re\Sigma_T^{AZ}(0)/s_W c_W m_Z^2$	✓	✓	-2	—
$\delta V_W^\mathcal{E}$	✓	✗	$\frac{-3+10c_W^2}{4c_W^2}$	$\frac{\sum_f N_c m_f^2}{2m_W^2}$
$\delta V_Z^\mathcal{E}$	✗	✓	$\frac{-3-6c_W^2+16c_W^4}{4c_W^2}$	$\frac{\sum_f N_c m_f^2}{2m_W^2}$
$\mathcal{C}_{\text{muon}}$	✓	✓	—	—

Table 4.1: *Coefficients of the bosonic and fermionic UV divergent parts of the relevant counterterms (which are divided by the common factor $g^2/(16\pi^2 \epsilon)$). The symbol ✓ (✗) indicates that the corresponding counterterm is present (absent) in $\mathcal{E}_{W,Z}$.*

parts, we know that the S field gives negligible contributions to the corrections of the muon decay and since there is no S field dependence in $\Sigma_T^{AZ}(0)$ [26], the new scalar contributions only affect the bosonic parts of $\widetilde{Re}\Sigma_T^{WW}(0)$, δm_Z^2 , δZ_Z , δZ_S , $\delta Z_{HS}^{\text{ios}}$ and $\delta V_V^\mathcal{E}$. The fermionic contributions of $\widetilde{Re}\Sigma_T^{WW}(0)$, δm_Z^2 , δZ_Z and $\delta V_V^\mathcal{E}$ are identical to those associated to the HVV vertex in the SM; in addition, their contributions to δZ_S and $\delta Z_{HS}^{\text{ios}}$ can be determined from the fermion loop terms in the SM δZ_H expression but now multiplied by s_α^2 and $c_\alpha s_\alpha$ and with external momenta fixed to m_S^2 (the definition of $\delta Z_{HS}^{\text{ios}}$ also contains the mixed two-point function with external momenta fixed to $(m_H^2 + m_S^2)/2$).

Notice that the renormalization of the vertex SW^+W^- is more complicated than the SZZ vertex since contributions due to the photons in the loop integrals, which are plagued by infrared (IR) singularities when the W bosons are on-shell, must be taken into account. The IR-cancellation is obtained considering soft-photon bremsstrahlung contributions [63] which, for the model under discussion, are shown in Fig.(4.2).

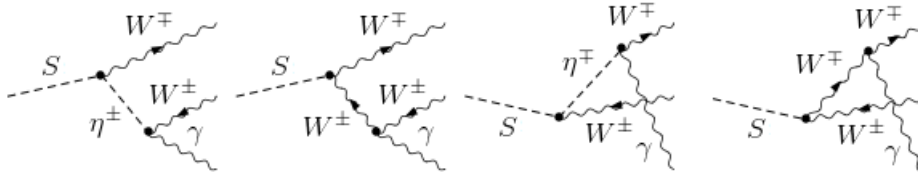


Figure 4.2: *Feynman diagrams of the photon bremsstrahlung associated to the first-order radiative corrected $SW^+W^-(\gamma)$ vertex.*

We call the external photon momenta as q_γ whose maximum value is $q_\gamma^{\max} = m_S(1 - 4x_W)/2$. In addition, to regularize the IR-divergences it is necessary to assign a virtual mass m_γ to the photon which works as an infrared regulator. Typically, a bremsstrahlung photon can be a soft or a hard photon. Differently from hard photons which are detected in the final state, the soft photons have typical energies smaller than the energy threshold of the experiment and they are not detected. To set an ideal boundary between the soft and hard region, we introduce a cutoff Λ_γ in such a way that the soft region corresponds to $m_\gamma \leq q_\gamma \leq \Lambda_\gamma$ while the hard region to $\Lambda_\gamma \leq q_\gamma \leq q_\gamma^{\max}$. The total photon-bremsstrahlung decay rate is then given by the sum of the soft and hard contributions:

$$\Gamma_{WW}^{\text{brem}} = \Gamma_{WW}^{\text{soft}} + \Gamma_{WW}^{\text{hard}} = \Gamma_{WW}^{\text{LO}}(\delta_W^{\text{soft}} + \delta_W^{\text{hard}}), \quad (4.13)$$

where we generally have $\Gamma_{ii} = \Gamma(S \rightarrow ii)$ and the correction factors δ_W^{soft} and δ_W^{hard} are extracted from [63]:

$$\delta_W^{\text{soft}} = \frac{\alpha_{\text{em}}}{\pi} \left\{ \mathcal{N}_0 \ln \left(\frac{4\Lambda_\gamma^2}{m_\gamma^2} \right) + (\mathcal{N}_0 + 1) \left[\frac{\mathcal{N}_1}{a_1} + \frac{2}{2r - 1} \right] \right\}, \quad (4.14)$$

$$\begin{aligned} \delta_W^{\text{hard}} = & \frac{\alpha_{\text{em}}}{\pi} \left\{ \mathcal{N}_0 \ln \left(\frac{m_S^2}{4\Lambda_\gamma^2} \right) + \frac{\mathcal{N}_2 (\mathcal{N}_0 + 1)}{a_1} + \frac{14}{3} \left(1 - \frac{t}{r} \sqrt{1 - \frac{1}{t}} \right) + \right. \\ & + \frac{1}{\mathcal{N}_3} \left[\frac{a_2 - a_1}{2r^2} \left(2 - \frac{1}{r} \right) + \frac{t}{3r} \sqrt{1 - \frac{1}{t}} \left(1 - \frac{t}{r} \right) \left(2 - \frac{4t - 1}{r} \right) \right] - \\ & \left. - 2 \ln \left(\frac{1 - (c_- d_+)^2}{1 - (c_- d_-)^2} \right) + 4 \left(\frac{t}{r} a_2 - b_- \right) \right\}, \quad (4.15) \end{aligned}$$

with,

$$\mathcal{N}_0 = [a_1(2 - 1/r)/(\sqrt{1 - 1/r})] - 1, \quad (4.16)$$

$$\mathcal{N}_1 = \text{Li}_2(c_-^2) + a_1(a_1 - 2b_-) - (\pi^2/6), \quad (4.17)$$

$$\begin{aligned} \mathcal{N}_2 = & \text{Li}_2((c_-d_+)^2) - \text{Li}_2((c_-d_-)^2) + \text{Li}_2(c_-)^4 + 4a_1(a_1 - b_+) + \\ & + 2a_2 \ln[(1 - (c_-d_+)^2)(1 - (c_-d_-)^2)] - (\pi^2/6), \end{aligned} \quad (4.18)$$

$$\mathcal{N}_3 = \sqrt{1 - 1/r} [1 - (1/r) + (3/4)r^2], \quad (4.19)$$

$$a_1 = \ln(c_+), a_2 = \ln(d_+), b_{\pm} = \ln(c_{\pm} \pm c_-), \quad (4.20)$$

$$c_{\pm} = \sqrt{r} \pm \sqrt{r-1}, d_{\pm} = \sqrt{t} \pm \sqrt{t-1}. \quad (4.21)$$

and $r = m_S^2/4m_W^2$, $t = r(1 - 2q_\gamma/m_S)^2$.

The m_γ and Λ_γ dependencies show up in δZ_W , $\delta V_W^\mathcal{E}$, δ_W^{soft} and δ_W^{hard} , as detailed in Tab.(4.2). The function \mathcal{N}_0 is defined in App.A.

	m_γ (IR regulator)	Λ_γ (IR cutoff)
δZ_W	$\frac{\alpha_{em}}{2\pi} \ln\left(\frac{m_W^2}{m_\gamma^2}\right)$	—
$\delta V_W^\mathcal{E}$	$\frac{\alpha_{em}}{2\pi} [\mathcal{N}_0 + 1] \ln\left(\frac{m_W^2}{m_\gamma^2}\right)$	—
δ_W^{soft}	$\frac{\alpha_{em}}{\pi} \mathcal{N}_0 \ln\left(\frac{m_W^2}{m_\gamma^2}\right)$	$\frac{\alpha_{em}}{\pi} \mathcal{N}_0 \ln\left(\frac{4\Lambda_\gamma^2}{m_W^2}\right)$
δ_W^{hard}	—	$\frac{\alpha_{em}}{\pi} \mathcal{N}_0 \ln\left(\frac{m_S^2}{4\Lambda_\gamma^2}\right)$

Table 4.2: IR-dependence on m_γ and Λ_γ in δZ_W , $\delta V_W^\mathcal{E}$, δ_W^{soft} and δ_W^{hard} .

Finally, the NLO total decay width which we call Γ_{VV}^{NLO} can be defined as:

$$\begin{aligned} \Gamma_{VV}^{\text{NLO}} = & \frac{G_F}{16\sqrt{2}\pi} m_S^3 s_\alpha^2 (1 + \delta_V) \sqrt{1 - 4x_V} (1 - 4x_V + 12x_V^2) \times \\ & \times \left\{ 1 + 2 \left[\delta\rho_{V'} + \delta V_V^\mathcal{E} + \frac{m_S^2}{2} \left(\frac{1 - 6x_V + 8x_V^2}{1 - 4x_V + 12x_V^2} \right) \delta V_V^\mathcal{D} \right] \right\} + \delta_V \Gamma_{WW}^{\text{brem}}, \end{aligned} \quad (4.22)$$

²Notice that for $q_\gamma = q_\gamma^{\text{max}}$, eq.(4.15) is reduced to,

$$\delta_W^{\text{hard}} = \frac{\alpha_{em}}{\pi} \left\{ \mathcal{N}_0 \ln\left(\frac{m_S^2}{4\Lambda_\gamma^2}\right) - 4b_- + \frac{14}{3} + \frac{(\mathcal{N}_0 + 1)}{a_1} \left[\text{Li}_2(c_-)^4 - \frac{\pi^2}{6} + 4a_1(a_1 - b_+) - \frac{2a_1}{4r^2 - 4r + 3} \right] \right\}.$$

where $\delta V_V^{\mathcal{D}}$ are the corrections from the coefficient \mathcal{D}_V and $\delta_V = 0, 1$ for $V = Z, W^\pm$ respectively. Notice that the first row of eq.(4.22) is the LO decay width of eq.(2.4). Now, two comments are in order:

i) using the m_γ -dependent contributions, reported in Tab.(4.2), we can verify the cancellation of the IR-divergences:

$$\{\Gamma_{WW}^{\text{NLO}}\}_{\text{IR}} = \{\Gamma_{WW}^{\text{LO}} [1 + \delta_W^{\text{soft}} + 2(\delta Z_W + \delta V_W^{\mathcal{E}})]\}_{\text{IR}} \propto \left[1 + \frac{\alpha_{\text{em}}}{\pi} \mathcal{N}_0 \ln \left(\frac{4\Lambda_\gamma^2}{m_W^2} \right) \right]; \quad (4.23)$$

ii) the combination of all terms in Tab.(4.2) is Λ_γ -independent at $\mathcal{O}(\alpha_{em})$.

4.2 NLO Decay Width to Fermions

The dominant decay channel with fermionic final state is $S \rightarrow \bar{t}t$. The tree-level amplitude of this process is given by:

$$\mathcal{M}^{\text{LO}} [S(k) \rightarrow \bar{t}(p)t(q)] = \mathcal{M}_{Sff}^{\text{LO}} = -i\bar{U}(p) \rho_t V(q), \quad (4.24)$$

where ρ_t has the following form:

$$\rho_t = e \frac{m_t}{2s_W m_W} s_\alpha. \quad (4.25)$$

Following the same treatment for the Feynman diagrams discussed in the previous section, we only report in Fig.(4.3) the contributions due to the insertion of the S field in the loops since loops with the SM fields are equivalent to those quoted in [64] with the external Higgs leg replaced by the new scalar singlet.

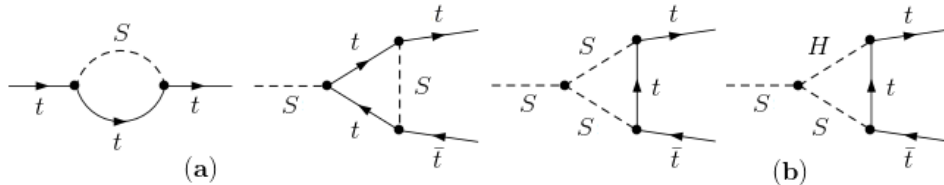


Figure 4.3: Fig.(a): S field contributions to the top quark self-energy; Fig.(b): S field contributions to the $S\bar{t}t$ vertex.

The bare coupling and the one-loop corrections to the $S\bar{t}t$ vertex can be expressed as:

$$\mathcal{V} = \rho_t(1 + T_t), \quad (4.26)$$

with T_t given by

$$T_t = \mathcal{A}_t + \mathcal{B}_t \not{k} + \mathcal{C}_t \not{q} + \mathcal{D}_t \not{k} \not{q} + \mathcal{E}_t \gamma_5 + \mathcal{F}_t \not{k} \gamma_5 + \mathcal{G}_t \not{q} \gamma_5 + \mathcal{H}_t \not{k} \not{q} \gamma_5, \quad (4.27)$$

where k and q are the four-momenta of the external top quarks. Obviously, the coefficients $\mathcal{A}_t, \dots, \mathcal{H}_t$ which appear in the T_t expression have to be UV-finite. In addition, it is possible to verify that the loop corrected decay rate is not affected by the γ_5 -terms at the NLO for the parity conserving [28]. The coupling counterterm $\delta\rho_t$ is enclosed in \mathcal{A}_t while all three-point functions are included in the remaining terms. We call the full set of NLO three-point corrections as δV_t . As set for the SVV case, we fix the external squared momenta in the $S(p)\bar{t}(k)t(q)$ vertex as: $[p^2, k^2, q^2] \rightarrow [m_S^2, m_t^2, m_t^2]$. Notice that this decay channel is also affected by QCD corrections. Therefore, we separately discuss the QCD-only contributions (denoted with a superscript "QCD") and the remaining electroweak corrections ("EW"). This distinction is needed for the counterterms $\delta m_t, \delta Z_{tV}, \delta V_t$.

• **EW Correction:**

We rewrite the EW expression of $\delta\rho_t$ as:

$$\begin{aligned} \delta\rho_t^{\text{EW}} = & \frac{\delta m_t^{\text{EW}}}{m_t} - \frac{\delta m_W^2}{2m_W^2} - \frac{\delta s_W^2}{2s_W^2} + \delta Z_{tV}^{\text{EW}} + \delta Z_e + \\ & + \frac{\delta Z_S}{2} + \frac{c_\alpha}{s_\alpha} \left(\frac{\delta Z_{HS}^{\text{ios}}}{2} - \delta\alpha^{\text{ios}} \right) + \frac{\delta s_\alpha^{\text{ios}}}{s_\alpha}. \end{aligned} \quad (4.28)$$

We can note the independence from the mixing angle counterterm which is eliminated by substituting $\delta s_\alpha^{\text{ios}} = c_\alpha \delta\alpha^{\text{ios}}$. By comparison with the gauge boson decay channel, the new counterterms are given by δm_t and δZ_{tV} which are defined in Subsect.(3.2.1-3.2.2). The application of the MOMS shift implies that $\delta\rho_t^{\text{EW}} \rightarrow \delta\rho_t^{\text{EW}'}$ which is then given by:

$$\delta\rho_t^{\text{EW}'} = \delta Z_{tV}^{\text{EW}} + \frac{\delta Z_S}{2} + \frac{c_\alpha}{s_\alpha} \frac{\delta Z_{HS}^{\text{ios}}}{2} + \frac{\delta m_t^{\text{EW}}}{m_t} - \frac{\widetilde{Re}\Sigma_T^{WW}(0)}{2m_W^2} + \frac{Re\Sigma_T^{AZ}(0)}{s_W c_W m_Z^2} - C_{\text{muon}}. \quad (4.29)$$

As a consequence of the external charged particles in the final state, the $S\bar{t}t$ vertex shows IR-divergences which are canceled by soft-photon bremsstrahlung contributions corresponding to the process $S \rightarrow \bar{t}t(\gamma)$ (shown in Fig.(4.4)) [64]. Using the $(m_\gamma, \Lambda_\gamma)$ -prescription, the total photon bremsstrahlung decay rate is given by:

$$\Gamma_{tt}^{\text{brem EW}} = \Gamma_{tt}^{\text{soft EW}} + \Gamma_{tt}^{\text{hard EW}} = \Gamma_{tt}^{\text{LO}} (\delta_t^{\text{soft EW}} + \delta_t^{\text{hard EW}}), \quad (4.30)$$

where $\delta_t^{\text{soft EW}}$ and $\delta_t^{\text{hard EW}}$ ³ are extracted from [64]:

³For $q_\gamma = q_\gamma^{\text{max}}$, eq.(4.32) is reduced to,

$$\begin{aligned} \delta_t^{\text{hard EW}} = & \frac{\alpha_{\text{em}}}{\pi} \left\{ \mathcal{N}_0 \ln \left(\frac{m_S^2}{4\Lambda_\gamma^2} \right) - 4b_- + \frac{26r - 29}{8(r-1)} + \right. \\ & \left. + \frac{(\mathcal{N}_0 + 1)(2 - 1/r)}{a_1} \left[\text{Li}_2(c_-)^4 - \frac{\pi^2}{6} + 4a_1(a_1 - b_+) - \frac{(8r^2 - 8r + 3)a_1}{8r(r-1)} \right] \right\}. \end{aligned}$$

$$\delta_t^{\text{soft EW}} = \frac{\alpha_{\text{em}}}{\pi} \left\{ \mathcal{N}_0 \ln \left(\frac{4\Lambda_\gamma^2}{m_\gamma^2} \right) + (\mathcal{N}_0 + 1) \left[\frac{\mathcal{N}_1}{a_1} + \frac{2}{2r-1} \right] \right\}, \quad (4.31)$$

$$\delta_t^{\text{hard EW}} = \frac{\alpha_{\text{em}}}{\pi} \left\{ \mathcal{N}_0 \ln \left(\frac{m_S^2}{4\Lambda_\gamma^2} \right) + \frac{\mathcal{N}_2(\mathcal{N}_0 + 1) + \mathcal{N}_4}{a_1} + \frac{26r-29}{8(r-1)} + \right. \\ \left. - 2 \ln \left(\frac{1 - (c-d_+)^2}{1 - (c-d_-)^2} \right) + 4 \left(\frac{t}{r} a_2 - b_- \right) \right\}, \quad (4.32)$$

with,

$$\mathcal{N}_4 = \frac{1}{8r(r-1)} (a_2 \mathcal{N}_5 + a_1 \mathcal{N}_6 + \mathcal{N}_7), \quad (4.33)$$

$$\mathcal{N}_5 = 8t^2 + 16tr - 32r^2 - 32t + 40r - 3, \quad (4.34)$$

$$\mathcal{N}_6 = 8r^2 - 8r + 3, \quad (4.35)$$

$$\mathcal{N}_7 = (9t - 2t^2 - 24tr) \sqrt{1 - 1/t}, \quad (4.36)$$

and the remaining quantities are the same mentioned for $S \rightarrow W^+W^-(\gamma)$ and defined below eq.(4.15). Notice that all these factors (listed in eqs.(4.16-4.21) and eqs.(4.33-4.36)) now have to be expressed in terms of $r = m_S^2/4m_t^2$.

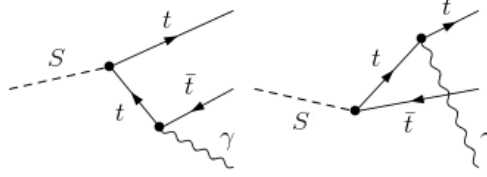


Figure 4.4: *Feynman diagrams of the photon bremsstrahlung associated to the first-order radiative corrected $S\bar{t}t(\gamma)$ vertex.*

- **QCD Correction:**

The total QCD corrections can be defined as:

$$\Delta V_t^{\text{QCD}} = \delta Z_{tV}^{\text{QCD}} + \frac{\delta m_t^{\text{QCD}}}{m_t} + \delta V_t^{\text{QCD}} + \frac{\delta_t^{\text{soft QCD}}}{2} + \frac{\delta_t^{\text{hard QCD}}}{2}, \quad (4.37)$$

where $\delta_t^{\text{soft QCD}}$ and $\delta_t^{\text{hard QCD}}$ stand for the soft and hard gluon emission corrections, respectively. These can be directly derived by $\delta_t^{\text{soft EW}}$ and $\delta_t^{\text{hard EW}}$ using the following replacements: $\alpha_{\text{em}} Q_t^2 \rightarrow 4\alpha_s/3$, $m_\gamma \rightarrow m_g$ and $\Lambda_\gamma \rightarrow \Lambda_g$ (with m_g and Λ_g acting as gluon mass regulator and cutoff energy). Notice that the scale of the momentum

transfer Q in the process is indicative of the effective strength of the strong interactions and this affects the running of α_s which is given at one-loop order by [50]:

$$\alpha_s(Q^2) = \frac{6}{33 - 2n_f} \frac{1}{\ln(Q^2/\Lambda_{\text{QCD}}^2)},$$

where Q is the typical scale related to the scalar singlet decay processes, $n_f = 6$ is the number of flavors when $m_S \geq 2m_t$ and $\Lambda_{\text{QCD}} \simeq 217$ MeV represents the basic QCD scale.

Since the only difference between $H_{\text{sm}} \rightarrow \bar{t}t(g)$ and $S \rightarrow \bar{t}t(g)$ processes lies in defining the external scalar field, we observe that the QCD one-loop factors corresponding to the SM and SSM cases (in terms of the respective scalar masses) are totally equivalent. These corrections are known in the SM and we report the results up to order $\mathcal{O}(\alpha_s^2)$ [65]:

$$\Delta V_t^{\text{QCD}} = \frac{C_F \alpha_s(m_S^2)}{\pi} \left\{ \frac{\mathcal{N}_8 + 17 \ln\left(\frac{c'_+}{c'_-}\right)}{2\beta} + \frac{21 - 13\beta \ln\left(\frac{c'_+}{c'_-}\right)}{16} - \frac{3 \left[2\beta - \ln\left(\frac{c'_+}{c'_-}\right) \right]}{32\beta^3} \right\}, \quad (4.38)$$

where $\beta = \sqrt{1 - 4m_t^2/m_S^2}$, $c'_\pm = m_S \pm \sqrt{m_S^2 - 4m_t^2}$ and \mathcal{N}_8 is defined as,

$$\mathcal{N}_8 = (1 + \beta^2) \left[4\text{Li}_2\left(\frac{c'_+}{c'_-}\right) + 2\text{Li}_2\left(-\frac{c'_+}{c'_-}\right) - \ln\frac{c'_+}{c'_-} \ln\frac{\beta^2}{(1 + \beta)^3} \right]. \quad (4.39)$$

Therefore, the NLO total decay width $\Gamma_{\bar{t}t}^{\text{NLO}}$ with the EW and QCD corrections is as follows:

$$\Gamma_{\bar{t}t}^{\text{NLO}} = s_\alpha^2 G_F N_c \frac{m_S m_t^2}{4\pi\sqrt{2}} \left(1 - \frac{4m_t^2}{m_S^2} \right)^{3/2} \times \left\{ 1 + 2 \left[\delta\rho_t^{\text{EW}'} + \delta V_t^{\text{EW}} + \Delta V_t^{\text{QCD}} \right] \right\} + \Gamma_{\bar{t}t}^{\text{brem,EW}}. \quad (4.40)$$

The definition of $\Gamma_{\bar{t}t}^{\text{NLO}}$ is UV- and IR- finite and this can be explicitly verified looking at the divergent parts of all counterterms. Some of these counterterms are in common with the SW^+W^- vertex and their divergent parts have been previously listed in Tab.(4.1) while for the remaining ones (δm_t , δZ_{tV} , δV_t , $\delta_t^{\text{soft EW}}$ and $\delta_t^{\text{hard EW}}$) the UV- and IR- divergent parts are separately quoted in Tab.(4.3) and Tab.(4.4).

Here, $C_F = 4/3$, $Q_t = +2/3$ is the top quark charge and the function \mathcal{N}_0 (see eq.(4.16)) has to be defined in terms of $r = m_t^2/4m_S^2$. Notice that the sum of all terms in Tab.(4.4) are Λ_γ and Λ_g -independent at $\mathcal{O}(\alpha_{\text{em}})$ and $\mathcal{O}(\alpha_s)$, respectively.

It is important to specify that the EW and the QCD corrections exhibit a threshold divergence if $m_S \rightarrow 2m_t = 346.68$ GeV; this is of the type $(\alpha_{\text{em},s}/\beta)$ where β is defined below eq.(4.38)

	UV ^{EW} _{bosonic}	UV ^{EW} _{fermionic}	UV ^{QCD} _{bosonic}	UV ^{QCD} _{fermionic}
δZ_{tV}	$-\frac{5}{36} - \frac{17}{72c_W^2}$	$-\frac{3m_t^2+m_b^2}{8m_W^2}$	$-\frac{C_F}{3}$	—
$\delta m_t/m_t$	$\frac{7}{12} - \frac{5}{24c_W^2}$	$\frac{3m_t^2-3m_b^2}{8m_W^2}$	$-C_F$	—
δV_t	$\frac{1}{18} + \frac{25}{36c_W^2}$	$\frac{m_b^2}{2m_W^2}$	$\frac{4}{3}C_F$	—

Table 4.3: *Coefficients of the bosonic and fermionic UV divergent parts (EW and QCD) of the new counterterms introduced for the $S\bar{t}t$ vertex. The EW and QCD coefficients are divided by the common factors $g^2/(16\pi^2 \epsilon)$ and $\alpha_s/(\pi \epsilon)$, respectively.*

	m_γ (IR regulator)	Λ_γ (IR cutoff)	m_g (IR regulator)	Λ_g (IR cutoff)
δZ_{tV}	$\frac{\alpha_{em} Q_t^2 \ln \frac{m_t}{m_\gamma}}{\pi}$	—	$\frac{C_F \alpha_s \ln \frac{m_t}{m_g}}{\pi}$	—
δV_t	$\frac{\alpha_{em} Q_t^2 [\mathcal{N}_0+1] \ln \frac{m_\gamma}{m_t}}{\pi}$	—	$\frac{C_F \alpha_s [\mathcal{N}_0+1] \ln \frac{m_g}{m_t}}{\pi}$	—
δ_t^{soft}	$\frac{\alpha_{em} Q_t^2 \mathcal{N}_0 \ln \frac{m_t}{m_\gamma}}{\pi}$	$\frac{\alpha_{em} Q_t^2 \mathcal{N}_0 \ln \frac{2\Lambda_\gamma}{m_\gamma}}{\pi}$	$\frac{C_F \alpha_s \mathcal{N}_0 \ln \frac{m_t}{m_g}}{\pi}$	$\frac{C_F \alpha_s \mathcal{N}_0 \ln \frac{2\Lambda_g}{m_g}}{\pi}$
δ_t^{hard}	—	$\frac{\alpha_{em} Q_t^2 \mathcal{N}_0 \ln \frac{m_S}{2\Lambda_\gamma}}{\pi}$	—	$\frac{C_F \alpha_s \mathcal{N}_0 \ln \frac{m_S}{2\Lambda_g}}{2\pi}$

Table 4.4: *EW and QCD IR-dependence on $m_{\gamma,g}$ and $\Lambda_{\gamma,g}$ of δZ_{tV} , δV_t , δ_t^{soft} and δ_t^{hard} .*

and represents the velocity of either fermion in the center-of-mass frame. For instance, the ΔV_t^{QCD} term is reduced to $\Delta V_t^{\text{QCD}} \simeq (\pi^2/2\beta) - 1$. Although this singularity is tamed by the LO factor β^3 (see eq.(2.14)) it, nevertheless, implies the breakdown of the perturbation theory at the threshold value. In this case, the NLO prediction can be improved by the resummation of all terms proportional to $(\alpha_{em,s}/\beta)^n$ which imply n -photon or gluon exchanges between the top and the antitop states. For the EW corrections, this procedure corresponds to use a non-relativistic Coulomb potential to describe the electromagnetic interactions between the decay products [66, 67]. On the other hand, this potential assumes a more complicated form for the QCD corrections but, in any case, we can avoid these singularities following alternative approaches, as those described in [68, 69]). However, we neglect the new NLO finite contributions arising from the procedure to cancel these threshold divergences since they are associated with the LO decay width results which are strongly suppressed for $m_S \simeq 2m_t$. Following [66, 69], we have verified that our results for the EW and QCD corrections become reliable once we exceed the physical threshold by more than 10 GeV. Therefore, we will perform the numerical analysis of the NLO corrections to the top quark final state for $m_S \geq 360$ GeV.

4.3 NLO Decay Width to Higgs Bosons

The three-level amplitude corresponding to the $S \rightarrow HH$ decay channel is simply due to the definition of the coupling C_{HHS} in eq.(1.21):

$$\mathcal{M}^{\text{LO}}[S(k) \rightarrow H(p)H(q)] = \mathcal{M}_{SHH}^{\text{LO}} = \rho_H \quad \text{with } \rho_H = C_{HHS}. \quad (4.41)$$

Therefore, the coupling ρ_H is a function of λ, κ, ρ and s_α, w, v . Notice that λ, κ, ρ , can be defined in terms of $m_H, m_S, \delta m_{HS}^2, T_H$ and T_S as mentioned in eqs.(1.39-1.41). As a consequence, the correction factor to the SHH coupling $\delta\rho_H$ will include the counterterms $\delta m_H^2, \delta m_S^2, \delta m_{HS}^{2\text{ios}} (\delta\alpha^{\text{ios}}), T_H, T_S$ and the Higgs vev counterterm δv which can be expressed in terms of $\delta Z_e, \delta m_W, \delta s_W$ (using $v = 2m_W s_W/e$).

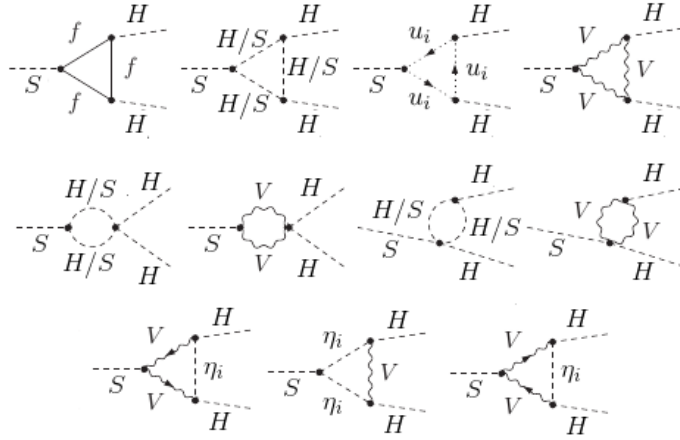


Figure 4.5: *Feynman diagrams associated to the SHH vertex corrections; u_i are the Ghosts and $\eta_i = \eta_0, \eta^\pm$ are the Goldstone bosons associated to the diagrams with $v = Z, W^\pm$, respectively.*

Including the field renormalization constant $\delta Z_S, \delta Z_H, \delta Z_{HS}^{\text{ios}}, \delta Z_{SH}^{\text{ios}}$, we can generally write $\delta\rho_H$ as:

$$\begin{aligned} \delta\rho_H = & c_1 \delta m_S^2 + c_2 \delta m_H^2 + c_3 \delta m_{HS}^{2\text{ios}} + c_4 \delta T_S + c_5 \delta T_H + \\ & + c_6 \left(\frac{\delta m_W^2}{2m_W^2} + \frac{\delta s_W^2}{2s_W^2} - \delta Z_e \right) + \delta Z_H + \frac{\delta Z_S}{2} + \frac{2C_{HHH} \delta Z_{HS}^{\text{ios}} + C_{HSS} \delta Z_{SH}^{\text{ios}}}{2C_{HHS}}, \end{aligned} \quad (4.42)$$

where the trilinear couplings C_{HHH}, C_{HSS} are given in eqs.(1.19-1.20) and the coefficients c_i ($i = 1, \dots, 6$) are defined as follows:

$$\begin{aligned}
c_1 &= \frac{1}{2m_H^2 + m_S^2}, & c_4 &= 3 \frac{c_\alpha s_\alpha (v^2 + w^2)}{v w (2m_H^2 + m_S^2) (c_\alpha w + s_\alpha v)}, \\
c_2 &= \frac{2}{2m_H^2 + m_S^2}, & c_5 &= 3 \frac{c_\alpha w - s_\alpha v}{v w (2m_H^2 + m_S^2)}, \\
c_3 &= \frac{s_\alpha w - c_\alpha v + (w/s_\alpha) - (v/c_\alpha)}{(2m_H^2 + m_S^2) (c_\alpha w + s_\alpha v)}, & c_6 &= \frac{c_\alpha w}{s_\alpha v + c_\alpha w}.
\end{aligned}$$

Notice that we have chosen the mixed mass counterterm prescription in terms of δm_{HS}^2 to simplify the structure of $\delta\rho_H$. After the application of the MOMS shift $\delta Z_e \rightarrow \delta Z'_e$, we get:

$$\begin{aligned}
\delta\rho_{H'} &= c_1 \delta m_H^2 + c_2 \delta m_S^2 + c_3 \delta m_{HS}^{2\text{ios}} + c_4 \delta T_H + & (4.43) \\
&+ c_5 \delta T_S + c_6 \left(\frac{\widetilde{Re}\Sigma_T^{WW}(0)}{2m_W^2} - \frac{Re\Sigma_T^{\gamma Z}(0)}{s_W c_W m_Z^2} + \frac{C_{\text{muon}}}{2} \right) + \\
&+ \delta Z_H + \frac{\delta Z_S}{2} + \frac{2C_{HHH} \delta Z_{HS}^{\text{ios}} + C_{HSS} \delta Z_{SH}^{\text{ios}}}{2C_{HHS}}.
\end{aligned}$$

Defining the three-point function corrections related to the SHH vertex as δV_H , whose Feynman diagrams are depicted in Fig.(4.5), we obtain the UV-divergence cancellation by the following sum: $\delta\rho_{H'} + \delta V_H$. This can be directly verified through the UV-divergence coefficients reported in Tab.(4.5).

In conclusion, the NLO total decay width Γ_{HH}^{NLO} is described by:

$$\Gamma_{HH}^{\text{NLO}} = \frac{(C_{HHS})^2}{32\pi m_H} \sqrt{1 - \frac{4m_H^2}{m_S^2}} \times \left\{ 1 + 2 \left[\delta\rho_{H'} + \delta V_H \right] \right\}. \quad (4.44)$$

4.4 NLO Total Decay Width

The NLO corrections to the total decay width of the scalar singlet particle can be expressed as the sum below:

$$\Gamma_{\text{TOT}}^{\text{NLO}} \simeq \Gamma_{WW}^{\text{NLO}} + \Gamma_{ZZ}^{\text{NLO}} + \Gamma_{tt}^{\text{NLO}} + \Gamma_{HH}^{\text{NLO}} + \sum_{ij} \Gamma_{ij}^{\text{LO}}, \quad (4.45)$$

where we only consider the LO contributions for the rare decays, represented by $ij = (gg, \gamma\gamma, Z\gamma, \bar{b}b, \bar{c}c, \bar{s}s, \bar{u}u, \bar{d}d, \tau^+\tau^-, \mu^+\mu^-, e^+e^-)$, being these channels already suppressed by the loop factor or the small fermion masses.

It is interesting to observe that we can define the NLO signal cross section at proton center-of-mass energy \sqrt{s} corresponding to the resonant process $pp \rightarrow S \rightarrow XY$ in terms of the

	UV _{bosonic}	UV _{fermionic}
δm_S^2	$\frac{s_\alpha^2 g^2 [9m_Z^2(1+2c_W^4) - 2m_S^2(1+2c_W^2)] - 2c_W^2 \left[\sum_{ij} \frac{2C_{ijS}^2}{1+\delta_{ij}} + \sum_{nm} m_n^2 C_{SSnm} \right]}{4c_W^2}$	$\frac{s_\alpha^2 g^2 \sum_f N_c (m_f^2 m_S^2 - 6m_f^4)}{2m_W^2}$
δm_H^2	$\frac{c_\alpha^2 g^2 [9m_Z^2(1+2c_W^4) - 2m_H^2(1+2c_W^2)] - 2c_W^2 \left[\sum_{ij} \frac{2C_{Hij}^2}{1+\delta_{ij}} + \sum_{nm} m_n^2 C_{HHnm} \right]}{4c_W^2}$	$\frac{c_\alpha^2 g^2 \sum_f N_c (m_f^2 m_H^2 - 6m_f^4)}{2m_W^2}$
$\delta m_{HS}^{\text{ios}2}$	$\frac{s_{2\alpha} g^2 [9m_Z^2(1+2c_W^4) - 2p^{*2}(1+2c_W^2)] - 4c_W^2 \left[\sum_{ij} \frac{2C_{Hij} C_{ijS}}{1+\delta_{ij}} + \sum_{nm} m_n^2 C_{HnmS} \right]}{8c_W^2}$	$\frac{s_{2\alpha} g^2 \sum_f N_c (m_f^2 p^{*2} - 6m_f^4)}{4m_W^2}$
δT_S	$\frac{-3s_\alpha g(1+2c_W^4) + c_W^4 \sum_{nm} C_{Snm} m_n^2}{2c_W^4}$	$\frac{2s_\alpha g \sum_f N_c m_f^4}{m_W}$
δT_H	$\frac{-3c_\alpha g(1+2c_W^4) + c_W^4 \sum_{nm} C_{Hnm} m_n^2}{2c_W^4}$	$\frac{2c_\alpha g \sum_f N_c m_f^4}{m_W}$
$c_6(\dots)$	$c_6 \frac{2c_W^2 + 1}{2c_W^2}$	$-\frac{c_6 \sum_f N_c m_f^2}{4m_W^2}$
δZ_H	$\frac{c_\alpha^2 g^2 (2c_W^2 + 1)}{2c_W^2}$	$-\frac{c_\alpha^2 g^2 \sum_f N_c m_f^2}{2m_W^2}$
δZ_S	$\frac{s_\alpha^2 g^2 (2c_W^2 + 1)}{2c_W^2}$	$-\frac{s_\alpha^2 g^2 \sum_f N_c m_f^2}{2m_W^2}$
$\delta Z_{HS}^{\text{ios}}$	$\frac{c_\alpha s_\alpha g^2 (2c_W^2 + 1)}{2c_W^2}$	$-\frac{s_{2\alpha} g^2 \sum_f N_c m_f^2}{4m_W^2}$
$\delta Z_{SH}^{\text{ios}}$	$\frac{c_\alpha s_\alpha g^2 (2c_W^2 + 1)}{2c_W^2}$	$-\frac{s_{2\alpha} g^2 \sum_f N_c m_f^2}{4m_W^2}$
δV_H	$\frac{c_\alpha g}{2} \sum_{kl} \frac{s_\alpha C_{Hkl} + c_\alpha C_{kls}}{[1+\delta_{kl}(2c_W^2-1)]} - \sum_{ij} \frac{2C_{Hij} C_{HijS} + C_{ijS} C_{HHij}}{1+\delta_{ij}}$	$-\frac{3c_\alpha^2 s_\alpha \sum_f N_c m_f^4}{m_W^3}$

Table 4.5: Coefficients of the bosonic and fermionic UV divergent parts of the counterterms associated with the SHH vertex. These are divided by the common factor $1/(16\pi^2 \epsilon)$. In this table $\{ij, nm, kl\}$ can be one of the combinations $ij = \{HH, SS, HS, \eta^+ \eta^-, \eta^0 \eta^0\}$, $nm = \{HH, SS, \eta^+ \eta^-, \eta^0 \eta^0\}$ and $kl = \{\eta^+ \eta^-, \eta^0 \eta^0\}$. Besides, $\delta_{ij, nm, kl}$ are equal to 1 for $\{HH, SS, \eta^0 \eta^0\}$ and to 0 for $\{HS, \eta^+ \eta^-\}$. The parenthesis (...) indicates the quantity in eq.(4.43) which multiplies the coefficient c_6 .

partial and total decay width expressions as,

$$\sigma(pp \rightarrow S \rightarrow XY) \simeq \frac{1}{m_S \Gamma_{\text{TOT}}^{\text{NLO}} s} \left[\sum_k C_{kk} \Gamma_{kk}^{\text{NLO}} \right] \Gamma_{XY}^{\text{NLO}}, \quad (4.46)$$

where $k = g, \gamma, b, c, s, u, d$ are the partons, XY are all possible decay channels of the particle associated with the resonance state and C_{kk} are the dimensionless partonic integrals defined as follows [71]:

$$C_{gg} = \frac{\pi^2}{8} \int_{m_S^2/s^2}^1 \frac{dx}{x} P_g(x) P_g(m_S^2/sx), \quad (4.47)$$

$$C_{\gamma\gamma} = 8\pi^2 \int_{m_S^2/s^2}^1 \frac{dx}{x} P_\gamma(x) P_\gamma(m_S^2/sx), \quad (4.48)$$

$$C_{\bar{q}q} = \frac{4\pi^2}{9} \int_{m_S^2/s^2}^1 \frac{dx}{x} [P_q(x) P_{\bar{q}}(m_S^2/sx) + P_{\bar{q}}(x) P_q(m_S^2/sx)]. \quad (4.49)$$

Numerical examples of $C_{\bar{k}k}$, computed using the MSTW2008NLO set of pdfs (P_k) at the scale $Q = m_S = 750$ GeV and $\sqrt{s} = 8, 13$ TeV, are given in Tab.(4.6) ⁴.

\sqrt{s}	$C_{\bar{b}b}$	$C_{\bar{c}c}$	$C_{\bar{s}s}$	$C_{\bar{d}d}$	$C_{\bar{u}u}$	C_{gg}	$C_{\gamma\gamma}$
8 TeV	1.07	2.7	7.2	89	158	174	11
13 TeV	15.3	36	83	627	1054	2137	54

Table 4.6: List of parton luminosity factors $C_{\bar{k}k}$ at the scale $Q = m_S = 750$ GeV and $\sqrt{s} = 8, 13$ TeV.

The higher order QCD corrections to the processes $gg, \bar{q}q \rightarrow S$ can be roughly expressed in terms of the so-called K-factors: $C_{gg, \bar{q}q} \rightarrow K_{gg, \bar{q}q} C_{gg, \bar{q}q}$ with $K_{gg} \simeq 2$ and $K_{\bar{q}q} \simeq 1.2$ (cf. [73, 74]).

4.5 NLO Application of the MF renormalization scheme

By applying the MF scheme prescription, we observe two main differences in the definitions of the Γ_i^{NLO} previously discussed. The first one is related to the mixing scalar sector counterterms and can be described by the following shifts: $\delta Z_{HS}^{\text{ios}} \rightarrow \delta Z_{HS}^{\text{mf}}$ and $\delta m_{HS}^2{}^{\text{ios}} (\delta\alpha^{\text{ios}}) \rightarrow \delta m_{HS}^2{}^{\text{mf}} (\delta\alpha^{\text{mf}})$. The second one lies in the insertion of the finite wave function corrections to the external scalar legs needed to absorb the residual factor which can be generated by the $H - S$ or $S - H$ oscillation if $\mu_R^2 \neq (m_H^2, m_S^2)$. Therefore, we must apply the following substitutions in order to obtain all NLO decay rates $S \rightarrow ZZ, W^+W^-, \bar{t}t, HH$ as a function of the MF counterterms:

$$\delta\rho_i'(\delta Z_{HS}^{\text{ios}}, \delta\alpha^{\text{ios}}) \rightarrow \delta\rho_i'(\delta Z_{HS}^{\text{mf}}, \delta\alpha^{\text{mf}}) + \delta\rho_i^{\text{WF}}. \quad (4.50)$$

Here, $\delta\rho_i^{\text{WF}}$ (with $i = Z, W, t, H$) are defined in the following way:

$$\delta\rho_Z^{\text{WF}} = \delta\rho_W^{\text{WF}} = \delta\rho_t^{\text{WF}} = \frac{c_\alpha}{s_\alpha} \hat{Z}_{SH} \quad , \quad \delta\rho_H^{\text{WF}} = \frac{C_{HHH}}{C_{HHS}} \hat{Z}_{SH} + 2 \frac{C_{HSS}}{C_{HHS}} \hat{Z}_{HS}, \quad (4.51)$$

⁴We obtain the same results of $C_{\bar{k}k}$ quoted in [72].

where $\hat{Z}_{SH,HS}$ are expressed in eq.(3.57). Using eq.(3.88) and eq.(3.92), we explicitly get:

$$\delta\rho_Z^{\text{WF}} = \delta\rho_W^{\text{WF}} = \delta\rho_t^{\text{WF}} = \frac{c_\alpha}{s_\alpha} \frac{\text{Re}\Sigma^{HS}(m_S^2) - \text{Re}\Sigma^{HS}(\mu_R^2) + \delta Z_{HS}^{\text{mf}}(m_S^2 - \mu_R^2)}{m_H^2 - m_S^2}, \quad (4.52)$$

$$\begin{aligned} \delta\rho_H^{\text{WF}} = & \frac{1}{C_{HHS}(m_H^2 - m_S^2)} \{ (2C_{HSS} - C_{HHH})[\text{Re}\Sigma^{HS}(\mu_R^2) + \mu_R^2 \delta Z_{HS}^{\text{mf}}] + \\ & + C_{HHH}[\text{Re}\Sigma^{HS}(m_S^2) + m_S^2 \delta Z_{HS}^{\text{mf}}] - 2C_{HSS}[\text{Re}\Sigma^{HS}(m_H^2) + m_H^2 \delta Z_{HS}^{\text{mf}}] \}. \end{aligned} \quad (4.53)$$

Chapter 5

Numerical Results

In this chapter, we will illustrate the numerical results for the NLO corrections to the scalar singlet decay rates discussed analytically in the previous chapters. It has to be specified that all amplitudes are computed with FEYNARTS [75] while their analytical processing was done with FORMCALC [75]. The outputs, written in terms of standard loop integrals [76, 77], have been evaluated with the help of PACKAGE-X [78].

In the evaluation of the corrections to the NLO decay rates we make use of the following quantity:

$$\mathcal{R}_i^{\text{SSM}} = [(\Gamma_i^{\text{NLO}}/\Gamma_i^{\text{LO}}) - 1], \quad (5.1)$$

with $i = WW, ZZ, HH, tt$ and TOT (which includes all decay channels). For the decay to top quarks, we will indicate whether the "EW + QCD" or only EW corrections are considered.

5.1 Dependence on s_α and w

We start evaluating $\mathcal{R}_i^{\text{SSM}}$ as a function of s_α for different values of m_S and w . It has to be considered that the maximally allowed ranges for $|s_\alpha|$ depend on the assumed singlet mass and such informations are summarized on Tab.(1.2). The numerical results are reported in Fig.(5.1). In the four panels we show separately the gauge boson channels $V = Z, W$; in the case of $V = W$ we fixed the momenta of the emitted photon-bremsstrahlung to its maximal value, $q_\gamma = q_\gamma^{\text{max}}$. For the considered final states we choose four fixed values of m_S : a high mass region with $m_S = (900, 1000)$ GeV and a low mass region with $m_S = (200, 300)$ GeV, $m_S = (300, 400)$ GeV and $m_S = (400, 500)$ GeV for $\mathcal{R}_{VV}^{\text{SSM}}$, $\mathcal{R}_{HH}^{\text{SSM}}$ and $\mathcal{R}_{tt}^{\text{SSM}}$, respectively. In order to roughly analyze the dependence on w , in the same plots we also show $\mathcal{R}_i^{\text{SSM}}$ computed for two different values of the singlet vev w : the smallest one (solid lines) is chosen according to the minimum reported in Tab.(1.2) while the largest is kept fixed at $w = 6.67v$ (dashed lines), which is a value used in [29] to determine the allowed intervals of s_α and, according to Tab.(1.2), valid for every m_S .

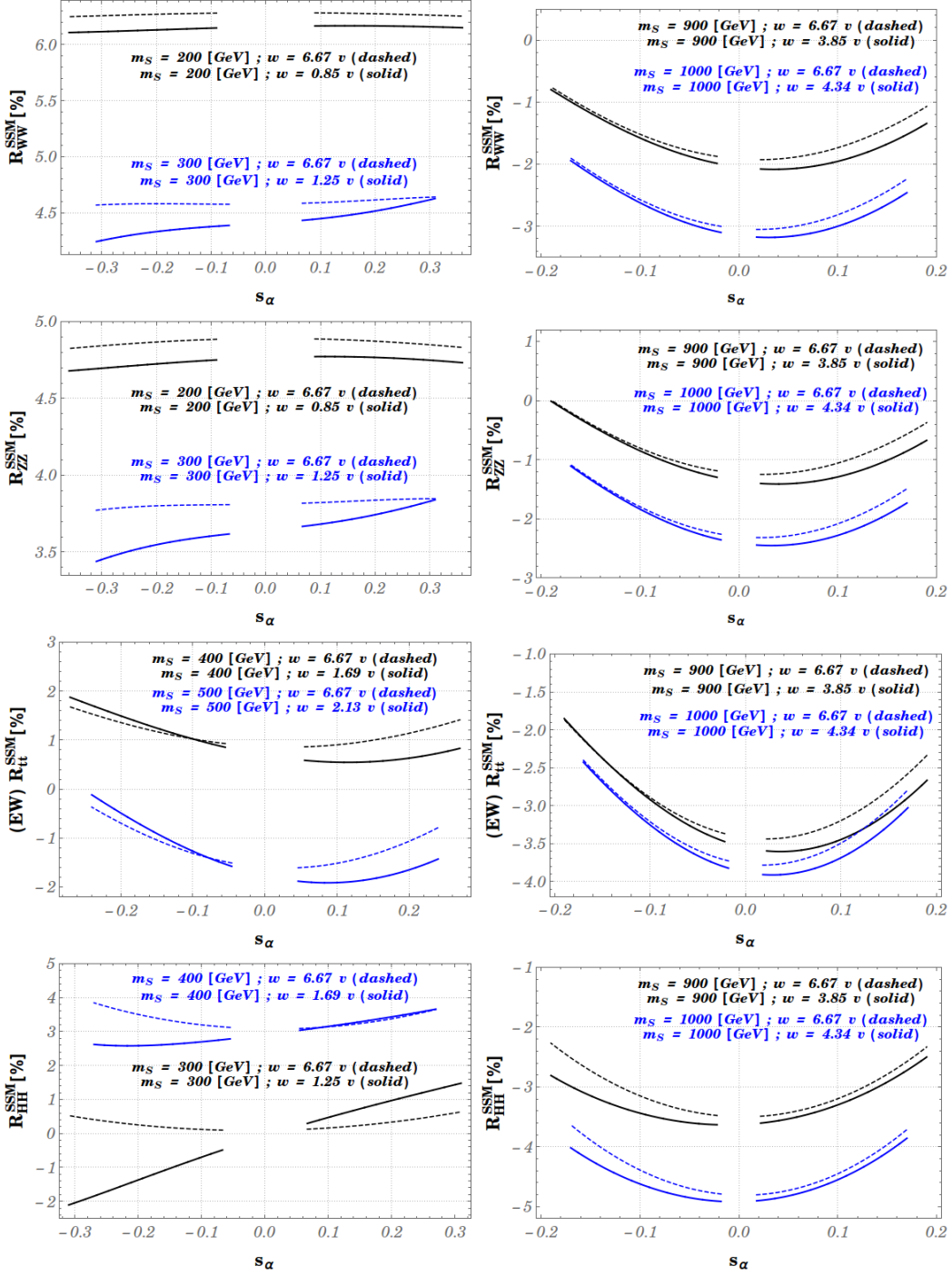


Figure 5.1: \mathcal{R}_i^{SSM} as a function of s_α , for different values of m_S (and the corresponding v_{ev} w). The range of s_α is the one deduced from Tab.(1.2). $\mathcal{R}_{WW,tt}^{SSM}$ are computed with $q_\gamma = q_\gamma^{max}$.

• **Low Mass Region**

We clearly see that the dependence on w corresponding to the gauge final states is not dramatic. For instance, the variation with w for both $\mathcal{R}_{ZZ}^{\text{SSM}}$ and $\mathcal{R}_{WW}^{\text{SSM}}$ amount to a maximum of $\mathcal{O}(8\%)$ when $m_S = 300$ GeV and $s_\alpha \sim -0.3$. For the fermionic final state we can note that the larger w -variations are associated with small correction values of $|\mathcal{R}_{tt}^{\text{SSM}}|$ which does not exceed $\mathcal{O}(2\%)$; an example is given by $\mathcal{R}_{tt}^{\text{SSM}}(w = 2.13v)/\mathcal{R}_{tt}^{\text{SSM}}(w = 6.67v) \sim 0.3$ for $m_S = 500$ GeV, $s_\alpha \sim -0.25$ and the corresponding correction values $\mathcal{R}_{tt}^{\text{SSM}} \sim (-0.1\%, -0.3\%)$ for $w = 2.13v$ and $6.67v$, respectively. On the other hand, the ratio $\mathcal{R}_{HH}^{\text{SSM}}$ shows a pronounced w -dependence especially in the case of s_α negative. This is due the fact that some of the loop contributions can be directly proportional to w and not strongly suppressed by the mixing.

We can also observe a dependence on s_α and its sign; in particular, the ratio $\mathcal{R}_{HH}^{\text{SSM}}$ shows large variations with s_α as expected for a process with mixed scalar fields as external particles; to be more quantitative: when $\mathcal{O}(3\%) \lesssim |\mathcal{R}_{HH}^{\text{SSM}}| \lesssim \mathcal{O}(4\%)$, for $m_S = 400$ GeV and $w = 1.69v$, the ratio $\mathcal{R}_{HH}^{\text{SSM}}(s_\alpha = 0.055)/\mathcal{R}_{HH}^{\text{SSM}}(s_\alpha = 0.27) \sim 0.75$ and in the case of $\mathcal{O}(1\%) \lesssim |\mathcal{R}_{HH}^{\text{SSM}}| \lesssim \mathcal{O}(2\%)$, for $m_S = 300$ GeV and $w = 1.25v$, we get $\mathcal{R}_{HH}^{\text{SSM}}(s_\alpha = 0.067)/\mathcal{R}_{HH}^{\text{SSM}}(s_\alpha = 0.31) \sim 0.2$. Regarding the ratios $\mathcal{R}_{WW,ZZ}^{\text{SSM}}$, these are weakly dependent on the mixing for $m_S \lesssim 300$ GeV while for $\mathcal{R}_{tt}^{\text{SSM}}$ this dependence is not totally negligible; for example, for $m_S = 400$ GeV and $w = 1.69v$, the ratio $\mathcal{R}_{tt}^{\text{SSM}}(s_\alpha = -0.055)/\mathcal{R}_{tt}^{\text{SSM}}(s_\alpha = -0.27) \sim 0.4$.

The reasons for such dependences on w and s_α are:

1. The loop interactions can be directly proportional to w and s_α .
2. The parameters κ , λ and ρ , entering $\mathcal{R}_i^{\text{SSM}}$ can be expressed as a function of w and s_α according to eq.(1.69).

On the other hand, the reason of different behaviors with respect to $\text{sign}(s_\alpha)$ has to be ascribed to those diagrams which contain odd powers of the coupling κ whose sign is only determined by $\text{sign}(s_\alpha)$. Typical Feynman diagrams with such a structure and that contribute to the mixing angle dependence of $\mathcal{R}_i^{\text{SSM}}$ are depicted in Fig.(5.2). Neglecting the loop integrals and using the approximate expressions in eq.(1.11) for simplicity, the couplings evaluated up to $\mathcal{O}(v^2/w^2)$ are the following:

$$\begin{aligned}
 \text{Fig.}(5.2\text{a}, 5.2\text{b}) \rightarrow & \quad (\text{SSH}) \sim \kappa v \quad , \quad (\text{HV}\eta^i) \propto \frac{m_V}{v} \quad , \quad (\text{SV}\eta^i) \propto s_\alpha \frac{m_V}{v} \sim \frac{\kappa m_V}{2\rho w} \quad , \\
 \text{Fig.}(5.2\text{c}) \rightarrow & \quad (\text{SSH}) \sim \kappa v \quad , \quad (\text{H}\bar{t}t) \propto \frac{m_t}{v} \quad , \quad (\text{S}\bar{t}t) \propto s_\alpha \frac{m_t}{v} \sim \frac{\kappa m_t}{2\rho w} \quad , \\
 \text{Fig.}(5.2\text{d}) \rightarrow & \quad (\text{SHH}) \sim \kappa w \quad , \quad (\text{HHH}) \propto \lambda_{\text{sm}} \quad , \quad (\text{SSH}) \propto \kappa \quad ,
 \end{aligned}$$

which in turn imply an overall dependence given by:

$$(\text{SSH}) \times (\text{SV}\eta^i) \times (\text{HV}\eta^i) \propto \frac{\kappa^2 m_V^2}{2\rho w} \sim \rho_V \kappa, \quad (5.2)$$

$$(\text{SSH}) \times (\text{S}\bar{t}t) \times (\text{H}\bar{t}t) \propto \frac{\kappa^2 m_t^2}{2\rho w} \sim \rho_t \kappa, \quad (5.3)$$

$$(\text{SSH}) \times (\text{SHH}) \times (\text{HHH}) \propto \kappa^2 \lambda_{\text{sm}} w \sim \rho_H \lambda_{\text{sm}} \kappa, \quad (5.4)$$

where $\lambda_{\text{sm}} \sim \lambda + \kappa^2/4\rho$ and $i = (3, \pm)$ for $V = Z, W^\pm$, respectively.

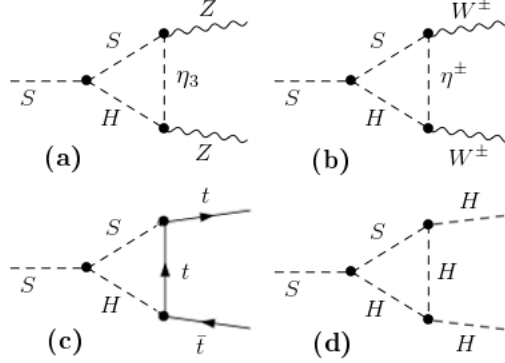


Figure 5.2: Examples of the Feynman diagrams contributing to the mixing angle dependence of $\mathcal{R}_i^{\text{SSM}}$.

- **High Mass Region**

In the region of larger masses, the w dependence in $\mathcal{R}_{VV}^{\text{SSM}}$ is more evident; for example, for $m_S = 900$ GeV and $s_\alpha \sim 0.2$, the ratio $\mathcal{R}_{VV}^{\text{SSM}}(w = 6.67v)/\mathcal{R}_{VV}^{\text{SSM}}(w = 3.85v) \sim (0.6, 0.8)$ for $V = Z, W$, respectively. For the top quark final state, the w dependence becomes pronounced when $|\mathcal{R}_{tt}^{\text{SSM}}| \gtrsim \mathcal{O}(3\%)$; for instance, it reaches the maximum variation, which is at the level of $\mathcal{O}(15\%)$, when $m_S = 900$ GeV and $s_\alpha \sim 0.2$. The ratio $\mathcal{R}_{HH}^{\text{SSM}}$ confirms the dependence on w , s_α and $\text{sign}(s_\alpha)$ discussed in the low mass case; the maximum s_α -variation of $\mathcal{R}_{HH}^{\text{SSM}}$ is of $\mathcal{O}(35\%)$ for $m_S = 900$ GeV and $w = 6.67v$ while the dependence on w reaches the maximum when $m_S = 900$ GeV and $s_\alpha \sim -0.2$: $\mathcal{R}_{HH}^{\text{SSM}}(w = 6.67v)/\mathcal{R}_{HH}^{\text{SSM}}(w = 3.85v) \sim 0.8$. Interestingly enough, in the high mass region the sign of the ratios $\mathcal{R}_i^{\text{SSM}}$ is negative for every choice of s_α and w .

5.2 Dependence on m_S

In this section we will scrutinize more in detail the dependence of $\mathcal{R}_i^{\text{SSM}}$ on the singlet mass for fixed values of s_α and w . In the upper plots of Fig.(5.3) we show the behavior of $\mathcal{R}_{VV}^{\text{SSM}}$ ($V = W$ on the left, $V = Z$ on the right) as a function of m_S for a fixed $s_\alpha = 0.17$ and $w = 4.34v$.

For the sake of comparison, we also computed the same ratio $\mathcal{R}_{VV}^{SM} = [(\Gamma_{VV}^{NLO}/\Gamma_{VV}^{LO}) - 1]$ in the SM (red line) leaving the Higgs mass as a free parameter (in practice, the SM with a heavy Higgs) and for which we obtained the same behaviors as those discussed in [57, 63]. In the plots, on the common x-axis we use the label m_{scalars} to indicate either m_H or m_S .

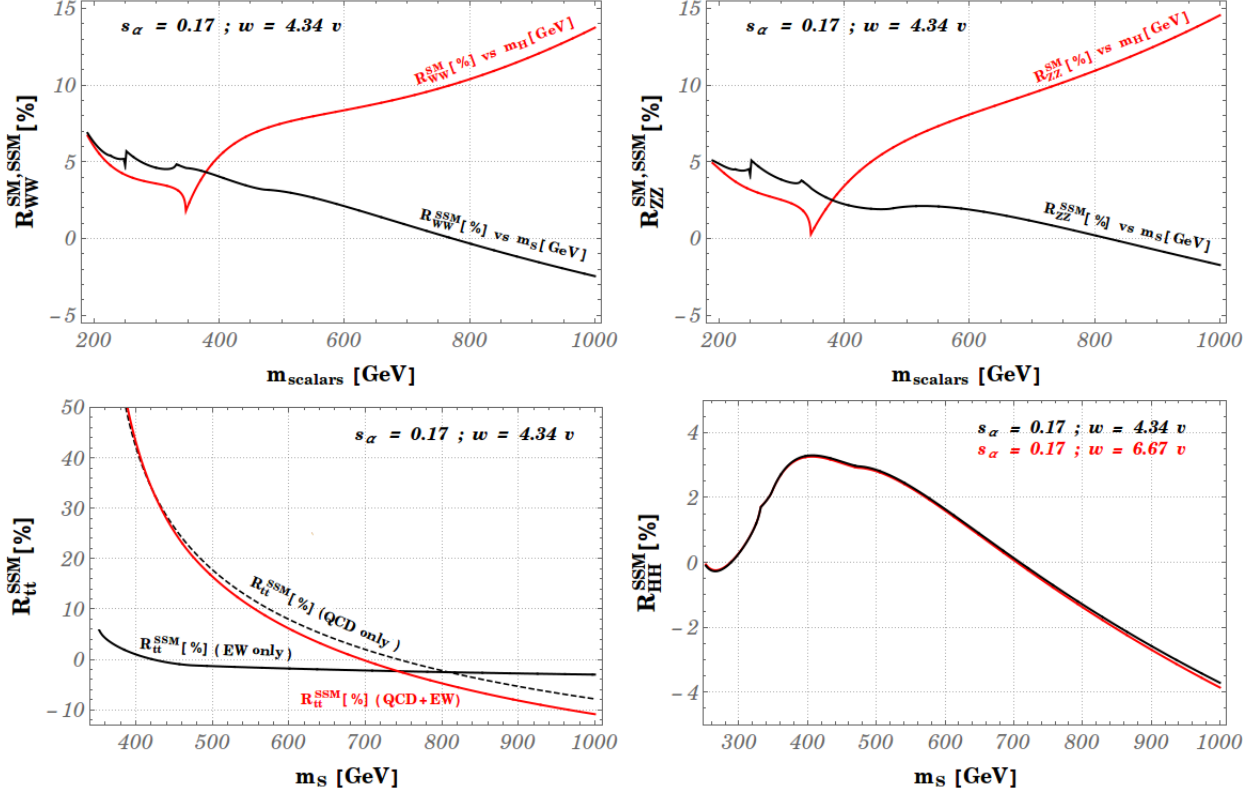


Figure 5.3: *Upper plots:* \mathcal{R}_{VV}^{SM} (red line) and \mathcal{R}_{VV}^{SSM} (black line) as a function of the scalar mass m_{scalars} . We fixed $s_\alpha = 0.17$, $w = 4.34 v$ and $q_\gamma = q_\gamma^{max}$. *Lower left plot:* EW and QCD contributions to \mathcal{R}_{tt}^{SSM} (thick and dashed black lines, respectively) and total contributions to \mathcal{R}_{tt}^{SSM} (red line) computed to $s_\alpha = 0.17$, $w = 4.34 v$ and $q_\gamma = q_\gamma^{max}$. *Lower right plot:* behavior of \mathcal{R}_{HH}^{SSM} for fixed values: $s_\alpha = 0.17$, $w = 4.34 v$ (black line) and $s_\alpha = 0.17$, $w = 6.67 v$ (red line).

We observe three main differences between the red and the black lines:

- **Finite peak at $m_S = 2m_H$:**

this appears in \mathcal{R}_{VV}^{SSM} due to the new coupling SHH which is obviously absent in the SM. These peaks are generated by the $\mathcal{B}_{0,1}(p^2, m^2, m^2)$ functions (reported in App.D) and their derivative with respect to p^2 which present a maximum (\mathcal{B}_0 and \mathcal{B}'_0) and minimum (\mathcal{B}_1 and \mathcal{B}'_1) for $p = 2m$.

- **Different peaks at $m_S = 2m_t$:**

in this case the main contributions are given by the fermionic loops which appear in δZ_S and $\delta V_V^{\mathcal{E}, \mathcal{D}}$. Differently from the SM ratio (red lines), in the SSM case these fermionic expressions contain an overall s_α^2 factor which induces the suppression of the considered peak.

- **High mass region behavior:**

it is clearly visible a different behavior for large values of m_S . This is mainly due to the new scalar contributions arising from the coefficient \mathcal{D}_V (see [57] for an explicit evaluation in the SM). For example, setting the mass of the heavy scalars to $m_{\text{scalars}} = 1000$ GeV and considering $V = Z$, we have:

$$\{\delta V_Z^{\mathcal{D}}\}^{\text{SM}} \sim (3.31 - 0.16 \lambda) \times 10^{-5} > 0 ,$$

whose positivity is determined by the fact that $\lambda = m_{\text{scalars}}^2/2v^2$. Instead, in the case of the SSM, we get:

$$\{\delta V_Z^{\mathcal{D}}\}^{\text{SSM}} \sim (4.97 - 2.27 \lambda - 2.07 \rho - 13.95 \kappa) \times 10^{-5} < 0$$

due to λ, ρ and κ which are all positive parameters for $s_\alpha = 0.17$ and $w = (4.34, 6.67)v$, see eq.(1.69).

In the lower plots of Fig.(5.3) we show the behavior of $\mathcal{R}_{tt, HH}^{\text{SSM}}$ as a function of m_S when $(s_\alpha, w) = (0.17, 4.34v)$, for $\mathcal{R}_{tt}^{\text{SSM}}$, and $(s_\alpha, w) = (0.17, 4.34v)$ and $(0.17, 6.67v)$, for $\mathcal{R}_{HH}^{\text{SSM}}$. In the case of the top quark final state, the QCD and EW contributions are represented by the dashed and the solid black lines, respectively, while the total sum (QCD plus EW) is depicted by the red line. We observe that the QCD contributions remain larger than the EW part for $m_S \lesssim 800$ GeV and dominate the region of $m_S \lesssim 450$ GeV. The EW contributions of $\mathcal{R}_{tt}^{\text{SSM}}$ are no larger than $\mathcal{O}(5\%)$ in all mass range and become negative for $m_S \gtrsim 400$ GeV. This implies a cancellation between the EW and QCD contributions in the mass range $400 \lesssim m_S \lesssim 750$ GeV while for larger masses these become totally negative driving toward negative values the global correction due to $\mathcal{R}_{tt}^{\text{SSM}}$. Concerning $\mathcal{R}_{HH}^{\text{SSM}}$, we note that it remains positive for $300 \lesssim m_S \lesssim 700$ GeV reaching a maximum value of order $\mathcal{O}(3.5\%)$ at $m_S \sim 400$ GeV. At $m_S = 2m_H$, we can observe that $\mathcal{R}_{HH}^{\text{SSM}}$ shows a similar behavior as the one mentioned for $\mathcal{R}_{VV}^{\text{SSM}}$. An additional slight variation of the curves is visible when $m_S \sim 470$ GeV. This variation arises exactly from the loop integral $\mathcal{B}_0(p^2, m_t^2, m_t^2)$ which appear in the definition of $\delta m_{HS}^{2\text{ios}}$ defined at $p^{*2} = (m_S^2 + m_H^2)/2$. As a consequence, the peak-condition becomes,

$$p^* = \sqrt{\frac{m_H^2 + m_S^2}{2}} = 2m_t \implies m_S = \sqrt{8m_t^2 - m_H^2} \sim 470 \text{ GeV}. \quad (5.5)$$

It is important to stress that we are not totally in agreement with the results obtained in [29]. In Tab.(5.1), we compare our results for $\mathcal{R}_{HH}^{\text{SSM}}$ with the numerical values of the corresponding quantity computed by the authors of [29]. To this aim, we only refer to the results collected in Tab.(6) of [29] calculated in the MOMS ¹ and iOS schemes for the following fixed values:

¹In [29], the results obtained in the MOMS scheme are indicated by δ_{GF} .

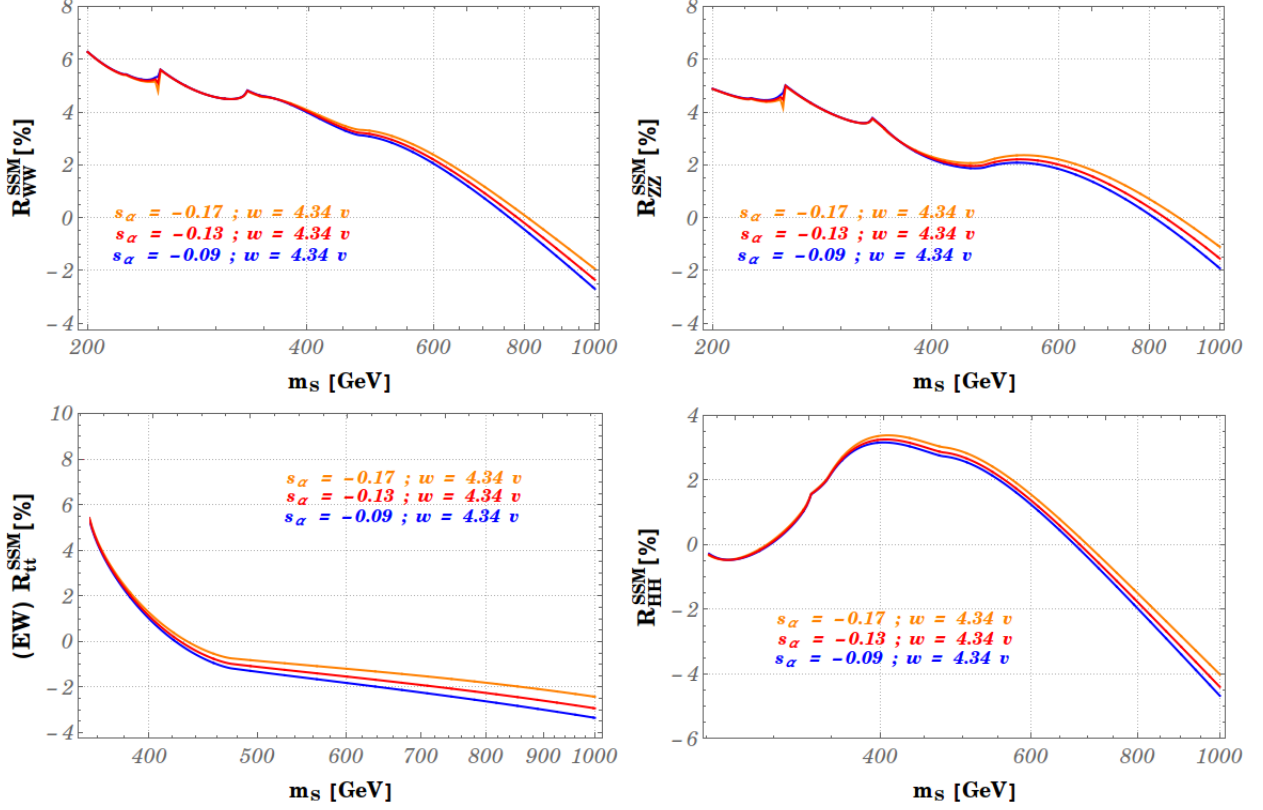


Figure 5.4: Ratio \mathcal{R}_i^{SSM} as a function of the singlet mass m_S for the three fixed values $s_\alpha = -0.09, -0.13$ and -0.17 . Ratio $\mathcal{R}_{WW,tt}^{SSM}$ are computed for $q_\gamma = q_\gamma^{max}$.

$m_S = 300, 500, 700$ GeV, $s_\alpha = 0.1, 0.2, 0.3$ and $w = 5v$. The deviations between our results and the ones of [29] seem to be roughly the same in all mass range, for each fixed value of s_α , at the level of $\mathcal{O}(3\%)$. Thus, the factor which generates this disagreement is almost completely independent on the singlet scalar mass. The reason for this discrepancy is still under investigation.

As it was shown in Fig.(5.1), the ratio \mathcal{R}_i^{SSM} depend on the sign and the assumed value of s_α and the variation with $sign(s_\alpha)$ is more evident when $s_\alpha < 0$; to be more quantitative we also study in detail the region of negative s_α . In Fig.(5.4), we show \mathcal{R}_i^{SSM} as a function of the singlet mass m_S for three fixed values of s_α , namely $s_\alpha = -0.09, -0.17$ (which are the two extremes of the considered range) and its central value $s_\alpha = -0.13$. Notice that the dependence on the scalar mixing angle starts to be significant for all ratios \mathcal{R}_i^{SSM} for $m_S \gtrsim 400$ GeV while it can be neglected for smaller masses. In addition, \mathcal{R}_{VV}^{SSM} becomes negative when the scalar mass is roughly larger than 800 GeV, \mathcal{R}_{tt}^{SSM} when $m_S \gtrsim 400$ GeV and \mathcal{R}_{HH}^{SSM} for mass values in the interval $300 \lesssim m_S \lesssim 800$ GeV, as it was the case for $s_\alpha > 0$ (see plots of Fig.(5.3)). As far as we know, the NLO corrections to the decay widths $\Gamma(S \rightarrow ZZ)$, $\Gamma(W^+W^-(\gamma))$ and

Set of Parameters		$\mathcal{R}_{HH}^{\text{SSM}} [\%]$	$\delta_{G_F} [\%]$
$w = 5v$		Our Results	Results of [29]
$m_S = 300 \text{ GeV}$	$s_\alpha = 0.1$	0.164	2.990
	$s_\alpha = 0.2$	0.343	3.100
	$s_\alpha = 0.3$	0.616	3.278
$m_S = 500 \text{ GeV}$	$s_\alpha = 0.1$	2.593	5.236
	$s_\alpha = 0.2$	2.959	5.518
	$s_\alpha = 0.3$	3.599	6.012
$m_S = 700 \text{ GeV}$	$s_\alpha = 0.1$	-0.304	2.473
	$s_\alpha = 0.2$	0.326	3.071
	$s_\alpha = 0.3$	1.424	4.195

Table 5.1: Comparison between the results of the NLO corrections to the decay rate $\Gamma(S \rightarrow HH)$ obtained in this thesis and those reported in Tab.(6) of [29] (called δ_{G_F}) for fixed values: $m_S = 300, 500, 700 \text{ GeV}$, $s_\alpha = 0.1, 0.2, 0.3$ and $w = 5v$.

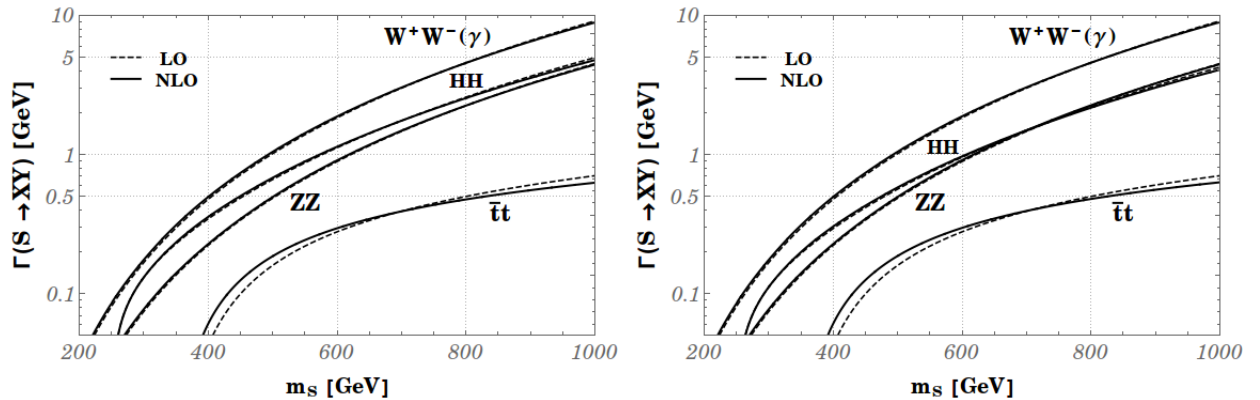


Figure 5.5: Leading order (dashed line) and next-to-leading order (solid line) results for $\Gamma(S \rightarrow XY)$ with $XY = ZZ, W^+W^-(\gamma), \bar{t}t, HH$ for $s_\alpha = 0.17$ (left plot), $s_\alpha = -0.17$ (right plot) and $w = 4.34v$. In the case $XY = W^+W^-(\gamma)$ and $\bar{t}t$, we have fixed $q_\gamma = q_\gamma^{\text{max}}$.

$\Gamma(S \rightarrow \bar{t}t(\gamma))$ have not been numerically computed before ^{2,3}. In order to briefly summa-

²Although we are not in agreement with the results in [29], they have shown for the first time the numerical results of the NLO corrected decay rate $\Gamma(S \rightarrow HH)$. Concerning the QCD-only corrections to $S \rightarrow \bar{q}q(g)$, these do not receive any new loop contributions beyond the SM results in [65].

³Analytical expressions of the NLO couplings $SVV, S\bar{f}f$ and SHH can be extracted by the amplitudes for the Higgs boson vertices in [55, 70], which are discussed for the SSM without \mathbb{Z}_2 -symmetry. In [55, 70], the numerical analysis is performed only for the corrections to the couplings $HV\bar{V}, H\bar{f}f$ and SHH .

riize the NLO EW results for the dominant decay channels obtained in this thesis, we list in Tab.(5.2) for fixed $(s_\alpha, w) = (0.17, 4.34 v)$ the ratios $\mathcal{R}_{ii}^{\text{SSM}}$ computed for $m_S = 1000$ GeV which involves the larger values of all NLO decay rates and for those singlet masses which give rise to the maximum correction values ($\mathcal{R}_{ii}^{\text{SSM max}}$), namely $m_S \simeq 200$ GeV ($\mathcal{R}_{WW}^{\text{SSM max}}$), $m_S \simeq 252$ GeV ($\mathcal{R}_{ZZ}^{\text{SSM max}}$), $m_S \simeq 360$ GeV ($\mathcal{R}_{tt}^{\text{SSM max}}$) and $m_S \simeq 406$ GeV ($\mathcal{R}_{HH}^{\text{SSM max}}$).

$s_\alpha = 0.17$ and $w = 4.34 v$				
m_S [GeV]	$\mathcal{R}_{WW}^{\text{SSM}}$ [%]	$\mathcal{R}_{ZZ}^{\text{SSM}}$ [%]	$\mathcal{R}_{HH}^{\text{SSM}}$ [%]	(EW) $\mathcal{R}_{tt}^{\text{SSM}}$ [%]
200	6.277	4.876	—	—
252	5.685	5.088	-0.065	—
360	4.523	2.923	2.657	4.229
406	3.952	2.172	3.256	0.676
1000	-2.239	-1.494	-3.857	-2.792

Table 5.2: Results of $\mathcal{R}_{ii}^{\text{SSM}}$ [%] (with $i = W, Z, H$ and t) for fixed values: $s_\alpha = 0.17$, $w = 4.34 v$ and $m_S = 200, 252, 360, 406$ and 1000 GeV. The bold numbers correspond to the maximum values of the ratios $\mathcal{R}_{ii}^{\text{SSM}}$ for the representative choice of variables.

Finally, in Fig.(5.5) we summarize our results for the decay widths $\Gamma(S \rightarrow XY)$ (with $XY = ZZ, W^+W^-(\gamma), \bar{t}t, HH$) as a function of m_S for the selected values $w = 4.34 v$ and $s_\alpha = \pm 0.17$. As expected from our previous considerations, the NLO results (solid line) are above the LO behavior (dashed line) in the small mass region but becomes generally smaller in the region of larger masses ($m_S \gtrsim 750$ GeV).

Having discussed the full set of quantities entering in the NLO total decay rate $\Gamma(S \rightarrow All)$ (see eq.(4.45)), we are now in the position to compute the ratio $\mathcal{R}_{\text{TOT}}^{\text{SSM}}$ that we report in Fig.(5.6) for fixed values $w = 4.34 v$ and $s_\alpha = \pm 0.17$. It can be useful for the considerations below to rewrite $\mathcal{R}_{\text{TOT}}^{\text{SSM}}$ in terms of the other single ratios as:

$$\mathcal{R}_{\text{TOT}}^{\text{SSM}} = \text{BR}_{SWW}^{\text{LO}} \mathcal{R}_{WW}^{\text{SSM}} + \text{BR}_{SZZ}^{\text{LO}} \mathcal{R}_{ZZ}^{\text{SSM}} + \text{BR}_{SHH}^{\text{LO}} \mathcal{R}_{HH}^{\text{SSM}} + \text{BR}_{Stt}^{\text{LO}} \mathcal{R}_{tt}^{\text{SSM}}. \quad (5.6)$$

We observe that the variation with s_α starts to be relevant for $m_S \gtrsim 250$ GeV. Since the dependence on the scalar mixing angle of $\mathcal{R}_{WW, ZZ, tt}^{\text{SSM}}$ become relevant for $m_S \gtrsim 400$ GeV (see for example Fig.(5.4)), this implies that the variation of $\mathcal{R}_{\text{TOT}}^{\text{SSM}}$ with s_α and its sign for the mass range $250 \lesssim m_S \lesssim 400$ GeV is mainly due to $\mathcal{R}_{HH}^{\text{SSM}}$ which is the only one that presents a not negligible mixing angle dependence in the low mass region. The behavior of the shapes depicted in Fig.(5.6) can be briefly analyzed in different mass regions:

- $200 \lesssim m_S \lesssim 2m_H$ GeV: this region is only affected by the gauge boson decay channels since the other processes are absent being kinematically not accessible. Notice that the

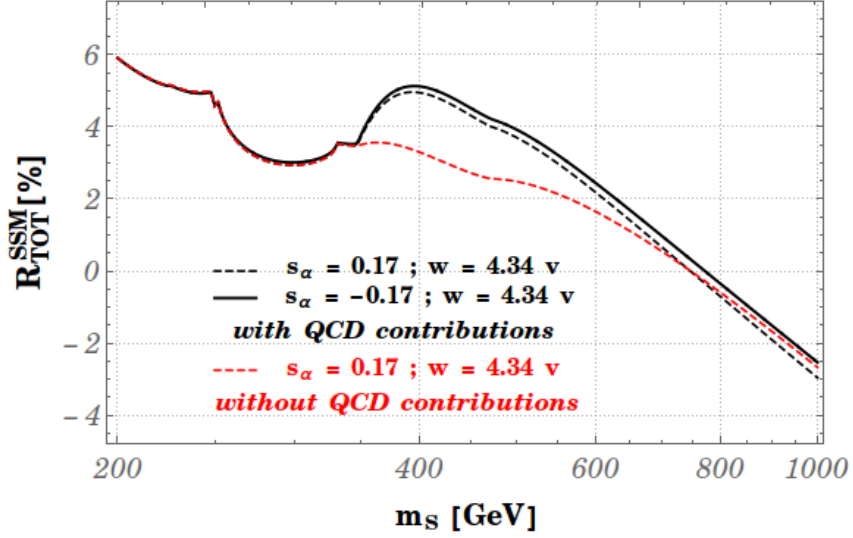


Figure 5.6: Behavior of $\mathcal{R}_{\text{TOT}}^{\text{SSM}}$ computed for fixed values, namely $s_\alpha = 0.17$ (black and red dashed lines), $s_\alpha = -0.17$ (black solid line) and $w = 4.34v$. The photon momenta in $\mathcal{R}_{\text{WW},tt}^{\text{SSM}}$ are fixed to $q_\gamma = q_\gamma^{\text{max}}$ and the QCD corrections of $\mathcal{R}_{tt}^{\text{SSM}}$ are only taken into account in the black lines.

WW branching fraction at the LO is larger than ZZ final state at the fixed values $w = 4.34v$ and $s_\alpha = \pm 0.17$; this implies that $\mathcal{R}_{\text{TOT}}^{\text{SSM}}$ are mainly influenced by the ratio $\mathcal{R}_{\text{WW}}^{\text{SSM}}$. In addition, the ratio $\mathcal{R}_{\text{TOT}}^{\text{SSM}}$ tends to decrease following the behavior of $\mathcal{R}_{\text{VV}}^{\text{SSM}}$ in the low mass region. Notice that the smooth peak at $m_S \sim 225$ GeV (near to the other one at $m_S = 2m_H$) is due to the loop integrals in $\delta m_{HS}^{2\text{ios}}$ when $p^* = 2m_Z$.

- $2m_H \lesssim m_S \lesssim 2m_t$ GeV: in this range, the correction to the total decay width is characterized by the additional contribution proportional to $\mathcal{R}_{\text{HH}}^{\text{SSM}}$. The loop functions entering in the counterterms δZ_S and $\delta V_{H,Z,W}$ generate the peaks at the extreme values $m_S = 2m_H, 2m_t$ while the variation of the curve at $m_S \sim 330$ GeV is due to the function $\mathcal{B}_0(p^{*2}, m_H^2, m_H^2)$ appearing in the counterterm $\delta m_{HS}^{2\text{ios}}$.
- $2m_t \lesssim m_S \lesssim 1000$ GeV: here, the $\mathcal{R}_{tt}^{\text{SSM}}$ contribution appears. Notice that the QCD effects are not negligible even though the LO decay rate of $S \rightarrow \bar{t}t$ is smaller than the other dominant decay widths for $m_S \gtrsim 400$ GeV. We observe that $\mathcal{R}_{\text{TOT}}^{\text{SSM}}$ tends to be negative in the high mass region according to the behavior of the individual ratios $\mathcal{R}_i^{\text{SSM}}$ discussed above. Since the counterterm $\delta m_{HS}^{2\text{ios}}$ appears in all expressions of partial decay rate corrections, we observe the slight variations of the $\mathcal{R}_{\text{TOT}}^{\text{SSM}}$ shapes at $m_S \sim 470$ GeV due to the function $\mathcal{B}_0(p^{*2}, m_t^2, m_t^2)$ computed for $p^* = 2m_t$.

For completeness, we conclude reporting in Tab.(5.3) an example of the cross section values at proton center-of-mass energy \sqrt{s} corresponding to the resonant process $pp \rightarrow S \rightarrow XY$

(defined in eq.(4.46)) for $XY = ZZ, W^+W^-, \bar{t}t, HH$ and fixed values, namely $m_S = 750$ GeV, $s_\alpha = \pm 0.17$ and $w = 4.34v$. First of all, we note that the QCD corrections to the partonic

$m_S = 750$ GeV , $w = 4.34v$	$s_\alpha = 0.17$		$s_\alpha = -0.17$	
without $K_{gg, \bar{q}q}$	LO [fb]	NLO [fb]	LO [fb]	NLO [fb]
$\sigma^{8\text{TeV}}(pp \rightarrow S \rightarrow W^+W^-)$	1.179	1.183	1.226	1.231
$\sigma^{8\text{TeV}}(pp \rightarrow S \rightarrow ZZ)$	0.578	0.582	0.601	0.606
$\sigma^{8\text{TeV}}(pp \rightarrow S \rightarrow \bar{t}t)$	0.141	0.137	0.147	0.146
$\sigma^{8\text{TeV}}(pp \rightarrow S \rightarrow HH)$	0.676	0.672	0.600	0.594
$\sigma^{13\text{TeV}}(pp \rightarrow S \rightarrow W^+W^-)$	5.485	5.502	5.705	5.726
$\sigma^{13\text{TeV}}(pp \rightarrow S \rightarrow ZZ)$	2.689	2.709	2.797	2.821
$\sigma^{13\text{TeV}}(pp \rightarrow S \rightarrow \bar{t}t)$	0.657	0.639	0.683	0.668
$\sigma^{13\text{TeV}}(pp \rightarrow S \rightarrow HH)$	3.147	3.127	2.792	2.763
with $K_{gg, \bar{q}q}$	LO [fb]	NLO [fb]	LO [fb]	NLO [fb]
$\sigma^{8\text{TeV}}(pp \rightarrow S \rightarrow W^+W^-)$	1.179	2.364	1.226	2.460
$\sigma^{8\text{TeV}}(pp \rightarrow S \rightarrow ZZ)$	0.578	1.164	0.601	1.212
$\sigma^{8\text{TeV}}(pp \rightarrow S \rightarrow \bar{t}t)$	0.141	0.275	0.147	0.287
$\sigma^{8\text{TeV}}(pp \rightarrow S \rightarrow HH)$	0.676	1.344	0.600	1.187
$\sigma^{13\text{TeV}}(pp \rightarrow S \rightarrow W^+W^-)$	5.485	10.996	5.705	11.444
$\sigma^{13\text{TeV}}(pp \rightarrow S \rightarrow ZZ)$	2.689	5.413	2.797	5.637
$\sigma^{13\text{TeV}}(pp \rightarrow S \rightarrow \bar{t}t)$	0.657	1.278	0.683	1.334
$\sigma^{13\text{TeV}}(pp \rightarrow S \rightarrow HH)$	3.147	6.250	2.792	5.521

Table 5.3: LO and NLO Cross sections $\sigma^{8,13\text{TeV}}(pp \rightarrow S \rightarrow W^+W^-, ZZ, \bar{t}t, HH)$ at proton center-of-mass energy $\sqrt{s} = 8$ and 13 TeV computed for fixed values, namely $m_S = 750$ GeV, $s_\alpha = \pm 0.17$ and $w = 4.34v$.

process $\Gamma(gg \rightarrow S)$ (numerically given by the K-factor, $K_{gg} \simeq 2$) affect the NLO cross section values for $\sqrt{s} = 8, 13$ TeV: $\sigma_{\text{NLO}}(pp \rightarrow S \rightarrow XY)/\sigma_{\text{LO}}(pp \rightarrow S \rightarrow XY) \sim 2$. Neglecting the K_{gg} contributions, the corrections to the scalar singlet decay rates imply that the NLO cross section $\sigma_{\text{NLO}}^{8,13\text{TeV}}(pp \rightarrow S \rightarrow XY)$ reaches a maximum variation of $\mathcal{O}(2\%)$ for each XY final states. Obviously, the process $pp \rightarrow S \rightarrow XY$ is a simple case to roughly quantify the impact of the NLO scalar singlet decay widths in the cross section corresponding to a scalar resonance but is not phenomenologically interesting since these effects are much smaller than the QCD corrections to the resonance production processes, mainly due to $gg \rightarrow S$. The corrections to the scalar singlet decay widths could become relevant in EW processes with leptons in the final states, like $pp(\bar{q}q) \rightarrow SZ \rightarrow XY \bar{l}l$, in the hadron colliders (see Fig.(5.7)).

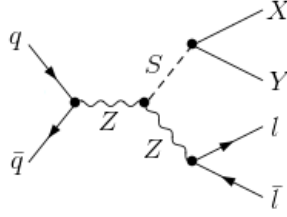


Figure 5.7: *Feynman diagram related to the process $\bar{q}q \rightarrow SZ \rightarrow XY \bar{l}$.*

5.3 A Comment on the Gauge Dependence

It has been verified by the authors of [29] that the physical quantities computed in the MF scheme prescription show a gauge-dependence for each possible value of the renormalization scale μ_R . As discussed in Sect.3.2.4, we demonstrated that the iOS and the MF schemes are equivalent at $p^{*2} = \mu_R^2 = (m_S^2 + m_H^2)/2$ and this would imply that the results obtained in terms of the MF counterterms is only gauge-independent if $\mu_R^2 = (m_S^2 + m_H^2)/2$. This is not totally in agreement with the results of [29] which show different values computed in the iOS scheme at $p^{*2} = (m_S^2 + m_H^2)/2$ and in the MF scheme $\mu_R^2 = (m_S^2 + m_H^2)/2$. Since the two renormalization schemes should give equivalent results for $p^* = \mu_R$, we are not able to explain the reason of the difference between the results computed in the MF and the iOS schemes of the Tab.(6) in [29]. To get an estimate of the gauge-dependence impact in the NLO decay rates, we define the following variable:

$$\Delta\Gamma_i = \frac{(\Gamma_i^{\text{NLO}})_{\text{ios}} - (\Gamma_i^{\text{NLO}})_{\text{mf}}}{(\Gamma_i^{\text{NLO}})_{\text{ios}}} \quad \text{with } i = ZZ, WW, tt, HH, \quad (5.7)$$

where $(\Gamma_i^{\text{NLO}})_{\text{ios}}$ and $(\Gamma_i^{\text{NLO}})_{\text{mf}}$ are the NLO decay widths computed in the iOS and MF prescription, respectively. The analysis of the gauge dependence is performed in terms of different values of μ_R which we fix in the following range: $m_H \leq \mu_R \leq m_S$ with $m_S = 400, 1000$ GeV. We can directly obtain the NLO decay rates in the MF scheme from those performed in the iOS scheme following the treatment described in Sect.4.5. As it is shown in Fig.(5.8), the gauge dependence generates $\Delta\Gamma_i$ included in the range $[-2, +3]\%$ for $m_S = 400$ GeV and 1000 GeV for each channel. Notice that the QCD corrections are μ_R -independent and survive only in the denominator of $\Delta\Gamma_{tt}$. Since the QCD corrections are positive for $m_S \lesssim 800$ GeV, their insertion reduces the gauge-dependence effects in the case of $m_S = 400$ GeV and vice versa for $m_S = 1000$ GeV. In addition, we clearly observe the peaks at $p = \mu_R = 2m_Z, 2m_H, 2m_t$ and the increasing gauge dependence effects as μ_R increases.

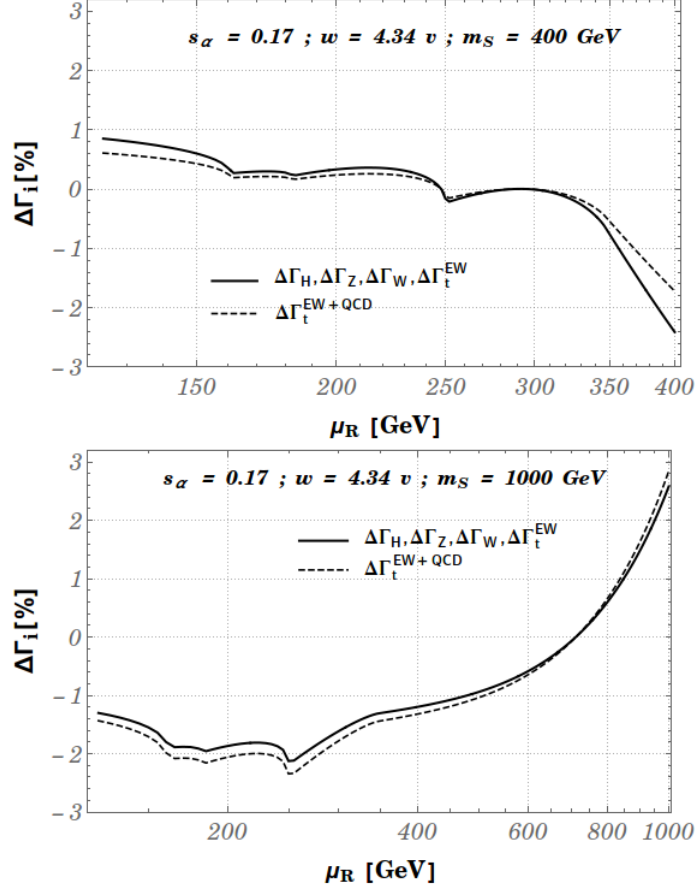


Figure 5.8: Ratio $\Delta\Gamma_i$ with $i = ZZ, WW, HH, tt$ as a function of the renormalization scale μ_R for fixed values $s_\alpha = 0.17$, $w = 4.34 v$ and $m_S = 400$ GeV (upper plot), 1000 GeV (lower plot). The $\Delta\Gamma_{tt}$ are analyzed with (solid line) and without (dashed line) the QCD corrections.

At $\mu_R = 296.35$ GeV (for $m_S = 400$ GeV) and 712.62 GeV (for $m_S = 1000$ GeV), we numerically found that $\Delta\Gamma_i = 0$ which implies that $(\Gamma_i^{\text{NLO}})_{\text{ios}} = (\Gamma_i^{\text{NLO}})_{\text{mf}}$. These μ_R values correspond exactly to the average geometrical mass $(m_S^2 + m_H^2)/2$ computed for $m_S = 400$ GeV and 1000 GeV. Therefore, we confirm that the MF and the iOS prescriptions converge to $\mu_R^2 = (m_S^2 + m_H^2)/2$.

Conclusions

In this thesis we have studied in details an extension of the SM which involves the presence of a new real scalar field s^0 , singlet under the SM gauge group. Its main effect is to mix with the SM-like scalar doublet ϕ via a quartic interaction of the form $\kappa|\phi|^2|s^0|^2$, giving rise to two mass eigenstates that we call H (the lighter) and S (the heaviest). We have limited our interests here to the study of the dominant decay rates of S to a pair of gauge bosons Z and W , to top quarks t and to lighter scalar bosons H ; as far as we know, the amplitudes of such vertices can be extracted by the one-loop self energies and vertex corrections quoted in [55, 70] but the one-loop corrections to the dominant heavy scalar decays have not been computed explicitly before (in the literature we only found the analysis of the one-loop corrections to $S \rightarrow HH$ [29, 70]). In order to ensure the gauge-independence in the NLO decay width results, we use the improved on-shell renormalization scheme (iOS) which gives a gauge-invariant expression for the counterterms corresponding to the mixed scalar sector, as it is shown in [29]. In the mass range analyzed in this thesis, $200 \leq m_S \leq 1000$ GeV which corresponds to mixing angles in the range $|s_\alpha| \in [0.09, 0.17]$, the decay rates of $S \rightarrow ZZ, W^+W^-, \bar{t}t, HH$ are kinematically accessible and we estimated that their EW one-loop corrections can be as large as $\mathcal{O}(6\%)$ in the W^+W^- channel, $\mathcal{O}(5\%)$ in the ZZ channel and $\mathcal{O}(4\%)$ in the HH and $\bar{t}t$ channels. The $\Gamma(S \rightarrow \bar{t}t)$ also receive the QCD loop contributions which for $m_S \lesssim 400$ GeV can be larger than $\mathcal{O}(50\%)$. Interestingly enough, the sign of the NLO corrections is not fixed a priori: for $300 \lesssim m_S \lesssim 700$ GeV, the quantity $\mathcal{R}_i^{\text{SSM}} = [(\Gamma_i^{\text{NLO}}/\Gamma_i^{\text{LO}}) - 1]$ with $i = ZZ, WW, \bar{t}t, HH$ is always positive for every values of α (if $\mathcal{R}_{\bar{t}t}^{\text{SSM}}$ also includes the QCD corrections) while for larger masses $\mathcal{R}_i^{\text{SSM}}$ can also become negative (the precise turning point depends on the assumed values of α and w). In addition, $\mathcal{R}_{HH}^{\text{SSM}}$ is the only ratio which becomes negative for $m_S \lesssim 300$ GeV. Regarding the dependence on α and its sign, $\mathcal{R}_i^{\text{SSM}}$ exhibits different behaviors in the mass range taken into account. In fact, these dependences are almost totally confined in the high mass region for masses somehow larger than 400 GeV. We have also studied the dependence of $\mathcal{R}_i^{\text{SSM}}$ on the singlet vev w ; we found that it is practically absent for masses $m_S \lesssim 400$ GeV whereas in the higher mass range it is not negligible (see for example the ratio $\mathcal{R}_{HH}^{\text{SSM}}$ in Fig.(5.3)); this condition becomes not completely reliable if we take a w value lower than $4.34v$; to give an example, for $m_S = 300$ GeV and $s_\alpha = 0.17$ the ratio $\mathcal{R}_{HH}^{\text{SSM}}(w = 4.34v)/\mathcal{R}_{HH}^{\text{SSM}}(w = 1.25v) \sim 0.35$. The NLO corrections to the total decay width reach a maximum of $\mathcal{O}(6\%)$ for $m_S = 200$ GeV and its s_α dependence becomes clearly visible for masses larger than $m_S \gtrsim 350$ GeV. For fixed values $(s_\alpha, w) = (0.17, 4.34v)$, the maximal

value of the difference between the ratio $\mathcal{R}_{\text{TOT}}^{\text{SSM}}$ including the EW and QCD corrections and the same EW-only quantity amounts to $\mathcal{O}(2\%)$ when $m_S = 400$ GeV.

Finally, we give a comment on the gauge-dependence defining the following variables: $\Delta\Gamma_i = [(\Gamma_i^{\text{NLO}})_{\text{ios}} - (\Gamma_i^{\text{NLO}})_{\text{mf}}]/(\Gamma_i^{\text{NLO}})_{\text{ios}}$, where $(\Gamma_i^{\text{NLO}})_{\text{mf}}$ represents the NLO decay width computed in terms of the counterterms associated with "minimal field" renormalization scheme (which needs the introduction of a renormalization scale μ_R and gives gauge-dependent results for physical observables if $\mu_R \neq \sqrt{(m_H^2 + m_S^2)/2}$). For fixed m_S values, we observe that the gauge dependence for the scale range $m_H \leq \mu_R \leq m_S$ generates $\Delta\Gamma_i$ included in the range $[-2, +3]\%$ when $m_S = 400$ GeV and 1000 GeV for each channel. Besides, for $\mu_R = 296.35$ GeV (when $m_S = 400$ GeV) and 712.62 GeV (when $m_S = 1000$ GeV) we found $\Delta\Gamma_i = 0$ and this implies that $(\Gamma_i^{\text{NLO}})_{\text{ios}} = (\Gamma_i^{\text{NLO}})_{\text{mf}}$. Since these μ_R values correspond exactly to the average geometrical mass $(m_S^2 + m_H^2)/2$ computed for $m_S = 400$ GeV and 1000 GeV, we confirm the equivalence of the MF and the iOS prescriptions when $\mu_R^2 = (m_S^2 + m_H^2)/2$ (analytically proven in Sect.3.2.4).

Acknowledgements

I would like to thank all the people who helped me during these three years of PhD and made this thesis possible. In particular, I am strongly indebted with Davide Meloni for his patience and illuminating advices. I am also very grateful to Giuseppe Degrossi and Roberto Franceschini for their precious comments and suggestions.

Appendix

In this appendix we explicitly quote all contributions to the two and three-point functions needed to evaluate the NLO order corrections for the scalar singlet decay channels discussed in this thesis. We work in the t'Hooft-Feynman gauge and give the amplitudes in terms of the Passarino-Veltman integrals. Besides we can generally decompose the self-energies and the three-point functions as follows:

- **Self-Energies of the Bosonic (B) and Fermionic Fields (F)**

$$\begin{aligned}\Sigma^{BB}(p^2) &= \{\Sigma^{BB}(p^2)\}_{\text{fer}} + \{\Sigma^{BB}(p^2)\}_{\text{bos}}, \\ \Sigma^F(p^2) &= m_F \Sigma_S^F(p^2) + \not{p} \Sigma_V^F(p^2) + \not{p} \gamma_5 \Sigma_A^F(p^2)\end{aligned}$$

- **Three-Point Functions with Bosonic (B) and Fermionic Final States (F)**

$$\begin{aligned}\delta V_B &= \{\delta V_B\}_{\text{fer}} + \{\delta V_B\}_{\text{bos}}, \\ \delta V_t &= \delta V_t^A + \delta V_t^B \not{k} + \delta V_t^C \not{q} + \delta V_t^D \not{k} \not{q} + \delta V_t^E \gamma_5 + \delta V_t^F \not{k} \gamma_5 + \delta V_t^G \not{q} \gamma_5 + \delta V_t^H \not{k} \not{q} \gamma_5,\end{aligned}$$

where "fer" and "bos" stand for fermionic and bosonic loop contributions.

A - SSM Tadpole Amplitudes

Tadpole for the H Field

$$\begin{aligned}\delta T_H &= \frac{g^2}{16\pi^2} m_W^2 \left\{ 3v m_b^2 c_\alpha \mathcal{A}_0(m_b^2) + \mathcal{A}_0(m_H^2) \left(-\frac{3}{8} \kappa v^3 c_\alpha s_\alpha^2 + \frac{3}{8} \kappa v^2 w c_\alpha^2 s_\alpha - \right. \right. \\ &\quad \left. \left. - \frac{3}{4} \lambda v^3 c_\alpha^3 + \frac{3}{4} \rho v^2 w s_\alpha^3 \right) + \mathcal{A}_0(m_S^2) \left(\frac{1}{4} \kappa v^3 c_\alpha s_\alpha^2 - \frac{3}{4} \lambda v^3 c_\alpha s_\alpha^2 - \right. \right. \\ &\quad \left. \left. - \frac{1}{4} \kappa v^2 w c_\alpha^2 s_\alpha + \frac{3}{4} \rho v^2 w c_\alpha^2 s_\alpha - \frac{1}{8} \kappa v^3 c_\alpha^3 + \frac{1}{8} \kappa v^2 w s_\alpha^3 \right) + \mathcal{A}_0(m_W^2) \left(-\frac{3}{2} v c_\alpha m_W^2 - \right. \right. \\ &\quad \left. \left. - \frac{1}{2} \lambda v^3 c_\alpha + \frac{1}{4} \kappa v^2 w s_\alpha \right) + \mathcal{A}_0(m_Z^2) \left(-\frac{3v c_\alpha m_W^2 s_W^4}{4c_W^2} - \frac{3}{2} v c_\alpha m_W^2 s_W^2 - \right. \right. \\ &\quad \left. \left. - \frac{3}{4} v c_\alpha c_W^2 m_W^2 - \frac{1}{4} \lambda v^3 c_\alpha + \frac{1}{8} \kappa v^2 w s_\alpha \right) + 3v c_\alpha m_t^2 \mathcal{A}_0(m_t^2) + v c_\alpha m_\tau^2 \mathcal{A}_0(m_\tau^2) + \right.\end{aligned}\tag{8}$$

$$+ 3vc_\alpha m_c^2 \mathcal{A}_0(m_c^2) + \frac{vc_\alpha m_W^2 m_Z^2 s_W^4}{2c_W^2} + vc_\alpha m_W^2 m_Z^2 + \frac{1}{2} m_W^4 vc_\alpha \left. \right\}, \quad (9)$$

Tadpole for the S Field

$$\begin{aligned} \delta T_S = & \frac{g^2}{16\pi^2} m_W^2 \left\{ 3vm_b^2 s_\alpha \mathcal{A}_0(m_b^2) + \mathcal{A}_0(m_H^2) \left(\frac{1}{4} \kappa v^3 c_\alpha^2 s_\alpha - \frac{3}{4} \lambda v^3 c_\alpha^2 s_\alpha + \right. \right. \\ & + \frac{1}{4} \kappa v^2 w c_\alpha s_\alpha^2 - \frac{3}{4} \rho v^2 w c_\alpha s_\alpha^2 - \frac{1}{8} \kappa v^2 w c_\alpha^3 - \frac{1}{8} \kappa v^3 s_\alpha^3 \left. \right) + \\ & + \mathcal{A}_0(m_S^2) \left(-\frac{3}{8} \kappa v^3 c_\alpha^2 s_\alpha - \frac{3}{8} \kappa v^2 w c_\alpha s_\alpha^2 - \frac{3}{4} \rho v^2 w c_\alpha^3 - \right. \\ & - \frac{3}{4} \lambda v^3 s_\alpha^3 \left. \right) + \mathcal{A}_0(m_W^2) \left(-\frac{1}{4} \kappa v^2 w c_\alpha - \frac{3}{2} v m_W^2 s_\alpha - \frac{1}{2} \lambda v^3 s_\alpha \right) + \\ & + \mathcal{A}_0(m_Z^2) \left(-\frac{3v m_W^2 s_\alpha s_W^4}{4c_W^2} - \frac{3}{4} v c_W^2 m_W^2 s_\alpha - \frac{1}{8} \kappa v^2 w c_\alpha - \frac{3}{2} v m_W^2 s_\alpha s_W^2 - \right. \\ & - \frac{1}{4} \lambda v^3 s_\alpha \left. \right) + 3vm_c^2 s_\alpha \mathcal{A}_0(m_c^2) + 3vm_t^2 s_\alpha \mathcal{A}_0(m_t^2) + vm_\tau^2 s_\alpha \mathcal{A}_0(m_\tau^2) + \\ & + \frac{vm_W^2 m_Z^2 s_\alpha s_W^4}{2c_W^2} + \frac{1}{2} v c_W^2 m_W^2 m_Z^2 s_\alpha + vm_W^2 m_Z^2 s_\alpha s_W^2 + m_W^4 v s_\alpha \left. \right\}. \quad (10) \end{aligned}$$

B - SSM Self-Energy Amplitudes

Self-Energy for the W Boson

$$\begin{aligned} \{\Sigma_T^{WW}(p^2)\}_{\text{fer}} = & \frac{g^2}{16\pi^2} \left\{ -6\mathcal{B}_{00}(p^2, m_b^2, m_t^2) - 6\mathcal{B}_{00}(p^2, 0, m_c^2) - 2\mathcal{B}_{00}(p^2, 0, m_\tau^2) - \right. \\ & - 10\mathcal{B}_{00}(p^2, 0, 0) - 3p^2 \mathcal{B}_1(p^2, m_b^2, m_t^2) + 3(m_t^2 - p^2) \mathcal{B}_0(p^2, m_b^2, m_t^2) - \\ & - 3p^2 \mathcal{B}_1(p^2, 0, m_c^2) + 3(m_c^2 - p^2) \mathcal{B}_0(p^2, 0, m_c^2) + p^2 \mathcal{B}_1(p^2, 0, m_\tau^2) + \\ & \left. + 5p^2 \mathcal{B}_1(p^2, 0, 0) + 3\mathcal{A}_0(m_b^2) + \mathcal{A}_0(m_\tau^2) \right\}, \quad (11) \end{aligned}$$

$$\{\Sigma_T^{WW}(p^2)\}_{\text{bos}} = \frac{g^2}{16\pi^2} \left\{ c_\alpha^2 \mathcal{B}_{00}(p^2, m_W^2, m_H^2) + (8c_W^2 + 1) \mathcal{B}_{00}(p^2, m_W^2, m_Z^2) + \right. \quad (12)$$

$$\begin{aligned}
& + s_\alpha^2 \mathcal{B}_{00}(p^2, m_W^2, m_S^2) + 8s_W^2 \mathcal{B}_{00}(p^2, 0, m_W^2) - c_\alpha^2 m_W^2 \mathcal{B}_0(p^2, m_H^2, m_W^2) + \\
& + \frac{\mathcal{B}_0(p^2, m_W^2, m_Z^2)(c_W^4(2m_Z^2 + 3p^2) - s_W^4 m_W^2)}{c_W^2} - 2p^2 c_W^2 \mathcal{B}_1(p^2, m_W^2, m_Z^2) - \\
& - m_W^2 s_\alpha^2 \mathcal{B}_0(p^2, m_S^2, m_W^2) + 2p^2 s_W^2 \mathcal{B}_1(p^2, 0, m_W^2) - s_W^2(m_W^2 - 5p^2) \mathcal{B}_0(p^2, 0, m_W^2) - \\
& - \left. \frac{1}{4} c_\alpha^2 \mathcal{A}_0(m_H^2) + \left(-3c_W^2 - \frac{1}{4}\right) \mathcal{A}_0(m_Z^2) - \frac{1}{4} s_\alpha^2 \mathcal{A}_0(m_S^2) - \frac{3}{2} \mathcal{A}_0(m_W^2) + \frac{2p^2}{3} \right\}. \quad (13)
\end{aligned}$$

Self-Energy for the Z Boson

$$\begin{aligned}
\{\Sigma_T^{ZZ}(p^2)\}_{\text{fer}} = & \frac{g^2}{16\pi^2} \left\{ -\frac{(32c_W^4 - 40c_W^2 + 17)(\mathcal{B}_{00}(p^2, m_c^2, m_c^2) + \mathcal{B}_{00}(p^2, m_t^2, m_t^2))}{3c_W^2} + \right. \\
& + \left(-\frac{8c_W^2}{3} - \frac{5}{3c_W^2} + \frac{4}{3}\right) \mathcal{B}_{00}(p^2, m_b^2, m_b^2) - \left(-8c_W^2 - \frac{5}{c_W^2} + 12\right) \mathcal{B}_{00}(p^2, m_\tau^2, m_\tau^2) + \\
& + \left(-32c_W^2 - \frac{22}{c_W^2} + 40\right) \mathcal{B}_{00}(p^2, 0, 0) + \frac{3m_b^2 \mathcal{B}_0(p^2, m_b^2, m_b^2)}{2c_W^2} + \left(\frac{4}{3}p^2 c_W^2 + \frac{5p^2}{6c_W^2} - \frac{2p^2}{3}\right) \times \\
& \times \mathcal{B}_1(p^2, m_b^2, m_b^2) + \frac{p^2(32c_W^4 - 40c_W^2 + 17)(\mathcal{B}_1(p^2, m_c^2, m_c^2) + \mathcal{B}_1(p^2, m_t^2, m_t^2))}{6c_W^2} + \\
& + \frac{3m_t^2 \mathcal{B}_0(p^2, m_t^2, m_t^2)}{2c_W^2} + \frac{m_\tau^2 \mathcal{B}_0(p^2, m_\tau^2, m_\tau^2)}{2c_W^2} + \left(4p^2 c_W^2 + \frac{5p^2}{2c_W^2} - 6p^2\right) \mathcal{B}_1(p^2, m_\tau^2, m_\tau^2) + \\
& + \frac{3m_c^2 \mathcal{B}_0(p^2, m_c^2, m_c^2)}{2c_W^2} + \mathcal{B}_1(p^2, 0, 0) \left(16p^2 c_W^2 + \frac{11p^2}{c_W^2} - 20p^2\right) + (\mathcal{A}_0(m_t^2) + \mathcal{A}_0(m_c^2)) \times \\
& \times \left(\frac{16c_W^2}{3} + \frac{17}{6c_W^2} - \frac{20}{3}\right) + \left(\frac{4c_W^2}{3} + \frac{5}{6c_W^2} - \frac{2}{3}\right) \mathcal{A}_0(m_b^2) + \left(4c_W^2 + \frac{5}{2c_W^2} - 6\right) \mathcal{A}_0(m_\tau^2) \left. \right\}, \quad (14)
\end{aligned}$$

$$\begin{aligned}
\{\Sigma_T^{ZZ}(p^2)\}_{\text{bos}} = & \frac{g^2}{16\pi^2} \left\{ \frac{c_\alpha^2 \mathcal{B}_{00}(p^2, m_Z^2, m_H^2)}{c_W^2} + \frac{s_\alpha^2 \mathcal{B}_{00}(p^2, m_Z^2, m_S^2)}{c_W^2} + \right. \\
& + \left(12c_W^2 + \frac{1}{c_W^2} - 4\right) \mathcal{B}_{00}(p^2, m_W^2, m_W^2) - \frac{c_\alpha^2 m_W^2 \mathcal{B}_0(p^2, m_H^2, m_Z^2)}{c_W^4} - \\
& - \frac{m_Z^2 s_\alpha^2 \mathcal{B}_0(p^2, m_S^2, m_Z^2)}{c_W^2} + 2p^2 c_W^2 \mathcal{B}_1(p^2, m_W^2, m_W^2) - \frac{c_\alpha^2 \mathcal{A}_0(m_H^2)}{4c_W^2} + \\
& + \left(-\frac{2m_W^2}{c_W^2} + 5p^2 c_W^2 + 4m_W^2\right) \mathcal{B}_0(p^2, m_W^2, m_W^2) - \frac{s_\alpha^2 \mathcal{A}_0(m_S^2)}{4c_W^2} - \\
& - \frac{\mathcal{A}_0(m_Z^2)}{4c_W^2} + \left(-6c_W^2 - \frac{1}{2c_W^2} + 2\right) \mathcal{A}_0(m_W^2) + \frac{2}{3} p^2 c_W^2 \left. \right\}. \quad (15)
\end{aligned}$$

Self-Energy for the $Z\gamma$ Mixing

$$\begin{aligned}
\{\Sigma_T^{\gamma Z}(p^2)\}_{\text{fer}} = & \frac{g^2}{16\pi^2} \frac{s_W}{3c_W} \left\{ (2 - 8c_W^2) \mathcal{B}_{00}(p^2, m_b^2, m_b^2) + (20 - 32c_W^2) \mathcal{B}_{00}(p^2, m_t^2, m_t^2) + \right. \\
& + (18 - 24c_W^2) \mathcal{B}_{00}(p^2, m_\tau^2, m_\tau^2) + (20 - 32c_W^2) \mathcal{B}_{00}(p^2, m_c^2, m_c^2) + \\
& + (60 - 96c_W^2) \mathcal{B}_{00}(p^2, 0, 0) + (4p^2 c_W^2 - p^2) \mathcal{B}_1(p^2, m_b^2, m_b^2) + \\
& + (16p^2 c_W^2 - 10p^2) \mathcal{B}_1(p^2, m_t^2, m_t^2) + (12p^2 c_W^2 - 9p^2) \mathcal{B}_1(p^2, m_\tau^2, m_\tau^2) + \\
& + (16p^2 c_W^2 - 10p^2) \mathcal{B}_1(p^2, m_c^2, m_c^2) + \mathcal{B}_1(p^2, 0, 0) (48p^2 c_W^2 - 30p^2) + \\
& + (4c_W^2 - 1) \mathcal{A}_0(m_b^2) + (16c_W^2 - 10) \mathcal{A}_0(m_t^2) + (12c_W^2 - 9) \mathcal{A}_0(m_\tau^2) + \\
& \left. + 2(8c_W^2 - 5) \mathcal{A}_0(m_c^2) \right\}, \tag{16}
\end{aligned}$$

$$\begin{aligned}
\{\Sigma_T^{\gamma Z}(p^2)\}_{\text{bos}} = & \frac{g^2}{16\pi^2} \frac{s_W}{c_W} \left\{ (12c_W^2 - 2) \mathcal{B}_{00}(p^2, m_W^2, m_W^2) + 2p^2 c_W^2 \mathcal{B}_1(p^2, m_W^2, m_W^2) + \right. \\
& \left. + (5p^2 c_W^2 + 2m_W^2) \mathcal{B}_0(p^2, m_W^2, m_W^2) + (1 - 6c_W^2) \mathcal{A}_0(m_W^2) + \frac{2}{3} p^2 c_W^2 \right\}. \tag{17}
\end{aligned}$$

Self-Energy for the γ Boson

$$\begin{aligned}
\{\Sigma_T^{\gamma\gamma}(p^2)\}_{\text{fer}} = & \frac{g^2}{16\pi^2} \frac{4s_W^2}{3} \left\{ -2\mathcal{B}_{00}(p^2, m_b^2, m_b^2) - 8\mathcal{B}_{00}(p^2, m_c^2, m_c^2) - \right. \\
& - 6\mathcal{B}_{00}(p^2, m_\tau^2, m_\tau^2) - 24\mathcal{B}_{00}(p^2, 0, 0) + p^2 \mathcal{B}_1(p^2, m_b^2, m_b^2) - 8\mathcal{B}_{00}(p^2, m_t^2, m_t^2) + \\
& + 4p^2 \mathcal{B}_1(p^2, m_c^2, m_c^2) + 4p^2 \mathcal{B}_1(p^2, m_t^2, m_t^2) + 3p^2 \mathcal{B}_1(p^2, m_\tau^2, m_\tau^2) + \\
& \left. + 12p^2 \mathcal{B}_1(p^2, 0, 0) + \mathcal{A}_0(m_b^2) + 4\mathcal{A}_0(m_c^2) + 4\mathcal{A}_0(m_t^2) + 3\mathcal{A}_0(m_\tau^2) \right\}, \tag{18}
\end{aligned}$$

$$\begin{aligned}
\{\Sigma_T^{\gamma\gamma}(p^2)\}_{\text{bos}} = & \frac{g^2}{16\pi^2} s_W^2 \left\{ 12\mathcal{B}_{00}(p^2, m_W^2, m_W^2) + 5p^2 \mathcal{B}_0(p^2, m_W^2, m_W^2) + \right. \\
& \left. + 2p^2 \mathcal{B}_1(p^2, m_W^2, m_W^2) - 6\mathcal{A}_0(m_W^2) + \frac{2p^2}{3} \right\}. \tag{19}
\end{aligned}$$

Self-Energy for the H Boson

$$\{\Sigma^{HH}(p^2)\}_{\text{fer}} = \frac{g^2}{16\pi^2} c_\alpha^2 \left\{ -\frac{6m_b^4 \mathcal{B}_0(p^2, m_b^2, m_b^2)}{m_W^2} - \frac{3p^2 m_b^2 \mathcal{B}_1(p^2, m_b^2, m_b^2)}{m_W^2} - \frac{6m_t^4 \mathcal{B}_0(p^2, m_t^2, m_t^2)}{m_W^2} - \frac{3p^2 m_t^2 \mathcal{B}_1(p^2, m_t^2, m_t^2)}{m_W^2} - \frac{3m_t^2 \mathcal{A}_0(m_t^2)}{m_W^2} - \frac{2m_\tau^4 \mathcal{B}_0(p^2, m_\tau^2, m_\tau^2)}{m_W^2} - \frac{p^2 m_\tau^2 \mathcal{B}_1(p^2, m_\tau^2, m_\tau^2)}{m_W^2} - \frac{m_\tau^2 \mathcal{A}_0(m_\tau^2)}{m_W^2} - \frac{6m_c^4 \mathcal{B}_0(p^2, m_c^2, m_c^2)}{m_W^2} - \frac{3p^2 c_\alpha^2 m_c^2 \mathcal{B}_1(p^2, m_c^2, m_c^2)}{m_W^2} - \frac{3m_c^2 \mathcal{A}_0(m_c^2)}{m_W^2} - \frac{3m_b^2 \mathcal{A}_0(m_b^2)}{m_W^2} \right\}, \quad (20)$$

$$\begin{aligned} \{\Sigma^{HH}(p^2)\}_{\text{bos}} = & \frac{g^2}{16\pi^2} \left\{ -\frac{3c_\alpha^2 m_Z^4}{2m_W^2} + \frac{p^2 c_\alpha^2 \mathcal{B}_1(p^2, m_Z^2, m_Z^2) m_Z^2}{2m_W^2} - 3c_\alpha^2 m_W^2 + \right. \\ & + \left(\frac{3v^2 \lambda c_\alpha^4}{4m_W^2} + \frac{3v^2 \kappa s_\alpha^2 c_\alpha^2}{4m_W^2} + \frac{3v^2 \rho s_\alpha^4}{4m_W^2} \right) \mathcal{A}_0(m_H^2) + \left(\frac{v^2 \kappa c_\alpha^4}{8m_W^2} - \frac{v^2 \kappa s_\alpha^2 c_\alpha^2}{2m_W^2} + \right. \\ & + \frac{3v^2 \lambda s_\alpha^2 c_\alpha^2}{4m_W^2} + \frac{3v^2 \rho s_\alpha^2 c_\alpha^2}{4m_W^2} + \frac{v^2 \kappa s_\alpha^4}{8m_W^2} \left. \right) \mathcal{A}_0(m_S^2) + \left(\frac{v^2 \lambda c_\alpha^2}{2m_W^2} + \frac{3c_\alpha^2}{2} + \frac{v^2 \kappa s_\alpha^2}{4m_W^2} \right) \mathcal{A}_0(m_W^2) + \\ & + \left(\frac{3m_Z^2 c_\alpha^2}{4m_W^2} + \frac{v^2 \lambda c_\alpha^2}{4m_W^2} + \frac{v^2 \kappa s_\alpha^2}{8m_W^2} \right) \mathcal{A}_0(m_Z^2) + \left(\frac{9v^4 \lambda^2 c_\alpha^6}{2m_W^2} - \frac{9v^3 w \kappa \lambda s_\alpha c_\alpha^5}{2m_W^2} + \frac{9v^2 w^2 \kappa^2 s_\alpha^2 c_\alpha^4}{8m_W^2} + \right. \\ & + \frac{9v^4 \kappa \lambda s_\alpha^2 c_\alpha^4}{2m_W^2} - \frac{9v^3 w \kappa^2 s_\alpha^3 c_\alpha^3}{4m_W^2} - \frac{9v^3 w \lambda \rho s_\alpha^3 c_\alpha^3}{m_W^2} + \frac{9v^4 \kappa^2 s_\alpha^4 c_\alpha^2}{8m_W^2} + \frac{9v^2 w^2 \kappa \rho s_\alpha^4 c_\alpha^2}{2m_W^2} - \\ & - \frac{9v^3 w \kappa \rho s_\alpha^5 c_\alpha}{2m_W^2} + \left. \frac{9v^2 w^2 \rho^2 s_\alpha^6}{2m_W^2} \right) \mathcal{B}_0(p^2, m_H^2, m_H^2) + \left(\frac{v^2 w^2 \kappa^2 c_\alpha^6}{4m_W^2} - \frac{v^3 w \kappa^2 s_\alpha c_\alpha^5}{m_W^2} + \right. \\ & + \frac{3v^3 w \kappa \lambda s_\alpha c_\alpha^5}{m_W^2} + \frac{v^4 \kappa^2 s_\alpha^2 c_\alpha^4}{m_W^2} - \frac{v^2 w^2 \kappa^2 s_\alpha^2 c_\alpha^4}{m_W^2} + \frac{9v^4 \lambda^2 s_\alpha^2 c_\alpha^4}{m_W^2} - \frac{6v^4 \kappa \lambda s_\alpha^2 c_\alpha^4}{m_W^2} + \frac{3v^2 w^2 \kappa \rho s_\alpha^2 c_\alpha^4}{m_W^2} + \\ & + \frac{5v^3 w \kappa^2 s_\alpha^3 c_\alpha^3}{2m_W^2} - \frac{6v^3 w \kappa \lambda s_\alpha^3 c_\alpha^3}{m_W^2} - \frac{6v^3 w \kappa \rho s_\alpha^3 c_\alpha^3}{m_W^2} + \frac{18v^3 w \lambda \rho s_\alpha^3 c_\alpha^3}{m_W^2} - \frac{v^4 \kappa^2 s_\alpha^4 c_\alpha^2}{m_W^2} + \\ & + \frac{v^2 w^2 \kappa^2 s_\alpha^4 c_\alpha^2}{m_W^2} + \frac{9v^2 w^2 \rho^2 s_\alpha^4 c_\alpha^2}{m_W^2} + \frac{3v^4 \kappa \lambda s_\alpha^4 c_\alpha^2}{m_W^2} - \frac{6v^2 w^2 \kappa \rho s_\alpha^4 c_\alpha^2}{m_W^2} - \frac{v^3 w \kappa^2 s_\alpha^5 c_\alpha}{m_W^2} + \\ & + \frac{3v^3 w \kappa \rho s_\alpha^5 c_\alpha}{m_W^2} + \left. \frac{v^4 \kappa^2 s_\alpha^6}{4m_W^2} \right) \mathcal{B}_0(p^2, m_H^2, m_S^2) + \left(\frac{v^4 \kappa^2 c_\alpha^6}{8m_W^2} + \frac{v^3 w \kappa^2 s_\alpha c_\alpha^5}{2m_W^2} - \right. \\ & - \frac{3v^3 w \kappa \rho s_\alpha c_\alpha^5}{2m_W^2} - \frac{v^4 \kappa^2 s_\alpha^2 c_\alpha^4}{2m_W^2} + \frac{v^2 w^2 \kappa^2 s_\alpha^2 c_\alpha^4}{2m_W^2} + \frac{9v^2 w^2 \rho^2 s_\alpha^2 c_\alpha^4}{2m_W^2} + \left. \frac{3v^4 \kappa \lambda s_\alpha^2 c_\alpha^4}{2m_W^2} - \right. \end{aligned}$$

$$\begin{aligned}
& - \frac{3v^2w^2\kappa\rho s_\alpha^2 c_\alpha^4}{m_W^2} - \frac{5v^3w\kappa^2 s_\alpha^3 c_\alpha^3}{4m_W^2} + \frac{3v^3w\kappa\lambda s_\alpha^3 c_\alpha^3}{m_W^2} + \frac{3v^3w\kappa\rho s_\alpha^3 c_\alpha^3}{m_W^2} - \frac{9v^3w\lambda\rho s_\alpha^3 c_\alpha^3}{m_W^2} + \\
& + \frac{v^4\kappa^2 s_\alpha^4 c_\alpha^2}{2m_W^2} - \frac{v^2w^2\kappa^2 s_\alpha^4 c_\alpha^2}{2m_W^2} + \frac{9v^4\lambda^2 s_\alpha^4 c_\alpha^2}{2m_W^2} - \frac{3v^4\kappa\lambda s_\alpha^4 c_\alpha^2}{m_W^2} + \frac{3v^2w^2\kappa\rho s_\alpha^4 c_\alpha^2}{2m_W^2} + \frac{v^3w\kappa^2 s_\alpha^5 c_\alpha}{2m_W^2} - \\
& - \frac{3v^3w\kappa\lambda s_\alpha^5 c_\alpha}{2m_W^2} + \frac{v^2w^2\kappa^2 s_\alpha^6}{8m_W^2} \Big) \mathcal{B}_0(p^2, m_S^2, m_S^2) + \left(\frac{\lambda^2 c_\alpha^2 v^4}{m_W^2} - \frac{w\kappa\lambda c_\alpha s_\alpha v^3}{m_W^2} + \frac{w^2\kappa^2 s_\alpha^2 v^2}{4m_W^2} - \right. \\
& - \frac{1}{2} p^2 c_\alpha^2 + 3c_\alpha^2 m_W^2 \Big) \mathcal{B}_0(p^2, m_W^2, m_W^2) + \left(\frac{\lambda^2 c_\alpha^2 v^4}{2m_W^2} - \frac{w\kappa\lambda c_\alpha s_\alpha v^3}{2m_W^2} + \frac{w^2\kappa^2 s_\alpha^2 v^2}{8m_W^2} + \right. \\
& \left. + \frac{3c_\alpha^2 m_Z^4}{2m_W^2} - \frac{p^2 c_\alpha^2 m_Z^2}{4m_W^2} \right) \mathcal{B}_0(p^2, m_Z^2, m_Z^2) + p^2 c_\alpha^2 \mathcal{B}_1(p^2, m_W^2, m_W^2) \Big\}, \tag{21}
\end{aligned}$$

Self-Energy for the S Boson

$$\begin{aligned}
\{\Sigma^{SS}(p^2)\}_{\text{fer}} = & \frac{g^2}{16\pi^2} s_\alpha^2 \left\{ - \frac{6m_b^4 \mathcal{B}_0(p^2, m_b^2, m_b^2)}{m_W^2} - \frac{3p^2 m_b^2 \mathcal{B}_1(p^2, m_b^2, m_b^2)}{m_W^2} - \right. \\
& - \frac{6m_t^4 \mathcal{B}_0(p^2, m_t^2, m_t^2)}{m_W^2} - \frac{3p^2 m_t^2 \mathcal{B}_1(p^2, m_t^2, m_t^2)}{m_W^2} - \frac{3m_t^2 \mathcal{A}_0(m_t^2)}{m_W^2} - \\
& - \frac{2m_\tau^4 \mathcal{B}_0(p^2, m_\tau^2, m_\tau^2)}{m_W^2} - \frac{p^2 m_\tau^2 \mathcal{B}_1(p^2, m_\tau^2, m_\tau^2)}{m_W^2} - \frac{m_\tau^2 \mathcal{A}_0(m_\tau^2)}{m_W^2} - \\
& - \frac{6m_c^4 \mathcal{B}_0(p^2, m_c^2, m_c^2)}{m_W^2} - \frac{3p^2 c_\alpha^2 m_c^2 \mathcal{B}_1(p^2, m_c^2, m_c^2)}{m_W^2} - \frac{3m_c^2 \mathcal{A}_0(m_c^2)}{m_W^2} \\
& \left. - \frac{3m_b^2 \mathcal{A}_0(m_b^2)}{m_W^2} \right\}, \tag{22}
\end{aligned}$$

$$\begin{aligned}
\{\Sigma^{SS}(p^2)\}_{\text{bos}} = & \frac{g^2}{16\pi^2} \left\{ - \frac{3s_\alpha^2 m_Z^4}{2m_W^2} + \frac{p^2 s_\alpha^2 \mathcal{B}_1(p^2, m_Z^2, m_Z^2) m_Z^2}{2m_W^2} - 3m_W^2 s_\alpha^2 + \left(\frac{v^2 \kappa c_\alpha^4}{8m_W^2} - \frac{v^2 \kappa s_\alpha^2 c_\alpha^2}{2m_W^2} + \right. \right. \\
& + \frac{3v^2 \lambda s_\alpha^2 c_\alpha^2}{4m_W^2} + \frac{3v^2 \rho s_\alpha^2 c_\alpha^2}{4m_W^2} + \frac{v^2 \kappa s_\alpha^4}{8m_W^2} \Big) \mathcal{A}_0(m_H^2) + \left(\frac{3v^2 \rho c_\alpha^4}{4m_W^2} + \frac{3v^2 \kappa s_\alpha^2 c_\alpha^2}{4m_W^2} + \frac{3v^2 \lambda s_\alpha^4}{4m_W^2} \right) \times \\
& \times \mathcal{A}_0(m_S^2) + \left(\frac{v^2 \kappa c_\alpha^2}{4m_W^2} + \frac{v^2 \lambda s_\alpha^2}{2m_W^2} + \frac{3s_\alpha^2}{2} \right) \mathcal{A}_0(m_W^2) + \left(\frac{v^2 \kappa c_\alpha^2}{8m_W^2} + \frac{3m_Z^2 s_\alpha^2}{4m_W^2} + \frac{v^2 \lambda s_\alpha^2}{4m_W^2} \right) \times \\
& \times \mathcal{A}_0(m_Z^2) + \left(\frac{v^2 w^2 \kappa^2 c_\alpha^6}{8m_W^2} - \frac{v^3 w \kappa^2 s_\alpha c_\alpha^5}{2m_W^2} + \frac{3v^3 w \kappa \lambda s_\alpha c_\alpha^5}{2m_W^2} + \frac{v^4 \kappa^2 s_\alpha^2 c_\alpha^4}{2m_W^2} - \frac{v^2 w^2 \kappa^2 s_\alpha^2 c_\alpha^4}{2m_W^2} + \right. \\
& \left. + \frac{9v^4 \lambda^2 s_\alpha^2 c_\alpha^4}{2m_W^2} - \frac{3v^4 \kappa \lambda s_\alpha^2 c_\alpha^4}{m_W^2} + \frac{3v^2 w^2 \kappa \rho s_\alpha^2 c_\alpha^4}{2m_W^2} + \frac{5v^3 w \kappa^2 s_\alpha^3 c_\alpha^3}{4m_W^2} - \frac{3v^3 w \kappa \lambda s_\alpha^3 c_\alpha^3}{m_W^2} - \right. \\
& \left. \right\} \tag{23}
\end{aligned}$$

$$\begin{aligned}
& - \frac{3v^3 w \kappa \rho s_\alpha^3 c_\alpha^3}{m_W^2} + \frac{9v^3 w \lambda \rho s_\alpha^3 c_\alpha^3}{m_W^2} - \frac{v^4 \kappa^2 s_\alpha^4 c_\alpha^2}{2m_W^2} + \frac{v^2 w^2 \kappa^2 s_\alpha^4 c_\alpha^2}{2m_W^2} + \frac{9v^2 w^2 \rho^2 s_\alpha^4 c_\alpha^2}{2m_W^2} + \frac{3v^4 \kappa \lambda s_\alpha^4 c_\alpha^2}{2m_W^2} - \\
& - \frac{3v^2 w^2 \kappa \rho s_\alpha^4 c_\alpha^2}{m_W^2} - \frac{v^3 w \kappa^2 s_\alpha^5 c_\alpha}{2m_W^2} + \frac{3v^3 w \kappa \rho s_\alpha^5 c_\alpha}{2m_W^2} + \frac{v^4 \kappa^2 s_\alpha^6}{8m_W^2} \Big) \mathcal{B}_0(p^2, m_H^2, m_H^2) + \left(\frac{v^4 \kappa^2 c_\alpha^6}{4m_W^2} + \right. \\
& + \frac{v^3 w \kappa^2 s_\alpha^5 c_\alpha}{m_W^2} - \frac{3v^3 w \kappa \rho s_\alpha^5 c_\alpha}{m_W^2} - \frac{v^4 \kappa^2 s_\alpha^2 c_\alpha^4}{m_W^2} + \frac{v^2 w^2 \kappa^2 s_\alpha^2 c_\alpha^4}{m_W^2} + \frac{9v^2 w^2 \rho^2 s_\alpha^2 c_\alpha^4}{m_W^2} + \frac{3v^4 \kappa \lambda s_\alpha^2 c_\alpha^4}{m_W^2} - \\
& - \frac{6v^2 w^2 \kappa \rho s_\alpha^2 c_\alpha^4}{m_W^2} - \frac{5v^3 w \kappa^2 s_\alpha^3 c_\alpha^3}{2m_W^2} + \frac{6v^3 w \kappa \lambda s_\alpha^3 c_\alpha^3}{m_W^2} + \frac{6v^3 w \kappa \rho s_\alpha^3 c_\alpha^3}{m_W^2} - \frac{18v^3 w \lambda \rho s_\alpha^3 c_\alpha^3}{m_W^2} + \\
& + \frac{v^4 \kappa^2 s_\alpha^4 c_\alpha^2}{m_W^2} - \frac{v^2 w^2 \kappa^2 s_\alpha^4 c_\alpha^2}{m_W^2} + \frac{9v^4 \lambda^2 s_\alpha^4 c_\alpha^2}{m_W^2} - \frac{6v^4 \kappa \lambda s_\alpha^4 c_\alpha^2}{m_W^2} + \frac{3v^2 w^2 \kappa \rho s_\alpha^4 c_\alpha^2}{m_W^2} + \frac{v^3 w \kappa^2 s_\alpha^5 c_\alpha}{m_W^2} - \\
& - \frac{3v^3 w \kappa \lambda s_\alpha^5 c_\alpha}{m_W^2} + \frac{v^2 w^2 \kappa^2 s_\alpha^6}{4m_W^2} \Big) \mathcal{B}_0(p^2, m_H^2, m_S^2) + \left(\frac{9v^2 w^2 \rho^2 c_\alpha^6}{2m_W^2} + \frac{9v^3 w \kappa \rho s_\alpha c_\alpha^5}{2m_W^2} + \frac{9v^4 \kappa^2 s_\alpha^2 c_\alpha^4}{8m_W^2} + \right. \\
& + \frac{9v^2 w^2 \kappa \rho s_\alpha^2 c_\alpha^4}{2m_W^2} + \frac{9v^3 w \kappa^2 s_\alpha^3 c_\alpha^3}{4m_W^2} + \frac{9v^3 w \lambda \rho s_\alpha^3 c_\alpha^3}{m_W^2} + \frac{9v^2 w^2 \kappa^2 s_\alpha^4 c_\alpha^2}{8m_W^2} + \frac{9v^4 \kappa \lambda s_\alpha^4 c_\alpha^2}{2m_W^2} + \\
& + \frac{9v^3 w \kappa \lambda s_\alpha^5 c_\alpha}{2m_W^2} + \frac{9v^4 \lambda^2 s_\alpha^6}{2m_W^2} \Big) \mathcal{B}_0(p^2, m_S^2, m_S^2) + \left(\frac{\lambda^2 s_\alpha^2 v^4}{m_W^2} + \frac{w \kappa \lambda c_\alpha s_\alpha v^3}{m_W^2} + \frac{w^2 \kappa^2 c_\alpha^2 v^2}{4m_W^2} - \right. \\
& - \frac{1}{2} p^2 s_\alpha^2 + 3m_W^2 s_\alpha^2 \Big) \mathcal{B}_0(p^2, m_W^2, m_W^2) + \left(\frac{\lambda^2 s_\alpha^2 v^4}{2m_W^2} + \frac{w \kappa \lambda c_\alpha s_\alpha v^3}{2m_W^2} + \frac{w^2 \kappa^2 c_\alpha^2 v^2}{8m_W^2} + \frac{3m_Z^4 s_\alpha^2}{2m_W^2} - \right. \\
& \left. - \frac{p^2 m_Z^2 s_\alpha^2}{4m_W^2} \right) \mathcal{B}_0(p^2, m_Z^2, m_Z^2) + p^2 s_\alpha^2 \mathcal{B}_1(p^2, m_W^2, m_W^2) \Big\}, \tag{24}
\end{aligned}$$

Self-Energy for the HS Mixing

$$\begin{aligned}
\{\Sigma^{HS}(p^2)\}_{\text{fer}} = & \frac{g^2}{16\pi^2} s_\alpha c_\alpha \left\{ - \frac{6m_b^4 \mathcal{B}_0(p^2, m_b^2, m_b^2)}{m_W^2} - \frac{3p^2 m_b^2 \mathcal{B}_1(p^2, m_b^2, m_b^2)}{m_W^2} - \right. \\
& - \frac{6m_t^4 \mathcal{B}_0(p^2, m_t^2, m_t^2)}{m_W^2} - \frac{3p^2 m_t^2 \mathcal{B}_1(p^2, m_t^2, m_t^2)}{m_W^2} - \frac{3m_t^2 \mathcal{A}_0(m_t^2)}{m_W^2} - \\
& - \frac{2m_\tau^4 \mathcal{B}_0(p^2, m_\tau^2, m_\tau^2)}{m_W^2} - \frac{p^2 m_\tau^2 \mathcal{B}_1(p^2, m_\tau^2, m_\tau^2)}{m_W^2} - \frac{m_\tau^2 \mathcal{A}_0(m_\tau^2)}{m_W^2} - \\
& - \frac{6m_c^4 \mathcal{B}_0(p^2, m_c^2, m_c^2)}{m_W^2} - \frac{3p^2 c_\alpha^2 m_c^2 \mathcal{B}_1(p^2, m_c^2, m_c^2)}{m_W^2} - \frac{3m_c^2 \mathcal{A}_0(m_c^2)}{m_W^2} - \\
& \left. - \frac{3m_b^2 \mathcal{A}_0(m_b^2)}{m_W^2} \right\}, \tag{25}
\end{aligned}$$

$$\begin{aligned}
\{\Sigma^{HS}(p^2)\}_{\text{bos}} = & \frac{g^2}{16\pi^2} \left\{ -\frac{3c_\alpha s_\alpha m_Z^4}{2m_W^2} + \frac{p^2 c_\alpha s_\alpha \mathcal{B}_1(p^2, m_Z^2, m_Z^2) m_Z^2}{2m_W^2} - 3c_\alpha m_W^2 s_\alpha + \right. \\
& + \left(-\frac{3v^2 \kappa s_\alpha c_\alpha^3}{8m_W^2} + \frac{3v^2 \lambda s_\alpha c_\alpha^3}{4m_W^2} + \frac{3v^2 \kappa s_\alpha^3 c_\alpha}{8m_W^2} - \frac{3v^2 \rho s_\alpha^3 c_\alpha}{4m_W^2} \right) \mathcal{A}_0(m_H^2) + \left(\frac{3v^2 \kappa s_\alpha c_\alpha^3}{8m_W^2} - \right. \\
& - \frac{3v^2 \rho s_\alpha c_\alpha^3}{4m_W^2} - \frac{3v^2 \kappa s_\alpha^3 c_\alpha}{8m_W^2} + \frac{3v^2 \lambda s_\alpha^3 c_\alpha}{4m_W^2} \left. \right) \mathcal{A}_0(m_S^2) + \left(-\frac{\kappa c_\alpha s_\alpha v^2}{4m_W^2} + \frac{\lambda c_\alpha s_\alpha v^2}{2m_W^2} + \frac{3c_\alpha s_\alpha}{2} \right) \times \\
& \times \mathcal{A}_0(m_W^2) + \left(-\frac{\kappa c_\alpha s_\alpha v^2}{8m_W^2} + \frac{\lambda c_\alpha s_\alpha v^2}{4m_W^2} + \frac{3c_\alpha m_Z^2 s_\alpha}{4m_W^2} \right) \mathcal{A}_0(m_Z^2) + \left(\frac{3v^3 w \kappa \lambda c_\alpha^6}{4m_W^2} - \right. \\
& - \frac{3v^2 w^2 \kappa^2 s_\alpha c_\alpha^5}{8m_W^2} + \frac{9v^4 \lambda^2 s_\alpha c_\alpha^5}{2m_W^2} - \frac{3v^4 \kappa \lambda s_\alpha c_\alpha^5}{2m_W^2} + \frac{9v^3 w \kappa^2 s_\alpha^2 c_\alpha^4}{8m_W^2} - \frac{15v^3 w \kappa \lambda s_\alpha^2 c_\alpha^4}{4m_W^2} + \\
& + \frac{9v^3 w \lambda \rho s_\alpha^2 c_\alpha^4}{2m_W^2} - \frac{3v^4 \kappa^2 s_\alpha^3 c_\alpha^3}{4m_W^2} + \frac{3v^2 w^2 \kappa^2 s_\alpha^3 c_\alpha^3}{4m_W^2} + \frac{3v^4 \kappa \lambda s_\alpha^3 c_\alpha^3}{m_W^2} - \frac{3v^2 w^2 \kappa \rho s_\alpha^3 c_\alpha^3}{m_W^2} - \\
& - \frac{9v^3 w \kappa^2 s_\alpha^4 c_\alpha^2}{8m_W^2} + \frac{15v^3 w \kappa \rho s_\alpha^4 c_\alpha^2}{4m_W^2} - \frac{9v^3 w \lambda \rho s_\alpha^4 c_\alpha^2}{2m_W^2} + \frac{3v^4 \kappa^2 s_\alpha^5 c_\alpha}{8m_W^2} - \frac{9v^2 w^2 \rho^2 s_\alpha^5 c_\alpha}{2m_W^2} + \\
& + \frac{3v^2 w^2 \kappa \rho s_\alpha^5 c_\alpha}{2m_W^2} - \frac{3v^3 w \kappa \rho s_\alpha^6}{4m_W^2} \left. \right) \mathcal{B}_0(p^2, m_H^2, m_H^2) + \left(\frac{v^3 w \kappa^2 c_\alpha^6}{4m_W^2} - \frac{v^4 \kappa^2 s_\alpha c_\alpha^5}{2m_W^2} + \right. \\
& + \frac{v^2 w^2 \kappa^2 s_\alpha c_\alpha^5}{2m_W^2} + \frac{3v^4 \kappa \lambda s_\alpha c_\alpha^5}{2m_W^2} - \frac{3v^2 w^2 \kappa \rho s_\alpha c_\alpha^5}{2m_W^2} - \frac{2v^3 w \kappa^2 s_\alpha^2 c_\alpha^4}{m_W^2} + \frac{9v^3 w \kappa \lambda s_\alpha^2 c_\alpha^4}{2m_W^2} + \\
& + \frac{9v^3 w \kappa \rho s_\alpha^2 c_\alpha^4}{2m_W^2} - \frac{9v^3 w \lambda \rho s_\alpha^2 c_\alpha^4}{m_W^2} + \frac{5v^4 \kappa^2 s_\alpha^3 c_\alpha^3}{4m_W^2} - \frac{5v^2 w^2 \kappa^2 s_\alpha^3 c_\alpha^3}{4m_W^2} + \frac{9v^4 \lambda^2 s_\alpha^3 c_\alpha^3}{m_W^2} - \\
& - \frac{9v^2 w^2 \rho^2 s_\alpha^3 c_\alpha^3}{m_W^2} - \frac{6v^4 \kappa \lambda s_\alpha^3 c_\alpha^3}{m_W^2} + \frac{6v^2 w^2 \kappa \rho s_\alpha^3 c_\alpha^3}{m_W^2} + \frac{2v^3 w \kappa^2 s_\alpha^4 c_\alpha^2}{m_W^2} - \frac{9v^3 w \kappa \lambda s_\alpha^4 c_\alpha^2}{2m_W^2} - \\
& - \frac{9v^3 w \kappa \rho s_\alpha^4 c_\alpha^2}{2m_W^2} + \frac{9v^3 w \lambda \rho s_\alpha^4 c_\alpha^2}{m_W^2} - \frac{v^4 \kappa^2 s_\alpha^5 c_\alpha}{2m_W^2} + \frac{v^2 w^2 \kappa^2 s_\alpha^5 c_\alpha}{2m_W^2} + \frac{3v^4 \kappa \lambda s_\alpha^5 c_\alpha}{2m_W^2} - \\
& - \frac{3v^2 w^2 \kappa \rho s_\alpha^5 c_\alpha}{2m_W^2} - \frac{v^3 w \kappa^2 s_\alpha^6}{4m_W^2} \left. \right) \mathcal{B}_0(p^2, m_H^2, m_S^2) + \left(\frac{3v^3 w \kappa \rho c_\alpha^6}{4m_W^2} + \frac{3v^4 \kappa^2 s_\alpha c_\alpha^5}{8m_W^2} - \right. \\
& - \frac{9v^2 w^2 \rho^2 s_\alpha c_\alpha^5}{2m_W^2} + \frac{3v^2 w^2 \kappa \rho s_\alpha c_\alpha^5}{2m_W^2} + \frac{9v^3 w \kappa^2 s_\alpha^2 c_\alpha^4}{8m_W^2} - \frac{15v^3 w \kappa \rho s_\alpha^2 c_\alpha^4}{4m_W^2} + \frac{9v^3 w \lambda \rho s_\alpha^2 c_\alpha^4}{2m_W^2} - \\
& - \frac{3v^4 \kappa^2 s_\alpha^3 c_\alpha^3}{4m_W^2} + \frac{3v^2 w^2 \kappa^2 s_\alpha^3 c_\alpha^3}{4m_W^2} + \frac{3v^4 \kappa \lambda s_\alpha^3 c_\alpha^3}{m_W^2} - \frac{3v^2 w^2 \kappa \rho s_\alpha^3 c_\alpha^3}{m_W^2} - \frac{9v^3 w \kappa^2 s_\alpha^4 c_\alpha^2}{8m_W^2} + \\
& + \frac{15v^3 w \kappa \lambda s_\alpha^4 c_\alpha^2}{4m_W^2} - \frac{9v^3 w \lambda \rho s_\alpha^4 c_\alpha^2}{2m_W^2} - \frac{3v^2 w^2 \kappa^2 s_\alpha^5 c_\alpha}{8m_W^2} + \frac{9v^4 \lambda^2 s_\alpha^5 c_\alpha}{2m_W^2} - \frac{3v^4 \kappa \lambda s_\alpha^5 c_\alpha}{2m_W^2} - \\
& \left. - \frac{3v^3 w \kappa \lambda s_\alpha^6}{4m_W^2} \right) \mathcal{B}_0(p^2, m_S^2, m_S^2) + \left(\frac{\lambda^2 c_\alpha s_\alpha v^4}{m_W^2} - \frac{w \kappa \lambda s_\alpha^2 v^3}{2m_W^2} + \frac{w \kappa \lambda c_\alpha^2 v^3}{2m_W^2} - \right.
\end{aligned}$$

(26)

$$\begin{aligned}
& -\frac{w^2\kappa^2c_\alpha s_\alpha v^2}{4m_W^2} + 3c_\alpha m_W^2 s_\alpha - \frac{1}{2}p^2 c_\alpha s_\alpha \Big) \mathcal{B}_0(p^2, m_W^2, m_W^2) + \left(\frac{\lambda^2 c_\alpha s_\alpha v^4}{2m_W^2} - \frac{w\kappa\lambda s_\alpha^2 v^3}{4m_W^2} + \right. \\
& + \frac{w\kappa\lambda c_\alpha^2 v^3}{4m_W^2} - \frac{w^2\kappa^2c_\alpha s_\alpha v^2}{8m_W^2} + \frac{3c_\alpha m_Z^4 s_\alpha}{2m_W^2} - \frac{p^2 c_\alpha m_Z^2 s_\alpha}{4m_W^2} \Big) \mathcal{B}_0(p^2, m_Z^2, m_Z^2) + \\
& \left. + p^2 c_\alpha s_\alpha \mathcal{B}_1(p^2, m_W^2, m_W^2) \right\}, \tag{27}
\end{aligned}$$

Self-Energies for the Top Quark

$$\begin{aligned}
\Sigma_S^t(p^2) = & \frac{g^2}{16\pi^2} \left\{ -\frac{c_\alpha^2 m_t^2 \mathcal{B}_0(p^2, m_H^2, m_t^2)}{4m_W^2} - \frac{m_t^2 s_\alpha^2 \mathcal{B}_0(p^2, m_S^2, m_t^2)}{4m_W^2} + \mathcal{B}_0(p^2, 0, m_t^2) \times \right. \\
& \times \left(\frac{16\pi v^2 \alpha_s}{3m_W^2} - \frac{16m_W^2}{9m_Z^2} + \frac{16}{9} \right) + \left(\frac{m_t^2}{4m_W^2} + \frac{4m_Z^2}{9m_W^2} + \frac{16m_W^2}{9m_Z^2} - \frac{20}{9} \right) \mathcal{B}_0(p^2, m_t^2, m_Z^2) - \\
& \left. - \frac{8\pi v^2 \alpha_s}{3m_W^2} - \frac{2m_Z^2}{9m_W^2} + \frac{2}{9} \right\}, \tag{28}
\end{aligned}$$

$$\begin{aligned}
\Sigma_V^t(p^2) = & \frac{g^2}{16\pi^2} \left\{ -\frac{c_\alpha^2 m_t^2 \mathcal{B}_1(p^2, m_t^2, m_H^2)}{4m_W^2} - \frac{m_t^2 s_\alpha^2 \mathcal{B}_1(p^2, m_t^2, m_S^2)}{4m_W^2} - \frac{17m_Z^2}{72m_W^2} + \frac{1}{9} + \right. \\
& + \mathcal{B}_0(p^2, 0, m_t^2) \left(\frac{8\pi v^2 \alpha_s}{3m_W^2} - \frac{8m_W^2}{9m_Z^2} + \frac{8}{9} \right) + \mathcal{B}_1(p^2, 0, m_t^2) \left(\frac{8\pi v^2 \alpha_s}{3m_W^2} - \frac{8m_W^2}{9m_Z^2} + \frac{8}{9} \right) + \\
& \left. + \left(-\frac{m_t^2}{4m_W^2} - \frac{17m_Z^2}{36m_W^2} - \frac{8m_W^2}{9m_Z^2} + \frac{10}{9} \right) \mathcal{B}_1(p^2, m_t^2, m_Z^2) - \frac{4\pi v^2 \alpha_s}{3m_W^2} \right\}, \tag{29}
\end{aligned}$$

$$\Sigma_A^t(p^2) = \frac{g^2}{16\pi^2} \left\{ \left(\frac{2}{3} - \frac{5m_Z^2}{12m_W^2} \right) \mathcal{B}_1(p^2, m_t^2, m_Z^2) - \frac{5m_Z^2}{24m_W^2} + \frac{1}{3} \right\}, \tag{30}$$

C - SSM Three Point Functions

One-Loop Corrections to SZZ Vertex

$$\begin{aligned}
\{\delta V_Z^\mathcal{E}(p^2, k^2, q^2)\}_{\text{fer}} = & \frac{g^2}{16\pi^2} \frac{1}{12m_W^2} \left\{ 4(4c_W^4 - 2c_W^2 + 7) \mathcal{B}_0(q^2, m_b^2, m_b^2) m_b^2 + \right. \\
& (16c_W^4 - 20c_W^2 + 13) m_c^2 \times \mathcal{B}_0(q^2, m_c^2, m_c^2) + (64m_t^2 c_W^4 - 80m_t^2 c_W^2 + 52m_t^2) \times \\
& \left. \mathcal{B}_0(q^2, m_t^2, m_t^2) \right\} \tag{31}
\end{aligned}$$

$$\begin{aligned}
& \times \mathcal{B}_0(q^2, m_t^2, m_t^2) + (48m_\tau^2 c_W^4 - 72m_\tau^2 c_W^2 + 36m_\tau^2) \mathcal{B}_0(q^2, m_\tau^2, m_\tau^2) + \left(8k^2 m_b^2 c_W^4 + \right. \\
& + p^2 m_b^2 c_W^4 - 8q^2 m_b^2 c_W^4 - 4k^2 m_b^2 c_W^2 - 4p^2 m_b^2 c_W^2 + 4q^2 m_b^2 c_W^2 + 36m_b^4 + 5k^2 m_b^2 + \\
& \left. + 5p^2 m_b^2 - 5q^2 m_b^2 \right) \mathcal{C}_0(k^2, q^2, p^2, m_b^2, m_b^2, m_b^2) + \left(32k^2 m_c^2 c_W^4 + 32p^2 m_c^2 c_W^4 - \right. \\
& - 32q^2 m_c^2 c_W^4 - 40k^2 m_c^2 c_W^2 - 40p^2 m_c^2 c_W^2 + 40q^2 m_c^2 c_W^2 + 36m_c^4 + 17k^2 m_c^2 + 17p^2 m_c^2 - \\
& \left. - 17q^2 m_c^2 \right) \mathcal{C}_0(k^2, q^2, p^2, m_c^2, m_c^2, m_c^2) + \left(32k^2 m_t^2 c_W^4 + 32p^2 m_t^2 c_W^4 - 32q^2 m_t^2 c_W^4 - \right. \\
& - 40k^2 m_t^2 c_W^2 - 40p^2 m_t^2 c_W^2 + 40q^2 m_t^2 c_W^2 + 36m_t^4 + 17k^2 m_t^2 + 17p^2 m_t^2 - 17q^2 m_t^2 \left. \right) \times \\
& \times \mathcal{C}_0(k^2, q^2, p^2, m_t^2, m_t^2, m_t^2) + \left(24k^2 m_\tau^2 c_W^4 + 24p^2 m_\tau^2 c_W^4 - 24q^2 m_\tau^2 c_W^4 - 36k^2 m_\tau^2 c_W^2 - \right. \\
& - 36p^2 m_\tau^2 c_W^2 + 36q^2 m_\tau^2 c_W^2 + 12m_\tau^4 + 15m_\tau^2(k^2 + p^2 - q^2) \left. \right) \mathcal{C}_0(k^2, q^2, p^2, m_\tau^2, m_\tau^2, m_\tau^2) + \\
& + (-64m_b^2 c_W^4 + 32m_b^2 c_W^2 - 40m_b^2) \mathcal{C}_{00}(k^2, q^2, p^2, m_b^2, m_b^2, m_b^2) + \left(-256m_c^2 c_W^4 + \right. \\
& \left. + 320m_c^2 c_W^2 - 136m_c^2 \right) \mathcal{C}_{00}(k^2, q^2, p^2, m_c^2, m_c^2, m_c^2) + (-256m_t^2 c_W^4 + 320m_t^2 c_W^2 - 136m_t^2) \times \\
& \times \mathcal{C}_{00}(k^2, q^2, p^2, m_t^2, m_t^2, m_t^2) + (-192c_W^4 + 288c_W^2 - 120) m_\tau^2 \mathcal{C}_{00}(k^2, q^2, p^2, m_\tau^2, m_\tau^2, m_\tau^2) + \\
& + (32k^2 m_b^2 c_W^4 - 16k^2 m_b^2 c_W^2 + 29k^2 m_b^2 + 9p^2 m_b^2 - 9q^2 m_b^2) \mathcal{C}_1(k^2, q^2, p^2, m_b^2, m_b^2, m_b^2) + \\
& + (128k^2 m_c^2 c_W^4 - 160k^2 m_c^2 c_W^2 + 77k^2 m_c^2 + 9p^2 m_c^2 - 9q^2 m_c^2) \mathcal{C}_1(k^2, q^2, p^2, m_c^2, m_c^2, m_c^2) + \\
& + (128k^2 m_t^2 c_W^4 - 160k^2 m_t^2 c_W^2 + 77k^2 m_t^2 + 9p^2 m_t^2 - 9q^2 m_t^2) \mathcal{C}_1(k^2, q^2, p^2, m_t^2, m_t^2, m_t^2) + \\
& + (96k^2 m_\tau^2 c_W^4 - 144k^2 m_\tau^2 c_W^2 + 63k^2 m_\tau^2 + 3p^2 m_\tau^2 - 3q^2 m_\tau^2) \mathcal{C}_1(k^2, q^2, p^2, m_\tau^2, m_\tau^2, m_\tau^2) + \\
& + m_b^2 \left(16k^2 c_W^4 + 16p^2 c_W^4 - 16q^2 c_W^4 - 8k^2 c_W^2 - 8p^2 c_W^2 + 8q^2 c_W^2 + 10k^2 + 28p^2 - 10q^2 \right) \times \\
& \times \mathcal{C}_2(k^2, q^2, p^2, m_b^2, m_b^2, m_b^2) + \left(64k^2 m_c^2 c_W^4 + 64p^2 m_c^2 c_W^4 - 64q^2 m_c^2 c_W^4 - 80k^2 m_c^2 c_W^2 - \right. \\
& - 80p^2 m_c^2 c_W^2 + 80q^2 m_c^2 c_W^2 + 34k^2 m_c^2 + 52p^2 m_c^2 - 34q^2 m_c^2 \left. \right) \mathcal{C}_2(k^2, q^2, p^2, m_c^2, m_c^2, m_c^2) + \\
& + m_t^2 (64k^2 c_W^4 + 64p^2 c_W^4 - 64q^2 c_W^4 - 80k^2 c_W^2 - 80p^2 c_W^2 + 80q^2 c_W^2 + 34k^2 + 52p^2 - 34q^2) \times \\
& \times \mathcal{C}_2(k^2, q^2, p^2, m_t^2, m_t^2, m_t^2) + \left(48k^2 m_\tau^2 c_W^4 + 48p^2 m_\tau^2 c_W^4 - 48q^2 m_\tau^2 c_W^4 - 72k^2 m_\tau^2 c_W^2 - \right. \\
& - 72p^2 m_\tau^2 c_W^2 + 72q^2 m_\tau^2 c_W^2 + 30k^2 m_\tau^2 + 36p^2 m_\tau^2 - 30q^2 m_\tau^2 \left. \right) \mathcal{C}_2(k^2, q^2, p^2, m_\tau^2, m_\tau^2, m_\tau^2) \left. \right\}, \tag{32}
\end{aligned}$$

$$\begin{aligned}
\{\delta V_Z^{\mathcal{D}}(p^2, k^2, q^2)\}_{\text{fer}} = & \frac{g^2}{16\pi^2} \frac{1}{6m_W^2} \left\{ - (8c_W^4 - 4c_W^2 + 5) \mathcal{C}_0(k^2, q^2, p^2, m_b^2, m_b^2, m_b^2) m_b^2 - \right. \\
& - 9\mathcal{C}_1(k^2, q^2, p^2, m_b^2, m_b^2, m_b^2) m_b^2 - (32c_W^4 - 40c_W^2 + 17) m_c^2 \mathcal{C}_0(k^2, q^2, p^2, m_c^2, m_c^2, m_c^2) - \\
& - (32m_t^2 c_W^4 - 40m_t^2 c_W^2 + 17m_t^2) \mathcal{C}_0(k^2, q^2, p^2, m_t^2, m_t^2, m_t^2) - m_\tau^2 (24c_W^4 - 36c_W^2 + 15) \times \\
& \times \mathcal{C}_0(k^2, q^2, p^2, m_\tau^2, m_\tau^2, m_\tau^2) - 9m_c^2 \mathcal{C}_1(k^2, q^2, p^2, m_c^2, m_c^2, m_c^2) - 3m_\tau^2 \mathcal{C}_1(k^2, q^2, p^2, m_\tau^2, m_\tau^2, m_\tau^2) - \\
& - 9m_t^2 \mathcal{C}_1(k^2, q^2, p^2, m_t^2, m_t^2, m_t^2) - (32m_b^2 c_W^4 - 16m_b^2 c_W^2 + 20m_b^2) \mathcal{C}_{12}(k^2, q^2, p^2, m_b^2, m_b^2, m_b^2) - \\
& - (128m_c^2 c_W^4 - 160m_c^2 c_W^2 + 68m_c^2) \mathcal{C}_{12}(k^2, q^2, p^2, m_c^2, m_c^2, m_c^2) - \left(128m_t^2 c_W^4 - 160m_t^2 c_W^2 + \right. \\
& \left. + 68m_t^2 \right) \mathcal{C}_{12}(k^2, q^2, p^2, m_t^2, m_t^2, m_t^2) - m_\tau^2 (96c_W^4 - 144c_W^2 + 60) \mathcal{C}_{12}(k^2, q^2, p^2, m_\tau^2, m_\tau^2, m_\tau^2) - \\
& - (32m_b^2 c_W^4 - 16m_b^2 c_W^2 + 20m_b^2) \mathcal{C}_2(k^2, q^2, p^2, m_b^2, m_b^2, m_b^2) - m_c^2 (128c_W^4 - 160c_W^2 + 68) \times \\
& \times \mathcal{C}_2(k^2, q^2, p^2, m_c^2, m_c^2, m_c^2) - (128m_t^2 c_W^4 - 160m_t^2 c_W^2 + 68m_t^2) \mathcal{C}_2(k^2, q^2, p^2, m_t^2, m_t^2, m_t^2) - \\
& - (96m_\tau^2 c_W^4 - 144m_\tau^2 c_W^2 + 60m_\tau^2) \mathcal{C}_2(k^2, q^2, p^2, m_\tau^2, m_\tau^2, m_\tau^2) - m_b^2 \left(32c_W^4 - 16c_W^2 + 20 \right) \times \\
& \times \mathcal{C}_{22}(k^2, q^2, p^2, m_b^2, m_b^2, m_b^2) - m_c^2 (128c_W^4 - 160c_W^2 + 68) \mathcal{C}_{22}(k^2, q^2, p^2, m_c^2, m_c^2, m_c^2) - \\
& - m_t^2 (128c_W^4 - 160c_W^2 + 68) \mathcal{C}_{22}(k^2, q^2, p^2, m_t^2, m_t^2, m_t^2) - m_\tau^2 (96c_W^4 - 144c_W^2 + 60) \times \\
& \left. \times \mathcal{C}_{22}(k^2, q^2, p^2, m_\tau^2, m_\tau^2, m_\tau^2) \right\}, \tag{33}
\end{aligned}$$

$$\begin{aligned}
\{V_Z^{\mathcal{E}}(p^2, k^2, q^2)\}_{\text{bos}} = & \frac{g^2}{16\pi^2} \frac{1}{8m_W^2 s_\alpha c_W^4} \left\{ - \frac{1}{m_Z^2} \left(4s_\alpha c_\alpha^2 \mathcal{B}_0(k^2, m_H^2, m_Z^2) m_W^4 + \right. \right. \\
& \left. \left. + 4s_\alpha^3 \mathcal{B}_0(k^2, m_S^2, m_Z^2) m_W^4 \right) - \frac{4c_\alpha^2 s_\alpha \mathcal{B}_0(q^2, m_H^2, m_Z^2) m_W^4}{m_Z^2} - \frac{4s_\alpha^3 \mathcal{B}_0(q^2, m_S^2, m_Z^2) m_W^4}{m_Z^2} - \right. \\
& - 8c_\alpha^2 s_\alpha \mathcal{C}_0(p^2, q^2, k^2, m_Z^2, m_Z^2, m_H^2) m_W^4 - 8s_\alpha^3 \mathcal{C}_0(p^2, q^2, k^2, m_Z^2, m_Z^2, m_S^2) m_W^4 - \\
& - (8m_W^2 s_\alpha c_W^8 - 16m_W^2 s_\alpha c_W^6 + 8m_W^2 s_\alpha c_W^4) \mathcal{B}_0(k^2, m_W^2, m_W^2) - \left(v w \kappa c_W^4 c_\alpha^5 - \right. \\
& \left. - 2v^2 \kappa c_W^4 s_\alpha c_\alpha^4 + 6v^2 \lambda c_W^4 s_\alpha c_\alpha^4 - 2v w \kappa c_W^4 s_\alpha^2 c_\alpha^3 + 6v w \rho c_W^4 s_\alpha^2 c_\alpha^3 + v^2 \kappa c_W^4 s_\alpha^3 c_\alpha^2 \right) \times \\
& \times \mathcal{B}_0(p^2, m_H^2, m_H^2) - \left(- 2v w \kappa c_\alpha s_\alpha^4 c_W^4 - 4v^2 \kappa c_\alpha^2 s_\alpha^3 c_W^4 + 12v^2 \lambda c_\alpha^2 s_\alpha^3 c_W^4 + 4v w \kappa c_\alpha^3 s_\alpha^2 c_W^4 - \right. \\
& \left. - 12v w \rho c_\alpha^3 s_\alpha^2 c_W^4 + 2v^2 \kappa c_\alpha^4 s_\alpha c_W^4 \right) \mathcal{B}_0(p^2, m_H^2, m_S^2) - \left(6v^2 \lambda c_W^4 s_\alpha^5 + 3v w \kappa c_W^4 c_\alpha s_\alpha^4 + \right. \\
& \left. + 3v^2 \kappa c_W^4 c_\alpha^2 s_\alpha^3 + 6v w \rho c_W^4 c_\alpha^3 s_\alpha^2 \right) \mathcal{B}_0(p^2, m_S^2, m_S^2) - \left(8v w \kappa c_\alpha c_W^8 + 48m_W^2 s_\alpha c_W^8 + \right. \tag{34}
\end{aligned}$$

$$\begin{aligned}
& + 16v^2\lambda s_\alpha c_W^8 - 8v\omega\kappa c_\alpha c_W^6 - 16v^2\lambda s_\alpha c_W^6 + 2v\omega\kappa c_\alpha c_W^4 + 4v^2\lambda s_\alpha c_W^4 \Big) \mathcal{B}_0(p^2, m_W^2, m_W^2) - \\
& - (v\omega\kappa c_\alpha c_W^4 + 2v^2\lambda s_\alpha c_W^4) \mathcal{B}_0(p^2, m_Z^2, m_Z^2) - (-8m_W^2 s_\alpha c_W^8 - 32m_W^2 s_\alpha c_W^6 + 8m_W^2 s_\alpha c_W^4) \times \\
& \times \mathcal{B}_0(q^2, m_W^2, m_W^2) - \left(4v\omega\kappa c_W^2 m_W^2 s_\alpha^5 - 8v^2\kappa c_W^2 m_W^2 s_\alpha^4 + 24v^2\lambda c_W^2 m_W^2 s_\alpha^4 - \right. \\
& - 8v\omega\kappa c_W^2 m_W^2 s_\alpha^3 c_\alpha^3 + 24v\omega\rho c_W^2 m_W^2 s_\alpha^2 c_\alpha^3 + 4v^2\kappa c_W^2 m_W^2 s_\alpha^3 c_\alpha^2 \Big) \mathcal{C}_0(k^2, p^2, q^2, m_Z^2, m_H^2, m_H^2) - \\
& - \left(4v^2\kappa c_W^2 m_W^2 s_\alpha^4 c_\alpha^4 + 8v\omega\kappa c_W^2 m_W^2 s_\alpha^3 c_\alpha^3 - 24v\omega\rho c_W^2 m_W^2 s_\alpha^2 c_\alpha^3 - 8v^2\kappa c_W^2 m_W^2 s_\alpha^3 c_\alpha^2 + \right. \\
& + 24v^2\lambda c_W^2 m_W^2 s_\alpha^3 c_\alpha^2 - 4v\omega\kappa c_W^2 m_W^2 s_\alpha^4 c_\alpha \Big) \mathcal{C}_0(k^2, p^2, q^2, m_Z^2, m_H^2, m_S^2) - \left(24v^2\lambda c_W^2 m_W^2 s_\alpha^5 + \right. \\
& + 12v\omega\kappa c_W^2 c_\alpha m_W^2 s_\alpha^4 + 12v^2\kappa c_W^2 c_\alpha^2 m_W^2 s_\alpha^3 + 24v\omega\rho c_W^2 c_\alpha^3 m_W^2 s_\alpha^2 \Big) \mathcal{C}_0(k^2, p^2, q^2, m_Z^2, m_S^2, m_S^2) - \\
& - c_W^4 \left(8v\omega\kappa c_\alpha m_W^2 c_W^4 - 40k^2 m_W^2 s_\alpha c_W^4 + 48p^2 m_W^2 s_\alpha c_W^4 - 40q^2 m_W^2 s_\alpha c_W^4 + 16v^2\lambda m_W^2 s_\alpha c_W^4 - \right. \\
& - 16v\omega\kappa c_\alpha m_W^2 c_W^2 - 48m_W^4 s_\alpha c_W^2 - 8k^2 m_W^2 s_\alpha c_W^2 - 16p^2 m_W^2 s_\alpha c_W^2 + 8q^2 m_W^2 s_\alpha c_W^2 - \\
& - 32v^2\lambda m_W^2 s_\alpha c_W^2 + 8v\omega\kappa c_\alpha m_W^2 + 16m_W^4 s_\alpha + 16v^2\lambda m_W^2 s_\alpha \Big) \mathcal{C}_0(k^2, q^2, p^2, m_W^2, m_W^2, m_W^2) - \\
& - \left(4v^2\kappa c_W^2 m_W^2 s_\alpha^4 c_\alpha^4 + 8v\omega\kappa c_W^2 m_W^2 s_\alpha^3 c_\alpha^3 - 24v\omega\rho c_W^2 m_W^2 s_\alpha^2 c_\alpha^3 - 8v^2\kappa c_W^2 m_W^2 s_\alpha^3 c_\alpha^2 + \right. \\
& + 24v^2\lambda c_W^2 m_W^2 s_\alpha^3 c_\alpha^2 - 4v\omega\kappa c_W^2 m_W^2 s_\alpha^4 c_\alpha \Big) \mathcal{C}_0(q^2, p^2, k^2, m_Z^2, m_H^2, m_S^2) - \left(-4v\omega\kappa c_W^4 c_\alpha^5 + \right. \\
& + 8v^2\kappa c_W^4 s_\alpha c_\alpha^4 - 24v^2\lambda c_W^4 s_\alpha c_\alpha^4 + 8v\omega\kappa c_W^4 s_\alpha^2 c_\alpha^3 - 24v\omega\rho c_W^4 s_\alpha^2 c_\alpha^3 - 4v^2\kappa c_W^4 s_\alpha^3 c_\alpha^2 \Big) \times \\
& \times \mathcal{C}_{00}(k^2, p^2, q^2, m_Z^2, m_H^2, m_H^2) - \left(4v\omega\kappa c_\alpha s_\alpha^4 c_W^4 + 8v^2\kappa c_\alpha^3 s_\alpha^4 c_W^4 - 24v^2\lambda c_\alpha^2 s_\alpha^3 c_W^4 - \right. \\
& - 8v\omega\kappa c_\alpha^3 s_\alpha^2 c_W^4 + 24v\omega\rho c_\alpha^3 s_\alpha^2 c_W^4 - 4v^2\kappa c_\alpha^4 s_\alpha c_W^4 \Big) \mathcal{C}_{00}(k^2, p^2, q^2, m_Z^2, m_H^2, m_S^2) - \\
& - c_W^4 \left(-24v^2\lambda s_\alpha^5 - 12v\omega\kappa c_\alpha s_\alpha^4 - 12v^2\kappa c_\alpha^2 s_\alpha^3 - 24v\omega\rho c_\alpha^3 s_\alpha^2 \right) \mathcal{C}_{00}(k^2, p^2, q^2, m_Z^2, m_S^2, m_S^2) - \\
& - \left(-32v\omega\kappa c_\alpha c_W^8 - 192m_W^2 s_\alpha c_W^8 - 64v^2\lambda s_\alpha c_W^8 + 32v\omega\kappa c_\alpha c_W^6 + 64m_W^2 s_\alpha c_W^6 + 64v^2\lambda s_\alpha c_W^6 - \right. \\
& - 8v\omega\kappa c_\alpha c_W^4 - 16m_W^2 s_\alpha c_W^4 - 16v^2\lambda s_\alpha c_W^4 \Big) \mathcal{C}_{00}(k^2, q^2, p^2, m_W^2, m_W^2, m_W^2) - \left(-4v\omega\kappa c_\alpha^3 c_W^4 - \right. \\
& - 8v^2\lambda c_\alpha^2 s_\alpha c_W^4 - 8c_\alpha^2 m_W^2 s_\alpha c_W^2 \Big) \mathcal{C}_{00}(p^2, q^2, k^2, m_Z^2, m_Z^2, m_H^2) - \left(-8v^2\lambda s_\alpha^3 c_W^4 - \right.
\end{aligned}$$

$$\begin{aligned}
& -4v\omega\kappa c_\alpha s_\alpha^2 c_W^4 - 8m_W^2 s_\alpha^3 c_W^2) \mathcal{C}_{00}(p^2, q^2, k^2, m_Z^2, m_Z^2, m_S^2) - \left(4v\omega\kappa c_\alpha s_\alpha^4 c_W^4 + \right. \\
& + 8v^2 \kappa c_\alpha^2 s_\alpha^3 c_W^4 - 24v^2 \lambda c_\alpha^2 s_\alpha^3 c_W^4 - 8v\omega\kappa c_\alpha^3 s_\alpha^2 c_W^4 + 24v\omega\rho c_\alpha^3 s_\alpha^2 c_W^4 - 4v^2 \kappa c_\alpha^4 s_\alpha c_W^4) \times \\
& \times \mathcal{C}_{00}(q^2, p^2, k^2, m_Z^2, m_H^2, m_S^2) - \left(-8k^2 m_W^2 s_\alpha c_W^8 - 8p^2 m_W^2 s_\alpha c_W^8 + 8q^2 m_W^2 s_\alpha c_W^8 - \right. \\
& - 32k^2 m_W^2 s_\alpha c_W^6) \mathcal{C}_1(k^2, q^2, p^2, m_W^2, m_W^2, m_W^2) - \left(-16p^2 m_W^2 s_\alpha c_W^8 - 16k^2 m_W^2 s_\alpha c_W^6 - \right. \\
& \left. - 16p^2 m_W^2 s_\alpha c_W^6 + 16q^2 m_W^2 s_\alpha c_W^6) \mathcal{C}_2(k^2, q^2, p^2, m_W^2, m_W^2, m_W^2) \right\}, \tag{35}
\end{aligned}$$

$$\begin{aligned}
\{\delta V_Z^{\mathcal{D}}(p^2, k^2, q^2)\}_{\text{bos}} &= \frac{g^2}{16\pi^2} \frac{1}{2m_W^2 c_W^2 s_\alpha} \left\{ \frac{4s_\alpha \mathcal{C}_1(k^2, q^2, p^2, m_W^2, m_W^2, m_W^2) m_W^4}{m_Z^2} + \right. \\
& + \frac{4(8c_W^4 - 4c_W^2 + 1) s_\alpha \mathcal{C}_0(k^2, q^2, p^2, m_W^2, m_W^2, m_W^2) m_W^4}{m_Z^2} + 2c_\alpha^2 s_\alpha \mathcal{C}_0(p^2, q^2, k^2, m_Z^2, m_Z^2, m_H^2) m_W^2 + \\
& + 2s_\alpha^3 \mathcal{C}_0(p^2, q^2, k^2, m_Z^2, m_Z^2, m_S^2) m_W^2 + 2c_\alpha^2 s_\alpha \mathcal{C}_2(p^2, q^2, k^2, m_Z^2, m_Z^2, m_H^2) m_W^2 + \\
& + 2s_\alpha^3 \mathcal{C}_2(p^2, q^2, k^2, m_Z^2, m_Z^2, m_S^2) m_W^2 + (v\omega\kappa c_W^2 c_\alpha^2 + 2v^2 \lambda c_W^2 s_\alpha c_\alpha^2 + 2m_W^2 s_\alpha c_\alpha^2) \times \\
& \times \mathcal{C}_1(p^2, q^2, k^2, m_Z^2, m_Z^2, m_H^2) + s_\alpha^2 (2v^2 \lambda c_W^2 s_\alpha + 2m_W^2 s_\alpha + v\omega\kappa c_W^2 c_\alpha) \mathcal{C}_1(p^2, q^2, k^2, m_Z^2, m_Z^2, m_S^2) + \\
& + (v\omega\kappa c_W^2 c_\alpha^3 + 2v^2 \lambda c_W^2 s_\alpha c_\alpha^2 + 2m_W^2 s_\alpha c_\alpha^2) \mathcal{C}_{11}(p^2, q^2, k^2, m_Z^2, m_Z^2, m_H^2) + \left(2v^2 \lambda c_W^2 s_\alpha^3 + \right. \\
& \left. + 2m_W^2 s_\alpha^3 + v\omega\kappa c_W^2 c_\alpha s_\alpha^2) \mathcal{C}_{11}(p^2, q^2, k^2, m_Z^2, m_Z^2, m_S^2) + \left(-v\omega\kappa c_W^2 c_\alpha^5 + 2v^2 \kappa c_W^2 s_\alpha c_\alpha^4 - \right. \\
& \left. - 6v^2 \lambda c_W^2 s_\alpha c_\alpha^4 + 2v\omega\kappa c_W^2 s_\alpha^2 c_\alpha^3 - 6v\omega\rho c_W^2 s_\alpha^2 c_\alpha^3 - v^2 \kappa c_W^2 s_\alpha^3 c_\alpha^2) \mathcal{C}_{12}(k^2, p^2, q^2, m_Z^2, m_H^2, m_S^2) + \right. \\
& + (-v^2 \kappa c_W^2 s_\alpha c_\alpha^4 - 2v\omega\kappa c_W^2 s_\alpha^2 c_\alpha^3 + 6v\omega\rho c_W^2 s_\alpha^2 c_\alpha^3 + 2v^2 \kappa c_W^2 s_\alpha^3 c_\alpha^2 - 6v^2 \lambda c_W^2 s_\alpha^3 c_\alpha^2 + v\omega\kappa c_W^2 s_\alpha^4 c_\alpha) \times \\
& \times \mathcal{C}_{12}(k^2, p^2, q^2, m_Z^2, m_H^2, m_S^2) + (-6v^2 \lambda c_W^2 s_\alpha^5 - 3v\omega\kappa c_W^2 c_\alpha s_\alpha^4 - 3v^2 \kappa c_W^2 c_\alpha^2 s_\alpha^3 - 6v\omega\rho c_W^2 c_\alpha^3 s_\alpha^2) \times \\
& \times \mathcal{C}_{12}(k^2, p^2, q^2, m_Z^2, m_S^2, m_S^2) + c_W^2 \left(8v\omega\kappa c_\alpha c_W^4 + 48m_W^2 s_\alpha c_W^4 + 16v^2 \lambda s_\alpha c_W^4 - 8v\omega\kappa c_\alpha c_W^2 - \right. \\
& \left. - 16m_W^2 s_\alpha c_W^2 - 16v^2 \lambda s_\alpha c_W^2 + 2v\omega\kappa c_\alpha + 4m_W^2 s_\alpha + 4v^2 \lambda s_\alpha) \mathcal{C}_{12}(k^2, q^2, p^2, m_W^2, m_W^2, m_W^2) + \right. \\
& + (v\omega\kappa c_W^2 c_\alpha^3 + 2v^2 \lambda c_W^2 s_\alpha c_\alpha^2 + 2m_W^2 s_\alpha c_\alpha^2) \mathcal{C}_{12}(p^2, q^2, k^2, m_Z^2, m_Z^2, m_H^2) + \left(2v^2 \lambda c_W^2 s_\alpha^3 + \right. \\
& \left. + 2m_W^2 s_\alpha^3 + v\omega\kappa c_W^2 c_\alpha s_\alpha^2) \mathcal{C}_{12}(p^2, q^2, k^2, m_Z^2, m_Z^2, m_S^2) + \left(-v^2 \kappa c_W^2 s_\alpha c_\alpha^4 - 2v\omega\kappa c_W^2 s_\alpha^2 c_\alpha^3 + \right.
\end{aligned}$$

$$\begin{aligned}
& + 6v\omega\rho c_W^2 s_\alpha^2 c_\alpha^3 + 2v^2 \kappa c_W^2 s_\alpha^3 c_\alpha^2 - 6v^2 \lambda c_W^2 s_\alpha^3 c_\alpha^2 + v\omega\kappa c_W^2 s_\alpha^4 c_\alpha \Big) \mathcal{C}_{12}(q^2, p^2, k^2, m_Z^2, m_H^2, m_S^2) + \\
& + \left(8v\omega\kappa c_\alpha c_W^6 + 48m_W^2 s_\alpha c_W^6 + 16v^2 \lambda s_\alpha c_W^6 - 8v\omega\kappa c_\alpha c_W^4 - 16m_W^2 s_\alpha c_W^4 - 16v^2 \lambda s_\alpha c_W^4 + \right. \\
& + 2v\omega\kappa c_\alpha c_W^2 + 4m_W^2 s_\alpha c_W^2 + 4v^2 \lambda s_\alpha c_W^2 \Big) \mathcal{C}_2(k^2, q^2, p^2, m_W^2, m_W^2, m_W^2) + \left(8v\omega\kappa c_\alpha c_W^6 + \right. \\
& + 48m_W^2 s_\alpha c_W^6 + 16v^2 \lambda s_\alpha c_W^6 - 8v\omega\kappa c_\alpha c_W^4 - 16m_W^2 s_\alpha c_W^4 - 16v^2 \lambda s_\alpha c_W^4 + 2v\omega\kappa c_\alpha c_W^2 + \\
& \left. + 4m_W^2 s_\alpha c_W^2 + 4v^2 \lambda s_\alpha c_W^2 \right) \mathcal{C}_{22}(k^2, q^2, p^2, m_W^2, m_W^2, m_W^2) \Big\}. \tag{36}
\end{aligned}$$

One-Loop Corrections to S $\overline{W}W$ Vertex

$$\begin{aligned}
\{\delta V_W^\mathcal{E}(p^2, k^2, q^2)\}_{\text{fer}} &= \frac{g^2}{16\pi^2} \frac{1}{m_W^2} \left\{ -6\mathcal{C}_{00}(p^2, q^2, k^2, m_b^2, m_b^2, m_t^2) m_b^2 + 3m_c^2 \mathcal{B}_0(q^2, 0, m_c^2) + \right. \\
& + m_\tau^2 \mathcal{B}_0(q^2, 0, m_\tau^2) + \left(\frac{3m_b^2}{m_W^2} + \frac{3m_t^2}{m_W^2} \right) m_W^2 \mathcal{B}_0(q^2, m_b^2, m_t^2) + \left(\frac{3m_c^4}{m_W^2} - \frac{3k^2 m_c^2}{m_W^2} \right) m_W^2 \times \\
& \times \mathcal{C}_0(k^2, p^2, q^2, 0, m_c^2, m_c^2) + m_W^2 \left(\frac{m_\tau^4}{m_W^2} - \frac{k^2 m_\tau^2}{m_W^2} \right) \mathcal{C}_0(k^2, p^2, q^2, 0, m_\tau^2, m_\tau^2) + \\
& + \left(\frac{3m_t^4}{m_W^2} - \frac{3k^2 m_t^2}{m_W^2} \right) m_W^2 \mathcal{C}_0(k^2, p^2, q^2, m_b^2, m_t^2, m_t^2) + \left(3m_b^4 + \frac{3k^2 m_b^2}{4} + \frac{3p^2 m_b^2}{4} - \frac{3q^2 m_b^2}{4} \right) \times \\
& \times \mathcal{C}_0(p^2, q^2, k^2, m_b^2, m_b^2, m_t^2) - 6m_c^2 \mathcal{C}_{00}(k^2, p^2, q^2, 0, m_c^2, m_c^2) - 2m_\tau^2 \mathcal{C}_{00}(k^2, p^2, q^2, 0, m_\tau^2, m_\tau^2) - \\
& - 6m_t^2 \mathcal{C}_{00}(k^2, p^2, q^2, m_b^2, m_t^2, m_t^2) + \left(\frac{-15k^2 - 3p^2 + 3q^2}{4} \right) m_c^2 \mathcal{C}_1(k^2, p^2, q^2, 0, m_c^2, m_c^2) + \\
& + \left(-\frac{5k^2 m_\tau^2}{4} - \frac{p^2 m_\tau^2}{4} + \frac{q^2 m_\tau^2}{4} \right) \mathcal{C}_1(k^2, p^2, q^2, 0, m_\tau^2, m_\tau^2) + \left(-\frac{15k^2 m_t^2}{4} - \frac{3p^2 m_t^2}{4} + \frac{3q^2 m_t^2}{4} \right) \times \\
& \times \mathcal{C}_1(k^2, p^2, q^2, m_b^2, m_t^2, m_t^2) + \left(\frac{3k^2 m_b^2}{2m_W^2} + \frac{3p^2 m_b^2}{m_W^2} - \frac{3q^2 m_b^2}{2m_W^2} \right) m_W^2 \mathcal{C}_1(p^2, q^2, k^2, m_b^2, m_b^2, m_t^2) + \\
& + \left(-\frac{9k^2 m_c^2}{4} + \frac{9p^2 m_c^2}{4} - \frac{3q^2 m_c^2}{4} \right) \mathcal{C}_2(k^2, p^2, q^2, 0, m_c^2, m_c^2) + \left(-\frac{3k^2 m_\tau^2}{4} + \frac{3p^2 m_\tau^2}{4} - \frac{q^2 m_\tau^2}{4} \right) \times \\
& \times \mathcal{C}_2(k^2, p^2, q^2, 0, m_\tau^2, m_\tau^2) + \left(-\frac{9k^2 m_t^2}{4m_W^2} + \frac{9p^2 m_t^2}{4m_W^2} - \frac{3q^2 m_t^2}{4m_W^2} \right) m_W^2 \mathcal{C}_2(k^2, p^2, q^2, m_b^2, m_t^2, m_t^2) + \\
& \left. + \left(\frac{15k^2 m_b^2}{4m_W^2} + \frac{3p^2 m_b^2}{4m_W^2} - \frac{3q^2 m_b^2}{4m_W^2} \right) m_W^2 \mathcal{C}_2(p^2, q^2, k^2, m_b^2, m_b^2, m_t^2) \right\}, \tag{37}
\end{aligned}$$

$$\begin{aligned}
\{\delta V_W^{\mathcal{D}}(p^2, k^2, q^2)\}_{\text{fer}} = & \frac{g^2}{16\pi^2} \frac{1}{m_W^2} \left\{ -\frac{3}{2} m_b^2 \mathcal{C}_0(p^2, q^2, k^2, m_b^2, m_b^2, m_t^2) - \right. \\
& - 6m_b^2 \mathcal{C}_1(p^2, q^2, k^2, m_b^2, m_b^2, m_t^2) + \frac{3}{2} m_t^2 \mathcal{C}_1(k^2, p^2, q^2, m_b^2, m_t^2, m_t^2) + \\
& + \frac{3}{2} m_c^2 \mathcal{C}_1(k^2, p^2, q^2, 0, m_c^2, m_c^2) + \frac{1}{2} m_\tau^2 \mathcal{C}_1(k^2, p^2, q^2, 0, m_\tau^2, m_\tau^2) - \\
& - 6m_b^2 \mathcal{C}_{11}(p^2, q^2, k^2, m_b^2, m_b^2, m_t^2) - 6m_b^2 \mathcal{C}_{12}(p^2, q^2, k^2, m_b^2, m_b^2, m_t^2) + \\
& + 6m_t^2 \mathcal{C}_{12}(k^2, p^2, q^2, m_b^2, m_t^2, m_t^2) + 6m_c^2 \mathcal{C}_{12}(k^2, p^2, q^2, 0, m_c^2, m_c^2) + \\
& + 2m_\tau^2 \mathcal{C}_{12}(k^2, p^2, q^2, 0, m_\tau^2, m_\tau^2) - \frac{3}{2} m_b^2 \mathcal{C}_2(p^2, q^2, k^2, m_b^2, m_b^2, m_t^2) + \\
& + \frac{3}{2} m_t^2 \mathcal{C}_2(k^2, p^2, q^2, m_b^2, m_t^2, m_t^2) + \frac{3}{2} m_c^2 \mathcal{C}_2(k^2, p^2, q^2, 0, m_c^2, m_c^2) + \\
& \left. + \frac{1}{2} m_\tau^2 \mathcal{C}_2(k^2, p^2, q^2, 0, m_\tau^2, m_\tau^2) \right\}, \tag{38}
\end{aligned}$$

$$\begin{aligned}
\{\delta V_W^{\mathcal{E}}(p^2, k^2, q^2)\}_{\text{bos}} = & \frac{g^2}{16\pi^2} \frac{1}{8} \left\{ -4\mathcal{B}_0(k^2, m_H^2, m_W^2) c_\alpha^2 - 4\mathcal{B}_0(q^2, m_H^2, m_W^2) c_\alpha^2 - 8m_W^2 \times \right. \\
& \times \mathcal{C}_0(p^2, q^2, k^2, m_W^2, m_W^2, m_H^2) c_\alpha^2 - 4s_W^2 \mathcal{B}_0(k^2, 0, m_W^2) - 4s_\alpha^2 \mathcal{B}_0(k^2, m_S^2, m_W^2) + \\
& + \left(-4c_W^2 + 8 - \frac{4}{c_W^2} \right) \mathcal{B}_0(k^2, m_W^2, m_Z^2) + \left(-\frac{vw\kappa c_\alpha^5}{m_W^2 s_\alpha} + \frac{2v^2 \kappa c_\alpha^4}{m_W^2} - \frac{6v^2 \lambda c_\alpha^4}{m_W^2} + \frac{2vw\kappa s_\alpha c_\alpha^3}{m_W^2} - \right. \\
& - \frac{6vw\rho s_\alpha c_\alpha^3}{m_W^2} - \left. \frac{v^2 \kappa s_\alpha^2 c_\alpha^2}{m_W^2} \right) \mathcal{B}_0(p^2, m_H^2, m_H^2) + \left(-\frac{2v^2 \kappa c_\alpha^4}{m_W^2} - \frac{4vw\kappa s_\alpha c_\alpha^3}{m_W^2} + \frac{12vw\rho s_\alpha c_\alpha^3}{m_W^2} + \right. \\
& + \frac{4v^2 \kappa s_\alpha^2 c_\alpha^2}{m_W^2} - \frac{12v^2 \lambda s_\alpha^2 c_\alpha^2}{m_W^2} + \left. \frac{2vw\kappa s_\alpha^3 c_\alpha}{m_W^2} \right) \mathcal{B}_0(p^2, m_H^2, m_S^2) + \left(-\frac{6v^2 \lambda s_\alpha^4}{m_W^2} - \frac{3vw\kappa c_\alpha s_\alpha^3}{m_W^2} - \right. \\
& - \frac{3v^2 \kappa c_\alpha^2 s_\alpha^2}{m_W^2} - \left. \frac{6vw\rho c_\alpha^3 s_\alpha}{m_W^2} \right) \mathcal{B}_0(p^2, m_S^2, m_S^2) + \left(-\frac{4\lambda v^2}{m_W^2} - \frac{2w\kappa c_\alpha v}{m_W^2 s_\alpha} - 24 \right) \mathcal{B}_0(p^2, m_W^2, m_W^2) + \\
& + \left(-\frac{2\lambda v^2}{m_W^2} - \frac{w\kappa c_\alpha v}{m_W^2 s_\alpha} - 24 \right) \mathcal{B}_0(p^2, m_Z^2, m_Z^2) + 20s_W^2 \mathcal{B}_0(q^2, 0, m_W^2) - 4s_\alpha^2 \mathcal{B}_0(q^2, m_S^2, m_W^2) + \\
& + \left(20c_W^2 + 16 - \frac{4}{c_W^2} \right) \mathcal{B}_0(q^2, m_W^2, m_Z^2) + \left(8c_W^2 k^2 - 8k^2 - 12p^2 + 16q^2 + 12p^2 c_W^2 - \right. \\
& - 16q^2 c_W^2 + 8v^2 \lambda c_W^2 - 24c_W^2 m_W^2 + 24m_W^2 - 8v^2 \lambda + \frac{4vw\kappa c_W^2 c_\alpha}{s_\alpha} - \left. \frac{4vw\kappa c_\alpha}{s_\alpha} \right) \times \\
& \times \mathcal{C}_0(k^2, p^2, q^2, 0, m_W^2, m_W^2) + \left(-\frac{4vw\kappa c_\alpha^5}{s_\alpha} + 8v^2 \kappa c_\alpha^4 - 24v^2 \lambda c_\alpha^4 + 8vw\kappa s_\alpha c_\alpha^3 - 24vw\rho s_\alpha c_\alpha^3 - \right.
\end{aligned}$$

$$\begin{aligned}
& -4v^2\kappa s_\alpha^2 c_\alpha^2 \Big) \mathcal{C}_0(k^2, p^2, q^2, m_W^2, m_H^2, m_H^2) + \left(-4v^2\kappa c_\alpha^4 - 8vw\kappa s_\alpha c_\alpha^3 + 24vwp s_\alpha c_\alpha^3 + \right. \\
& + 8v^2\kappa s_\alpha^2 c_\alpha^2 - 24v^2\lambda s_\alpha^2 c_\alpha^2 + 4vw\kappa s_\alpha^3 c_\alpha \Big) \mathcal{C}_0(k^2, p^2, q^2, m_W^2, m_H^2, m_S^2) + \left(-24v^2\lambda s_\alpha^4 - \right. \\
& - 12vw\kappa c_\alpha s_\alpha^3 - 12v^2\kappa c_\alpha^2 s_\alpha^2 - 24vwp c_\alpha^3 s_\alpha \Big) \mathcal{C}_0(k^2, p^2, q^2, m_W^2, m_S^2, m_S^2) + \left(-\frac{8m_Z^4}{m_W^2} + \right. \\
& + 16m_Z^2 + 4k^2 - 20p^2 + 20q^2 + \frac{16m_W^2}{c_W^2} - 8m_W^2 \Big) \mathcal{C}_0(k^2, p^2, q^2, m_W^2, m_Z^2, m_Z^2) - \\
& - 8m_W^2 s_\alpha^2 \mathcal{C}_0(p^2, q^2, k^2, m_W^2, m_W^2, m_S^2) + \left(28c_W^2 k^2 - 4k^2 - 8p^2 + 4q^2 - 8p^2 c_W^2 + 12q^2 c_W^2 - \right. \\
& - 8v^2\lambda c_W^2 + 24c_W^2 m_W^2 - 8m_W^2 + 16v^2\lambda - \frac{4vw\kappa c_W^2 c_\alpha}{s_\alpha} + \frac{8vw\kappa c_\alpha}{s_\alpha} - \frac{4vw\kappa c_\alpha}{c_W^2 s_\alpha} - \frac{8v^2\lambda}{c_W^2} \Big) \times \\
& \times \mathcal{C}_0(p^2, q^2, k^2, m_W^2, m_W^2, m_Z^2) + \left(-4v^2\kappa c_\alpha^4 - 8vw\kappa s_\alpha c_\alpha^3 + 24vwp s_\alpha c_\alpha^3 + 8v^2\kappa s_\alpha^2 c_\alpha^2 - \right. \\
& - 24v^2\lambda s_\alpha^2 c_\alpha^2 + 4vw\kappa s_\alpha^3 c_\alpha \Big) \mathcal{C}_0(q^2, p^2, k^2, m_W^2, m_H^2, m_S^2) + 64s_W^2 \mathcal{C}_{00}(k^2, p^2, q^2, 0, m_W^2, m_W^2) + \\
& + \left(\frac{4vw\kappa c_\alpha^5}{m_W^2 s_\alpha} - \frac{8v^2\kappa c_\alpha^4}{m_W^2} + \frac{24v^2\lambda c_\alpha^4}{m_W^2} - \frac{8vw\kappa s_\alpha c_\alpha^3}{m_W^2} + \frac{24vwp s_\alpha c_\alpha^3}{m_W^2} + \frac{4v^2\kappa s_\alpha^2 c_\alpha^2}{m_W^2} \right) \times \\
& \times \mathcal{C}_{00}(k^2, p^2, q^2, m_W^2, m_H^2, m_H^2) + \left(\frac{4v^2\kappa c_\alpha^4}{m_W^2} + \frac{8vw\kappa s_\alpha c_\alpha^3}{m_W^2} - \frac{24vwp s_\alpha c_\alpha^3}{m_W^2} - \frac{8v^2\kappa s_\alpha^2 c_\alpha^2}{m_W^2} + \right. \\
& + \frac{24v^2\lambda s_\alpha^2 c_\alpha^2}{m_W^2} - \frac{4vw\kappa s_\alpha^3 c_\alpha}{m_W^2} \Big) \mathcal{C}_{00}(k^2, p^2, q^2, m_W^2, m_H^2, m_S^2) + \left(\frac{24v^2\lambda s_\alpha^4}{m_W^2} + \frac{12vw\kappa c_\alpha s_\alpha^3}{m_W^2} + \right. \\
& + \frac{12v^2\kappa c_\alpha^2 s_\alpha^2}{m_W^2} + \frac{24vwp c_\alpha^3 s_\alpha}{m_W^2} \Big) \mathcal{C}_{00}(k^2, p^2, q^2, m_W^2, m_S^2, m_S^2) + \left(\frac{8\lambda v^2}{m_W^2} + \frac{4w\kappa c_\alpha v}{m_W^2 s_\alpha} + \frac{8}{c_W^2} + 64 \right) \times \\
& \times \mathcal{C}_{00}(k^2, p^2, q^2, m_W^2, m_Z^2, m_Z^2) + \left(\frac{4vw\kappa c_\alpha^3}{m_W^2 s_\alpha} + \frac{8v^2\lambda c_\alpha^2}{m_W^2} + 8c_\alpha^2 \right) \mathcal{C}_{00}(p^2, q^2, k^2, m_W^2, m_W^2, m_H^2) + \\
& + s_\alpha \left(\frac{8v^2\lambda s_\alpha}{m_W^2} + 8s_\alpha + \frac{4vw\kappa c_\alpha}{m_W^2} \right) \mathcal{C}_{00}(p^2, q^2, k^2, m_W^2, m_W^2, m_S^2) + \left(\frac{8\lambda v^2}{m_W^2} + \frac{4w\kappa c_\alpha v}{m_W^2 s_\alpha} + 64c_W^2 + \right. \\
& + 8 \Big) \mathcal{C}_{00}(p^2, q^2, k^2, m_W^2, m_W^2, m_Z^2) + \left(\frac{4v^2\kappa c_\alpha^4}{m_W^2} + \frac{8vw\kappa s_\alpha c_\alpha^3}{m_W^2} - \frac{24vwp s_\alpha c_\alpha^3}{m_W^2} - \frac{8v^2\kappa s_\alpha^2 c_\alpha^2}{m_W^2} + \right. \\
& + \frac{24v^2\lambda s_\alpha^2 c_\alpha^2}{m_W^2} - \frac{4vw\kappa s_\alpha^3 c_\alpha}{m_W^2} \Big) \mathcal{C}_{00}(q^2, p^2, k^2, m_W^2, m_H^2, m_S^2) + \left(36c_W^2 k^2 - 36k^2 - 4p^2 + 4q^2 + \right. \\
& + 4c_W^2(p^2 - q^2) \Big) \mathcal{C}_1(k^2, p^2, q^2, 0, m_W^2, m_W^2) + 4(-5k^2 - p^2 + q^2) \mathcal{C}_1(k^2, p^2, q^2, m_W^2, m_Z^2, m_Z^2) + \\
& + (16c_W^2 k^2 - 8k^2 - 8p^2 + 8q^2 + 24p^2 c_W^2 - 16q^2 c_W^2) \mathcal{C}_1(p^2, q^2, k^2, m_W^2, m_W^2, m_Z^2) +
\end{aligned}$$

$$\begin{aligned}
& + (20c_W^2 k^2 - 20k^2 + 20p^2 - 12q^2 - 20p^2 c_W^2 + 12q^2 c_W^2) \mathcal{C}_2(k^2, p^2, q^2, 0, m_W^2, m_W^2) + \\
& + (-12k^2 + 12p^2 - 4q^2) \mathcal{C}_2(k^2, p^2, q^2, m_W^2, m_Z^2, m_Z^2) + 4(9c_W^2 k^2 - 4k^2 + p^2 c_W^2 - q^2 c_W^2) \times \\
& \quad \times \mathcal{C}_2(p^2, q^2, k^2, m_W^2, m_W^2, m_Z^2) \Big\}, \tag{39}
\end{aligned}$$

$$\begin{aligned}
\{\delta V_W^D(p^2, k^2, q^2)\}_{\text{bos}} = & \frac{g^2}{16\pi^2} \frac{1}{2} \Big\{ 2\mathcal{C}_0(p^2, q^2, k^2, m_W^2, m_W^2, m_H^2) c_\alpha^2 + \\
& + 2\mathcal{C}_2(p^2, q^2, k^2, m_W^2, m_W^2, m_H^2) c_\alpha^2 + 8\mathcal{C}_0(k^2, p^2, q^2, m_W^2, m_Z^2, m_Z^2) + 2s_\alpha^2 \times \\
& \times \mathcal{C}_0(p^2, q^2, k^2, m_W^2, m_W^2, m_S^2) + (8c_W^2 + 2) \mathcal{C}_0(p^2, q^2, k^2, m_W^2, m_W^2, m_Z^2) + (8c_W^2 - 8) \times \\
& \times \mathcal{C}_1(k^2, p^2, q^2, 0, m_W^2, m_W^2) - \frac{2\mathcal{C}_1(k^2, p^2, q^2, m_W^2, m_Z^2, m_Z^2)}{c_W^2} + \left(\frac{v\omega\kappa c_\alpha^3}{m_W^2 s_\alpha} + \frac{2v^2 \lambda c_\alpha^2}{m_W^2} + 2c_\alpha^2 \right) \times \\
& \times \mathcal{C}_1(p^2, q^2, k^2, m_W^2, m_W^2, m_H^2) + \left(\frac{2v^2 \lambda s_\alpha^2}{m_W^2} + 2s_\alpha^2 + \frac{v\omega\kappa c_\alpha s_\alpha}{m_W^2} \right) \mathcal{C}_1(p^2, q^2, k^2, m_W^2, m_W^2, m_S^2) + \\
& + \left(\frac{2\lambda v^2}{m_W^2} + \frac{\omega\kappa c_\alpha v}{m_W^2 s_\alpha} + 16c_W^2 + 2 \right) \mathcal{C}_1(p^2, q^2, k^2, m_W^2, m_W^2, m_Z^2) + \left(\frac{v\omega\kappa c_\alpha^3}{m_W^2 s_\alpha} + \frac{2v^2 \lambda c_\alpha^2}{m_W^2} + 2c_\alpha^2 \right) \times \\
& \times \mathcal{C}_{11}(p^2, q^2, k^2, m_W^2, m_W^2, m_H^2) + \left(\frac{2v^2 \lambda s_\alpha^2}{m_W^2} + 2s_\alpha^2 + \frac{v\omega\kappa c_\alpha s_\alpha}{m_W^2} \right) \mathcal{C}_{11}(p^2, q^2, k^2, m_W^2, m_W^2, m_S^2) + \\
& + \left(\frac{2\lambda v^2}{m_W^2} + \frac{\omega\kappa c_\alpha v}{m_W^2 s_\alpha} + 16c_W^2 + 2 \right) \mathcal{C}_{11}(p^2, q^2, k^2, m_W^2, m_W^2, m_Z^2) + (16c_W^2 - 16) \times \\
& \times \mathcal{C}_{12}(k^2, p^2, q^2, 0, m_W^2, m_W^2) + \left(-\frac{v\omega\kappa c_\alpha^5}{m_W^2 s_\alpha} + \frac{2v^2 \kappa c_\alpha^4}{m_W^2} - \frac{6v^2 \lambda c_\alpha^4}{m_W^2} + \frac{2v\omega\kappa s_\alpha c_\alpha^3}{m_W^2} - \frac{6v\omega\rho s_\alpha c_\alpha^3}{m_W^2} - \right. \\
& \left. - \frac{v^2 \kappa s_\alpha^2 c_\alpha^2}{m_W^2} \right) \mathcal{C}_{12}(k^2, p^2, q^2, m_W^2, m_H^2, m_H^2) + \left(-\frac{v^2 \kappa c_\alpha^4}{m_W^2} - \frac{2v\omega\kappa s_\alpha c_\alpha^3}{m_W^2} + \frac{6v\omega\rho s_\alpha c_\alpha^3}{m_W^2} + \frac{2v^2 \kappa s_\alpha^2 c_\alpha^2}{m_W^2} - \right. \\
& \left. - \frac{6v^2 \lambda s_\alpha^2 c_\alpha^2}{m_W^2} + \frac{v\omega\kappa s_\alpha^3 c_\alpha}{m_W^2} \right) \mathcal{C}_{12}(k^2, p^2, q^2, m_W^2, m_H^2, m_S^2) + \left(-\frac{6v^2 \lambda s_\alpha^4}{m_W^2} - \frac{3v\omega\kappa c_\alpha s_\alpha^3}{m_W^2} - \right. \\
& \left. - \frac{3v^2 \kappa c_\alpha^2 s_\alpha^2}{m_W^2} - \frac{6v\omega\rho c_\alpha^3 s_\alpha}{m_W^2} \right) \mathcal{C}_{12}(k^2, p^2, q^2, m_W^2, m_S^2, m_S^2) + \left(-\frac{2\lambda v^2}{m_W^2} - \frac{\omega\kappa c_\alpha v}{m_W^2 s_\alpha} - \frac{2}{c_W^2} - 16 \right) \times \\
& \times \mathcal{C}_{12}(k^2, p^2, q^2, m_W^2, m_Z^2, m_Z^2) + \left(\frac{v\omega\kappa c_\alpha^3}{m_W^2 s_\alpha} + \frac{2v^2 \lambda c_\alpha^2}{m_W^2} + 2c_\alpha^2 \right) \mathcal{C}_{12}(p^2, q^2, k^2, m_W^2, m_W^2, m_H^2) + \\
& + \left(\frac{2v^2 \lambda s_\alpha^2}{m_W^2} + 2s_\alpha^2 + \frac{v\omega\kappa c_\alpha s_\alpha}{m_W^2} \right) \mathcal{C}_{12}(p^2, q^2, k^2, m_W^2, m_W^2, m_S^2) + \left(\frac{2\lambda v^2}{m_W^2} + \frac{\omega\kappa c_\alpha v}{m_W^2 s_\alpha} + 16c_W^2 + 2 \right) \times \\
& \times \mathcal{C}_{12}(p^2, q^2, k^2, m_W^2, m_W^2, m_Z^2) + \left(-\frac{v^2 \kappa c_\alpha^4}{m_W^2} - \frac{2v\omega\kappa s_\alpha c_\alpha^3}{m_W^2} + \frac{6v\omega\rho s_\alpha c_\alpha^3}{m_W^2} + \frac{2v^2 \kappa s_\alpha^2 c_\alpha^2}{m_W^2} - \right. \\
& \left. - \frac{6v^2 \lambda s_\alpha^2 c_\alpha^2}{m_W^2} + \frac{v\omega\kappa s_\alpha^3 c_\alpha}{m_W^2} \right) \mathcal{C}_{12}(q^2, p^2, k^2, m_W^2, m_H^2, m_S^2) + (8c_W^2 - 8) \mathcal{C}_2(k^2, p^2, q^2, 0, m_W^2, m_W^2) -
\end{aligned}$$

$$\begin{aligned}
& - \frac{2\mathcal{C}_2(k^2, p^2, q^2, m_W^2, m_Z^2, m_Z^2)}{c_W^2} + 2s_\alpha^2 \mathcal{C}_2(p^2, q^2, k^2, m_W^2, m_W^2, m_S^2) + (8c_W^2 - 6) \times \\
& \times \mathcal{C}_2(p^2, q^2, k^2, m_W^2, m_W^2, m_Z^2) \Big\}. \tag{40}
\end{aligned}$$

One-Loop Corrections to SHH Vertex

$$\begin{aligned}
\{\delta V_H(p^2, k^2, q^2)\}_{\text{fer}} = & \frac{g^2}{16\pi^2} \frac{c_\alpha^2}{vm_W^2 C_{HHS}} \Big\{ -18s_\alpha \mathcal{B}_0(q^2, m_b^2, m_b^2) m_b^4 - \\
& -18m_c^4 s_\alpha \mathcal{B}_0(q^2, m_c^2, m_c^2) - 18m_t^4 s_\alpha \mathcal{B}_0(q^2, m_t^2, m_t^2) - 6m_\tau^4 s_\alpha \mathcal{B}_0(q^2, m_\tau^2, m_\tau^2) - \left(24m_b^6 + \right. \\
& \left. + 3k^2 m_b^4 + 3p^2 m_b^4 - 3q^2 m_b^4\right) s_\alpha \mathcal{C}_0(k^2, q^2, p^2, m_b^2, m_b^2, m_b^2) - \left(24m_c^6 + 3k^2 m_c^4 + 3p^2 m_c^4 - \right. \\
& \left. - 3q^2 m_c^4\right) s_\alpha \mathcal{C}_0(k^2, q^2, p^2, m_c^2, m_c^2, m_c^2) - (24m_t^6 + 3k^2 m_t^4 + 3p^2 m_t^4 - 3q^2 m_t^4) s_\alpha \times \\
& \times \mathcal{C}_0(k^2, q^2, p^2, m_t^2, m_t^2, m_t^2) - m_\tau^4 (8m_\tau^2 + k^2 + p^2 - q^2) s_\alpha \mathcal{C}_0(k^2, q^2, p^2, m_\tau^2, m_\tau^2, m_\tau^2) - \\
& - (18k^2 m_b^4 + 6p^2 m_b^4 - 6q^2 m_b^4) s_\alpha \mathcal{C}_1(k^2, q^2, p^2, m_b^2, m_b^2, m_b^2) - (18k^2 m_c^4 + 6p^2 m_c^4 - 6q^2 m_c^4) s_\alpha \times \\
& \times \mathcal{C}_1(k^2, q^2, p^2, m_c^2, m_c^2, m_c^2) - (18k^2 m_t^4 + 6p^2 m_t^4 - 6q^2 m_t^4) s_\alpha \mathcal{C}_1(k^2, q^2, p^2, m_t^2, m_t^2, m_t^2) - \\
& - (6k^2 m_\tau^4 + 2p^2 m_\tau^4 - 2q^2 m_\tau^4) s_\alpha \mathcal{C}_1(k^2, q^2, p^2, m_\tau^2, m_\tau^2, m_\tau^2) - (6k^2 m_b^4 + 18p^2 m_b^4 - 6q^2 m_b^4) s_\alpha \times \\
& \times \mathcal{C}_2(k^2, q^2, p^2, m_b^2, m_b^2, m_b^2) - (6k^2 m_c^4 + 18p^2 m_c^4 - 6q^2 m_c^4) s_\alpha \mathcal{C}_2(k^2, q^2, p^2, m_c^2, m_c^2, m_c^2) - \\
& - (6k^2 m_t^4 + 18p^2 m_t^4 - 6q^2 m_t^4) s_\alpha \mathcal{C}_2(k^2, q^2, p^2, m_t^2, m_t^2, m_t^2) - (2k^2 m_\tau^4 + 6p^2 m_\tau^4 - 2q^2 m_\tau^4) s_\alpha \times \\
& \times \mathcal{C}_2(k^2, q^2, p^2, m_\tau^2, m_\tau^2, m_\tau^2) \Big\}, \tag{41}
\end{aligned}$$

$$\begin{aligned}
\{\delta V_H(p^2, k^2, q^2)\}_{\text{bos}} = & \frac{g^2}{16\pi^2} \frac{c_\alpha^2}{vm_W^2 C_{HHS}} \Big\{ -48c_\alpha^2 s_\alpha m_W^4 - 24c_\alpha^2 m_Z^4 s_\alpha + v^3 C_{HHH} C_{HHS} \times \\
& \times \mathcal{B}_0(k^2, m_H^2, m_H^2) + 2v^3 C_{HHS} C_{HHSS} \mathcal{B}_0(k^2, m_H^2, m_S^2) + v^3 C_{HSS} C_{HSSS} \mathcal{B}_0(k^2, m_S^2, m_S^2) + \\
& + (32c_\alpha^2 s_\alpha m_W^4 + 2v^3 C_{HS\eta^+\eta^-} C_{H\eta^+\eta^-}) \mathcal{B}_0(k^2, m_W^2, m_W^2) + (16c_\alpha^2 s_\alpha m_Z^4 + v^3 C_{H\eta_3\eta_3} C_{HS\eta_3\eta_3}) \times \\
& \times \mathcal{B}_0(k^2, m_Z^2, m_Z^2) + v^3 C_{HHHH} C_{HHS} \mathcal{B}_0(p^2, m_H^2, m_H^2) + 2v^3 C_{HHHS} C_{HSS} \mathcal{B}_0(p^2, m_H^2, m_S^2) + \\
& + v^3 C_{HHSS} C_{SSS} \mathcal{B}_0(p^2, m_S^2, m_S^2) + (32c_\alpha^2 s_\alpha m_W^4 + 2v^3 C_{HH\eta^+\eta^-} C_{S\eta^+\eta^-}) \mathcal{B}_0(p^2, m_W^2, m_W^2) + \\
& + (16c_\alpha^2 s_\alpha m_Z^4 + v^3 C_{HH\eta_3\eta_3} C_{S\eta_3\eta_3}) \mathcal{B}_0(p^2, m_Z^2, m_Z^2) + v^3 C_{HHH} C_{HHHS} \mathcal{B}_0(q^2, m_H^2, m_H^2) + \\
& + 2v^3 C_{HHS} C_{HHSS} \mathcal{B}_0(q^2, m_H^2, m_S^2) + v^3 C_{HSS} C_{HSSS} \mathcal{B}_0(q^2, m_S^2, m_S^2) + \left(8c_\alpha^2 s_\alpha m_W^4 - \right. \\
& \left. - 4vc_\alpha^2 C_{S\eta^+\eta^-} m_W^2 - 8vc_\alpha C_{H\eta^+\eta^-} s_\alpha m_W^2 + 2v^3 C_{HS\eta^+\eta^-} C_{H\eta^+\eta^-}\right) \mathcal{B}_0(q^2, m_W^2, m_W^2) +
\end{aligned}$$

$$\begin{aligned}
& + \left(4c_\alpha^2 s_\alpha m_Z^4 + v^3 C_{H\eta_3\eta_3} C_{HS\eta_3\eta_3} - \frac{2vc_\alpha^2 m_W^2 C_{S\eta_3\eta_3}}{c_W^2} - \frac{4vc_\alpha m_W^2 C_{H\eta_3\eta_3} s_\alpha}{c_W^2} \right) \mathcal{B}_0 (q^2, m_Z^2, m_Z^2) + \\
& + 2v^3 C_{HHS}^2 C_{SSS} \mathcal{C}_0 (k^2, p^2, q^2, m_H^2, m_S^2, m_S^2) + 2v^3 C_{HHH}^2 C_{HHS} \mathcal{C}_0 (k^2, q^2, p^2, m_H^2, m_H^2, m_H^2) + \\
& + 2v^3 C_{HHH} C_{HHS} C_{HSS} \mathcal{C}_0 (k^2, q^2, p^2, m_H^2, m_H^2, m_S^2) + 2v^3 C_{HHS} C_{HSS}^2 \mathcal{C}_0 (k^2, q^2, p^2, m_H^2, m_S^2, m_S^2) + \\
& + 2v^3 C_{HSS}^2 C_{SSS} \mathcal{C}_0 (k^2, q^2, p^2, m_S^2, m_S^2, m_S^2) + \left(96c_\alpha^2 s_\alpha m_W^6 - 4vc_\alpha^2 C_{S\eta^+\eta^-} m_W^4 - 20k^2 c_\alpha^2 s_\alpha m_W^4 - \right. \\
& - 20p^2 c_\alpha^2 s_\alpha m_W^4 - 12q^2 c_\alpha^2 s_\alpha m_W^4 - 8vc_\alpha C_{H\eta^+\eta^-} s_\alpha m_W^4 + 4p^2 vc_\alpha^2 C_{S\eta^+\eta^-} m_W^2 - 4q^2 vc_\alpha^2 C_{S\eta^+\eta^-} m_W^2 - \\
& - 4k^2 vc_\alpha C_{H\eta^+\eta^-} s_\alpha m_W^2 - 8p^2 vc_\alpha C_{H\eta^+\eta^-} s_\alpha m_W^2 + 4q^2 vc_\alpha C_{H\eta^+\eta^-} s_\alpha m_W^2 + 4v^3 C_{H\eta^+\eta^-}^2 C_{S\eta^+\eta^-} \left. \right) \times \\
& \times \mathcal{C}_0 (k^2, q^2, p^2, m_W^2, m_W^2, m_W^2) + \left(\frac{60c_\alpha^2 s_\alpha m_W^6}{c_W^6} + \frac{2p^2 vc_\alpha^2 C_{S\eta_3\eta_3} m_W^2}{c_W^2} - \frac{2q^2 vc_\alpha^2 C_{S\eta_3\eta_3} m_W^2}{c_W^2} - \right. \\
& - \frac{2vc_\alpha^2 m_Z^2 C_{S\eta_3\eta_3} m_W^2}{c_W^2} - \frac{4vc_\alpha m_Z^2 C_{H\eta_3\eta_3} s_\alpha m_W^2}{c_W^2} - \frac{2k^2 vc_\alpha C_{H\eta_3\eta_3} s_\alpha m_W^2}{c_W^2} - \frac{4p^2 vc_\alpha C_{H\eta_3\eta_3} s_\alpha m_W^2}{c_W^2} + \\
& + \frac{2q^2 vc_\alpha C_{H\eta_3\eta_3} s_\alpha m_W^2}{c_W^2} + 2v^3 C_{H\eta_3\eta_3}^2 C_{S\eta_3\eta_3} - 12c_\alpha^2 m_Z^6 s_\alpha - 10k^2 c_\alpha^2 m_Z^4 s_\alpha - 10p^2 c_\alpha^2 m_Z^4 s_\alpha - \\
& - 6q^2 c_\alpha^2 m_Z^4 s_\alpha \left. \right) \mathcal{C}_0 (k^2, q^2, p^2, m_Z^2, m_Z^2, m_Z^2) + 2v^3 C_{HHS} C_{HSS}^2 \mathcal{C}_0 (p^2, k^2, q^2, m_H^2, m_S^2, m_S^2) + \\
& + 2v^3 C_{HHS}^3 \mathcal{C}_0 (p^2, q^2, k^2, m_H^2, m_H^2, m_S^2) + 2v^3 C_{HHH} C_{HHS} C_{HSS} \mathcal{C}_0 (q^2, p^2, k^2, m_H^2, m_H^2, m_S^2) + \\
& + \left(-24k^2 c_\alpha^2 s_\alpha m_W^4 - 8p^2 c_\alpha^2 s_\alpha m_W^4 + 8q^2 c_\alpha^2 s_\alpha m_W^4 + 4k^2 vc_\alpha^2 C_{S\eta^+\eta^-} m_W^2 - 4p^2 vc_\alpha^2 C_{S\eta^+\eta^-} m_W^2 + \right. \\
& + 4q^2 vc_\alpha^2 C_{S\eta^+\eta^-} m_W^2 - 16k^2 vc_\alpha C_{H\eta^+\eta^-} s_\alpha m_W^2 \left. \right) \mathcal{C}_1 (k^2, q^2, p^2, m_W^2, m_W^2, m_W^2) + \left(-12k^2 c_\alpha^2 s_\alpha m_Z^4 - \right. \\
& - 4p^2 c_\alpha^2 s_\alpha m_Z^4 + 4q^2 c_\alpha^2 s_\alpha m_Z^4 + \frac{2k^2 vc_\alpha^2 m_W^2 C_{S\eta_3\eta_3}}{c_W^2} - \frac{2p^2 vc_\alpha^2 m_W^2 C_{S\eta_3\eta_3}}{c_W^2} + \frac{2q^2 vc_\alpha^2 m_W^2 C_{S\eta_3\eta_3}}{c_W^2} - \\
& - \frac{8k^2 vc_\alpha m_W^2 C_{H\eta_3\eta_3} s_\alpha}{c_W^2} \left. \right) \mathcal{C}_1 (k^2, q^2, p^2, m_Z^2, m_Z^2, m_Z^2) + m_W^2 \left(-8k^2 c_\alpha^2 s_\alpha m_W^2 - 24p^2 c_\alpha^2 s_\alpha m_W^2 + \right. \\
& + 8q^2 c_\alpha^2 s_\alpha m_W^2 + 4k^2 vc_\alpha^2 C_{S\eta^+\eta^-} - 4p^2 vc_\alpha^2 C_{S\eta^+\eta^-} - 4q^2 vc_\alpha^2 C_{S\eta^+\eta^-} - 8k^2 vc_\alpha C_{H\eta^+\eta^-} s_\alpha - \\
& - 8p^2 vc_\alpha C_{H\eta^+\eta^-} s_\alpha + 8q^2 vc_\alpha C_{H\eta^+\eta^-} s_\alpha \left. \right) \mathcal{C}_2 (k^2, q^2, p^2, m_W^2, m_W^2, m_W^2) + \left(-4k^2 c_\alpha^2 s_\alpha m_Z^4 - \right. \\
& - 12p^2 c_\alpha^2 s_\alpha m_Z^4 + 4q^2 c_\alpha^2 s_\alpha m_Z^4 + \frac{2k^2 vc_\alpha^2 m_W^2 C_{S\eta_3\eta_3}}{c_W^2} - \frac{2p^2 vc_\alpha^2 m_W^2 C_{SS\eta_3}}{c_W^2} - \frac{2q^2 vc_\alpha^2 m_W^2 C_{S\eta_3\eta_3}}{c_W^2} - \\
& - \frac{4k^2 vc_\alpha m_W^2 C_{H\eta_3\eta_3} s_\alpha}{c_W^2} - \frac{4p^2 vc_\alpha m_W^2 C_{H\eta_3\eta_3} s_\alpha}{c_W^2} + \frac{4q^2 vc_\alpha m_W^2 C_{H\eta_3\eta_3} s_\alpha}{c_W^2} \left. \right) \times \\
& \times \mathcal{C}_2 (k^2, q^2, p^2, m_Z^2, m_Z^2, m_Z^2) \left. \right\}. \tag{42}
\end{aligned}$$

One-Loop Corrections to Stt Vertex

$$\begin{aligned}
\delta V_t^A(p^2, k^2, q^2) = & \frac{g^2}{16\pi^2} \frac{1}{144m_W^2} \left\{ -72c_\alpha^2 \mathcal{C}_0(p^2, q^2, k^2, m_t^2, m_t^2, m_H^2) m_t^4 - \right. \\
& -72s_\alpha^2 \mathcal{C}_0(p^2, q^2, k^2, m_t^2, m_t^2, m_S^2) m_t^4 - 36c_\alpha^2 \mathcal{B}_0(q^2, m_H^2, m_t^2) m_t^2 - 36s_\alpha^2 \mathcal{B}_0(q^2, m_S^2, m_t^2) m_t^2 + \\
& + 32m_W^2 - 32m_Z^2 - 384\pi v^2 \alpha_s - 256(-3\pi \alpha_s v^2 - m_W^2 s_W^2) \mathcal{B}_0(q^2, 0, m_t^2) + \left(36m_t^2 + \right. \\
& + 256c_W^2 m_W^2 - 320m_W^2 + 100m_Z^2 \left. \right) \mathcal{B}_0(q^2, m_t^2, m_Z^2) + \left(384\pi q^2 \alpha_s v^2 + 1536\pi m_t^2 \alpha_s v^2 - \right. \\
& - 384k^2 \pi \alpha_s v^2 - 384p^2 \pi \alpha_s v^2 - 128k^2 m_W^2 - 128p^2 m_W^2 + 128q^2 m_W^2 + 128k^2 c_W^2 m_W^2 + \\
& + 128p^2 c_W^2 m_W^2 - 128q^2 c_W^2 m_W^2 - 512c_W^2 m_t^2 m_W^2 + 512m_t^2 m_W^2 \left. \right) \mathcal{C}_0(k^2, p^2, q^2, 0, m_t^2, m_t^2) + \\
& + \left(-\frac{36v\omega\kappa m_t^2 c_\alpha^5}{s_\alpha} + 72v^2 \kappa m_t^2 c_\alpha^4 - 216v^2 \lambda m_t^2 c_\alpha^4 + 72v\omega\kappa m_t^2 s_\alpha c_\alpha^3 - 216v\omega\rho m_t^2 s_\alpha c_\alpha^3 - \right. \\
& - 36v^2 \kappa m_t^2 s_\alpha^2 c_\alpha^2 \left. \right) \mathcal{C}_0(k^2, p^2, q^2, m_t^2, m_H^2, m_H^2) + m_t^2 \left(-36v^2 \kappa c_\alpha^4 - 72v\omega\kappa s_\alpha c_\alpha^3 + \right. \\
& + 216v\omega\rho s_\alpha c_\alpha^3 + 72v^2 \kappa s_\alpha^2 c_\alpha^2 - 216v^2 \lambda s_\alpha^2 c_\alpha^2 + 36v\omega\kappa s_\alpha^3 c_\alpha \left. \right) \mathcal{C}_0(k^2, p^2, q^2, m_t^2, m_H^2, m_S^2) + \\
& + m_t^2 (-216v^2 \lambda s_\alpha^4 - 108v\omega\kappa c_\alpha s_\alpha^3 - 108v^2 \kappa c_\alpha^2 s_\alpha^2 - 216v\omega\rho c_\alpha^3 s_\alpha) \mathcal{C}_0(k^2, p^2, q^2, m_t^2, m_S^2, m_S^2) + \\
& + \left(512m_W^4 - 640m_Z^2 m_W^2 + 164m_Z^4 + 72v^2 \lambda m_t^2 - 36k^2 m_Z^2 + \frac{36v\omega\kappa c_\alpha m_t^2}{s_\alpha} \right) \times \\
& \times \mathcal{C}_0(k^2, p^2, q^2, m_t^2, m_Z^2, m_Z^2) + (72m_t^4 + 512c_W^2 m_W^2 m_t^2 - 640m_W^2 m_t^2 + 128m_Z^2 m_t^2) \times \\
& \times \mathcal{C}_0(p^2, q^2, k^2, m_t^2, m_t^2, m_Z^2) + \left(-36v^2 \kappa m_t^2 c_\alpha^4 - 72v\omega\kappa m_t^2 s_\alpha c_\alpha^3 + 216v\omega\rho m_t^2 s_\alpha c_\alpha^3 + \right. \\
& + 72v^2 \kappa m_t^2 s_\alpha^2 c_\alpha^2 - 216v^2 \lambda m_t^2 s_\alpha^2 c_\alpha^2 + 36v\omega\kappa m_t^2 s_\alpha^3 c_\alpha \left. \right) \mathcal{C}_0(q^2, p^2, k^2, m_t^2, m_H^2, m_S^2) + \\
& + \left(384\pi q^2 \alpha_s v^2 - 384k^2 \pi \alpha_s v^2 - 384p^2 \pi \alpha_s v^2 - 128k^2 m_W^2 - 128p^2 m_W^2 + 128q^2 m_W^2 + \right. \\
& + 128k^2 c_W^2 m_W^2 + 128p^2 c_W^2 m_W^2 - 128q^2 c_W^2 m_W^2 \left. \right) \mathcal{C}_1(k^2, p^2, q^2, 0, m_t^2, m_t^2) + \left(9k^2 m_Z^2 - \right. \\
& - 9p^2 m_Z^2 + 9q^2 m_Z^2 \left. \right) \mathcal{C}_1(k^2, p^2, q^2, m_t^2, m_Z^2, m_Z^2) + (-36k^2 c_\alpha^2 m_t^2 - 36p^2 c_\alpha^2 m_t^2 - 36q^2 c_\alpha^2 m_t^2) \times \\
& \times \mathcal{C}_1(p^2, q^2, k^2, m_t^2, m_t^2, m_H^2) - 36m_t^2 s_\alpha^2 (k^2 + p^2 + q^2) \mathcal{C}_1(p^2, q^2, k^2, m_t^2, m_t^2, m_S^2) + \\
& + (36k^2 m_t^2 + 36p^2 m_t^2 + 36q^2 m_t^2 - 320p^2 m_W^2 + 256p^2 c_W^2 m_W^2 + 64p^2 m_Z^2) \times
\end{aligned}$$

$$\begin{aligned}
& \times \mathcal{C}_1(p^2, q^2, k^2, m_t^2, m_t^2, m_Z^2) + \left(384\pi q^2 \alpha_s v^2 - 384k^2 \pi \alpha_s v^2 + 384p^2 \pi \alpha_s v^2 - 128m_W^2(k^2 + \right. \\
& \left. + p^2 + q^2 + k^2 c_W^2 - p^2 c_W^2 - q^2 c_W^2) \right) \mathcal{C}_2(k^2, p^2, q^2, 0, m_t^2, m_t^2) + \left(-27k^2 m_Z^2 + 27p^2 m_Z^2 - \right. \\
& \left. - 63q^2 m_Z^2 \right) \mathcal{C}_2(k^2, p^2, q^2, m_t^2, m_Z^2, m_Z^2) + (-54k^2 c_\alpha^2 m_t^2 - 18p^2 c_\alpha^2 m_t^2 + 18q^2 c_\alpha^2 m_t^2) \times \\
& \times \mathcal{C}_2(p^2, q^2, k^2, m_t^2, m_t^2, m_H^2) - 18m_t^2 s_\alpha^2 (3k^2 + p^2 - q^2) \mathcal{C}_2(p^2, q^2, k^2, m_t^2, m_t^2, m_S^2) + \\
& + \left(54k^2 m_t^2 + 18p^2 m_t^2 - 18q^2 m_t^2 - 160k^2 m_W^2 - 160p^2 m_W^2 + 160q^2 m_W^2 + 128k^2 c_W^2 m_W^2 + \right. \\
& \left. + 128p^2 c_W^2 m_W^2 - 128q^2 c_W^2 m_W^2 + 32k^2 m_Z^2 + 32p^2 m_Z^2 - 32q^2 m_Z^2 \right) \mathcal{C}_2(p^2, q^2, k^2, m_t^2, m_t^2, m_Z^2) \left. \right\}, \tag{43}
\end{aligned}$$

$$\begin{aligned}
\delta V_t^{\mathcal{B}}(p^2, k^2, q^2) &= \frac{g^2}{16\pi^2} \frac{1}{72m_W^2} \left\{ 18c_\alpha^2 \mathcal{C}_0(p^2, q^2, k^2, m_t^2, m_t^2, m_H^2) m_t^3 \right. \\
& + 18s_\alpha^2 \mathcal{C}_0(p^2, q^2, k^2, m_t^2, m_t^2, m_S^2) m_t^3 + 36c_\alpha^2 \mathcal{C}_1(p^2, q^2, k^2, m_t^2, m_t^2, m_H^2) m_t^3 + \\
& + 36s_\alpha^2 \mathcal{C}_1(p^2, q^2, k^2, m_t^2, m_t^2, m_S^2) m_t^3 - 64(-3\pi \alpha_s v^2 - m_W^2 s_W^2) \mathcal{C}_0(k^2, p^2, q^2, 0, m_t^2, m_t^2) m_t - \\
& - 9m_Z^2 \mathcal{C}_0(k^2, p^2, q^2, m_t^2, m_Z^2, m_Z^2) m_t + (18m_t^3 + 64c_W^2 m_W^2 m_t - 80m_W^2 m_t + 34m_Z^2 m_t) \times \\
& \times \mathcal{C}_0(p^2, q^2, k^2, m_t^2, m_t^2, m_Z^2) + (36m_t^3 + 128c_W^2 m_W^2 m_t - 160m_W^2 m_t + 68m_Z^2 m_t) \times \\
& \times \mathcal{C}_1(p^2, q^2, k^2, m_t^2, m_t^2, m_Z^2) + \left(-18v^2 \kappa m_t c_\alpha^4 - 36v\omega \kappa m_t s_\alpha c_\alpha^3 + 108v\omega \rho m_t s_\alpha c_\alpha^3 + \right. \\
& \left. + 36v^2 \kappa m_t s_\alpha^2 c_\alpha^2 - 108v^2 \lambda m_t s_\alpha^2 c_\alpha^2 + 18v\omega \kappa m_t s_\alpha^3 c_\alpha \right) \mathcal{C}_1(q^2, p^2, k^2, m_t^2, m_H^2, m_S^2) + \\
& + (384\pi m_t \alpha_s v^2 - 128c_W^2 m_t m_W^2 + 128m_t m_W^2) \mathcal{C}_2(k^2, p^2, q^2, 0, m_t^2, m_t^2) + \left(-\frac{18v\omega \kappa m_t c_\alpha^5}{s_\alpha} + \right. \\
& \left. + 36v^2 \kappa m_t c_\alpha^4 - 108v^2 \lambda m_t c_\alpha^4 + 36v\omega \kappa m_t s_\alpha c_\alpha^3 - 108v\omega \rho m_t s_\alpha c_\alpha^3 - 18v^2 \kappa m_t s_\alpha^2 c_\alpha^2 \right) \times \\
& \times \mathcal{C}_2(k^2, p^2, q^2, m_t^2, m_H^2, m_H^2) + \left(-18v^2 \kappa m_t c_\alpha^4 - 36v\omega \kappa m_t s_\alpha c_\alpha^3 + 108v\omega \rho m_t s_\alpha c_\alpha^3 + \right. \\
& \left. + 36v^2 \kappa m_t s_\alpha^2 c_\alpha^2 - 108v^2 \lambda m_t s_\alpha^2 c_\alpha^2 + 18v\omega \kappa m_t s_\alpha^3 c_\alpha \right) \mathcal{C}_2(k^2, p^2, q^2, m_t^2, m_H^2, m_S^2) + \\
& + m_t (-108v^2 \lambda s_\alpha^4 - 54v\omega \kappa c_\alpha s_\alpha^3 - 54v^2 \kappa c_\alpha^2 s_\alpha^2 - 108v\omega \rho c_\alpha^3 s_\alpha) \mathcal{C}_2(k^2, p^2, q^2, m_t^2, m_S^2, m_S^2) + \\
& + \left(-\frac{128m_W^4}{m_t} + \frac{160m_Z^2 m_W^2}{m_t} - \frac{68m_Z^4}{m_t} - 18m_t m_Z^2 - 36v^2 \lambda m_t - \frac{18v\omega \kappa c_\alpha m_t}{s_\alpha} \right) \times \\
& \left. \times \mathcal{C}_2(k^2, p^2, q^2, m_t^2, m_Z^2, m_Z^2) \right\}, \tag{44}
\end{aligned}$$

$$\begin{aligned}
\delta V_t^C(p^2, k^2, q^2) = & \frac{g^2}{16\pi^2} \frac{1}{72m_W^2} \left\{ 18c_\alpha^2 \mathcal{C}_0(p^2, q^2, k^2, m_t^2, m_t^2, m_H^2) m_t^3 + \right. \\
& + 18s_\alpha^2 \mathcal{C}_0(p^2, q^2, k^2, m_t^2, m_t^2, m_S^2) m_t^3 + 36c_\alpha^2 \mathcal{C}_1(p^2, q^2, k^2, m_t^2, m_t^2, m_H^2) m_t^3 + \\
& + 36s_\alpha^2 \mathcal{C}_1(p^2, q^2, k^2, m_t^2, m_t^2, m_S^2) m_t^3 + 36c_\alpha^2 \mathcal{C}_2(p^2, q^2, k^2, m_t^2, m_t^2, m_H^2) m_t^3 + \\
& + 36s_\alpha^2 \mathcal{C}_2(p^2, q^2, k^2, m_t^2, m_t^2, m_S^2) m_t^3 + 64m_t (-3\pi\alpha_s v^2 - m_W^2 s_W^2) \mathcal{C}_0(k^2, p^2, q^2, 0, m_t^2, m_t^2) + \\
& + 9m_Z^2 \mathcal{C}_0(k^2, p^2, q^2, m_t^2, m_Z^2, m_Z^2) m_t + (18m_t^3 + 64c_W^2 m_W^2 m_t - 80m_W^2 m_t + 34m_Z^2 m_t) \times \\
& \times \mathcal{C}_0(p^2, q^2, k^2, m_t^2, m_t^2, m_Z^2) - 128m_t (3\pi\alpha_s v^2 - s_W^2 m_W^2) \mathcal{C}_1(k^2, p^2, q^2, 0, m_t^2, m_t^2) + \\
& + m_t \left(\frac{18v\omega\kappa c_\alpha^5}{s_\alpha} - 36v^2 \kappa c_\alpha^4 + 108v^2 \lambda c_\alpha^4 - 36v\omega\kappa s_\alpha c_\alpha^3 + 108v\omega\rho s_\alpha c_\alpha^3 + 18v^2 \kappa s_\alpha^2 c_\alpha^2 \right) \times \\
& \times \mathcal{C}_1(k^2, p^2, q^2, m_t^2, m_H^2, m_H^2) + \left(18v^2 \kappa m_t c_\alpha^4 + 36v\omega\kappa m_t s_\alpha c_\alpha^3 - 108v\omega\rho m_t s_\alpha c_\alpha^3 - \right. \\
& \left. - 36v^2 \kappa m_t s_\alpha^2 c_\alpha^2 + 108v^2 \lambda m_t s_\alpha^2 c_\alpha^2 - 18v\omega\kappa m_t s_\alpha^3 c_\alpha \right) \mathcal{C}_1(k^2, p^2, q^2, m_t^2, m_H^2, m_S^2) + \\
& + m_t (108v^2 \lambda s_\alpha^4 + 54v\omega\kappa c_\alpha s_\alpha^3 + 54v^2 \kappa c_\alpha^2 s_\alpha^2 + 108v\omega\rho c_\alpha^3 s_\alpha) \mathcal{C}_1(k^2, p^2, q^2, m_t^2, m_S^2, m_S^2) + \\
& + \left(\frac{128m_W^4}{m_t} - \frac{160m_Z^2 m_W^2}{m_t} + \frac{68m_Z^4}{m_t} + 18m_t m_Z^2 + 36v^2 \lambda m_t + \frac{18v\omega\kappa c_\alpha m_t}{s_\alpha} \right) \times \\
& \times \mathcal{C}_1(k^2, p^2, q^2, m_t^2, m_Z^2, m_Z^2) + (36m_t^3 + 128c_W^2 m_W^2 m_t - 160m_W^2 m_t + 68m_Z^2 m_t) \times \\
& \times \mathcal{C}_1(p^2, q^2, k^2, m_t^2, m_t^2, m_Z^2) + (36m_t^3 + 128c_W^2 m_W^2 m_t - 160m_W^2 m_t + 68m_Z^2 m_t) \times \\
& \times \mathcal{C}_2(p^2, q^2, k^2, m_t^2, m_t^2, m_Z^2) + m_t \left(18v^2 \kappa c_\alpha^4 + 36v\omega\kappa s_\alpha c_\alpha^3 - 108v\omega\rho s_\alpha c_\alpha^3 - 36v^2 \kappa s_\alpha^2 c_\alpha^2 + \right. \\
& \left. + 108v^2 \lambda s_\alpha^2 c_\alpha^2 - 18v\omega\kappa s_\alpha^3 c_\alpha \right) \mathcal{C}_2(q^2, p^2, k^2, m_t^2, m_H^2, m_S^2) \left. \right\}, \tag{45}
\end{aligned}$$

$$\begin{aligned}
\delta V_t^D(p^2, k^2, q^2) = & \frac{g^2}{16\pi^2} \frac{1}{8m_W^2} \left\{ -3m_Z^2 \mathcal{C}_1(k^2, p^2, q^2, m_t^2, m_Z^2, m_Z^2) + \right. \\
& + 2c_\alpha^2 m_t^2 \mathcal{C}_2(p^2, q^2, k^2, m_t^2, m_t^2, m_H^2) + 2m_t^2 s_\alpha^2 \mathcal{C}_2(p^2, q^2, k^2, m_t^2, m_t^2, m_S^2) - \\
& \left. - 2m_t^2 \mathcal{C}_2(p^2, q^2, k^2, m_t^2, m_t^2, m_Z^2) - 3m_Z^2 \mathcal{C}_2(k^2, p^2, q^2, m_t^2, m_Z^2, m_Z^2) \right\}, \tag{46}
\end{aligned}$$

$$\begin{aligned}
\delta V_t^E(p^2, k^2, q^2) = & \frac{g^2}{16\pi^2} \frac{1}{48m_W^2} \left\{ (8c_W^2 - 5) m_Z^2 (- (k^2 + 3p^2 - 3q^2)) \times \right. \\
& \left. \times \mathcal{C}_1(k^2, p^2, q^2, m_t^2, m_Z^2, m_Z^2) - (8c_W^2 - 5) m_Z^2 (3k^2 - 3p^2 - q^2) \mathcal{C}_2(k^2, p^2, q^2, m_t^2, m_Z^2, m_Z^2) \right\}, \tag{47}
\end{aligned}$$

$$\begin{aligned}
\delta V_t^{\mathcal{F}}(p^2, k^2, q^2) = & \frac{g^2}{16\pi^2} \frac{1}{24m_W^2} \left\{ - (8c_W^2 - 5) m_t m_Z^2 \mathcal{C}_0(k^2, p^2, q^2, m_t^2, m_Z^2, m_Z^2) + \right. \\
& + 2 (8c_W^2 - 5) m_t m_Z^2 \mathcal{C}_0(p^2, q^2, k^2, m_t^2, m_t^2, m_Z^2) + 4 (8c_W^2 - 5) m_t m_Z^2 \times \\
& \times \mathcal{C}_1(p^2, q^2, k^2, m_t^2, m_t^2, m_Z^2) - \left. \frac{(8c_W^2 - 5) m_Z^4 (2c_W^2 m_t^2 + 4m_W^2) \mathcal{C}_2(k^2, p^2, q^2, m_t^2, m_Z^2, m_Z^2)}{m_t m_W^2} \right\}, \tag{48}
\end{aligned}$$

$$\begin{aligned}
\delta V_t^{\mathcal{G}}(p^2, k^2, q^2) = & \frac{g^2}{16\pi^2} \frac{1}{24m_W^2} \left\{ (8c_W^2 - 5) m_t m_Z^2 \mathcal{C}_0(k^2, p^2, q^2, m_t^2, m_Z^2, m_Z^2) + \right. \\
& + 2 (8c_W^2 - 5) m_t m_Z^2 \mathcal{C}_0(p^2, q^2, k^2, m_t^2, m_t^2, m_Z^2) + \frac{(8c_W^2 - 5) m_Z^4 (2c_W^2 m_t^2 + 4m_W^2)}{m_t m_W^2} \times \\
& \times \mathcal{C}_1(k^2, p^2, q^2, m_t^2, m_Z^2, m_Z^2) + \\
& \left. + 4 (8c_W^2 - 5) m_t m_Z^2 \mathcal{C}_1(p^2, q^2, k^2, m_t^2, m_t^2, m_Z^2) + 4 (8c_W^2 - 5) m_t m_Z^2 \mathcal{C}_2(p^2, q^2, k^2, m_t^2, m_t^2, m_Z^2) \right\}, \tag{49}
\end{aligned}$$

$$\begin{aligned}
\delta V_t^{\mathcal{H}}(p^2, k^2, q^2) = & \frac{g^2}{16\pi^2} \frac{1}{24m_W^2} \left\{ (8c_W^2 - 5) m_Z^2 \mathcal{C}_1(k^2, p^2, q^2, m_t^2, m_Z^2, m_Z^2) - \right. \\
& \left. - (8c_W^2 - 5) m_Z^2 \mathcal{C}_2(k^2, p^2, q^2, m_t^2, m_Z^2, m_Z^2) \right\}. \tag{50}
\end{aligned}$$

D - Loop Integral Expressions: \mathcal{A}_0 , \mathcal{B}_0 , \mathcal{B}_{00} , \mathcal{B}_1

Now let us report the loop integrals which are expressed in the $\overline{\text{MS}}$ renormalization scheme:

$$\Delta[p^2] = \frac{1}{\epsilon} + \log \left[\frac{\mu^2}{p^2} \right] \tag{51}$$

$$\mathcal{K}[p, m_a, m_b] = \sqrt{m_a^4 + (m_b^2 - p^2)^2 - 2m_a^2(m_b^2 + p^2)} \tag{52}$$

$$\mathcal{Q}[p, m] = \sqrt{1 - \frac{4m^2}{p^2}} \log \left[1 - \frac{p^2}{2m^2} \left(1 + \sqrt{1 - \frac{4m^2}{p^2}} \right) \right], \tag{53}$$

$$\mathcal{A}_0(m^2) = m^2(1 + \Delta[m^2]), \quad (54)$$

$$\mathcal{B}_0(p^2, 0, 0) = 2 + \Delta[-p^2], \quad (55)$$

$$\mathcal{B}_0(p^2, m^2, m^2) = 2 + \Delta[m^2] - \mathcal{Q}[p, m], \quad (56)$$

$$\mathcal{B}_0(p^2, 0, m^2) = 2 + \Delta[-m^2] + \left(1 - \frac{m^2}{p^2}\right) \log \left[\frac{m^2}{m^2 - p^2} \right] \quad (57)$$

$$\begin{aligned} \mathcal{B}_0(p^2, m_a^2, m_b^2) = 2 + \Delta[m_b^2] + \frac{\mathcal{K}[p, m_a, m_b]}{p^2} \log \left[\frac{2m_a m_b}{m_a^2 + m_b^2 - p^2 - \mathcal{K}[p, m_a, m_b]} \right] + \\ + \left(\frac{m_b^2}{p^2} - \frac{m_a^2}{p^2} - 1 \right) \log \left[\frac{m_a}{m_b} \right], \end{aligned} \quad (58)$$

$$\mathcal{B}_{00}(p^2, 0, 0) = -p^2 \left(\frac{2}{9} + \frac{\Delta[-p^2]}{12} \right) \quad (59)$$

$$\mathcal{B}_{00}(p^2, m^2, m^2) = -\frac{2p^2}{9} + \frac{m^2}{6}(\Delta[m^2] + 7) + \frac{p^2 - 4m^2}{12}(\mathcal{Q}[p, m] - \Delta[m^2]), \quad (60)$$

$$\begin{aligned} \mathcal{B}_{00}(p^2, 0, m^2) = \frac{m^2}{12} \left(7 - \frac{m^2}{p^2} \right) - \frac{2p^2}{9} + \left(\frac{3m^2 - p^2}{12} \right) \Delta[m^2] + \\ + \frac{(m^2 - p^2)^3}{12p^4} \log \left[\frac{m^2}{m^2 - p^2} \right], \end{aligned} \quad (61)$$

$$\begin{aligned} \mathcal{B}_{00}(p^2, m_a^2, m_b^2) = \frac{7(m_a^2 + m_b^2)}{12} - \frac{2p^2}{9} - \frac{m_a^4 - 2m_a^2 m_b^2 + m_b^4}{12p^2} + \left(\frac{m_a^2 + m_b^2}{4} - \frac{p^2}{12} \right) \times \\ \times \left(\Delta[m_b^2] + \log \left[\frac{m_b}{m_a} \right] \right) - \frac{1}{12p^4} \left\{ \frac{[(m_a^2 - m_b^2)^3 + 3p^2(m_b^4 - m_a^4)]}{4} \log \left[\frac{m_b}{m_a} \right] - \right. \\ \left. - \mathcal{K}^3[p, m_a, m_b] \log \left[\frac{2m_a m_b}{m_a^2 + m_b^2 - p^2 - \mathcal{K}[p, m_a, m_b]} \right] \right\}, \end{aligned} \quad (62)$$

$$\mathcal{B}_1(p^2, 0, 0) = -1 - \frac{\Delta[-p^2]}{2} \quad (63)$$

$$\mathcal{B}_1(p^2, m^2, m^2) = -1 + \frac{\mathcal{Q}[p, m] - \Delta[m^2]}{2}, \quad (64)$$

$$\mathcal{B}_1(p^2, 0, m^2) = -1 + \frac{m^2}{2p^2} - \frac{\Delta[m^2]}{2} - \frac{(m^2 - p^2)^2}{2p^4} \log \left[\frac{m^2}{m^2 - p^2} \right], \quad (65)$$

$$\begin{aligned} \mathcal{B}_1(p^2, m_a^2, m_b^2) = -1 - \frac{\Delta[m_b^2]}{2} + \frac{1}{2p^2} \left\{ m_b^2 - m_a^2 + \frac{2m_a^2 p^2 + \mathcal{K}^2[p, m_a, m_b]}{p^2} \log \left[\frac{m_a}{m_b} \right] \right. \\ \left. - \frac{m_a^2 - m_b^2 + p^2}{p^2} \mathcal{K}[p, m_a, m_b] \log \left[\frac{2m_a m_b}{m_a^2 + m_b^2 - p^2 - \mathcal{K}[p, m_a, m_b]} \right] \right\}. \end{aligned} \quad (66)$$

Bibliography

- [1] G. Aad *et al.* [ATLAS Collaboration], Phys. Lett. B **716** (2012) 1 doi:10.1016/j.physletb.2012.08.020 [arXiv:1207.7214 [hep-ex]].
- [2] S. Chatrchyan *et al.* [CMS Collaboration], Phys. Lett. B **716** (2012) 30 doi:10.1016/j.physletb.2012.08.021 [arXiv:1207.7235 [hep-ex]].
- [3] P. W. Higgs, Phys. Rev. Lett. **13** (1964) 508. doi:10.1103/PhysRevLett.13.508
- [4] P. W. Higgs, Phys. Lett. **12** (1964) 132. doi:10.1016/0031-9163(64)91136-9
- [5] F. Englert and R. Brout, Phys. Rev. Lett. **13** (1964) 321. doi:10.1103/PhysRevLett.13.321
- [6] G. S. Guralnik, C. R. Hagen and T. W. B. Kibble, Phys. Rev. Lett. **13** (1964) 585. doi:10.1103/PhysRevLett.13.585
- [7] R. M. Schabinger and J. D. Wells, Phys. Rev. D **72** (2005) 093007 doi:10.1103/PhysRevD.72.093007 [hep-ph/0509209].
- [8] G. M. Pruna and T. Robens, Phys. Rev. D **88** (2013) no.11, 115012 doi:10.1103/PhysRevD.88.115012 [arXiv:1303.1150 [hep-ph]]; C. Englert, T. Plehn, D. Zerwas and P. M. Zerwas, Phys. Lett. B **703**, 298 (2011) doi:10.1016/j.physletb.2011.08.002 [arXiv:1106.3097 [hep-ph]]; B. Batell, S. Gori and L. T. Wang, JHEP **1206**, 172 (2012) doi:10.1007/JHEP06(2012)172 [arXiv:1112.5180 [hep-ph]].
- [9] D. Buttazzo, F. Sala and A. Tesi, JHEP **1511** (2015) 158 doi:10.1007/JHEP11(2015)158 [arXiv:1505.05488 [hep-ph]].
- [10] T. Robens and T. Stefaniak, Eur. Phys. J. C **75**, 104 (2015) doi:10.1140/epjc/s10052-015-3323-y [arXiv:1501.02234 [hep-ph]].
- [11] T. Robens and T. Stefaniak, Eur. Phys. J. C **76** (2016) no.5, 268 doi:10.1140/epjc/s10052-016-4115-8 [arXiv:1601.07880 [hep-ph]].
- [12] I. M. Lewis and M. Sullivan, arXiv:1701.08774 [hep-ph]

- [13] S. Dawson and I. M. Lewis, Phys. Rev. D **92**, no. 9, 094023 (2015) doi:10.1103/PhysRevD.92.094023 [arXiv:1508.05397 [hep-ph]].
- [14] C. Y. Chen, S. Dawson and I. M. Lewis, Phys. Rev. D **91**, no. 3, 035015 (2015) doi:10.1103/PhysRevD.91.035015 [arXiv:1410.5488 [hep-ph]].
- [15] F. Bezrukov, M. Y. Kalmykov, B. A. Kniehl and M. Shaposhnikov, JHEP **1210**, 140 (2012) doi:10.1007/JHEP10(2012)140 [arXiv:1205.2893 [hep-ph]]; S. Alekhin, A. Djouadi and S. Moch, Phys. Lett. B **716**, 214 (2012) doi:10.1016/j.physletb.2012.08.024 [arXiv:1207.0980 [hep-ph]]; D. Buttazzo, G. Degrossi, P. P. Giardino, G. F. Giudice, F. Sala, A. Salvio and A. Strumia, JHEP **1312**, 089 (2013) doi:10.1007/JHEP12(2013)089 [arXiv:1307.3536 [hep-ph]].
- [16] J. Elias-Miro, J. R. Espinosa, G. F. Giudice, H. M. Lee and A. Strumia, JHEP **1206**, 031 (2012) doi:10.1007/JHEP06(2012)031 [arXiv:1203.0237 [hep-ph]].
- [17] A. Falkowski, C. Gross and O. Lebedev, JHEP **1505** (2015) 057 doi:10.1007/JHEP05(2015)057 [arXiv:1502.01361 [hep-ph]].
- [18] B. Patt and F. Wilczek, hep-ph/0605188.
- [19] G. Aad *et al.* [ATLAS Collaboration], Phys. Rev. D **92** (2015) no.1, 012006 doi:10.1103/PhysRevD.92.012006 [arXiv:1412.2641 [hep-ex]].
- [20] V. Khachatryan *et al.* [CMS Collaboration], JHEP **1510** (2015) 144 doi:10.1007/JHEP10(2015)144 [arXiv:1504.00936 [hep-ex]].
- [21] G. Aad *et al.* [ATLAS Collaboration], Eur. Phys. J. C **75** (2015) no.9, 412 doi:10.1140/epjc/s10052-015-3628-x [arXiv:1506.00285 [hep-ex]].
- [22] G. Aad *et al.* [ATLAS Collaboration], Phys. Rev. Lett. **114** (2015) no.8, 081802 doi:10.1103/PhysRevLett.114.081802 [arXiv:1406.5053 [hep-ex]].
- [23] V. Khachatryan *et al.* [CMS Collaboration], Phys. Lett. B **749** (2015) 560 doi:10.1016/j.physletb.2015.08.047 [arXiv:1503.04114 [hep-ex]].
- [24] V. Barger, P. Langacker, M. McCaskey, M. J. Ramsey-Musolf and G. Shaughnessy, Phys. Rev. D **77**, 035005 (2008) doi:10.1103/PhysRevD.77.035005 [arXiv:0706.4311 [hep-ph]]; W. L. Guo and Y. L. Wu, JHEP **1010**, 083 (2010) doi:10.1007/JHEP10(2010)083 [arXiv:1006.2518 [hep-ph]]; A. Biswas and D. Majumdar, Pramana **80**, 539 (2013) doi:10.1007/s12043-012-0478-z [arXiv:1102.3024 [hep-ph]].
- [25] J. A. Casas, D. G. Cerdeño, J. M. Moreno and J. Quilis, arXiv:1701.08134 [hep-ph].
- [26] D. López-Val and T. Robens, Phys. Rev. D **90** (2014) 114018 doi:10.1103/PhysRevD.90.114018 [arXiv:1406.1043 [hep-ph]].

- [27] G. Chalons, D. Lopez-Val, T. Robens and T. Stefaniak, arXiv:1611.03007 [hep-ph].
- [28] M. E. Peskin and D. V. Schroeder, Reading, USA: Addison-Wesley (1995) 842 p
- [29] F. Bojarski, G. Chalons, D. Lopez-Val and T. Robens, JHEP **1602** (2016) 147 doi:10.1007/JHEP02(2016)147 [arXiv:1511.08120 [hep-ph]].
- [30] A. Alloul, N. D. Christensen, C. Degrande, C. Duhr and B. Fuks, Comput. Phys. Commun. **185** (2014) 2250 doi:10.1016/j.cpc.2014.04.012 [arXiv:1310.1921 [hep-ph]].
- [31] G. Aad *et al.* [ATLAS Collaboration], Phys. Lett. B **716** (2012) 1 doi:10.1016/j.physletb.2012.08.020 [arXiv:1207.7214 [hep-ex]].
- [32] G. Degrande, S. Di Vita, J. Elias-Miro, J. R. Espinosa, G. F. Giudice, G. Isidori and A. Strumia, JHEP **1208** (2012) 098 doi:10.1007/JHEP08(2012)098 [arXiv:1205.6497 [hep-ph]].
- [33] A. Denner, Fortsch. Phys. **41** (1993) 307 doi:10.1002/prop.2190410402 [arXiv:0709.1075 [hep-ph]].
- [34] F. Boudjema and E. Chopin, Z. Phys. C **73** (1996) 85 doi:10.1007/s002880050298 [hep-ph/9507396];
- [35] G. Belanger, F. Boudjema, J. Fujimoto, T. Ishikawa, T. Kaneko, K. Kato and Y. Shimizu, Phys. Rept. **430** (2006) 117 doi:10.1016/j.physrep.2006.02.001 [hep-ph/0308080].
- [36] L. D. Faddeev and V. N. Popov, Phys. Lett. **25B** (1967) 29. doi:10.1016/0370-2693(67)90067-6
- [37] C. Becchi, A. Rouet and R. Stora, Annals Phys. **98** (1976) 287. doi:10.1016/0003-4916(76)90156-1 ; M. Z. Iofa and I. V. Tyutin, Teor. Mat. Fiz. **27** (1976) 38 [Theor. Math. Phys. **27** (1976) 316]. doi:10.1007/BF01036547
- [38] J. F. Gunion, H. E. Haber and J. Wudka, Phys. Rev. D **43** (1991) 904. doi:10.1103/PhysRevD.43.904
- [39] J. Alcaraz *et al.* [ALEPH and DELPHI and L3 and OPAL Collaborations and LEP Electroweak Working Group], hep-ex/0612034.
- [40] T. Aaltonen *et al.* [CDF Collaboration], Phys. Rev. Lett. **108** (2012) 151803 doi:10.1103/PhysRevLett.108.151803 [arXiv:1203.0275 [hep-ex]].
- [41] V. M. Abazov *et al.* [D0 Collaboration], Phys. Rev. D **89** (2014) no.1, 012005 doi:10.1103/PhysRevD.89.012005 [arXiv:1310.8628 [hep-ex]].
- [42] The ATLAS collaboration [ATLAS Collaboration], ATLAS-CONF-2014-009.

- [43] [CMS Collaboration], CMS-PAS-HIG-13-005.
- [44] G. Aad *et al.* [ATLAS and CMS Collaborations], JHEP **1608** (2016) 045 doi:10.1007/JHEP08(2016)045 [arXiv:1606.02266 [hep-ex]].
- [45] B. W. Lee, C. Quigg and H. B. Thacker, Phys. Rev. Lett. **38** (1977) 883. doi:10.1103/PhysRevLett.38.883
- [46] W. Y. Keung and W. J. Marciano, Phys. Rev. D **30** (1984) 248. doi:10.1103/PhysRevD.30.248
- [47] J. R. Ellis, M. K. Gaillard and D. V. Nanopoulos, Nucl. Phys. B **106** (1976) 292. doi:10.1016/0550-3213(76)90382-5
- [48] M. A. Shifman, A. I. Vainshtein, M. B. Voloshin and V. I. Zakharov, Sov. J. Nucl. Phys. **30** (1979) 711 [Yad. Fiz. **30** (1979) 1368].
- [49] L. Bergstrom and G. Hulth, Nucl. Phys. B **259** (1985) 137 Erratum: [Nucl. Phys. B **276** (1986) 744]. doi:10.1016/0550-3213(86)90074-X, 10.1016/0550-3213(85)90302-5
- [50] C. Patrignani *et al.* [Particle Data Group], Chin. Phys. C **40** (2016) no.10, 100001. doi:10.1088/1674-1137/40/10/100001
- [51] S. S. Schweber, Princeton, USA: Univ. Pr. (1994) 732 p
- [52] C. G. Bollini and J. J. Giambiagi, Nuovo Cim. B **12** (1972) 20. doi:10.1007/BF02895558
- [53] G. 't Hooft and M. J. G. Veltman, Nucl. Phys. B **44** (1972) 189. doi:10.1016/0550-3213(72)90279-9
- [54] D. A. Ross and J. C. Taylor, Nucl. Phys. B **51** (1973) 125 Erratum: [Nucl. Phys. B **58** (1973) 643]. doi:10.1016/0550-3213(73)90608-1, 10.1016/0550-3213(73)90505-1
- [55] S. Kanemura, M. Kikuchi and K. Yagyu, Nucl. Phys. B **907** (2016) 286 doi:10.1016/j.nuclphysb.2016.04.005 [arXiv:1511.06211 [hep-ph]].
- [56] S. Heinemeyer, Int. J. Mod. Phys. A **21** (2006) 2659 doi:10.1142/S0217751X06031028 [hep-ph/0407244].
- [57] B. A. Kniehl, Nucl. Phys. B **352** (1991) 1. doi:10.1016/0550-3213(91)90126-I
- [58] A. Sirlin, Phys. Rev. D **22** (1980) 971. doi:10.1103/PhysRevD.22.971
- [59] J. R. Espinosa and Y. Yamada, Phys. Rev. D **67** (2003) 036003 doi:10.1103/PhysRevD.67.036003 [hep-ph/0207351].

- [60] D. Binosi and J. Papavassiliou, Phys. Rept. **479** (2009) 1 doi:10.1016/j.physrep.2009.05.001 [arXiv:0909.2536 [hep-ph]].
- [61] S. Kanemura, M. Kikuchi, K. Sakurai and K. Yagyu, Phys. Rev. D **96** (2017) no.3, 035014 doi:10.1103/PhysRevD.96.035014 [arXiv:1705.05399 [hep-ph]].
- [62] D. Lopez-Val and J. Sola, Phys. Rev. D **81** (2010) 033003 doi:10.1103/PhysRevD.81.033003 [arXiv:0908.2898 [hep-ph]].
- [63] B. A. Kniehl, Nucl. Phys. B **357** (1991) 439. doi:10.1016/0550-3213(91)90476-E
- [64] B. A. Kniehl, Nucl. Phys. B **376** (1992) 3. doi:10.1016/0550-3213(92)90065-J
- [65] M. Drees and K. i. Hikasa, Phys. Lett. B **240** (1990) 455 Erratum: [Phys. Lett. B **262** (1991) 497]. doi:10.1016/0370-2693(90)91130-4
- [66] J. S. Schwinger, REDWOOD CITY, USA: ADDISON-WESLEY (1989) 318 P. (ADVANCED BOOK CLASSICS SERIES)
- [67] B. A. Kniehl, Phys. Rept. **240** (1994) 211. doi:10.1016/0370-1573(94)90037-X
- [68] M. Drees and K. i. Hikasa, Phys. Rev. D **41** (1990) 1547. doi:10.1103/PhysRevD.41.1547
- [69] M. J. Strassler and M. E. Peskin, Phys. Rev. D **43** (1991) 1500. doi:10.1103/PhysRevD.43.1500
- [70] S. Kanemura, M. Kikuchi and K. Yagyu, Nucl. Phys. B **917** (2017) 154 doi:10.1016/j.nuclphysb.2017.02.004 [arXiv:1608.01582 [hep-ph]]. 11 citations counted in INSPIRE as of 17 May 2017
- [71] A. D. Martin, W. J. Stirling, R. S. Thorne and G. Watt, Eur. Phys. J. C **63** (2009) 189 doi:10.1140/epjc/s10052-009-1072-5 [arXiv:0901.0002 [hep-ph]].
- [72] R. Franceschini, G. F. Giudice, J. F. Kamenik, M. McCullough, F. Riva, A. Strumia and R. Torre, JHEP **1607** (2016) 150 doi:10.1007/JHEP07(2016)150 [arXiv:1604.06446 [hep-ph]].
- [73] A. Djouadi, Phys. Rept. **457** (2008) 1 doi:10.1016/j.physrep.2007.10.004 [hep-ph/0503172].
- [74] A. Djouadi, Phys. Rept. **459** (2008) 1 doi:10.1016/j.physrep.2007.10.005 [hep-ph/0503173].
- [75] T. Hahn, Comput. Phys. Commun. **140** (2001) 418 doi:10.1016/S0010-4655(01)00290-9 [hep-ph/0012260].

- [76] G. 't Hooft and M. J. G. Veltman, Nucl. Phys. B **153** (1979) 365. doi:10.1016/0550-3213(79)90605-9
- [77] G. Passarino and M. J. G. Veltman, Nucl. Phys. B **160** (1979) 151. doi:10.1016/0550-3213(79)90234-7
- [78] H. H. Patel, Comput. Phys. Commun. **197** (2015) 276 doi:10.1016/j.cpc.2015.08.017 [arXiv:1503.01469 [hep-ph]].